

The Impact of Neonatal Basal Forebrain Cholinergic Lesion on the Behavioural and Neural Effects of Aging, Cerebral Hypoperfusion, and Environmental Enrichment

By Kerry Rennie

A thesis submitted to the
Faculty of Graduate and Postdoctoral Affairs
in partial fulfillment of
the requirements for the degree of

Doctor of Philosophy
Psychology
Specialization in Neuroscience

Department of Psychology
and Institute of Neuroscience

Carleton University
Ottawa, Ontario
©2011 Kerry Rennie



Library and Archives
Canada

Published Heritage
Branch

395 Wellington Street
Ottawa ON K1A 0N4
Canada

Bibliothèque et
Archives Canada

Direction du
Patrimoine de l'édition

395, rue Wellington
Ottawa ON K1A 0N4
Canada

Your file *Votre référence*
ISBN: 978-0-494-81579-3
Our file *Notre référence*
ISBN: 978-0-494-81579-3

NOTICE:

The author has granted a non-exclusive license allowing Library and Archives Canada to reproduce, publish, archive, preserve, conserve, communicate to the public by telecommunication or on the Internet, loan, distribute and sell theses worldwide, for commercial or non-commercial purposes, in microform, paper, electronic and/or any other formats.

The author retains copyright ownership and moral rights in this thesis. Neither the thesis nor substantial extracts from it may be printed or otherwise reproduced without the author's permission.

In compliance with the Canadian Privacy Act some supporting forms may have been removed from this thesis.

While these forms may be included in the document page count, their removal does not represent any loss of content from the thesis.

AVIS:

L'auteur a accordé une licence non exclusive permettant à la Bibliothèque et Archives Canada de reproduire, publier, archiver, sauvegarder, conserver, transmettre au public par télécommunication ou par l'Internet, prêter, distribuer et vendre des thèses partout dans le monde, à des fins commerciales ou autres, sur support microforme, papier, électronique et/ou autres formats.

L'auteur conserve la propriété du droit d'auteur et des droits moraux qui protègent cette thèse. Ni la thèse ni des extraits substantiels de celle-ci ne doivent être imprimés ou autrement reproduits sans son autorisation.

Conformément à la loi canadienne sur la protection de la vie privée, quelques formulaires secondaires ont été enlevés de cette thèse.

Bien que ces formulaires aient inclus dans la pagination, il n'y aura aucun contenu manquant.


Canada

Abstract

Dysfunction of the basal forebrain cholinergic system (BFCS) has been implicated in the cognitive decline that occurs during normal aging and in Alzheimer's disease. However, cholinergic dysfunction alone may be insufficient to precipitate aging- or Alzheimer's-associated cognitive deficits. Rather, cognitive status may better reflect the interaction of a dysfunctional cholinergic system with pathological or other factors across the lifespan. Here we employed postnatal day 7 lesions of the BFCS using 192-IgG-saporin in rats in combination with aging, cerebral hypoperfusion induced by permanent carotid artery ligation (2VO), or environmental enrichment (EE) to explore this hypothesis.

Neonatal forebrain cholinergic lesion (N192S) was found to synergize with both aging and 2VO to produce memory impairments in the working memory version of the Morris water maze. While N192S precipitated cognitive dysfunction in aged and 2VO rats, in neither case, however, was there evidence of Alzheimer's-like neuropathology such as CA1 cell loss, astrogliosis or dendritic atrophy. Aged lesioned rats did show subtle alterations in dendritic morphology suggestive of a shifting of dendritic material away from the cell body. Furthermore, 2VO resulted in significant dendritic hypertrophy in CA1 pyramidal cells. While this occurred in both N192S and control rats, branch order analysis revealed that some of the 2VO-induced changes were apparent only in the N192S rats.

The third study assessed the impact of N192S on the proliferation, differentiation and survival of newborn cells in rats that were housed in either enriched or standard

conditions. Surprisingly, EE failed to increase neurogenesis, thereby preventing determination of the effects of N192S on EE-induced neurogenesis. However, N192S reduced the number of 5-bromo-2-deoxyuridine-immunopositive (BrdU⁺) cells 1 day after BrdU exposure but did not alter the number of cells expressing the cell cycle marker Ki-67. Neither the number of BrdU⁺ cells 28 days after BrdU exposure, nor the proportion of BrdU⁺ cells that adopted a neuronal or glial identity was affected by N192S. The most plausible explanation for these novel results is that N192S accelerates the death of newborn cells, but does not alter their overall survival rate or phenotypic differentiation.

Acknowledgements

Over the several years that I have spent at Carleton I have been surrounded by an amazing group of people, who have taught me so much, and who have made my time here memorable. Firstly, I would like to thank my supervisor, Bruce Pappas. Bruce, I feel privileged to have had the opportunity to work with you and learn from you. I hope that I will someday be the kind of researcher that you are, and that I will demonstrate the same commitment to my students that you have always shown me. Wherever I end up in the future, I know that I will always have you to thank for starting me out along my career path.

I also owe a debt of gratitude to Teresa Fortin. Teresa, you are an excellent teacher and a fountain of knowledge, and I want to thank you for all the times you have provided advice and helped me trouble-shoot protocols. My first response every time I encountered a problem in the lab was “I’ll just ask Teresa” – and I don’t think there was ever a time when you didn’t have an answer for me. I also appreciate that I can always locate you in the building by listening for your laugh. To Ann, Collinda, Shari, and Shannon, thank you for taking excellent care of my rats (and way back, the gerbils). Thank you for the work you do every day that is so much appreciated and under-acknowledged.

For my first introduction to life at the lab, I have to thank Maxine De Butte-Smith. Max, thank you for everything you taught me and for continuing to stay in touch over the past several years. I hope to keep running into you at conferences! I might still be slicing brains and tracing dendrites if it weren’t for the help of Mylène Fréchette and

Chloé Ward. I can't thank you each enough, both for your assistance and for your companionship. Mylène, my favourite times at the lab were the years that we worked together, and I am fortunate to have had you as a labmate, and to have you still as a friend. I also want to extend my thanks to several past and present students who I have been lucky enough to work with and who have spent so much time in the Pappas lab that I will always consider them to be honorary Pappas lab members: Jenn, Tania, Dan, and Livia, thank you for your friendship and your company during the long hours of counting. The past several years would have been a much less enjoyable experience without you.

I owe a huge thank you to Pat McGuire. Pat, it would be impossible to tell you (but I hope you know) how much your support means to me. I could not have asked for a better friend to go through all the ups and downs of the past several years with. Finally, while the faculty, staff and students at Carleton have taught me everything I know about neuroscience, I learned everything else from my family, and this thesis would not have been possible without their support. To Mom, Dad, Sarah, and Erica: thank you.

TABLE OF CONTENTS

Title Page.....	i
Abstract.....	ii
Acknowledgements.....	v
Table of Contents.....	vii
List of Figures.....	xi
List of Appendices.....	xv
List of Abbreviations.....	xvi
1. General Introduction.....	1
1.1. Organization of the Basal Forebrain Cholinergic System.....	2
1.2. The Basal Forebrain Cholinergic System in Aging and AD.....	3
1.3. Cholinergic Lesion Using 192-IgG Saporin.....	4
1.4. Behavioural Effects of Neonatal Cholinergic Lesion.....	6
1.5. Effects of Neonatal Cholinergic Lesion on Dendritic Morphology.....	9
1.6. Adult Neurogenesis.....	11
1.7. Cholinergic Involvement in the Regulation of Neurogenesis.....	15
1.8. Research Plan.....	17
2. Study 1: The effects of neonatal cholinergic lesion on age-related neural and behavioural changes.....	19
2.1. Introduction.....	19
2.2. Methods.....	22
2.2.1. Animals.....	22
2.2.2. Breeding.....	23
2.2.3. Cholinergic Lesion.....	23
2.2.4. Water Maze Testing.....	24
2.2.5. Tissue Collection.....	25
2.2.6. Verification of the Cholinergic Lesion.....	26
2.2.7. Ki-67 Staining and Analysis.....	27
2.2.8. DCX Staining and Analysis.....	28
2.2.9. GFAP Staining and Analysis.....	28

2.2.10. APP Staining and Analysis.....	29
2.2.11. CA1 Pyramidal Cell Counts.....	30
2.2.12. Golgi Analysis.....	31
2.3. Results.....	32
2.3.1. General.....	32
2.3.2. Water Maze.....	32
2.3.3. Cued Platform.....	40
2.3.4. Ki-67 Counts.....	40
2.3.5. DCX Counts.....	43
2.3.6. GFAP Immunoreactivity.....	43
2.3.7. APP Immunoreactivity.....	43
2.3.8. CA1 Cell Number.....	54
2.3.9. CA1 Pyramidal Cell Morphology.....	54
2.3.9.1. Branch Order Analysis – Apical Dendrites.....	54
2.3.9.2. Branch Order Analysis – Basal Dendrites.....	61
2.4. Discussion.....	70
2.4.1. Effects of Aging and N192S on Spatial Working Memory.....	70
2.4.2. Effects of Aging and N192S on Neurogenesis.....	72
2.4.3. Effects of N192S on the CA1 Sector in Aged Rats.....	73
2.5. Conclusions.....	75
3. Study 2: The effects of neonatal cholinergic lesion on the behavioural and neural consequences of chronic cerebral hypoperfusion.....	77
3.1. Introduction.....	77
3.2. Methods.....	79
3.2.1. Animals.....	79
3.2.2. Cholinergic Lesion.....	80
3.2.3. Carotid Artery Occlusion.....	81
3.2.4. Open Field.....	81
3.2.5. Elevated Plus.....	82
3.2.6. Water Maze Testing.....	82
3.2.7. Pupillary Reflex.....	83
3.2.8. BrdU Administration.....	84
3.2.9. Tissue Collection.....	84

3.2.10. Verification of the Cholinergic Lesion.....	85
3.2.11. CA1 Pyramidal Cell Counts.....	86
3.2.12. GFAP Staining and Analysis.....	86
3.2.13. Ki67 Staining and Analysis.....	87
3.2.14. DCX Staining and Analysis.....	88
3.2.15. BrdU Staining and Analysis.....	89
3.2.16. Golgi Analysis.....	90
3.3 Results.....	91
3.3.1. General.....	91
3.3.2. Open Field.....	94
3.3.3. Elevated Plus.....	105
3.3.4. Water Maze.....	105
3.3.4.1. Run 1.....	105
3.3.4.2. Run 2.....	110
3.3.4.3. Run 3.....	117
3.3.4.4. Cued Platform.....	132
3.3.5. CA1 Cell Number.....	132
3.3.6. GFAP Immunoreactivity.....	132
3.3.7. Ki67 Counts.....	132
3.3.8. DCX Counts.....	137
3.3.9. BrdU Counts.....	137
3.3.10. CA1 Pyramidal Cell Morphology.....	137
3.3.10.1. Branch Order Analysis.....	144
3.4 Discussion.....	152
3.4.1. Combined Effects of N192S and 2VO.....	152
3.4.2. Effects of 2VO.....	162
3.4.3. Effects of N192S.....	164
3.5 Conclusions.....	167
4. Study 3: The effects of neonatal cholinergic lesion on hippocampal neurogenesis....	168
4.1. Introduction.....	168
4.2. Methods.....	170
4.2.1. Animals.....	170
4.2.2. Breeding.....	170

4.2.3. Cholinergic Lesion.....	171
4.2.4. Housing.....	172
4.2.5. Behavioural Monitoring.....	172
4.2.6. BrdU Labelling.....	173
4.2.7. Tissue Collection.....	173
4.2.8. Verification of the Cholinergic Lesion.....	173
4.2.9. Quantification of Cell Proliferation.....	175
4.2.10. Quantification of Immature Neurons.....	176
4.2.11. Quantification of Cell Survival.....	177
4.2.12. Determination of Cellular Fate Choice.....	178
4.3. Results.....	179
4.3.1. General.....	179
4.3.2. BrdU Counts – 2 Hour Survival.....	182
4.3.3. Ki-67 Counts.....	182
4.3.4. DCX Counts.....	185
4.3.5. Correlations.....	185
4.3.6. BrdU Counts – 28 Day Survival.....	185
4.3.7. Differentiation.....	190
4.4. Discussion.....	195
4.4.1. Effects of N192S on Neurogenesis.....	195
4.4.2. Combined Effects of N192S and Enrichment on Neurogenesis....	209
4.5. Conclusions.....	210
5. General Discussion and Conclusions.....	212
6. References.....	218
7. Appendix 1.....	246
8. Appendix 2.....	269
9. Appendix 3.....	286

List of Figures

Figure 2.1	Verification of the cholinergic lesion.....	34
Figure 2.2	Swim speed in the water maze.....	37
Figure 2.3	Path length in the water maze.....	39
Figure 2.4	Cued platform water maze.....	42
Figure 2.5	Ki-67+ cells in the dorsal and ventral dentate gyrus.....	45
Figure 2.6	DCX+ cells in the dorsal and ventral dentate gyrus.....	47
Figure 2.7	GFAP immunoreactivity in the hippocampus.....	49
Figure 2.8	APP immunoreactivity in the hippocampus.....	51
Figure 2.9	APP immunoreactivity in the parietal and entorhinal cortex.....	53
Figure 2.10	Number of CA1 pyramidal cells.....	56
Figure 2.11	Apical and basal dendritic complexity of CA1 pyramidal cells.....	58
Figure 2.12	Apical and basal spine analysis of CA1 pyramidal cells.....	60
Figure 2.13	Analysis of apical and basal branch number by branch order.....	63
Figure 2.14	Analysis of apical and basal branch length by branch order.....	65
Figure 2.15	Analysis of apical and basal spines by branch order.....	67
Figure 2.16	Analysis of apical and basal spine density by branch order.....	69
Figure 3.1	Verification of the cholinergic lesion.....	93
Figure 3.2	Distance travelled in the open field.....	96
Figure 3.3	Number of lines crossed in the open field.....	98
Figure 3.4	Distance travelled in the inner squares of the open field.....	100

Figure 3.5	Number of entries into the central area of the open field.....	102
Figure 3.6	Latency to enter the central area of the open field.....	104
Figure 3.7	Elevated plus: number of open and closed arm entries.....	107
Figure 3.8	Exploratory behaviour on the elevated plus maze.....	109
Figure 3.9	Path length in the water maze: run 1.....	112
Figure 3.10	Latency in the water maze: run 1.....	114
Figure 3.11	Swim speed in the water maze: run 1.....	116
Figure 3.12	Path length in the water maze: run 2.....	119
Figure 3.13	Latency in the water maze: run 2.....	121
Figure 3.14	Swim speed in the water maze: run 2.....	123
Figure 3.15	Path length in the water maze: run 3.....	125
Figure 3.16	Latency in the water maze: run 3.....	127
Figure 3.17	Swim speed in the water maze: run 3.....	129
Figure 3.18	Cued platform water maze.....	131
Figure 3.19	CA1 pyramidal cell number.....	134
Figure 3.20	GFAP immunoreactivity in the hippocampus.....	136
Figure 3.21	Ki-67+ cell number in the hippocampus.....	139
Figure 3.22	DCX+ cell number in the hippocampus.....	141
Figure 3.23	BrdU+ cell number in the hippocampus.....	143
Figure 3.24	Representative CA1 cell tracings.....	146
Figure 3.25	Analysis of dendritic complexity in CA1 pyramidal cells.....	148

Figure 3.26	Spine analysis of CA1 pyramidal cells.....	150
Figure 3.27	Analysis of apical and basal branch number by branch order.....	154
Figure 3.28	Analysis of apical and basal branch length by branch order.....	156
Figure 3.29	Analysis of apical and basal spines by branch order.....	158
Figure 3.30	Analysis of apical and basal spine density by branch order.....	160
Figure 4.1	Verification of the cholinergic lesion.....	181
Figure 4.2	BrdU+ cells 2 hours after the final BrdU injection.....	184
Figure 4.3	Ki-67+ cell number.....	187
Figure 4.4	DCX+ cell number.....	189
Figure 4.5	BrdU+ cells 28 days after the final BrdU injection.....	192
Figure 4.6	Percentage of surviving BrdU+ cells.....	194
Figure 4.7	Percentage of BrdU+ cells expressing NeuN, S100B or neither.....	197
Figure 4.8	Total neurogenesis.....	199
Figure 4.9	Total astroglialogenesis.....	201
Figure A1.1	Dorsal and ventral hippocampus.....	248
Figure A1.2	Parietal and entorhinal cortices.....	250
Figure A1.3	Sample cresyl violet staining.....	252
Figure A1.4	Sample BrdU staining.....	254
Figure A1.5	Sample Ki-67 staining.....	256
Figure A1.6	Sample DCX staining.....	258
Figure A1.7	Sample GFAP staining (DAB).....	260

Figure A1.8	Sample GFAP staining (fluorescent).....	262
Figure A1.9	Sample APP staining.....	264
Figure A1.10	Sample BrdU/NeuN and BrdU/S100B staining.....	266
Figure A1.11	Sample Golgi staining.....	268
Figure A2.1	Behaviour monitoring: enrichment, solitary behaviours (set A).....	273
Figure A2.2	Behaviour monitoring: enrichment, solitary behaviours (set B).....	275
Figure A2.3	Behaviour monitoring: enrichment, social behaviours.....	277
Figure A2.4	Behaviour monitoring: enrichment, object-directed behaviours.....	279
Figure A2.5	Behaviour monitoring: standard housing, solitary behaviours (set A)....	281
Figure A2.6	Behaviour monitoring: standard housing, solitary behaviours (set B)....	283
Figure A2.7	Behaviour monitoring: standard housing, social behaviours.....	285

List of Appendices

Appendix 1: Anatomy and sample photomicrographs.....	246
Appendix 2: Supplementary material for study 3.....	269
Appendix 3: ANOVA summary tables.....	286

LIST OF ABBREVIATIONS

192S	192-IgG-saporin
2VO	two vessel occlusion (occlusion of the common carotid arteries)
ACh	acetylcholine
AChE	acetylcholinesterase
AD	Alzheimer's disease
ANOVA	analysis of variance
APP	amyloid precursor protein
BDNF	brain-derived neurotrophic factor
BFCS	basal forebrain cholinergic system
BrdU	5-bromo-2-deoxyuridine
CA	cornu ammonis
CBF	cerebral blood flow
ChAT	choline acetyltransferase
DAB	diaminobenzidine
DAPI	4',6-diamidino-2-phenylindole
DCX	doublecortin
DG	dentate gyrus
EE	environmental enrichment
GCL	granule cell layer
GFAP	glial fibrillary acidic protein
hDB	horizontal limb of the diagonal band of Broca
LTP	long-term potentiation
MCI	mild cognitive impairment
MS	medial septum

N192S	neonatal lesion using 192-IgG-saporin
NB	nucleus basalis complex
NeuN	neuronal nuclei
NGF	nerve growth factor
NS	not significant
p75	low affinity nerve growth factor receptor
PB	phosphate buffer
PBS	phosphate-buffered saline
PCNA	proliferating cell nuclear antigen
PFA	paraformaldehyde
PFC	prefrontal cortex
PND	postnatal day
PSA-NCAM	polysialyated neural cell adhesion molecule
r	Pearson's product-moment correlation coefficient
RAM	radial arm maze
S	standard housing
SGZ	subgranular zone
SVZ	subventricular zone
TUNEL	terminal deoxynucleotidyl transferase dUTP nick end labelling
vDB	vertical limb of the diagonal band of Broca

1. General Introduction

Acetylcholine (ACh) acts as a modulatory neurotransmitter in the brain. Axons arising from the basal forebrain cholinergic system (BFCS) extend diffusely into the neocortex, hippocampus and amygdala, and are in a prime position to influence the activity of these structures and the processes they mediate. Consistent with a key role for the BFCS in modulating cognitive functions mediated by cortical and limbic structures, defective cholinergic transmission has been implicated in both the cognitive decline that occurs during normal aging (Bartus et al., 1982) and the pathological impairments observed in patients suffering from Alzheimer's disease (AD; Bartus et al., 1982; Mesulam 2004). However, attempts at modelling aging- and AD-related cognitive deficits by lesioning the BFCS in rodents have frequently failed to produce robust learning and memory deficits (Baxter et al., 1996; Chappell et al., 1998; Dornan et al., 1996; Fletcher et al., 2007; McMahan et al., 1997; Vuckovich et al., 2004). Rather than ruling out a role for cholinergic dysfunction in the cognitive decline associated with aging or AD, these results might instead suggest the possibility that disruption of the cholinergic system leads to cognitive impairments only when it occurs within a background of other age-related changes (Gallagher and Colombo 1995). Furthermore, it has been postulated that cognitive deficits that emerge with age may be rooted in early dysfunction of the BFCS (Pappas and Sherren 2003; Sarter and Bruno 2004). Cholinergic deficits beginning early in life might affect neural processes throughout the life of an organism, from brain development (affecting the initial structural and functional framework of the brain), to plastic events occurring in the adult brain, to the brain's response to other pathological factors that occur as the brain ages. The three experiments

described in this thesis are based on the premise that lesioning of the BFCS during the early postnatal period in rodents provides a model to explore the effects of cholinergic disruption across the lifespan.

Previous studies have shown that neonatal BFCS lesion alters structural features of the hippocampus and neocortex that are laid down during early postnatal development (Fréchette et al., 2009; Hohmann and Berger-Sweeney 1998; Robertson et al., 1998; Sherren and Pappas 2005). However, very little research has addressed the possibility that neonatal cholinergic lesion might change the way the brain responds to other events, either positive or pathological, across the lifespan. The studies described here examine the interaction between neonatal cholinergic lesion and 1) aging, 2) cerebral hypoperfusion, a common condition associated with aging, AD and cognitive impairment, and 3) environmental enrichment, an experimental paradigm that has been shown to have many beneficial consequences for the brain and cognitive functioning. Throughout these studies, the hippocampus was the focus of interest, owing to its susceptibility to aging-, AD- and enrichment-induced changes, its contributions to cognitive functioning, and the fact that it is heavily innervated by the BFCS. In particular, an emphasis has been placed on the effects of the lesion on hippocampus-dependent spatial working memory, CA1 cell number and dendritic morphology, and hippocampal neurogenesis.

1.1. Organization of the Basal Forebrain Cholinergic System

Much of the brain's cholinergic innervation derives from the BFCS, a network of subcortical nuclei encompassing the medial septum (MS), vertical and horizontal limbs of the diagonal band (vDB and hDB, respectively), and nucleus basalis complex (NB)

(Mesulam et al., 1983). The BFCS represents the major source of cholinergic innervation to the neocortex, hippocampus, amygdala and olfactory bulb, each of which is preferentially innervated by axons arising from distinct nuclei of the BFCS (Mesulam et al., 1983). The cholinergic projection to most neocortical regions originates in the nucleus basalis magnocellularis, with the exception of the retrosplenial and cingulate cortices which are innervated by the septum, and the entorhinal and olfactory cortices which receive projections from the lateral hDB (Eckenstein et al., 1988). Within the hippocampus, cholinergic fibres originating from MS and vDB terminate on pyramidal and granule cells, as well as on inhibitory interneurons (Frotscher and L  r  n  th 1985). Cholinergic fibres terminate in a laminar pattern in the dentate gyrus (DG), with dense acetylcholinesterase (AChE) and choline acetyltransferase (ChAT) staining at the boundary between the granule cell layer (GCL) and the molecular layer (Leranth and Hajszan 2007; Mathisen and Blackstad 1964). Though the density of cholinergic terminals is minimal throughout most of the GCL (Leranth and Hajszan 2007) the subgranular zone (SGZ), which borders the inner GCL, exhibits a higher density of cholinergic fibres (Kaneko et al., 2006). Most of the ChAT-positive boutons within the DG form symmetric synapses on the dendritic shafts of granule cells (Clarke 1985), with only a minor innervation of interneurons (Frotscher and L  r  n  th 1986). In both CA1 and CA3 sectors, cholinergic axons are found at relatively high density in stratum pyramidale and stratum oriens (Aznavour et al., 2002). In CA1, ChAT-immunoreactive axons are also present, but at lower density, in stratum radiatum and stratum lacunosum-moleculare (Aznavour et al., 2002).

1.2. The Basal Forebrain Cholinergic System in Aging and Alzheimer's Disease

Cholinergic dysfunction emerges with aging (Bartus et al., 1982; Terry and Buccafusco 2003), and progressive impairment of the cholinergic system has been proposed as a mechanism to explain cognitive decline in normally aging populations, as well as AD ('The cholinergic hypothesis,' Bartus et al., 1982). AD in particular is characterized by dysfunction of the cholinergic system. Post-mortem analysis of AD brains showed evidence of impaired cholinergic activity in the cortex (reviewed in Auld et al., 2002; Mesulam 2004), including reduced ChAT activity (Bowen et al., 1976; Davies and Maloney 1976), impairments in high affinity choline uptake (the rate-limiting step in ACh synthesis; Rylett et al., 1983), and decreased ACh release (Nilsson et al., 1986). These changes are accompanied by a loss of cholinergic neurons in the NB (Henke and Lang 1983). Furthermore, the expression of both muscarinic and nicotinic ACh receptors is reduced in hippocampus and neocortex of AD brains (Court et al., 2001; London et al., 1989; Mash et al., 1985; Mesulam 2004). Cortical cholinergic denervation is considered to be a hallmark feature of the AD brain (Mesulam 2004) and likely has significant functional relevance, as changes in cholinergic markers have been found to correlate with the severity of dementia (Baskin et al., 1999; Bierer et al., 1995; Mesulam 2004; Minger et al., 2000; Pappas et al., 2000).

1.3 Cholinergic Lesion using 192 IgG Saporin

Early studies aimed at investigating the role of the BFCS in rodents used either electrolytic or excitotoxic lesions, which damage fibres of passage and/or noncholinergic cell types in addition to the intended damage to cholinergic cells in the basal forebrain (Wrenn and Wiley 1998). The development of the immunotoxin 192 IgG-saporin (192S) first allowed researchers to exclusively target BFCS neurons which, in the adult brain, are

distinguished from almost all other cell types by their expression of the low affinity nerve growth factor receptor p75^{NTR}. The toxin consists of a monoclonal antibody to p75^{NTR} coupled to a ribosome-inactivating plant toxin (saporin). After binding to the p75 receptor, the complex is internalized and arrests protein synthesis, leading to cell death (Wiley et al., 1991). Infusion of 192S into the adult brain results in almost complete loss of BFCS neurons, and substantial reductions in cholinergic markers in the BFCS target areas (Heckers et al., 1994; Waite et al., 1994; Wiley et al., 1991). Cholinergic innervation of the amygdala is spared, owing to a lack of p75 receptors on BFCS neurons innervating the amygdala (Heckers et al., 1994).

192S can also be used in neonatal rats. Cells destined to become BFCS neurons are born between embryonic days 12 and 17 in the rat (Semba and Fibiger 1988), migrate within a few days of their birth, and begin to express cholinergic markers shortly thereafter (Armstrong et al., 1987). Cholinergic fibres emanating from the basal forebrain can be detected within the neocortex early in the first postnatal week, and slightly later in the hippocampus (Gould et al., 1991; Koh and Loy 1989). The p75 receptor is expressed on basal forebrain neurons beginning from embryonic day 15 (Yan and Johnson 1988) and continues to be expressed at high levels into adulthood. The toxin is commonly administered by intraventricular infusion on postnatal day (PND) 7 to maximize destruction of cholinergic neurons in the basal forebrain at the time when their projections are reaching the hippocampus and cortex, and when p75 receptor expression is high. PND 7 lesions cause substantial reductions in the number of p75-expressing basal forebrain neurons (in the range of 75-90%) along with large, long lasting reductions (~75%) in ChAT activity in the cortex and hippocampus (Pappas et al., 2000; Sherren

and Pappas 2005; Sherren et al., 1999). In addition, whereas cholinergic innervation recovers after electrolytic lesions performed in the very early postnatal period (Arters et al., 1998), the loss of BFCS neurons observed after 192S lesions performed on PND 7 is still evident in 22-month-old animals (Pappas et al., 2005), and is almost certainly permanent. Noncholinergic, parvalbumin-expressing cells in the basal forebrain show relative (Sherren et al., 1999) or complete (Leanza et al., 1996) sparing after neonatal treatment with 192S (N192S). Early in development additional cell groups, including striatal cholinergic interneurons (Koh and Loy 1989) and cerebellar Purkinje cells (Cohen-Cory et al., 1989; Koh and Higgins 1991; Yan and Johnson 1988), also display p75 expression. However, p75 expression declines rapidly in the striatum over the first few days after birth to nearly nonexistent levels (Koh and Loy 1989), and levels of ChAT activity in the striatum are only slightly reduced after intracerebroventricular infusion of 192S on PND 7 (Sherren and Pappas 2005). Though Purkinje cells maintain moderate levels of p75 expression in the first weeks after birth, they too are preserved after neonatal toxin infusion (Leanza et al., 1996). Thus PND 7 192S infusions produce robust, long-lasting, and relatively selective loss of BFCS neurons.

1.4. Behavioural Effects of Neonatal Cholinergic Lesion

Neonatal BFCS lesions were expected to impair rats' learning and/or memory, especially in light of the effects of the lesion on cortical and hippocampal morphogenesis (discussed later). However, lesioning of the BFCS in the early postnatal period has generally revealed only modest effects on rodent behaviour. For instance, lesioned rats tested during the preweaning period show alterations in exploratory behaviour in the open field (Ricceri et al., 1997; Scattoni et al., 2003; Sherren et al., 1999), hole-board test

(Ricceri et al., 1997) and elevated plus maze (Sherren et al., 1999), as well as deficits in passive avoidance acquisition (Ricceri et al., 1997; Ricceri et al., 2002) but these effects have often been found to be transient, disappearing as rats reach adulthood (Ricceri et al., 1999; Sherren et al., 1999).

Memory functions in adulthood after neonatal cholinergic lesion appear to be surprisingly intact. Delayed spatial alternation is not affected by N192S (Pappas et al., 1996a; Pappas et al., 2000), and performance on the reference memory version of the Morris Water Maze, in which rats must learn to find a submerged platform hidden in the same location on every trial, is consistently unimpaired by the lesion when the rats are tested as adults (Leanza et al., 1996; Pappas et al., 1996a; Pappas et al., 2000; Ricceri et al., 1999; Sherren et al., 1999).

Radial arm maze testing has provided some insight into the behavioural profile of N192S lesioned rats. While Scattoni et al (2006) failed to find an overall effect of the lesion on a 4-arms-baited, 4-arms-unbaited version of the radial arm maze, using a difficult 10-arm maze Pappas et al. (2000) demonstrated an increase in baited arm re-entries (working memory errors) but not unbaited arm entries (reference memory errors) in lesioned rats. Furthermore, a water-based version of the radial arm maze used by Pappas et al. (2005) showed that lesioned rats made more reference and working memory errors during training. Nevertheless, the lesioned rats did improve, and eventually attained control levels of performance. It was noted that both the control rats and the lesioned animals markedly reduced the number of errors committed in the days subsequent to the first error-free trial, which is a typical problem-solving pattern (Pappas et al., 2005). The day on which the first error-free trial was run was simply delayed in the

lesioned group. Thus it has been suggested that cholinergic lesioned rats might suffer from a problem-solving deficit (Pappas et al., 2005; Pappas and Sherren 2003), or show behavioural alterations only when task requirements are complex (Ricceri 2003). Of note, rats subjected to N192S lesion exhibit prominent memory impairments in a standard reference memory water maze task at 22 months of age compared to age-matched controls (Pappas et al., 2005). Taken together, these results suggest that aging might exacerbate cognitive deficits that are present, though subtle, in younger adult animals subjected to neonatal cholinergic lesion (Pappas et al., 2005). Of note in this regard, there is now a consensus that AD begins at least a decade before behavioural symptoms are evident (Preclinical Alzheimer's Disease Workgroup, 2010). Indeed, the fact that individuals suffering from Alzheimer's dementia showed subtle cognitive limitations much earlier in life suggests that dementia may have its origins decades before aging (Riley et al., 2005; Snowden et al., 1996).

Working memory involves maintaining new information in storage in order to use it to guide behaviour (Dudchenko 2004), and is believed to be a central component of a variety of cognitive abilities (de Fockert 2005). In rodent working memory tasks, the animals are required to rapidly acquire new information and then use it within the same session to achieve a goal (often a food reward or access to a safe location). Working memory can be assessed in the water maze using a procedure very similar to the standard reference memory version of the water maze (Morris 1984). In the working memory version the submerged platform is hidden in a new location on each day of testing. On each day the rat is given a discovery trial in which to locate the submerged platform, and memory for the platform location is assessed in subsequent trials, since learning occurs

across trials within a session (Morris 1984; Steele and Morris 1999). This task is hippocampus-dependent, as rats subjected to ibotenic acid-induced complete hippocampal lesions are unable to learn new platform locations (Steele and Morris 1999). Recently, the working memory ability of rats subjected to N192S was assessed and it was found that N192S by itself had no effect on the ability to remember a new platform location (Fréchette et al., 2009). However, since working memory is vulnerable to the effects of aging and AD, it is of interest here to determine whether N192S might render working memory ability more susceptible to the negative effects of aging or age-associated pathological factors such as cerebral hypoperfusion.

1.5. Effects of Neonatal Cholinergic Lesion on Dendritic Morphology

The function of a neuron is reflected in the shape of its dendritic arbour (Kolb et al., 2001). Synaptic contacts are made primarily on the dendrites and spines of pyramidal neurons (Nieuwenhuys 1994; Schade and Baxter 1960), and it is assumed that the length and complexity of the dendrites, as well as the density of spines, reflect the degree of connectivity of the neuron.

The time when cholinergic fibres begin to invade the hippocampus and neocortex coincides with a period of extensive synaptogenesis in the target areas (Crain et al., 1973). Taken together with data indicating that ACh acts as a morphogen *in vitro* (Lauder and Schambra 1999), this suggests that BFCS input might participate in shaping the cytoarchitecture of cells in the hippocampus and neocortex at this critical stage of development (Berger-Sweeney 1998). In accordance with this suggestion, cholinergic lesions during the early postnatal period have been shown to alter dendritic structure in cortical neuron populations. Pyramidal cells in layer V of the medial prefrontal cortex

(Sherren and Pappas 2005), layer II/III of the retrosplenial cortex (Sherren and Pappas 2005), and layer III of the anterior cingulate cortex (Sherren 2003) all show reduced dendritic length in adult rats subjected to PND 7 cholinergic lesions.

Recently, the effect of N192S on hippocampal CA1 pyramidal cells was examined. These neurons generally have a single apical trunk that arises from the soma and passes through stratum radiatum, ending in an apical tuft within stratum lacunosum-moleculare. While traversing stratum radiatum, the apical tree gives off oblique branches, and occasionally bifurcates (Bannister and Larkman 1995). Multiple basal trees emerge from the cell body to ramify in stratum oriens, with most branching occurring proximal to the soma (Bannister and Larkman 1995). In young rats subjected to N192S, the CA1 cells show a reduction in apical branching and spines, particularly on distal branches, as well as a decrease in the length of the basal dendrites (Fréchette et al., 2009) suggesting a reduction in the synaptic connectivity of these cells.

Dendrites retain the capacity to be shaped by changes in both the internal and external environment across the lifespan (Holtmaat and Svoboda 2009; Leuner and Gould 2010). Recent research suggests that the BFCS might modulate ongoing structural plasticity. For example, reorganization of the motor cortex associated with motor skill learning is prevented in animals subjected to BFCS lesions (Conner et al., 2003; Ramanathan et al., 2009). In addition, neonatal electrolytic lesions of the NB in mice (Nishimura et al., 2002) and 192S lesions of the BFCS in rats (Zhu and Waite 1998) have been shown to impair the structural plasticity of the barrel cortex in response to whisker follicle removal. Two of the studies described herein were designed to assess the impact

of N192S on dendritic remodelling of CA1 pyramidal cells after chronic cerebral hypoperfusion, as well as its effect on age-related changes in dendritic structure.

1.6. Adult Neurogenesis

The adult brain was once considered to be a stable structure, having lost the capacity to generate new neurons. Altman and colleagues challenged this view in a series of papers published in the 1960s by demonstrating that tritiated thymidine, which is incorporated into newly synthesized DNA during cell division, could be detected in neuron-like cells in restricted regions of the brain after administration to adult rats (Altman and Das 1965; Altman 1969). The existence and significance of adult-born neurons were later supported by studies showing that cells born in the adult brain were capable of surviving for long periods of time (Kaplan and Hinds 1977), receiving synaptic input (Kaplan and Bell 1983), and projecting axons to target cells (Stanfield and Trice 1988). The development of 5-bromo-2-deoxyuridine (BrdU), a thymidine analog capable of incorporation into DNA, and which can be detected immunohistochemically in the brain, has greatly facilitated research in this area. It is now generally accepted that neurogenesis, the production of neurons from progenitor cells, continues in two regions of the adult brain: the subventricular zone (SVZ) and the SGZ of the DG (Gould 2007). The SVZ lies along the lateral wall of the lateral ventricles, and cells born in this region migrate through the rostral migratory stream to the olfactory bulb, where they become mature granule cells or periglomerular interneurons. The SGZ is located along the hilar border of the DG GCL and produces neurons that migrate into the GCL to become mature granule cells (Gould 2007).

Adult neurogenesis proceeds in stages akin to those occurring during the initial

development of the brain, and involves proliferation, differentiation, migration, maturation and integration of newborn neurons (Christie and Cameron 2006). Neural progenitor cells undergo mitosis to produce newborn daughter cells, some of which then begin to exhibit neuronal features, migrate into existing cell layers, and become functionally integrated into the neural circuitry, eventually behaving as mature neurons. In the DG, neurons develop in a series of stages defined both by their morphology and by the expression of endogenous stage-specific markers.

The primary progenitor cells in the SGZ are believed to be cells with characteristics of radial astrocytes (Doetsch 2003; Filippov et al., 2003; Garcia et al., 2004; Seri et al., 2001; Seri et al., 2004). These cells, which express nestin as well as astrocytic markers including glial fibrillary acidic protein (GFAP), and vimentin, sit at the border of the GCL and hilus, and extend a long apical process through the GCL into the molecular layer of the DG (Kempermann et al., 2004; Kronenberg et al., 2003; Seri et al., 2004). The process of neurogenesis begins with the asymmetrical division of progenitor cells to regenerate one radial astrocyte-type cell, and another daughter cell that forms part of the transiently amplifying, highly proliferative cell population. The transiently amplifying cells express nestin but not astrocytic markers, and divide symmetrically to produce post-mitotic lineage-specific cells that will eventually become neurons (Seri et al., 2004). As these cells differentiate along a neuronal lineage, they begin to express doublecortin (DCX), a microtubule associated protein (Gleeson et al., 1999; Kronenberg et al., 2003) and lose nestin expression (Kempermann et al., 2004). Finally, adult-born neurons express markers of mature granule cells, including the proteins neuronal nuclei (NeuN) and calbindin (Kempermann et al., 2004).

The progression of cells from unspecified proliferative cells to mature granule cells is accompanied by the death of a subset of the newly born cells. Under normal conditions, approximately half of the newly generated cells do not survive the first month (Dayer et al., 2003). Of the newly generated cells remaining at 4 weeks after their birth, approximately 85% express neuronal markers (Christie and Cameron 2006), and new neurons that survive the first month are capable of surviving for very long periods (Kempermann et al., 2003). It has been estimated that nearly 9000 cells are born in the DG of the male rat daily (Cameron and McKay 2001). Thus, even after accounting for the substantial cell death that occurs in the first month after birth, and the fact that not all newborn cells become neurons, it appears that neurogenesis in the adult DG can significantly add to the total size of the granule cell population (Cameron and McKay 2001).

Adult-generated neurons develop morphological features of mature granule cells. Immature granule cells have simple apical and basal dendrites (Schmidt-Hieber et al., 2004), and as they mature, the dendrites grow and increase in complexity (van Praag et al., 2002) and the cell extends a long axon from the GCL to CA3 (Hastings and Gould 1999; Markakis and Gage 1999; Stanfield and Trice 1988). Furthermore, evidence is accumulating that adult-born neurons display functional characteristics of mature granule cells and are functionally integrated into the circuitry of the hippocampus (Jessberger and Kempermann 2003; Schmidt-Hieber et al., 2004; Song et al., 2002; van Praag et al., 2002; Wang et al., 2000). However, in comparison to mature granule cells, newborn neurons exhibit increased likelihood of action potential generation when stimulated by a low intensity stimulus (Schmidt-Hieber et al., 2004) and have a lower threshold for the

induction of long term potentiation (LTP) (Schmidt-Hieber et al., 2004; Wang et al., 2000). These findings suggest that adult-born neurons may make a unique contribution to hippocampal functioning (Gould et al., 1999; Kempermann 2002; Ming and Song 2005; Shors 2004). Accordingly, adult-born granule neurons appear to be preferentially recruited into circuits supporting the acquisition and expression of spatial memory (Kee et al., 2007; Ramirez-Amaya et al., 2006), and furthermore, behavioural studies suggest that neurogenesis may in fact be necessary for some types of learning and memory. Reducing the number of newly generated neurons in the hippocampus by treatment with the antiproliferative agent methylazoxymethanol acetate impairs trace eyeblink conditioning (Shors et al., 2001) and trace fear conditioning (Shors et al., 2002). Irradiation, which also reduces cell proliferation, has been shown to impair spatial memory in the Barnes maze (Raber et al., 2004), long-term spatial memory in the water maze (Snyder et al., 2005), contextual but not cued fear conditioning (Saxe et al., 2006; Winocur et al., 2006), and memory for a delayed non-matching to sample task (Winocur et al., 2006). Thus adult neurogenesis appears to have functional relevance for at least some cognitive processes.

Neurogenesis can be regulated at many of the distinct stages that comprise the overall process. In particular, the rate of proliferation and the degree to which the population of new cells undergoes neuronal fate specification are modifiable. In addition, the large proportion of cells that die within their first month of life under standard conditions provides a significant window for increasing neurogenesis by enhancing the survival of cells that would otherwise perish. The rate at which adult neurogenesis occurs is subject to regulation by a number of factors, including hormonal, pharmacological,

behavioural, environmental and genetic variables.

1.7. Cholinergic Involvement in the Regulation of Neurogenesis

The DG receives dense cholinergic input from the BFCS (Aznavour et al., 2002) and newborn neurons in the DG express both muscarinic and nicotinic ACh receptor subunits (Kaneko et al., 2006). It might be expected, therefore, that cholinergic input could have some influence on neurogenesis. In fact, evidence for cholinergic involvement in the regulation of neurogenesis is beginning to accumulate. In vitro, proliferation of neural stem and progenitor cells obtained from the embryonic cortex of the rat is enhanced by the action of ACh on muscarinic receptors (Ma et al., 2000). In vivo, manipulations that remove the cholinergic input to the hippocampus negatively impact adult hippocampal neurogenesis. For example, van der Borght and colleagues (2005) examined the effects of MS lesions on proliferation and newborn cell survival, and found that lesioning the MS, which is the major source of cholinergic input to the hippocampus, substantially decreased the survival of newly generated DG cells (Van der Borght et al., 2005). Fimbria/fornix axotomy also decreased the number of BrdU-labelled cells in the GCL (Fontana et al., 2006). However, neither of these manipulations selectively removes cholinergic input to the hippocampus, and the results may have been caused by destruction of other cell types.

A handful of studies have examined the rate of neurogenesis after selective lesions of the BFCS in adult rats, and all have found neurogenesis to be decreased in these animals (Aztiria et al., 2007; Cooper-Kuhn et al., 2004; Mohapel et al., 2005). However, the authors of these studies reached differing conclusions regarding the particular stage of neurogenesis that was affected by the lesion. Cooper-Kuhn, Winkler

and Kuhn (2004) injected BrdU on days 3, 5 and 7 after 192S infusion, and examined the number and phenotype of BrdU-positive cells in the DG 28 days later. While the total number of BrdU⁺ cells was unaffected, the lesion had the effect of decreasing the number of newly generated cells that expressed markers of mature neurons, and increased the number of dying cells. The authors suggest that the loss of cholinergic input reduces the viability of the newborn neurons, and therefore interpret these data as an indication that ACh has a selective survival-promoting effect on neurons (Cooper-Kuhn et al., 2004). In contrast, Mohapel and colleagues (2005) found that adult cholinergic lesion had a more pronounced effect on cell proliferation than on newborn cell survival. Aztiria et al (2007) administered BrdU to cholinergically lesioned rats for 14 days, and found a severe reduction in labelled cells shortly after the last BrdU injection. Unfortunately, the repeated injection of BrdU over several days makes it impossible to dissociate the effects of the lesion on proliferation and survival. Overall, the evidence is very suggestive of a modulatory role of the cholinergic system on hippocampal neurogenesis, but a more detailed investigation of this phenomenon is required to determine which stages of neurogenesis are under cholinergic control.

A recent study in our laboratory found that neonatal lesion of the forebrain cholinergic system in rats reduced the number of cells expressing DCX, a marker for immature neurons, in the DG (Fréchette et al., 2009). Furthermore, the results suggested that lesioned rats were non-responsive to the effect of enrichment on neurogenesis. However, the design of the study did not allow a detailed examination of the precise effects of the cholinergic lesion on neurogenesis in that the impact of cholinergic denervation on proliferation, differentiation, and cell survival could not be distinguished.

Experiment 3 of this thesis was designed to examine these issues.

1.8. Research Plan

The finding that cognitive impairments emerge with age in rats subjected to neonatal cholinergic lesion (Pappas et al., 2005) suggests that cholinergic lesion interacts with the aging process. It is expected that this interaction would also be evident in terms of neural changes. While it is known that young adult rats show altered cortical and hippocampal cytoarchitecture and impaired neurogenesis after neonatal cholinergic lesion, there is currently no data on cytoarchitecture or neurogenesis in aged lesioned rats. Experiment 1 therefore examined spatial working memory and neurogenesis in 12-month-old (middle-aged) and 21month-old (aged) lesioned and control rats. In addition, CA1 cell counts and dendritic structure were analyzed in aged rats after neonatal cholinergic lesion.

Experiment 2 did not involve aged rats; however, it combined an age-related neuropathological factor, chronic cerebral hypoperfusion, with neonatal cholinergic lesion. The rationale underlying this is that chronic reduction of cerebral blood flow represents a significant risk factor for AD (de la Torre 2002) and the combination of cholinergic dysfunction and cerebral hypoperfusion may be particularly damaging. This experiment investigated the impact of pre-existing cholinergic lesion on the behavioural and neural consequences of chronic cerebral hypoperfusion induced by permanent occlusion of the carotid arteries.

Experiment 3, as outlined earlier, involved a detailed analysis of the effects of neonatal cholinergic lesion on neurogenesis and neurogenic responsiveness to environmental enrichment. This experiment, while not obviously connected to the theme

of the first two, was initiated because of the aforementioned findings by our laboratory that N192S affected neurogenesis. These findings occurred while experiments 1 and 2 were underway and were deemed sufficiently provocative and important to warrant our immediate followup.

2. Study #1: The Effects of Neonatal Cholinergic Lesion on Age-Related Neural and Behavioural Changes

2.1. Introduction

The purpose of the present study was to determine whether the effects of N192S on spatial working memory, neurogenesis and dendritic morphology of CA1 pyramidal cells are more severe in aged (21-month-old) compared to middle-aged (12-month-old) rats. We hypothesized that N192S and aging would interact to cause a working memory impairment, which would be accompanied by more drastic dendritic alterations and reductions in neurogenesis than those that have been documented in the young adult animal after neonatal cholinergic lesion.

Across a number of cognitive domains, aging is associated with a decline in function (Drag and Bieliauskas 2010; Grady and Craik 2000; Zec 1995). Aging is also a major risk factor for the development of AD (Lindsay et al., 2002). Working memory in particular has consistently been shown to decline with age, in both humans (Belleville et al., 1996; Dobbs and Rule 1989; Foos and Wright 1992; Salthouse et al., 1991; Wingfield et al., 1988) and rodents (Frick et al., 1995; Means and Kennard 1991; Sabolek et al., 2004; Shukitt-Hale et al., 1998; Veng et al., 2003), and to be impaired in patients suffering from mild cognitive impairment (Saunders and Summers 2010) or AD (Belleville et al., 2003; Carlesimo et al., 1998; Kensinger et al., 2003; Stopford et al., 2007; Vecchi et al., 1998; Waters and Caplan 2002). It is thought that a wide range of cognitive functions rely on working memory, and that impaired working memory might

be a core deficit underlying several aging- and AD-related cognitive impairments (de Fockert 2005; Germano and Kinsella 2005; White and Ruske 2002).

Hippocampal ACh levels are increased in rats while performing a working memory task (Fadda et al., 1996), and activation of the septohippocampal and nucleus basalis-cortical cholinergic pathways may be particularly associated with retaining information over an interval during working memory tasks (Durkin and Toumane 1992; Durkin 1994). Evidence from both rodents and humans suggests that changes in the cholinergic system may contribute to age-related impairments in working memory (Duzel et al., 2010; Ikegami 1994). Furthermore, in humans afflicted with AD the number of p75-expressing nucleus basalis cholinergic neurons (Mufson et al., 2002) and the level of cholinesterase activity (Bohnen et al., 2005) were both found to correlate with working memory performance, further supporting a role for the BFCS in working memory. Surprisingly, a number of studies have found working memory performance to be spared or only mildly affected following cholinergic lesions in the adult rodent (Chappell et al., 1998; Connor et al., 1992; McMahan et al., 1997; Paban et al., 2005; Vuckovich et al., 2004), calling into question the importance of the BFCS in age- or AD- related working memory impairments.

However, Sarter and Bruno (1998) have advocated for the use of aging as an intervening variable when studying the effects of basal forebrain cholinergic lesions. Aging is associated with a host of neural changes (Caserta et al., 2009; Lister and Barnes 2009; Yankner et al., 2008), and it is possible that cholinergic manipulation might result in substantial cognitive impairments only when it occurs within a background of these other age-related changes (Gallagher and Colombo 1995). Accordingly, interactions between adult cholinergic lesions and aging have been demonstrated on the radial arm

maze (Wellman and Pelley 1999), sustained attention task (Burk et al., 2002), stimulus discriminability (Stoehr et al., 1997) and reference memory version of the water maze (Bannon et al., 1996), with age-related impairments on these tasks being more severe in lesioned animals. Only a single study has evaluated the effects of aging on the cognitive abilities of rats subjected to neonatal cholinergic lesion, and similar to the adult lesion studies it found that reference memory deficits emerged with aging in lesioned rats (Pappas et al., 2005; Pappas et al., 2000). The age-dependency of other cognitive abilities, including working memory, in N192S rats has never been investigated.

The rate of adult hippocampal neurogenesis declines precipitously with age (Bizon and Gallagher 2003; Klempin and Kempermann 2007; Kuhn et al., 1996; Olariu et al., 2007b; Rao et al., 2006b), mainly as a result of a reduction in the number and/or rate of division of progenitor cells (Olariu et al., 2007a; Rao et al., 2006a; Walter et al., 2010). Reductions in neurogenesis have been proposed to contribute to age-related cognitive decline (Drapeau et al., 2007). In fact, among aged subjects, those with preserved memory function exhibit higher levels of neurogenesis than their cognitively impaired counterparts (Drapeau et al., 2003). While it is known that neurogenesis is disrupted by adult (Cooper-Kuhn et al., 2004; Mohapel et al., 2005) and neonatal (Fréchette et al., 2009) cholinergic lesions, the interactive effects of cholinergic lesions and aging are as yet unexplored.

Aging is associated with changes in the dendritic morphology of cortical and hippocampal pyramidal neurons. The majority of studies report that cortical pyramidal neurons undergo progressive dendritic regression with age in both humans and rodents (Brabander et al., 1998; Dickstein et al., 2007; Nakamura et al., 1985; Scheibel et al., 1975; Wang et al., 2009). With respect to hippocampal CA1 cells, whereas no change in

dendritic complexity was detected in aged human tissue (Hanks and Flood 1991), both an increase (Pyapali and Turner 1996) and a decrease (Markham et al., 2005; Lolova, 1989) in dendritic branching with age has been observed in rats. CA1 pyramidal cells are sensitive to the effects of N192S, showing decreased apical branching and basal branch length, and a reduction in the number of apical spines compared to sham lesioned controls (Fréchette et al., 2009). Experiment 1 followed up on this earlier study by examining the dendritic morphology of CA1 cells in aged N192S rats. It was expected that age would augment the changes previously seen in younger 192S rats.

2.2. Methods

2.2.1. Animals

All rats were housed throughout the experiment under a reversed light cycle with free access to standard rat chow and water. On PND 7, rat pups underwent stereotaxic surgery to infuse either the immunotoxin 192S or a vehicle solution into the lateral ventricles (see below). The pups were weaned on PND 21-23, and pair-housed until it was determined that the rats were too large to share a cage, at which point each rat was single-housed with a small amount of paper nesting material. The rats were assigned to a survival time of 12 or 21 months of age. Within each age group, some of the rats underwent behavioural testing in the working memory version of the Morris Water Maze, and the remaining rats were used to assess neurogenesis and CA1 pyramidal cell morphology. All care and handling of the animals followed established guidelines of the Canadian Council on Animal Care, and the experiment was approved by the Carleton University Animal Care Committee.

2.2.2. Breeding

Four male and eight female Sprague-Dawley rats (Harlan, Indianapolis, IN) were used as breeders. After a one-week acclimation period, the rats were housed in groups of three (one male with two females). The females were inspected daily and were removed from the cage and single-housed when they began to show obvious indications of pregnancy. The females were monitored daily until the pups were born. The day of birth was designated as PND 0. On PND 3 or PND 4, the litters were culled to a maximum of 10 pups. Though only males were used in this study, sufficient females were kept in order to maintain a minimum litter size of 8 whenever possible. The pups were subjected to stereotaxic surgery on PND 7 (see below) and weaned on PND 21-23. Each breeder was used to produce at least two litters. The females were given a minimum of one week of rest after weaning before being paired with another male.

2.2.3. Cholinergic Lesion

On PND7, the pups underwent stereotaxic surgery to infuse either 192S (Advanced Targeting Systems, San Diego, CA), or vehicle (10mM pH 7.2 phosphate-buffered saline (PBS)) into the lateral ventricles. Pups were removed from the home cage 4 at a time and brought to the surgical suite, where they were placed on a heating pad. Each pup was anaesthetized using 4% isoflurane/oxygen, then placed in a plaster mould mounted on a stereotaxic frame. The pups were maintained on 1.5-2% isoflurane for the duration of the surgery. One ear was punched for rat identification. A dorsal midline incision was made in the scalp and tissue overlying the skull was blunt deflected. Two holes were drilled in the skull at +/- 1.8 mm lateral to Bregma. A needle attached to a 5 μ l

syringe (Hamilton, Reno, NV) was lowered to a depth of 3.5 mm ventral to the dura, aimed at the lateral ventricles. 1.5 μ l of 0.2 μ g/ μ l 192S was infused into each ventricle (300 ng per ventricle) over 2 minutes. The needle was left in place for a further 2 minutes to allow the solution to diffuse away from the injection site, then slowly retracted to prevent the toxin from being drawn back up into the needle. The incision was closed using tissue adhesive (Vetbond, 3M, London, ON), and the pup was placed with its littermates on a heating pad. When all pups had regained consciousness, they were placed back in the home cage. Approximately half of the rats in each litter were assigned to each treatment group, such that group assignments were balanced as evenly as possible across litters.

2.2.4. Water Maze Testing

At the age of 12 or 21 months, approximately half of the rats in each treatment group were tested in the working memory version of the water maze. Rats tested in the water maze were given 5 daily trials for 5 consecutive days on a hidden platform task in which the platform location was changed daily, but remained in a constant position within each daily session. On each daily trial, the rat was placed on one of 8 submersible platforms around the perimeter of the pool. The platform was then lowered, forcing the rat to search for the hidden platform, which was submerged 2cm below the surface of the water. If the rat failed to find the platform within 90 seconds, it was gently guided to the platform by the experimenter. The rat was allowed to remain on the platform for 30 seconds before being placed on a new starting platform. The swim paths were recorded by an overhead camera connected to a computer running SMART tracking software (San Diego Instruments, San Diego, CA). The latency to find the platform as well as the

distance traveled and the average swim speed were recorded for each trial. The 21 month old rats were additionally tested on a cued platform version of the maze following the fifth day of working memory training. The platform was moved to a novel location and a yellow plastic container was hung 12 inches above the platform. Each rat was given 5 trials of 90 second duration to swim to the cued platform. If the rat did not find the platform, it was guided to the platform by the experimenter. The rats were allowed to sit on the platform for 30 seconds before being moved to a new start location for the next trial. The total path length, latency and swim speed to find the platform were recorded using an overhead camera coupled to the SMART tracking system.

2.2.5. Tissue Collection

Within 2-4 days of completing water maze testing, all rats (including non-tested rats) were sacrificed by sodium pentobarbital overdose, and were transcardially perfused with 100ml of 0.9% saline. The 12 month old rats were additionally perfused with 400ml of 4% paraformaldehyde (PFA) in phosphate buffer (PB), and their brains were removed and stored in PFA overnight. The 21 month old rats were not perfused with PFA. Instead, their brains were removed without fixative, taking care not to touch the brain with metal instruments. The brains were bisected using a glass coverslip. The right hemispheres were placed in Golgi fix (0.01% mercuric chloride, 0.01% potassium dichromate and 0.008% potassium chromate in distilled water; Glaser and Van der Loos 1981). The left hemispheres were drop-fixed in 4% PFA overnight. The following day, the brains stored in PFA were rinsed in PB several times over the next 24 hours. The brains were then processed through graded sucrose concentrations (10%, 20% and 30% sucrose in PB with azide). After at least 2 days in 30% sucrose, the brains were sliced in

the coronal orientation on a cryostat at a thickness of 40 μ m. The sections were stored in PB with azide (for immediate staining) or were transferred into cryoprotectant for long-term storage at -20°C.

2.2.6. Verification of the Cholinergic Lesion

AChE staining and p75^{NTR} immunohistochemistry were used to confirm the cholinergic lesion. For AChE, four sections spanning the hippocampus were stained. Briefly, floated sections were rinsed in 0.1M sodium acetate, then incubated overnight in a reaction solution of 0.68% sodium acetate, 0.1% cupric sulfate, 0.12% glycine and 0.1% acetylthiocholine iodide in distilled water, pH 5.0. The next day the sections were rinsed in sodium acetate, then developed in 1% sodium sulphide, pH 7.5 for 10 minutes. After rinsing in sodium acetate, the sections were washed in distilled water, mounted, air dried overnight, then dehydrated, cleared and coverslipped. The sections were visually inspected using an Olympus BX-51 microscope with a 10x objective lens.

Sections containing the vDB, hDB, and MS were immunohistochemically stained to detect p75^{NTR}, the low affinity nerve growth factor receptor which is targeted by 192S. Briefly, floated sections were rinsed in PBS and incubated overnight at room temperature in a dilution solution containing mouse anti-NGF receptor antibody (1:2000; Chemicon, Billerica, MA), 0.3% lambda carrageenan, 0.3% bovine serum albumin and 0.3% triton x-100 in PBS. The sections were then incubated for 2 hours at room temperature in biotinylated sheep anti-mouse immunoglobulin (1:100; GE Healthcare, Oakville, ON), followed by a 2 hour incubation in streptavidin biotinylated horseradish peroxidase complex (1:100; GE Healthcare). In order to visualize the antibody complex, the sections

were reacted in 0.02% 3,3-diaminobenzidine (DAB), 0.6% ammonium nickel sulphate and 0.01% hydrogen peroxide in 50mM Tris buffer, pH 7.4, then rinsed in PBS, mounted, and air-dried overnight. After counterstaining with 0.085% pyronin Y in acetate buffer, the sections were dehydrated, cleared and coverslipped. The number of cells in the MS/vDB and hDB that stained positive for p75 was counted manually using a BX-51 microscope (Olympus) at 20x magnification. Any rat that suffered less than a 60% reduction in the number of p75⁺ cells compared to the average of the control group was excluded from further analyses. Since we have found that loss of p75⁺ cells and reductions in AChE staining in the hippocampus as determined by densitometry are in very good agreement (see Study #3 and Frechette et al., 2009), the cholinesterase-stained sections were used to visually confirm the lesion here. Densitometry was not performed in this experiment.

2.2.7. Ki-67 Staining and Analysis

Every 8th section through the hippocampus was immunohistochemically stained to detect the cell cycle marker Ki-67. Floated sections were rinsed three times in PBS with azide, then blocked in 0.3% hydrogen peroxide in PBS. After a further three rinses in PBS, the sections were incubated overnight at 4°C in a solution containing mouse anti-Ki-67 antibody (1:500; Dako, Mississauga, ON) diluted in 0.3% lambda carrageenan, 0.3% bovine serum albumin and 0.3% triton x-100 in PBS. On the following day the sections were incubated first in sheep anti-mouse antibody (1:100; GE Healthcare) for 2 hours at room temperature, then in streptavidin biotinylated horseradish peroxidase complex (1:100; GE Healthcare). After a 2-hour incubation, the antibody complex was visualized using a DAB reaction as described above. The sections were counterstained in

pyronin Y, then dehydrated, cleared and coverslipped. Ki-67-expressing cells in the dorsal and ventral DG GCL and SGZ were counted manually using an Olympus BX-51 microscope with a 100x oil objective lens. The SGZ was defined as a three-cell-diameter thick region lying between the GCL and the hilus of the DG. The dorsal and ventral hippocampus were considered separately (see Figure A1.1 in Appendix 1), as it has been noted that some treatments preferentially affect dorsal or ventral hippocampal neurogenesis (Banar et al., 2006). A photomicrograph showing sample Ki-67 staining is included in Appendix 1 (Figure A1.5).

2.2.8. DCX Staining and Analysis

DCX expression was immunohistochemically detected in every 8th section through the entire hippocampus. Briefly, floated sections were rinsed in PBS, blocked in 0.3% hydrogen peroxide, blocked in 3% normal horse serum, then incubated in primary goat anti-DCX antibody (1:250; Santa Cruz Biotechnology, Santa Cruz, CA) overnight at room temperature. The sections were then incubated for 2 hours in biotinylated horse anti-goat antibody (1:100; Vector Laboratories, Burlingame, CA) followed by a 2-hour incubation in streptavidin-biotinylated horseradish peroxidase complex (1:100; GE Healthcare). The antibody complex was visualized using a DAB reaction as described above. After counterstaining in pyronin Y, the sections were dehydrated, cleared and coverslipped. DCX-expressing cells in the dorsal and ventral DG were counted manually using an Olympus BX-51 microscope with a 40x objective lens. Appendix 1 contains a photomicrograph showing DCX staining in the hippocampus (Figure A1.6).

2.2.9. GFAP Staining and Analysis

Three sections containing the hippocampus from each brain in the 21-month-old groups were immunofluorescently stained to detect the expression of GFAP. Floated sections were rinsed in PBS, then incubated in a blocking solution containing 0.3% bovine serum albumin, 0.3% lambda carrageenan and 0.3% triton-x 100 in PBS for 30 minutes. After a PBS rinse, the sections were incubated in mouse anti-GFAP antibody (1:1000; Sigma, Oakville, ON) in 0.3% Triton X-100 in PBS with azide overnight at 4°C. The following day the sections were rinsed in PBS, then incubated for one hour in goat anti-mouse Alexa 555 (1:500; Invitrogen, Burlington, ON). The sections were then rinsed three times in PBS, mounted onto gelatin-dipped slides, and coverslipped immediately with anti-fade mounting medium containing 4',6-diamidino-2-phenylindole (DAPI; Prolong Gold; Invitrogen). From each section, three images of the DG, three of the CA1 sector, three of the CA3 sector, and one of the hilus were acquired using StereoInvestigator software (MBF Biosciences) and a 40x objective. The images were loaded into Image J software (National Institutes of Health, Bethesda, MD) and a thresholding function was used to determine the percent area showing positive staining. Sample GFAP staining is shown in Appendix 1, Figure A1.8.

2.2.10. Amyloid Precursor Protein Staining and Analysis

Five sections containing the dorsal hippocampus, five sections containing parietal cortex (corresponding to primary sensory cortex, barrel field from Paxinos and Watson 1998) and four sections containing lateral entorhinal cortex from each brain were immunohistochemically stained to detect amyloid precursor protein (APP). Figure A1.2 in Appendix 1 shows the cortical areas chosen for analysis. Floated sections were rinsed three times in PBS with azide, then incubated for 30 minutes in a 10% formic acid

solution (diluted in PBS). After a further three rinses, the sections were placed in 3% hydrogen peroxide for 30 minutes, followed by another three PBS rinses. The sections were incubated overnight at room temperature in a solution containing anti-APP (1:1000; Millipore MAB348) diluted in 0.3% lambda carrageenan, 0.3% bovine serum albumin and 0.3% triton x-100 in PBS. On the following day, the sections were incubated first in secondary anti-mouse antibody (1:100; GE Healthcare) for 2 hours, then in streptavidin-biotinylated horseradish peroxidase complex (1:100; GE Healthcare) for a further 2 hours, after which a DAB reaction was performed to visualize the antibody complex. The sections were mounted onto gel-coated slides, air-dried overnight, then dehydrated, cleared and coverslipped. The percent area that was positively immunostained was calculated in two images of the CA1 region, two images of the CA3 region, two images of the DG and one image of the hilus from each of the five hippocampal sections using Image J, and averaged across all five sections to obtain a single score for each hippocampal region for each animal. The images were acquired using the 40x objective lens of an Olympus BX-51 microscope. For the parietal and entorhinal cortices, images of layers I-IV and layers V-VI were acquired and analyzed separately, using a 20x objective lens.

2.2.11. CA1 Pyramidal Cell Counts

Every 8th section through the entire hippocampus was stained using cresyl violet. The sections were mounted on gel-dipped slides, then dehydrated in graded ethanols. After a short incubation in clearane, the sections were rehydrated in graded ethanol solutions, then stained in 1% cresyl violet for 20 seconds. The sections were rinsed, then placed in differentiator for 3 minutes. The sections were then dehydrated, cleared and

coverslipped. CA1 pyramidal cells were counted in the dorsal and ventral hippocampus using the optical fractionator feature of StereoInvestigator software (MBF Biosciences, Williston, VT) and an Olympus BX-51 microscope with a 100x objective lens. Cells were counted within an 18 μ m x 18 μ m x 10 μ m counting frame, and the grid size was set at 85 μ m x 85 μ m. These counting parameters yielded approximately 625 sampling sites in the dorsal CA1 and 200 sampling sites in the ventral CA1. Sample cresyl violet staining is shown in Figure A1.3 of Appendix 1.

2.2.12. Golgi Analysis

The right hemisphere of each brain was left in Golgi solution for 14 days, then rinsed three times in distilled water, once for four hours, once for three hours, and the third time overnight. The brains were transferred to a 10% sucrose solution for 8 hours, then into a 20% sucrose solution overnight. The next day they were transferred to 30% sucrose for storage. After a minimum of 4 days in 30% sucrose, the brains were sliced on a vibratome (World Precision Instruments) at a thickness of 200 μ m, and mounted immediately on 2% gelatin-dipped slides. The sections were stored in a humidifying plastic box for up to five days, then stained. After a brief wash in distilled water, the sections were placed in ammonium hydroxide for 40 minutes, washed in distilled water, then incubated in diluted film fix (Kodak, Toronto, ON) for 40 minutes. The sections were then washed twice in distilled water, dehydrated in ethanol, cleared, and coverslipped with Permount (Fisher, Ottawa, ON).

The cell bodies and entire apical and basal dendritic fields of CA1 pyramidal cells from the dorsal hippocampus of five randomly chosen rats per group were traced using

NeuroLucida software (MBF Biosciences) and an Olympus BX-51 microscope with a 100x oil objective. Cells within the middle third of the tissue section were chosen, and only cells with the entire dendritic structure contained within the three-dimensional space of a single section were traced. Additionally, only cells whose dendrites could clearly be distinguished from those of neighbouring cells were chosen. In total, 10 cells from each brain were traced. NeuroLucida Explorer (MBF Biosciences) was used to obtain data on total dendritic length, dendritic branching and total number of spines and spine density. Sample golgi staining is shown in Figure A1.11 of Appendix 1.

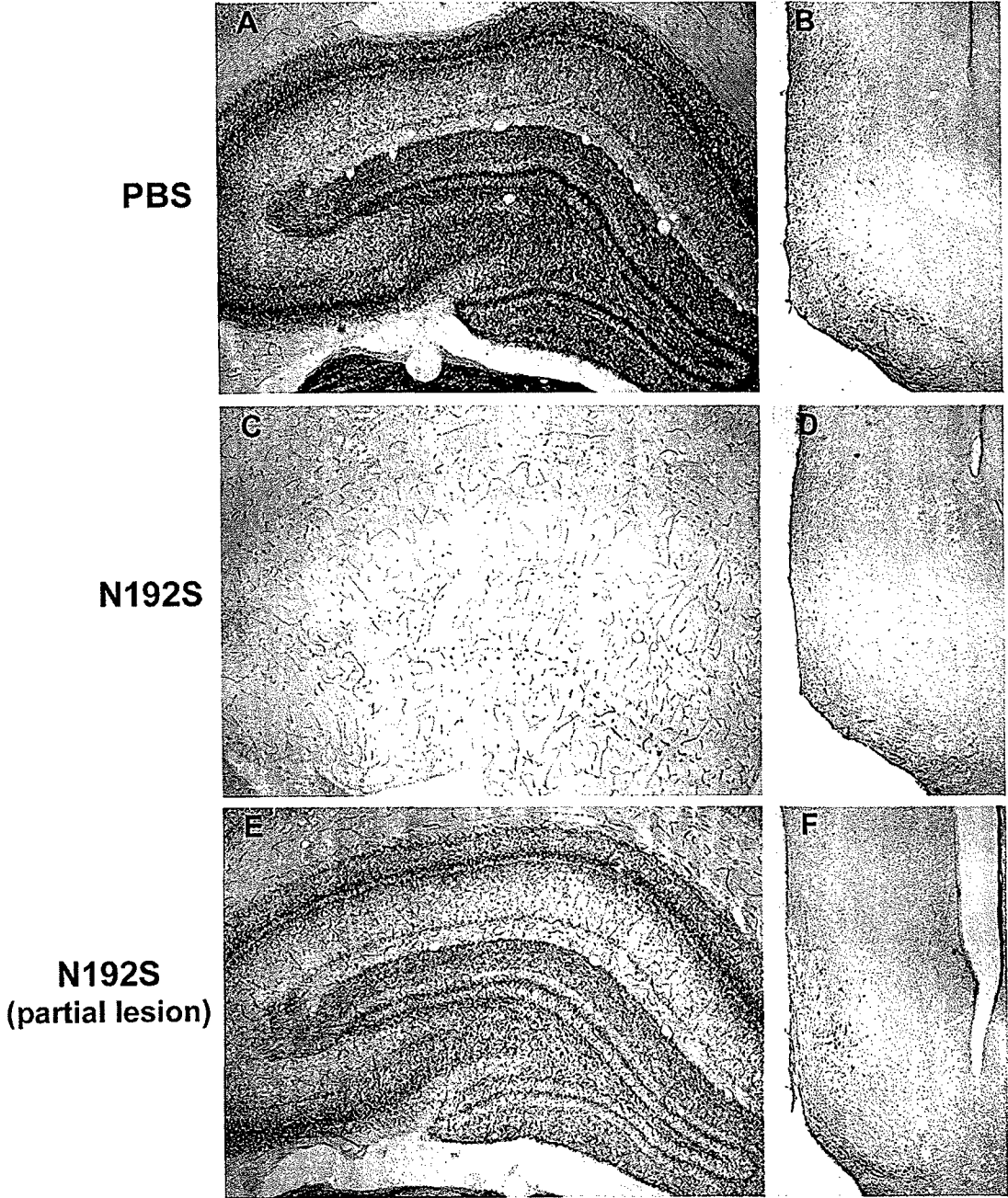
2.3. Results

2.3.1. General

In the MS and vDB, N192S reduced the number of p75⁺ cells to ~13% of controls ($F_{1,54}=130.7$, $p<.001$), while the number of cells in the hDB was reduced to ~21% of controls ($F_{1,54}=196.7$, $p<.001$). In addition, AChE staining in the hippocampus was substantially reduced by the toxin. Rats that did not show extensive reductions in p75⁺ cells in the basal forebrain or loss of AChE staining in the hippocampus were excluded from further analyses and their behavioural data were discarded. The final numbers of animals included in each group were as follows: PBS-12 months (water maze: n=10, histology: n=9); PBS-21 months (water maze: n=7, histology: n=8); N192S-12 months (water maze: n=7, histology: n=6); N1292S-21 months (water maze: n=7, histology: n=9). Photomicrographs of hippocampal sections stained for AChE and sections of the MS and vDB immunohistochemically stained for p75 from a control animal and a N192S animal showing a satisfactory and unacceptable lesion are shown in Figure 2.1.

Figure 2.1. Verification of the cholinergic lesion. Sample photomicrographs showing acetylcholinesterase staining in the hippocampus (A,C,E) and p75-positive cells in the medial septum and diagonal band of Broca (B,D,F) of a control rat (A,B), N192S rat (C,D) and a N192S rat with an incomplete lesion (E,F). All images were acquired using a 4X objective lens.

**Verification of the Cholinergic Lesion:
AChE and p75 Staining**



2.3.2. Water Maze

At 12 or 21 months of age, N192S and PBS rats were tested on a working memory version of the Morris water maze. Latency and distance to find the platform as well as the swim speed were recorded for each of 5 daily trials on the 5 days of testing. The data were analyzed using repeated-measures ANOVA with age and lesion as between-subjects factors and days and trials as within-subjects factors.

Lesioned rats swam more slowly than controls ($F_{1,27}=7.62, p=.001$). There was also a significant main effect of age on swim speed ($F_{1,27}=8.59, p=.007$) and a significant lesion by age interaction effect ($F_{1,27}=6.31, p=.018$). Overall, 21-month-old control rats swam faster than 12-month-old controls, while 12- and 21-month-old lesioned rats swam at similar speeds (see Figure 2.2).

Since the latency data were contaminated by group differences in swim speed, only the distance data are presented here. Neither age ($F_{1,27}=1.98, NS$) nor lesion ($F_{1,27}=.002, NS$) influenced the distance required to find the platform on the first trial of each day, indicating that there were no group differences in the ability to find the new platform location. There was no overall lesion effect on swim distance ($F_{1,27}=.91, NS$), and the main effect of age also narrowly missed reaching significance ($F_{1,27}=3.62, p=.068$). The lesion by age interaction effect was also nonsignificant ($F_{1,27}=.32$). However, the day by lesion by age effect on swim distance was significant ($F_{4,108}=3.85, p=.006$), indicating that an age by lesion interaction effect differed across days of testing. Figure 2.3 shows that 21 month old N192S rats performed more poorly on the last two days of testing. One-way ANOVAs with post-hoc Tukey's tests were performed on the

Figure 2.2. Swim speed in the water maze. The data are presented as averages (\pm SEM) across trials 2 through 5 on each day, since the first trial of each day is a discovery trial and does not represent working memory ability. A significant N192S by age interaction was observed ($F_{1,27}=6.31$, $p=.018$). One-way ANOVAs with post-hoc Tukey's test indicated that 21-month PBS rats swam significantly faster compared to all other groups on days 3 and 4 (indicated by '*'), and compared to both 12-month groups on day 5 (indicated by '&'). On day 1, the 21-month N192S rats swam more slowly than the 12-month PBS rats (indicated by '#'; all p 's $<.05$).

Swim Speed in the Water Maze

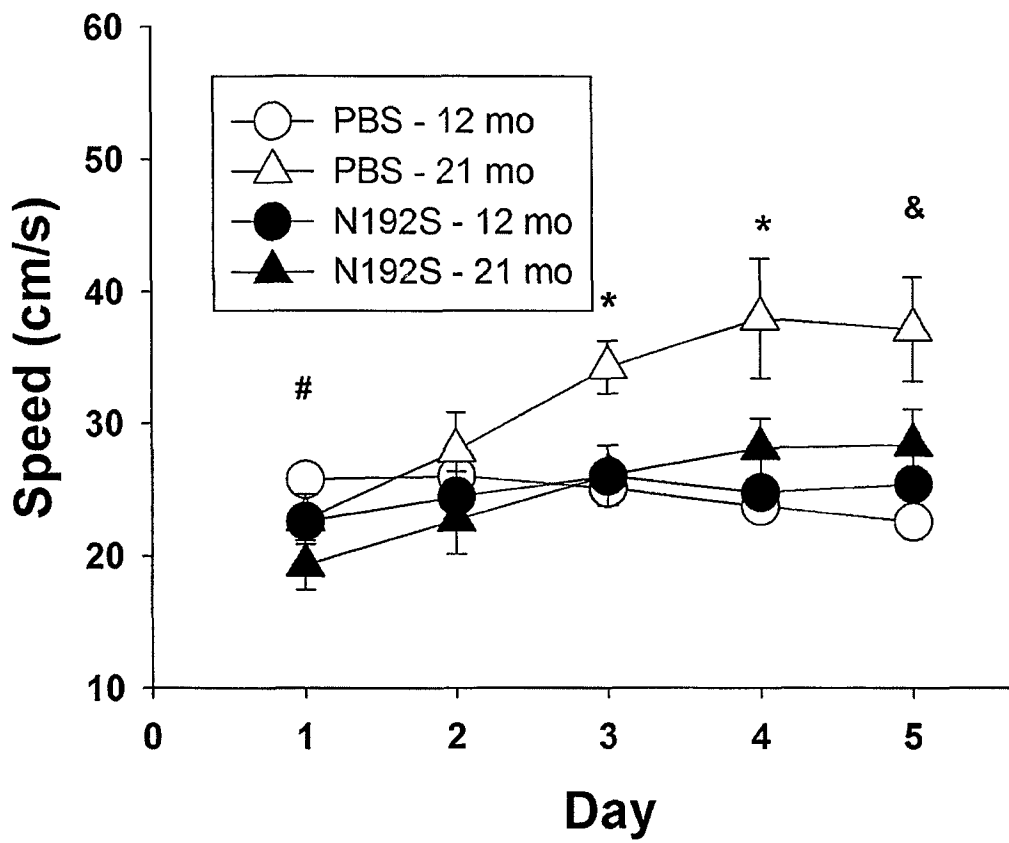
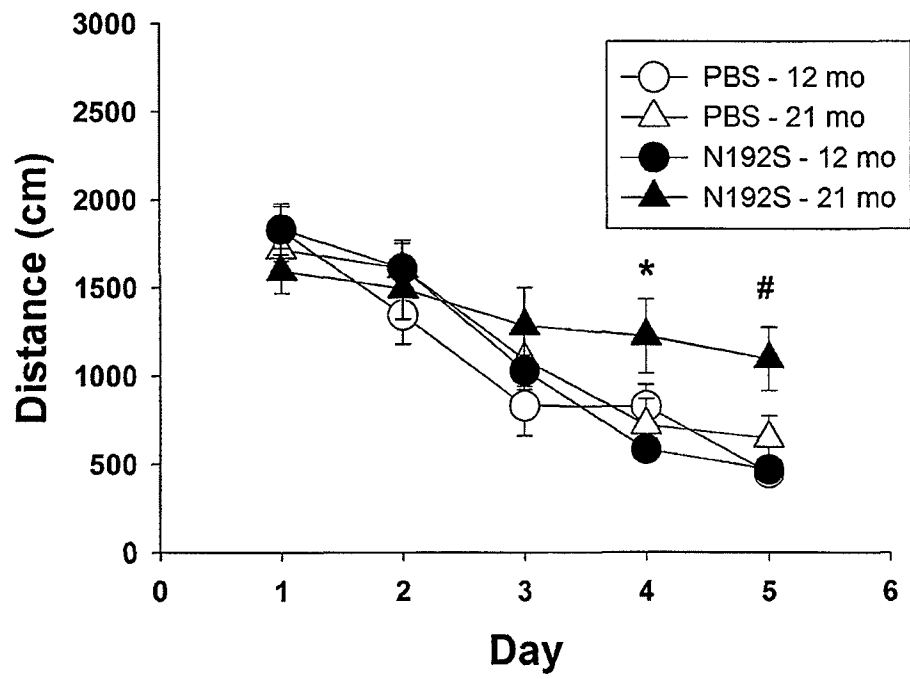


Figure 2.3. Path length to find the hidden platform. The data are presented as averages (\pm SEM) across trials 2 through 5 on each day, since the first trial of each day is a discovery trial and does not represent working memory ability. Only the day by N192S by age interaction was significant ($F_{4,108}=3.85$, $p=.006$). One-way ANOVAs with post-hoc Tukey's tests were performed on the daily averages to assess group differences on each day. On day 4, the 21-month N192S rats required greater swim distances to find the platform than 12-month N192S rats ($p<.05$; indicated by '#') and on day 5, the 21-month N192S rats swam significantly greater distances than all other groups (all p 's $<.05$; indicated by '*').

Water Maze Working Memory Version



daily averages to assess group differences on each day. On day 4, the 21-month N192S rats required greater swim distances to find the platform than 12-month N192S rats ($p < .05$) and on day 5, the 21-month N192S rats swam significantly greater distances than all other groups (all p 's $< .05$).

2.3.3. Cued Platform

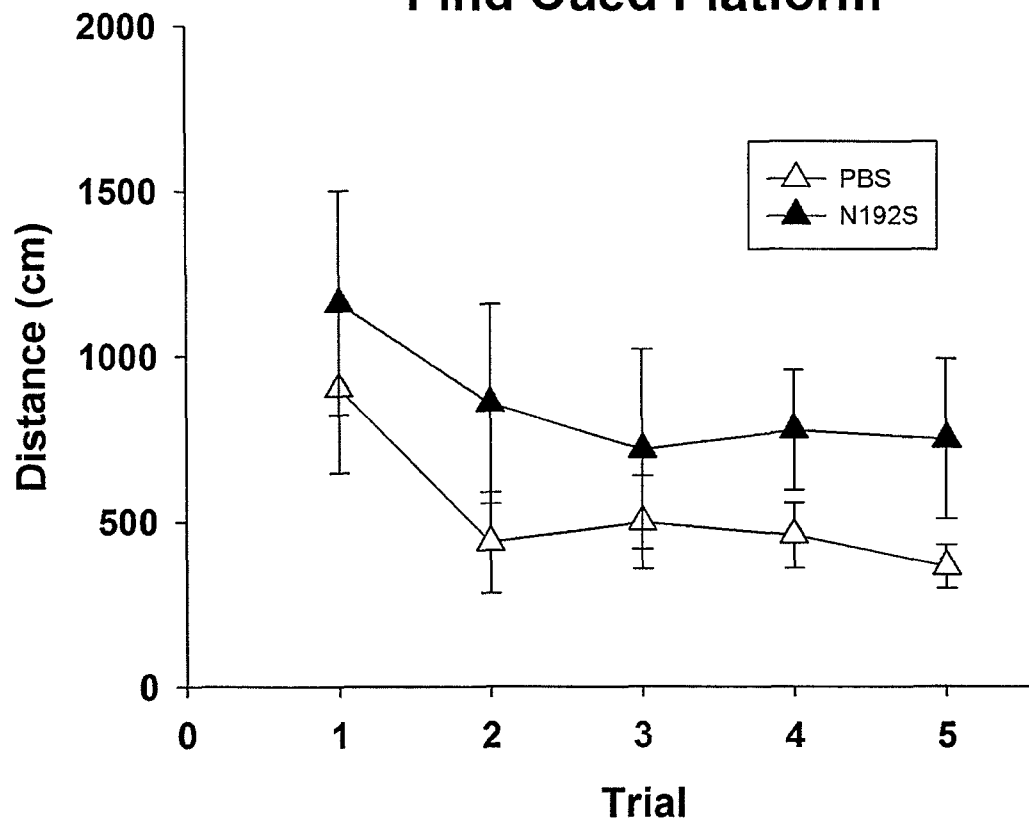
In order to rule out the possibility that the impairment observed in the 21-month-old lesioned rats was due to motivational, visual or motor factors, the 21-month-old control and lesioned rats were tested on a cued platform version of the water maze (see Figure 2.4). The distance travelled by the lesioned rats on the cued platform trials was not different from controls ($F_{1,12}=2.79$, NS). In addition, there were no significant interaction effects. Independent samples t-tests on the data from each trial indicated that the groups did not differ on any single trial (all p 's $> .05$).

2.3.4. Ki-67 Counts

Ki67-immunoreactive cells were counted manually in the DG and SGZ of 12- and 21-month-old lesioned and control rats. The data were analyzed using a two-way ANOVA with age and lesion as independent variables. As shown in Figure 2.5, aging caused a significant decrease in the number of Ki-67-positive cells in both the dorsal ($F_{1,28}=19.09$, $p < .001$) and ventral ($F_{1,28}=6.97$, $p = .013$) DG. N192S did not impact the number of cells staining positive for Ki-67 in either the dorsal ($F_{1,28} < 1$) or ventral ($F_{1,28} < 1$) DG. The age effect was equivalent in both control and lesioned rats, as there was no age by lesion interaction in either the dorsal ($F_{1,28} < 1$) or ventral ($F_{1,28}=1.90$,

Figure 2.4. Path length to find the cued platform. Path lengths did not differ significantly between 21-month old PBS and N192S rats ($F_{1,12}=2.79$, NS).

Distance Traveled to Find Cued Platform



$p=.17$) DG. Across both groups, the number of Ki-67⁺ cells decreased by 60% from 12 months of age to 21 months in the dorsal DG, and by 55% in the ventral DG.

2.3.5. DCX Counts

The DCX results mirrored those for Ki-67. N192S had no effect on the number of DCX-positive cells in either the dorsal ($F_{1,28}<1$) or ventral ($F_{1,28}<1$) DG. However, there was a substantial reduction in the number of DCX-positive cells from 12 to 21 months of age in both the dorsal ($F_{1,28}=33.29$, $p<.001$) and ventral ($F_{1,28}=38.58$, $p<.001$) DG. Aging had a similar impact on lesioned and non lesioned rats, as evidenced by the lack of age by lesion interaction effects in either hippocampal sector (both p 's $>.05$). 21-month-old rats showed a 66% reduction in the number of dorsal DCX-stained cells compared to 12-month-old rats, and a 74% reduction in the ventral DG (see Figure 2.6).

2.3.6. GFAP Immunoreactivity

The percent area staining positive for GFAP in the CA1, CA3, DG and hilus of the hippocampi of 21-month-old rats was analyzed using independent samples t-tests (see Figure 2.7). GFAP immunoreactivity in all hippocampal sectors analyzed was unaffected by N192S (all p 's $>.05$).

2.3.7. APP Immunoreactivity

APP immunoreactivity was not altered by N192S in any hippocampal sector, or in either the superficial or deep layers of the parietal or entorhinal cortices (all p 's $>.05$) of 21-month-old rats. These data are illustrated in Figures 2.8 (hippocampus) and 2.9 (cortical areas).

Figure 2.5. Ki-67⁺ cells in the dorsal (top panel) and ventral (bottom panel) dentate gyrus. 21-month-old animals had fewer Ki-67⁺ cells than 12-month-old animals in both the dorsal ($F_{1,28}=19.09$, $p<.001$) and ventral ($F_{1,28}=6.97$, $p=.013$) DG. N192S had no effect on the number of Ki-67⁺ cells in either hippocampal sector.

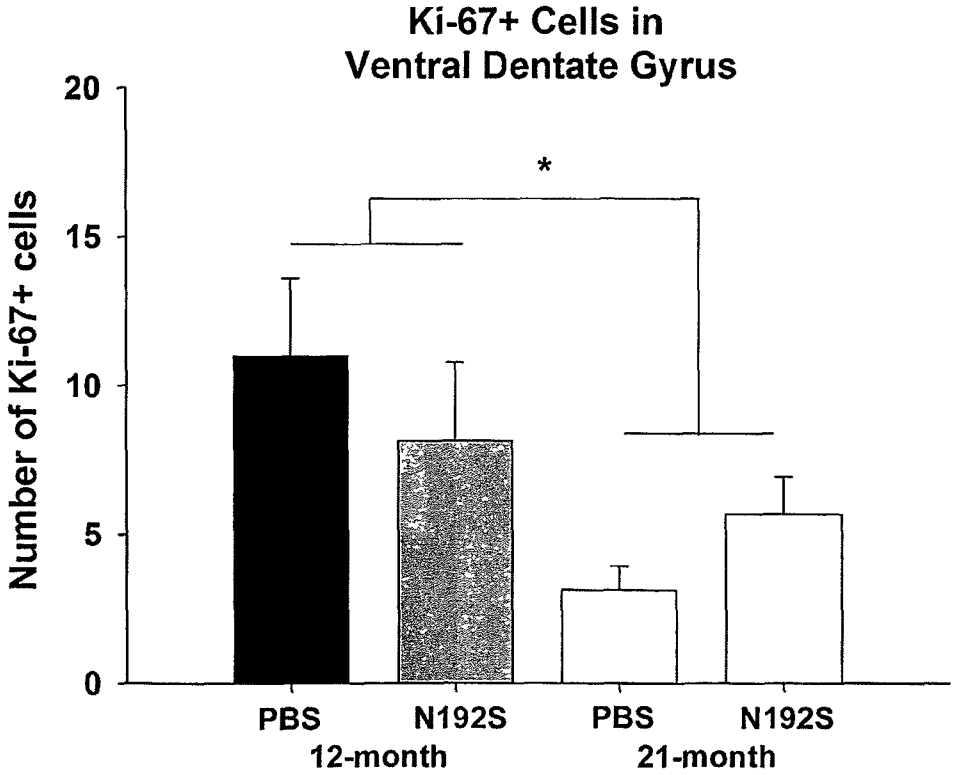
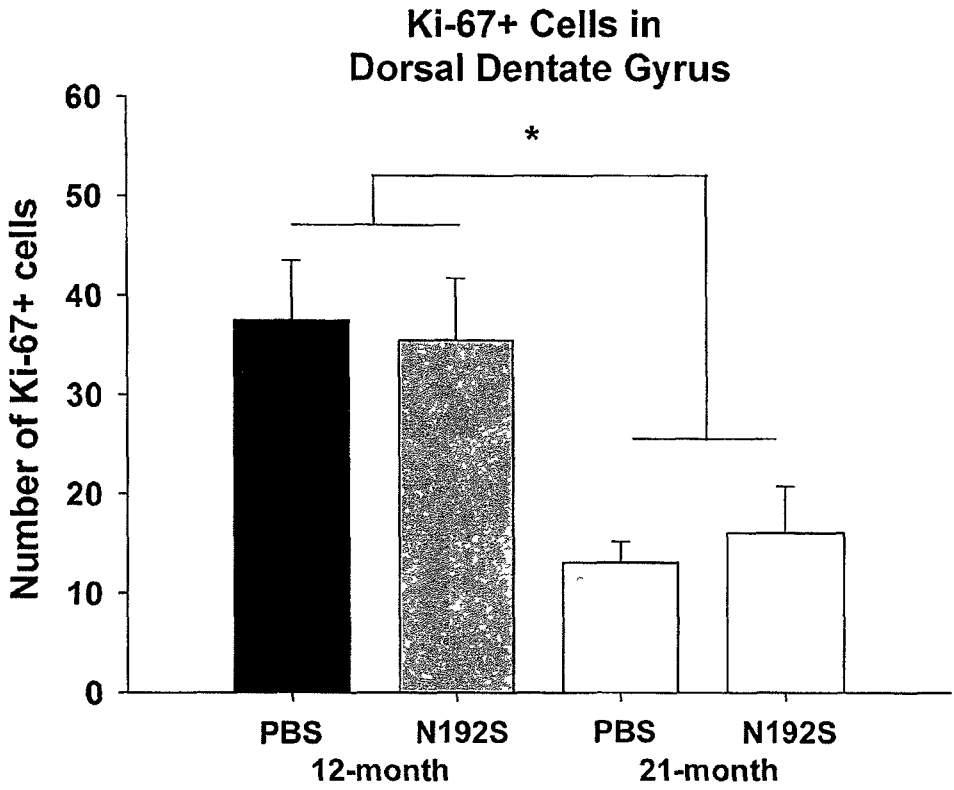


Figure 2.6. DCX⁺ cells in the dorsal (top panel) and ventral (bottom panel) dentate gyrus. For both control and N192S rats, aging reduced the number of DCX⁺ cells in both the dorsal ($F_{1,28}=33.29$, $p<.001$) and ventral ($F_{1,28}=38.58$, $p<.001$) DG.

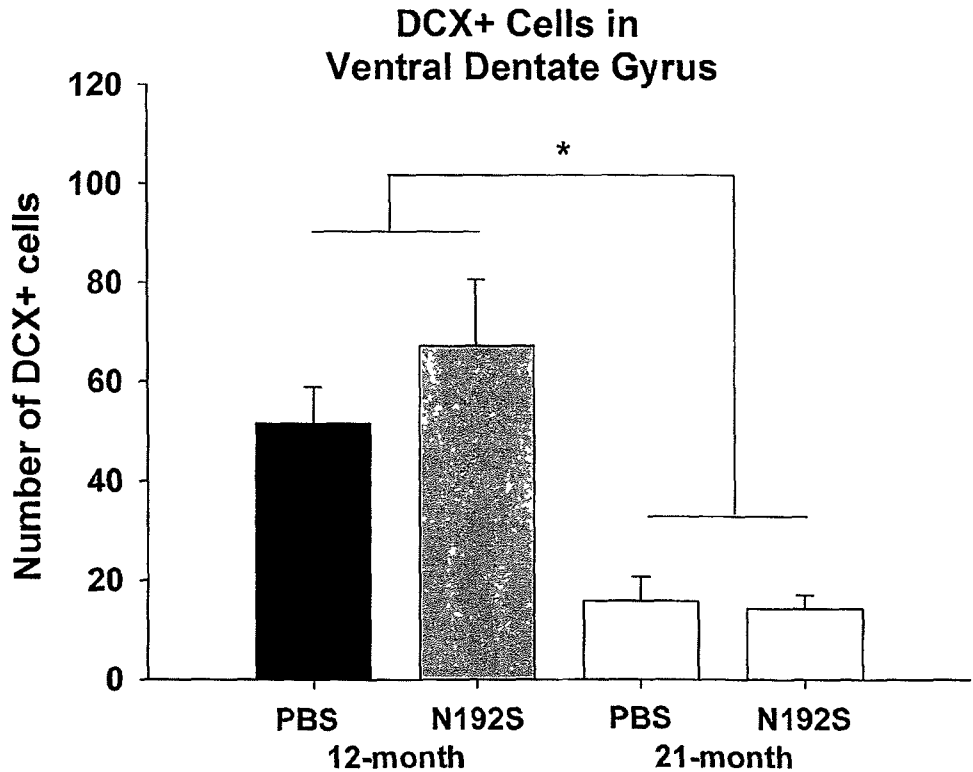
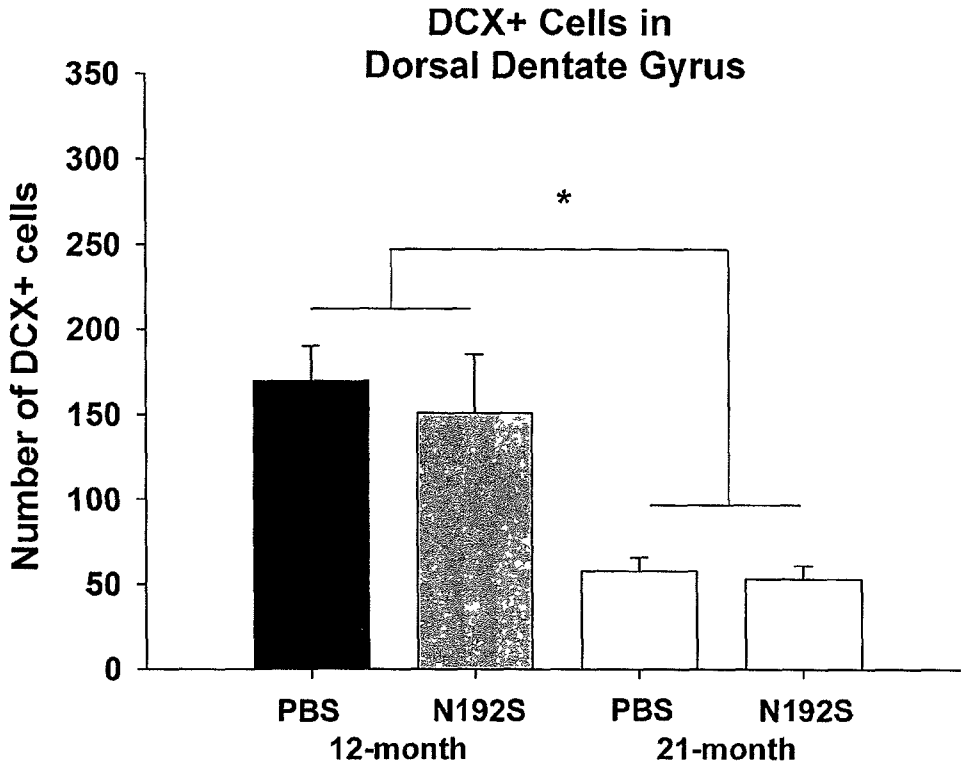


Figure 2.7. GFAP immunoreactivity in the hippocampus. There were no group differences in the percent area staining positive for GFAP in any hippocampal subregion.

GFAP Immunoreactivity in the Hippocampus

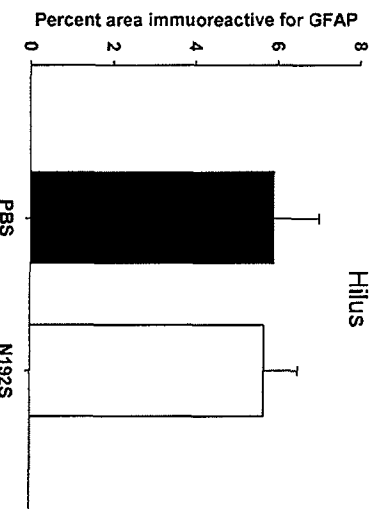
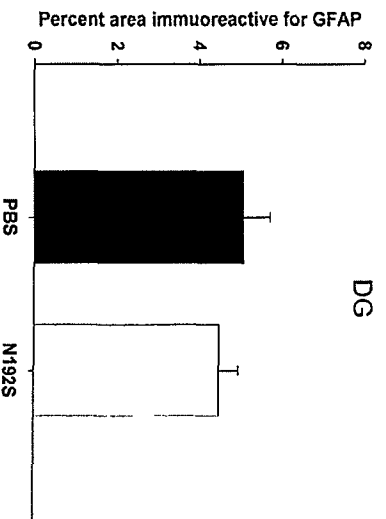
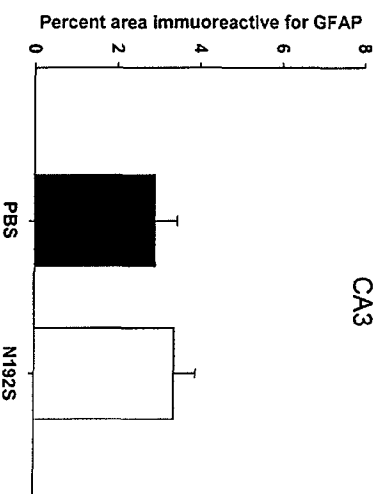
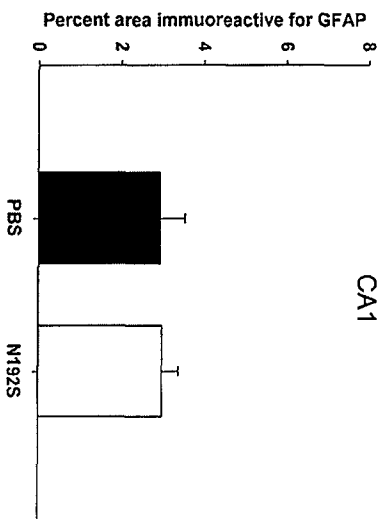


Figure 2.8. APP immunoreactivity in the hippocampus. There were no group differences in the percent area staining positive for APP in any hippocampal subregion.

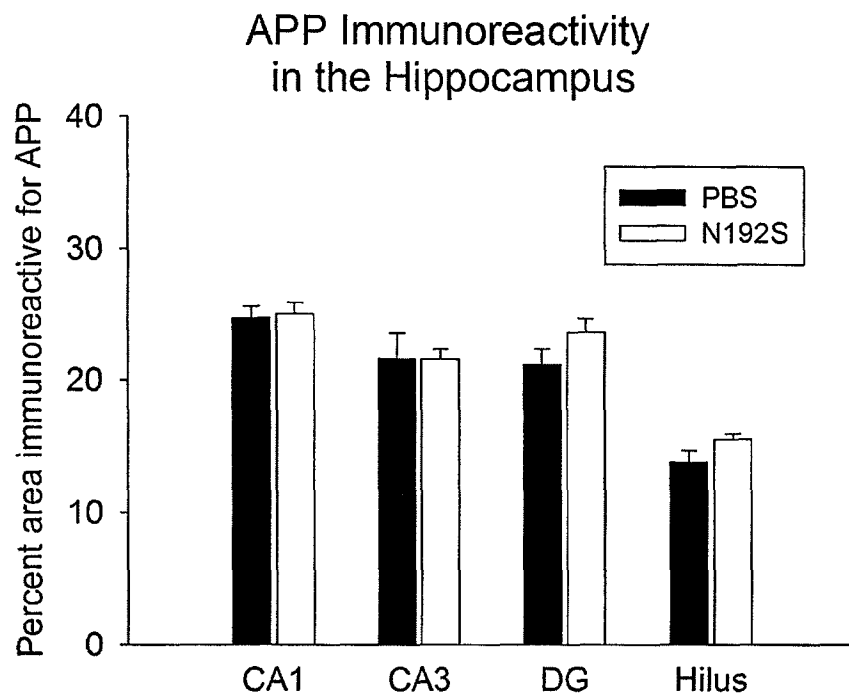
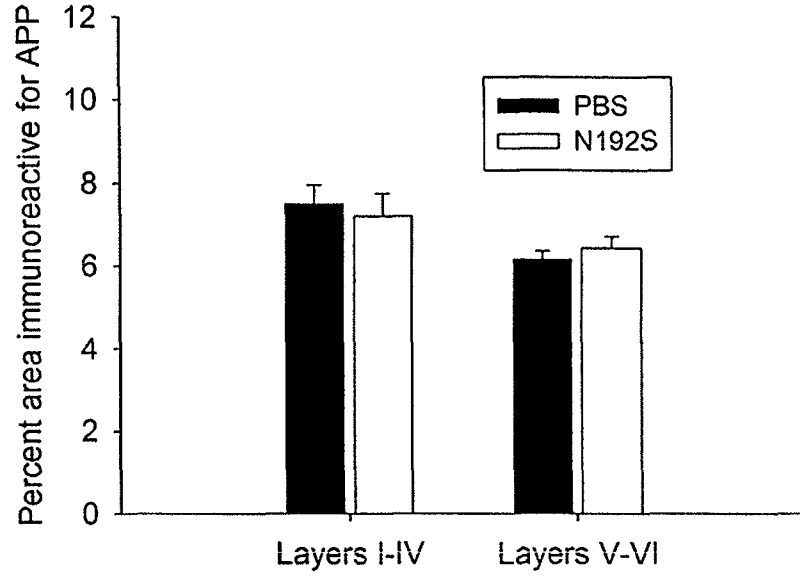
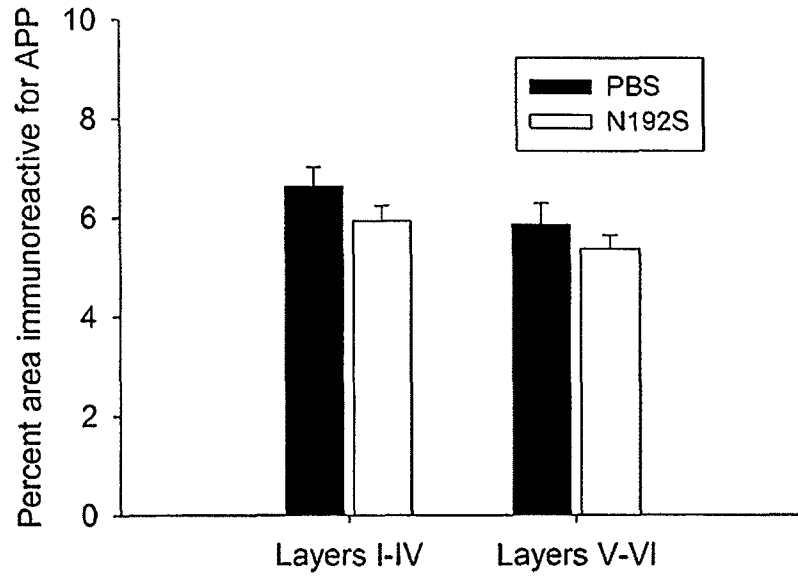


Figure 2.9. APP immunoreactivity in the parietal (top panel) and entorhinal (bottom panel) cortex. There were no group differences in the percent area staining positive for APP in layers I-IV or layers V-VI in either cortical region.

APP Immunoreactivity in the Parietal Cortex



APP Immunoreactivity in the Entorhinal Cortex



2.3.8. CA1 Cell Number

The numbers of CA1 cells in the dorsal and ventral hippocampal CA1 sectors of 21-month-old lesioned and control rats were estimated using stereological cell counting. N192S did not alter the number of pyramidal cells in the dorsal ($t_{15}=1.15$, NS) or ventral ($t_{15}<1$) CA1. These data are depicted in Figure 2.10.

2.3.9. CA1 Pyramidal Cell Morphology

Five control and five N192S rats from the 21-month age group were randomly selected for Golgi analysis. The cell body as well as the complete apical and basal dendritic trees of 10 dorsal CA1 pyramidal cells per brain were traced using NeuroLucida software. The cell body area, total number of apical and basal trees, branches, segments and spines as well as total apical and basal dendritic length and spine density were analyzed using independent samples t-tests. N192S rats did not differ from controls on any of these aggregate measures of cell morphology (all p 's $>.05$; see Figures 2.11 and 2.12).

2.3.9.1. Branch Order Analysis – Apical Dendrites

Repeated measures ANOVAs with branch order as the within-subjects variable and group as the between subjects variable were conducted to determine whether the distribution of branch segments, branch length, total spines or spine density across branch orders was altered by N192S. Independent samples t-tests were used to examine group differences at individual branch orders. The branch order data are shown in Figures 2.13 (branch number), 2.14 (branch length), 2.15 (spines) and 2.16 (spine density).

Figure 2.10. Number of CA1 pyramidal cells. There were no differences between 21-month-old PBS and N192S rats in terms of pyramidal cell number in either the dorsal or ventral CA1 (both p 's > .05)

Dorsal and Ventral CA1 Cell Counts

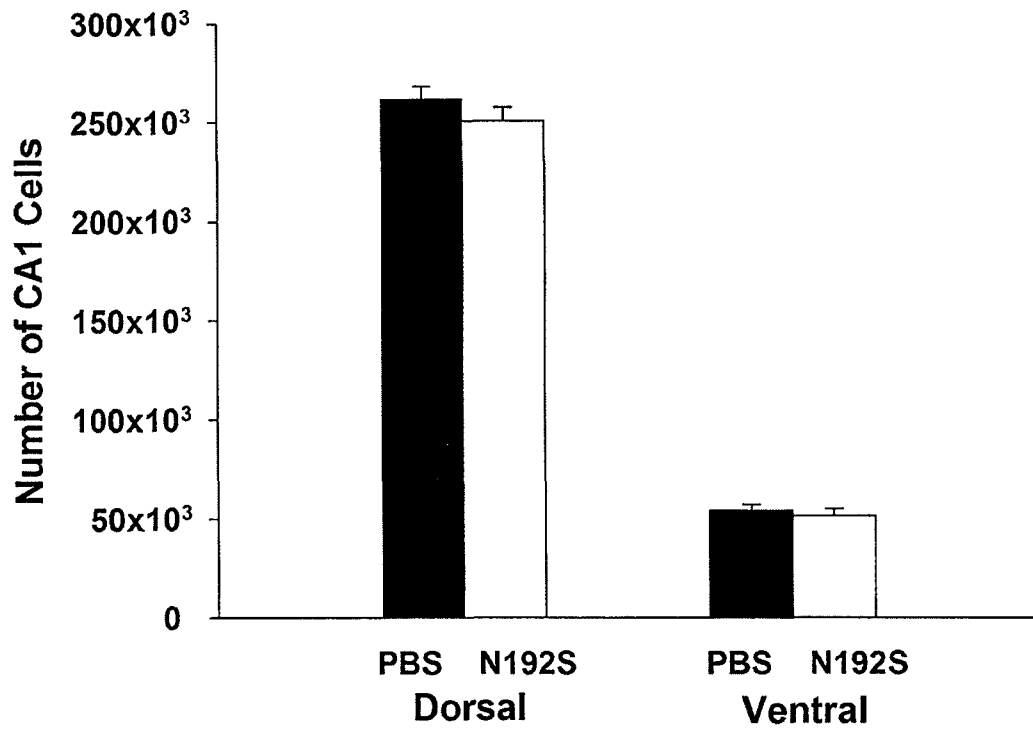


Figure 2.11. Apical and basal dendritic complexity of CA1 pyramidal cells. There were no group differences in terms of total number of segments (top), maximum branch number (middle) or total branch length (bottom).

Golgi Analysis of CA1 Pyramidal Neurons Summary Measures of Dendritic Complexity

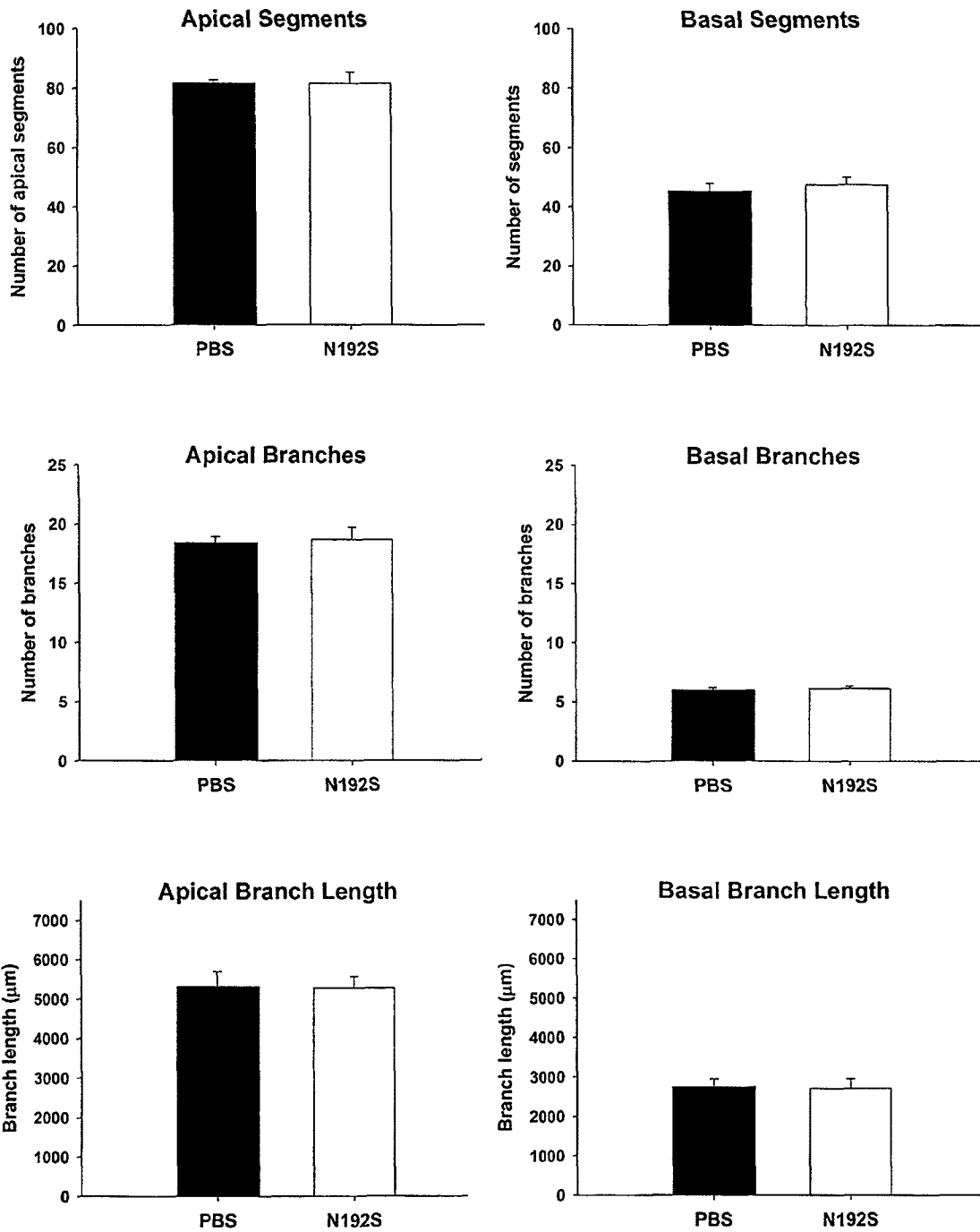
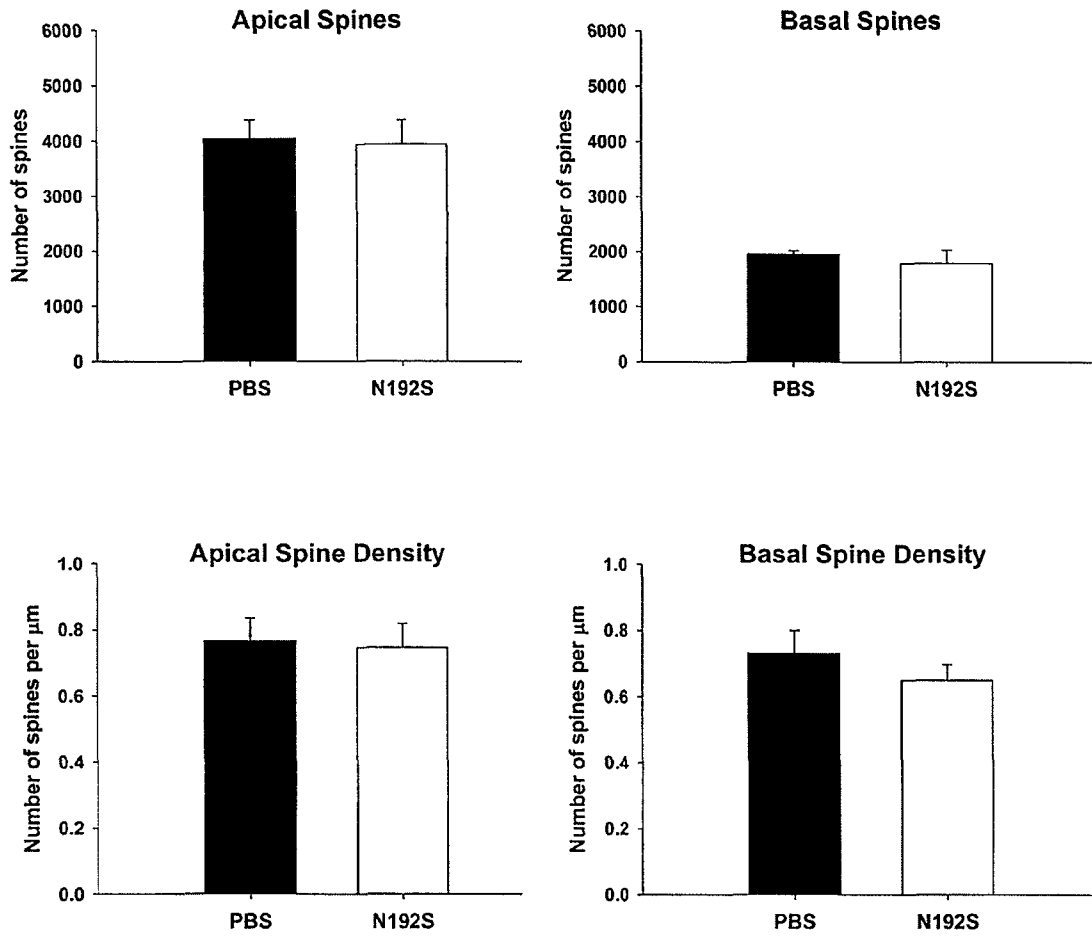


Figure 2.12. Apical and basal spine analysis of CA1 pyramidal cells. Neither the total number of spines (top) nor the spine density (bottom) differed between groups (both p's >.05).

Golgi Analysis of CA1 Pyramidal Neurons Summary of Spine Measures



The branch order by lesion effect on apical branch number was nonsignificant ($F_{29,232}=1.36$), and there were no lesion effects at any single branch order (all t 's $>.05$). However, the branch order by lesion effect on apical branch length ($F_{29,232}=1.70$, $p=.017$) and apical spine density ($F_{19,152}=2$, $p=.011$) were both significant, and the branch order by lesion effect on apical spines narrowly missed reaching significance ($F_{29,232}=1.46$, $p=.064$). This indicates that the distribution of apical branch length and apical spine density across branch orders was significantly altered by N192S. As illustrated in Figures 2.14 and 2.16, there is a general trend towards decreased dendritic material at low/middle branch orders, and increased material at higher branch orders in N192S rats. Individual t -tests at each branch order indicated that apical branch length was significantly increased by N192S at branch order 13 ($t_8=-2.36$, $p=.045$), but decreased at branch order 15 ($t_8=2.63$, $p=.03$). N192S increased the number of apical spines at branch order 18 ($t_8=-3.05$, $p=.016$), and increased spine density at branch orders 24 ($t_7=-2.36$, $p=.05$) and 25 ($t_6=-3.50$, $p=.013$).

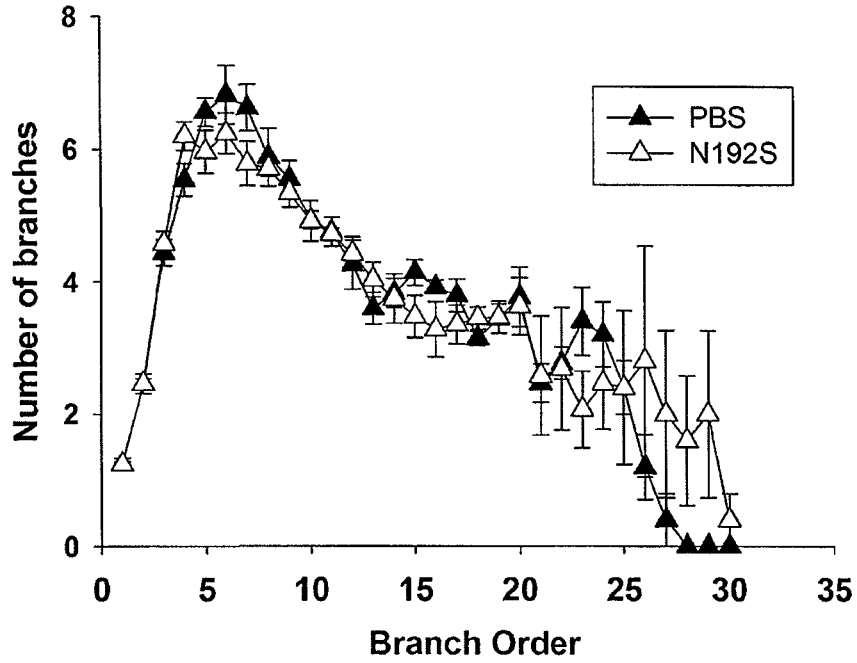
2.3.9.2. Branch Order Analysis - Basal Dendrites

The branch order by lesion effects on basal branch number ($F_{8,64}=2.16$, $p=.042$), basal length ($F_{8,64}=3.05$, $p=.006$) and basal spines ($F_{8,64}=4.06$, $p=.001$) were all significant. In contrast, the branch order by lesion effect on basal spine density was nonsignificant ($F_{6,48}<1$). Similar to what was seen in the apical dendrites, the basal dendrites of N192S rats showed decreases in branch number, length and spines at lower branch orders and increases at higher branch orders. The only significant group difference at a single branch order was found at branch order 7 ($t_8=-2.75$, $p=.025$) where N192S rats had increased numbers of this order.

Figure 2.13. Analysis of apical and basal branch number by branch order. N192S altered the overall distribution of basal ($F_{8,64}=2.16$, $p=.042$), but not apical ($p>.05$) branches across branch orders. More 7th order basal branches were observed in N192S than PBS rats ($t_8=-2.75$, $p=.025$).

Branch Number by Branch Order Analysis

Apical Dendrites



Basal Dendrites

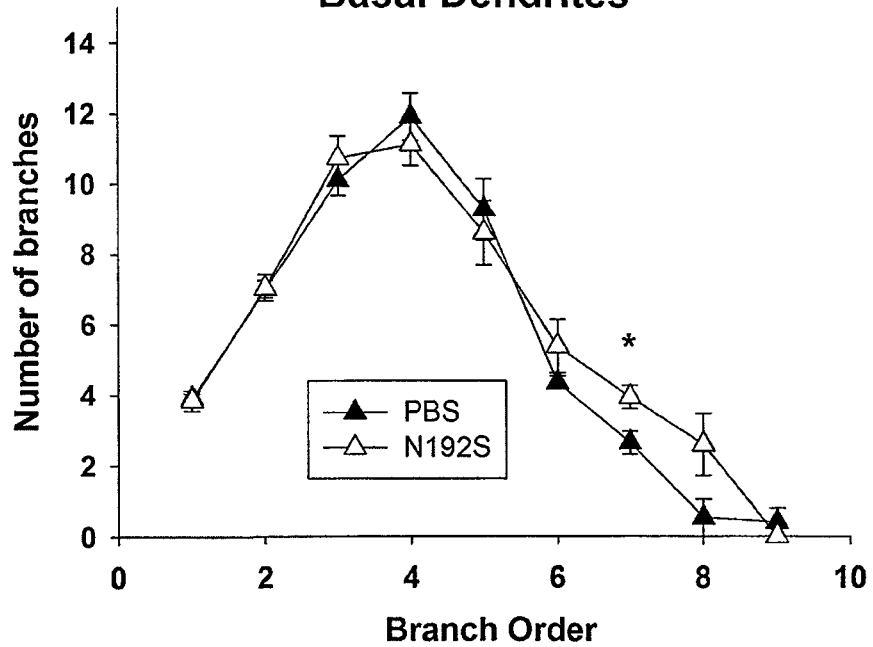


Figure 2.14. Analysis of apical and basal branch length by branch order. The distributions of both apical ($F_{29,232}=1.70$, $p=.017$) and basal ($F_{8,64}=3.05$, $p=.006$) branch length was altered by N192S. Apical length was significantly increased by N192S at branch order 13 ($t_8=-2.36$, $p=.045$), but decreased at branch order 15 ($t_8=2.63$, $p=.03$). Group differences in the basal dendrites did not reach significance at any particular branch order (all p 's $>.05$).

Branch Length by Branch Order Analysis

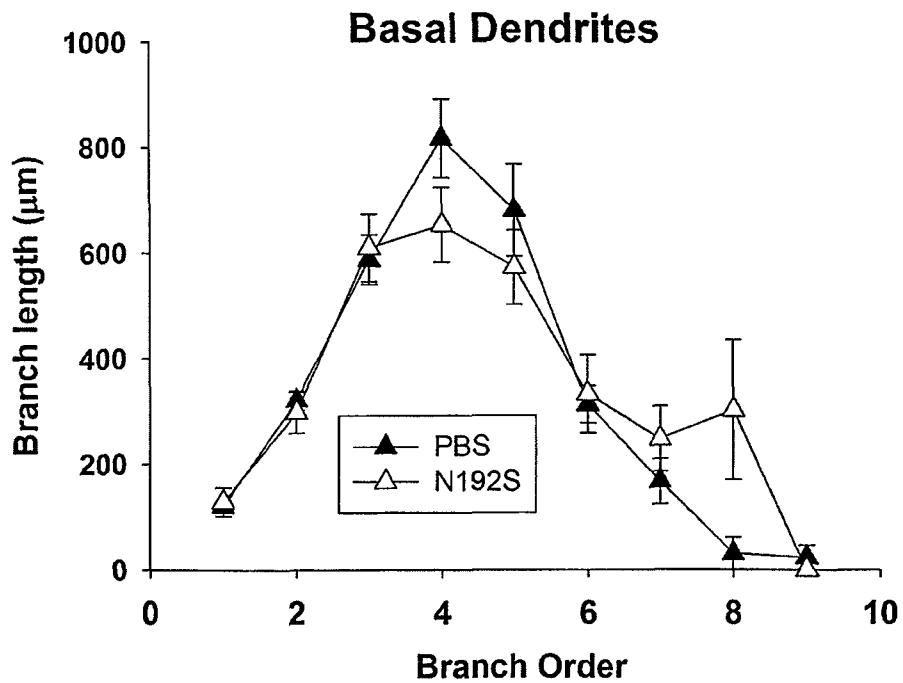
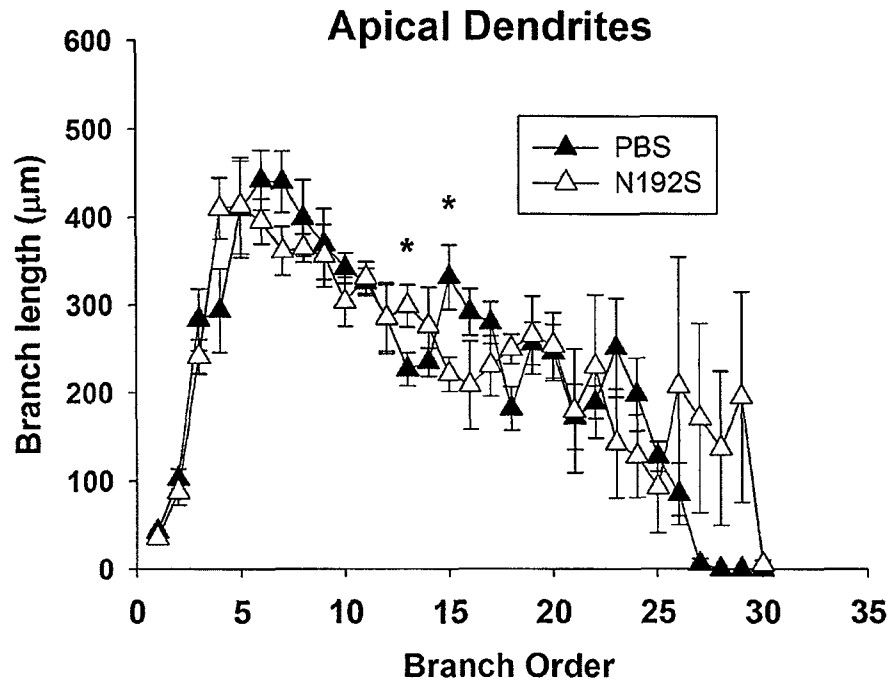


Figure 2.15. Analysis of apical and basal spines by branch order. The branch order by N192S effect on apical spines narrowly missed reaching significance ($F_{29,232}=1.46$, $p=.064$), but the interaction effect was significant for the basal dendrites ($F_{8,64}=4.06$, $p=.001$). N192S increased the number of apical spines at branch order 18 ($t_8=-3.05$, $p=.016$), but did not have a significant effect on basal spines at any particular branch order.

Number of Spines by Branch Order Analysis

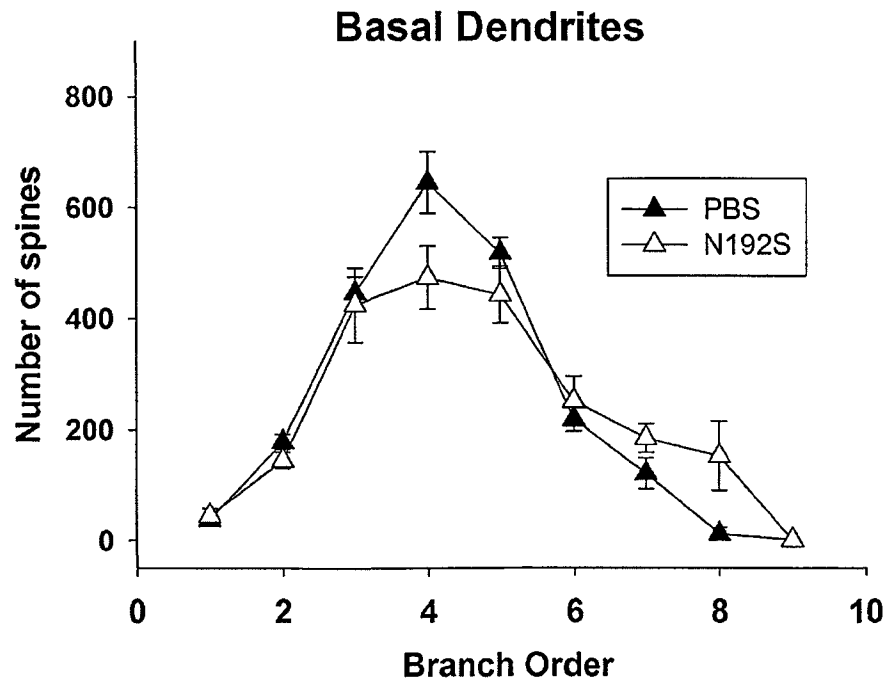
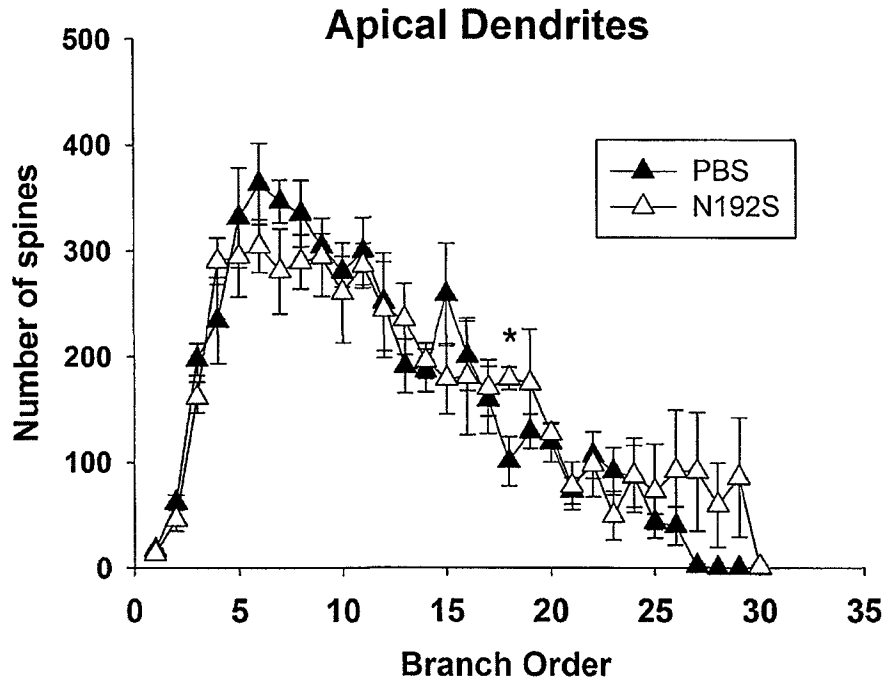
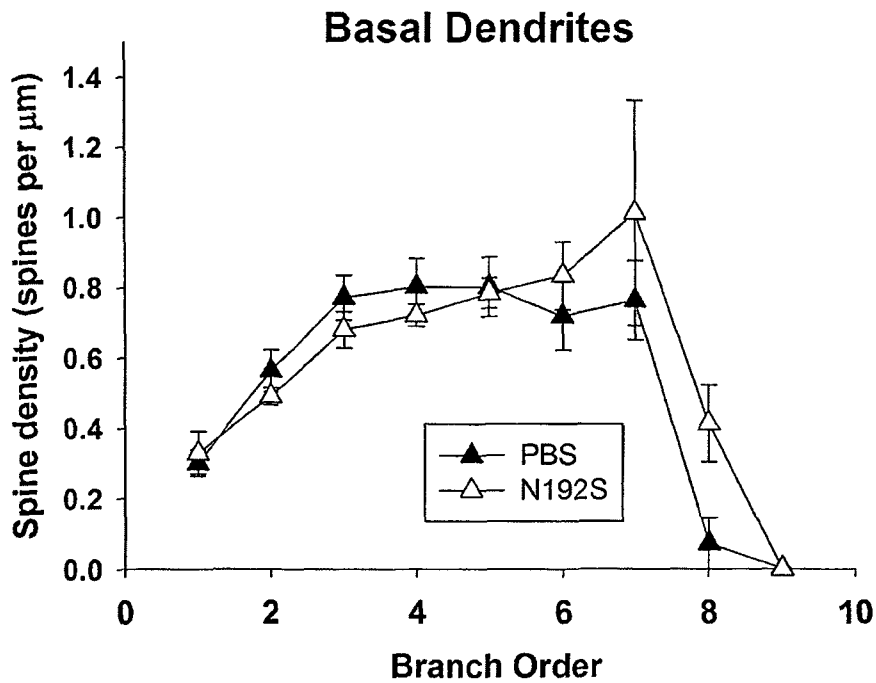
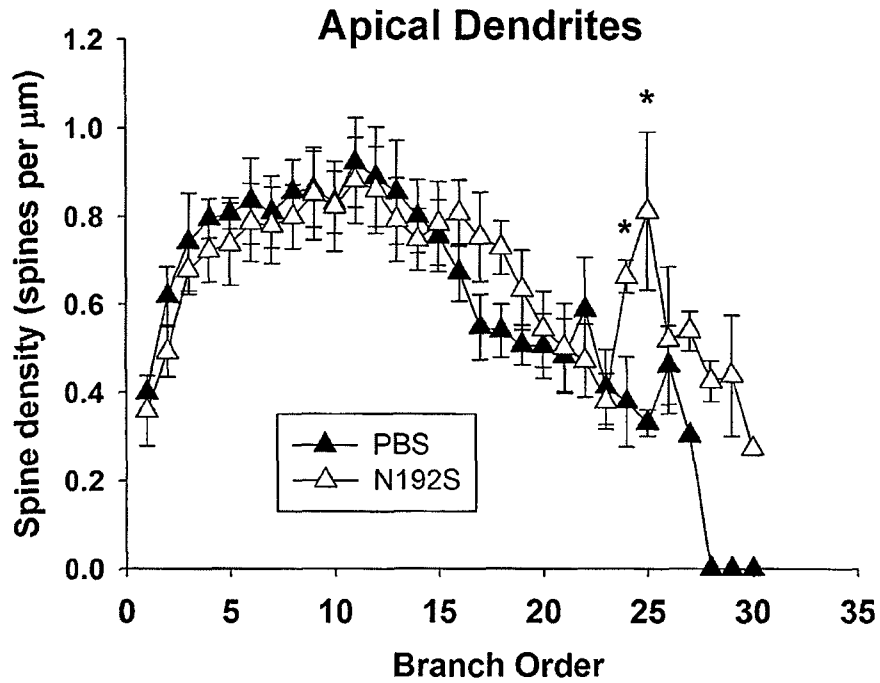


Figure 2.16. Analysis of apical and basal spine density by branch order. The apical spine density distribution across branch orders was altered by N192S ($F_{19,152}=2$, $p=.011$), and N192S rats exhibited increased spine density at branch orders 24 ($t_7=-2.36$, $p=.05$) and 25 ($t_6=-3.50$, $p=.013$). The branch order by N192S effect on basal spine density was nonsignificant ($p>.05$), and there were no basal branch orders at which there were group differences in spine density.

Spine Density by Branch Order Analysis



2.4. Discussion

The present study was designed to examine the effects of neonatal cholinergic lesion on spatial working memory, neurogenesis and CA1 cytoarchitecture in aging rats. The data reveal an interactive effect of N192S and aging on spatial working memory, and demonstrate subtle changes in the dendritic morphology of CA1 cells in aged N192S rats.

2.4.1. Effects of Aging and N192S on Spatial Working Memory

In terms of swim distance, 21-month-old (aged) N192S rats were impaired relative to both 12-month-old (middle aged) N192S rats and aged PBS animals in the last days of testing. In contrast, middle-aged and aged PBS rats performed equivalently, and there was no difference between middle-aged N192S and PBS rats. N192S therefore impaired performance only in aged rats, and aging impaired performance only in lesioned rats, indicating that aging and cholinergic lesion interact to produce cognitive deficits. Importantly, the groups did not differ in their ability to find the platform on the first trial of each day or on the cued platform test, indicating that aged N192S rats' impairment was not due to an inability to use general maze strategies.

While a number of studies have reported working memory deficits after cholinergic lesions of the medial septal area (Fitz et al., 2006; Shen et al., 1996; Walsh et al., 1996) or entire basal forebrain (Wrenn et al., 1999), or ibotenic acid lesions of the NB (Wellman and Pellemounter 1999) in the adult rat, several others have found no or very little effect of BFCS lesions on working memory (Chappell et al., 1998; Connor et al., 1992; McMahan et al., 1997; Paban et al., 2005; Vuckovich et al., 2004). Wrenn et al. (1999) suggested that working memory deficits become apparent only after a threshold

for cholinergic depletion has been reached (greater than 85% loss of p75⁺ cells in the MS/vDB and greater than 70% loss in the NB/hDB). However, the loss of p75⁺ cells in the present study surpassed this threshold without producing working memory deficits in middle-aged animals. This discrepancy may be due to the difference in age at the time of lesion. Rats subjected to the lesion as neonates might show a greater resistance to its cognitive effects, or have an increased capacity for compensation. It is also possible that a different task might reveal a working memory deficit in middle-aged animals after N192S. Wrenn et al. used a radial arm maze task that requires rats to hold in memory a list of previously entered arms as they search for food rewards, which is likely more difficult than remembering a single platform location in the water maze. Furthermore, Fitz et al (2006) demonstrated that administering a mild aversive stimulus prior to training on a delayed match-to-position T-maze task eliminated the working memory deficit seen after intraseptal 192-saporin injections, suggesting that aversive stimuli can mask a working memory deficit in lesioned rats. The use of a less aversive task might therefore reveal a working memory deficit in young or middle-aged N192S rats. Nevertheless, the choice of task in the present study allowed us to clearly demonstrate the more severe effects of N192S in aged rats compared to middle-aged rats.

The present results, as well as previous work in this laboratory (Pappas et al., 2005) suggest that a prior cholinergic lesion renders the brain more vulnerable to the effects of aging on both spatial working and reference memory. This agrees with a number of studies demonstrating the interactive behavioural effects of adult cholinergic lesion and aging. For example, deficits on a sustained attention task became evident in rats subjected to adult BFCS lesion only when they reached the age of 31 months (Burk et al., 2002). The ability to discriminate between sensory stimuli was also more severely

affected in 18-month-old than in 3-month-old BFCS-lesioned rats (Stoehr et al., 1997), and water maze performance was impaired in old but not young adult rats after intraseptal injections of 192-IgG-saporin (Bannon et al., 1996). Collectively, these studies suggest that changes in the aging brain are permissive to the detrimental effects of cholinergic deafferentation.

The interactive effects of N192S and aging on working memory performance might occur for a number of reasons. While the extent of p75⁺ cell loss was no greater in aged than in middle-aged N192S rats, the functional capacity of the residual BFCS might have differed between the age groups. The ability of a meaningful stimulus to enhance the release of cortical ACh is impaired in aged rats subjected to partial cholinergic deafferentation, but not in young lesioned rats (Fadel et al., 1999). Hippocampal ACh efflux is normally increased during performance of a working memory task (Fadda et al., 1996) and it is possible that working memory performance was impaired in aged lesion rats owing to a failure to stimulate ACh release from the remaining BFCS neurons.

2.4.2. Effects of Aging and N192S on Neurogenesis

The numbers of Ki-67⁺ and DCX⁺ cells in both the dorsal and ventral DG were substantially reduced in aged compared to middle-aged rats. The reduction in cells immunopositive for Ki-67 suggests reduced cell proliferation in the aging brain, in agreement with a number of other studies showing age-related reductions in proliferation (Cameron and McKay 1999; Heine et al., 2004; Kuhn et al., 1996; Rao et al., 2005) rather than survival or differentiation of new cells (Rao et al., 2005). Although previous studies report that the greatest age-related reductions in neurogenesis occur prior to the age of 12 months and that the rate of neurogenesis remains relatively stable thereafter (Heine et al.,

2004; Kuhn et al., 1996; Rao et al., 2005; Rennie et al., 2009), Rao et al. (2006b) found a ~49% decrease in Ki-67⁺ cells between 12 and 24 months of age in the Fischer 344 rat, in close agreement with the present results.

The effect of age on neurogenesis was not modulated by N192S, as animals in both treatment groups showed equal reductions in Ki-67⁺ and DCX⁺ cells with age. Furthermore, N192S on its own did not significantly affect neurogenesis. This is somewhat surprising, as we have found reduced numbers of DCX⁺ cells in the dorsal DG after N192S in younger rats (3-week-old rats: unpublished results; 9-week-old rats: Fréchette et al., 2009, see also Study #3 in this thesis). Though nonsignificant, there was an 11% reduction in dorsal DCX⁺ cells in 12-month-old N192S rats, and an 8% reduction in 21-month-olds, whereas we observed an 18% decrease in DCX⁺ cells at nine weeks of age in N192S rats (see Study #3). Together, these findings suggest that with age, the influence of the cholinergic system on neurogenesis is diminished.

Effects of N192S on the CA1 Sector in Aged Rats

While N192S did not cause CA1 cell loss, it did change the dendritic structure of CA1 pyramidal neurons in aged rats. The branch order by lesion effects on apical branch length and spine density, and basal branch number, length and spines indicates that the distributions of these parameters were altered by the lesion. In particular, there appeared to be a shift in the dendritic material away from the cell soma and towards the more distal area of the dendritic trees. This pattern differs from previously observed effects of N192S in young (9-week-old) rat, which included an overall reduction in basal branch length and a decrease in the number of apical spines distal to the cell body (Fréchette et al., 2009). The effects of N192S on CA1 dendritic morphology appear to be age-dependent.

Similar to our observations here for the effects of N192S on CA1 neurons, the effects of adult cholinergic lesions on the dendritic morphology of layer II/III frontal cortex pyramidal neurons are age-dependent (Works et al., 2004). While the lesion produced minimal effects in 3-month-old rats, 24-month-old rats subjected to the lesion showed marked dendritic regression in both the apical and basal trees. Whether the difference between that study and the results of the present study are due to differences in the cell type examined, or are related to the difference in the age at which the lesion was performed is unknown. Notably, in the Works et al. study dendritic morphology was examined only two weeks after the lesions, and as noted by the authors, deafferentation may lead to a period of regression/atrophy followed by reactive proliferation of the dendrites (Caceres and Steward 1983). It may be the case in that study that the proliferative period was simply delayed in the aged rats, and that the impact of age on the effects of cholinergic lesion on dendritic structure might be less pronounced if the brains were examined at a longer post-lesion interval (Works et al., 2004). Further examination of the age-dependency of lesion effects on cortical and hippocampal dendritic structure is warranted.

The functional properties of a neuron are influenced by the shape of the dendritic arbour (Mainen and Sejnowski 1996). The location of a synapse affects the ability of the corresponding input to drive membrane potential changes at the site of action potential generation (Williams and Stuart 2003). The apparent shift in dendritic material away from the cell body may therefore affect the efficiency of CA1 inputs at driving action potential generation. In addition, distal apical dendrites of CA1 cells receive input from the entorhinal cortex via the perforant path, while proximal apical dendrites form synapses with Schaffer collaterals carrying information from CA3 (Witter and Amaral

2004). The altered distribution of apical dendritic length and spines in N192S rats might indicate a change in the balance of these inputs and their influence over the receiving cell.

The expression of amyloid precursor protein, from which beta-amyloid peptides are derived, is elevated in the brains of Alzheimer's patients (Cummings et al., 1992) and aging itself is associated with an upregulation of APP (Sivanandam and Thakur 2010). We hypothesized that N192S might increase the expression of APP in the aged brain, and therefore assessed APP immunoreactivity in the hippocampus and cortex of aged N192S and control rats. However, consistent with a lack of change in mRNA or protein levels in the hippocampus and cortex in 6-month-old rats after N192S (Ricceri et al., 2004) the levels of APP were not significantly different between N192S and PBS rats in any hippocampal sector or in the parietal or entorhinal cortex in 21-month-old rats. Thus even with advanced age, N192S does not appear to alter the expression of APP. Surprisingly, this contrasts with the upregulation of APP protein expression observed in the hippocampus and cortex after adult cholinergic lesion (Leanza 1998; Lin et al., 1998).

2.5. Conclusions

The effects of N192S on CA1 pyramidal cells in aged rats do not mimic the changes associated with AD. Severe CA1 atrophy occurs in the AD brain, with pyramidal cell loss in the range of 50-70% (Bobinski et al., 1998; Kril et al., 2002; Rössler et al., 2002; West et al., 1994b). Furthermore, the remaining CA1 cells show severe atrophy of both the apical and basal dendritic trees (Hanks and Flood 1991). In addition, AD brains show increased astrocytic reactivity in the hippocampus and temporal cortex (Muramori et al., 1998; Sheng et al., 1994; Van Eldik and Griffin 1994; Vijayan et al., 1991), as well as increased APP expression (Cummings et al., 1992). We hypothesized that aged N192S

rats might model these neuropathological changes. However, compared to age-matched controls, 21-month-old N192S rats did not show CA1 cell loss in the dorsal or ventral hippocampus, nor did they exhibit astrogliosis or APP upregulation in any hippocampal subfield. Finally, rather than exhibiting widespread dendritic atrophy, the CA1 cells of aged N192S rats showed subtle alterations in the distribution of dendritic material along the length of the dendritic tree. Thus the combination of aging and cholinergic lesion is not sufficient to reproduce the neuropathological features of AD.

In summary, N192S interacts with the aging process to precipitate cognitive impairments which are not accompanied by CA1 cell loss or hippocampal astrogliosis. However, the dendritic morphology of CA1 cells in aged N192S rats show alterations that could potentially affect hippocampal function. The memory deficit seen in aged N192S rats might also be associated with structural alterations in other brain regions. For instance, the prefrontal cortex (PFC) mediates working memory and pyramidal cells in this area show reduced dendritic complexity in adult rats after N192S (Sherren and Pappas 2005). An examination of PFC pyramidal cells in aged N192S rats is therefore warranted. Furthermore, as pointed out by Flood (1993), the ability of dendrites to continue to exhibit plasticity with age might be just as, or more, important than the absolute size or complexity of the dendritic arbour at any given time. Thus, it would be informative to determine whether age-related changes in dendritic plasticity are modulated by N192S.

3. Study #2. The Effects of Neonatal Cholinergic Lesion on the Behavioural and Neural Consequences of Chronic Cerebral Hypoperfusion

3.1. Introduction

Dysfunction of the BFCS is a hallmark feature of AD, and is believed by many to contribute not only to the cognitive impairments observed in AD patients, but also to the neuropathological features of the disease (Bartus et al., 1982; Mesulam 2004). However, it is clear that other factors play a part in AD susceptibility. One such factor might be chronically impaired oxygen/nutrient delivery to the brain due to peripheral or central vascular pathology (de la Torre 2009; Dickstein et al., 2010; de la Torre 2002).

Several established risk factors for AD are directly related to cardiovascular function, including atherosclerosis, stroke, high cholesterol, cardiac disease, and atrial fibrillation (Kalaria 2000; Stampfer 2006; de la Torre 2002). Other factors connected with AD risk such as smoking, alcoholism, depression and low educational attainment also share a common link in that each is associated with reduced cerebral blood flow (CBF; de la Torre 2004; de la Torre 2002). Notably, many of these factors are present long before cognitive impairments become apparent, suggesting a causal relationship between these cerebrovascular risk factors and AD (Stampfer 2006; de la Torre 2002). In fact, reductions in CBF predict the progression from mild cognitive impairment (MCI) to AD (Johnson et al., 1998; Johnson and Albert 2000), and differences in CBF differentiate MCI patients from cognitively intact controls (Okamura et al., 2002). AD is also associated with pathological alterations of the cerebral microvasculature. Postmortem AD brains show evidence of deformed microvessels in areas of the brain that are typically

most affected by amyloid plaques and neurofibrillary tangles (Kalaria 1996). The basement membrane and walls of cortical capillaries are thickened, the lumen is narrowed, and there is a loss or degeneration of pericytes (Kalaria 1996; de la Torre 2002). Both nutrient and oxygen delivery to the parenchyma are impaired as a result of cerebral hypoperfusion and impaired integrity of the vasculature, likely leading to a state of chronic energy shortage for the hypoperfused tissue (de la Torre 2006).

Animal models support a role for chronic cerebral hypoperfusion in neurodegeneration. Permanent occlusion of the common carotid arteries (2VO) in the rat results in a moderate reduction of hippocampal CBF (to 50% of control values) immediately after 2VO onset (Tsuchiya et al., 1992) which gradually normalizes over the ensuing months (Farkas et al., 2007). At long survival times, the brains of rats subjected to 2VO show microvascular changes similar to those seen in AD, including degenerative pericytes, collagen accumulation, and thickening of the basement membrane (De Jong et al., 1997). In addition, 2VO produces a delayed loss of CA1 neurons (Bennett et al., 1998; Ni et al., 1994; Ni et al., 1995; Pappas et al., 1996b) accompanied by impaired reference (Bennett et al., 1998; de la Torre et al., 1998; Liu et al., 2005; Pappas et al., 1996b) and working (Bennett et al., 1998; Ni et al., 1994) memory, as well as deficits in brightness discrimination (Tanaka et al., 1996), object recognition, and Y maze performance (Sarti et al., 2002).

Given that AD is associated with both cholinergic dysfunction and cerebrovascular abnormalities, it was of interest to examine the combined effects of cholinergic lesion and 2VO. Cholinergic dysfunction and cerebral hypoperfusion might synergize to produce cognitive deficits and/or neuropathology. For instance, BFCS

neurons innervate cortical microvessels (Vaucher and Hamel 1995), and cholinergic signalling stimulates vasodilation, thereby modulating cerebral blood flow (Sato et al., 2002). Cholinergic lesion might be expected to further reduce cerebral blood flow after 2VO, or prevent the compensatory response to 2VO which normally helps return CBF to baseline levels.

In the present study the effects of single and combined neonatal cholinergic lesion and cerebral hypoperfusion induced by 2VO on spatial working memory, CA1 cell number and cytoarchitecture were examined. It was hypothesized that a pre-existing cholinergic deficit would render the brain more vulnerable to the behavioural and neuropathological effects of cerebral hypoperfusion.

3.2. Methods

3.2.1. Animals

Four male and eight female Sprague-Dawley rats (Harlan, Indianapolis, IN) were used as breeders. After one week of acclimation to the animal facility, rats were triple-housed (one male with two females) for breeding. The rats were inspected daily and females were removed from the male's cage and single-housed when they began to show obvious signs of pregnancy. The females were monitored daily until the pups were born. The day of birth was designated as PND 0. The litters were culled on PND3 or PND4. Though only female pups were used in this study, sufficient male pups were kept in order to maintain a constant litter size of 8. The pups were subjected to stereotaxic surgery on PND7, and at 21 days of age the pups were weaned and the females were housed 4 per cage for one month, after which they were housed 2 per cage. The rats were always

housed with other similarly-treated animals. At 6 months of age, they underwent carotid artery occlusion surgery or sham surgery after which they were single-housed. The rats had free access to food and water throughout the experiment. All care and handling of the animals followed established guidelines of the Canadian Council on Animal Care, and the experiment was approved by the Carleton University Animal Care Committee.

3.2.2. Cholinergic Lesion

On PND7, the pups underwent stereotaxic surgery to infuse either the cholinotoxin 192S (Advanced Targeting Systems, San Diego, CA), or vehicle (10mM pH 7.2 PBS) into the lateral ventricles. Pups were removed from the home cage 4 at a time and brought to the surgical suite, where they were placed on a heating pad. Each pup was anaesthetized using isoflurane/oxygen, then placed in a plaster mould mounted on a stereotaxic frame. One ear was punched for rat identification. A dorsal midline incision was made in the scalp and tissue overlying the skull was blunt deflected. Two holes were drilled in the skull at +/- 1.8 mm lateral to Bregma. A needle attached to a 5 μ l syringe (Hamilton, Reno, NV) was lowered to a depth of 3.5 mm ventral to the dura, aimed at the lateral ventricles. 1.5 μ l of 0.2 μ g/ μ l 192-IgG-saporin was infused into each ventricle (300 ng per ventricle) over 2 minutes. The needle was left in place for a further 2 minutes to allow the solution to diffuse away from the injection site, then slowly retracted to prevent the toxin from being drawn back up into the needle tract. The incision was closed using tissue adhesive (Vetbond, 3M, London, ON), and the pup was placed with its littermates on a heating pad. When all pups had regained consciousness, they were placed back in the home cage.

3.2.3. Carotid Artery Occlusion (2VO)

At six months of age, the rats underwent 2VO or sham surgery. Anaesthesia was initiated with 4% isoflurane in oxygen, then maintained using 1.75-2% isoflurane for the duration of the surgery. After making a ventral midline incision, the musculature overlying the carotid sheath was dissected apart, and the carotid artery was carefully separated from the vagus nerve. Two lengths of 4-0 silk thread were placed around each carotid artery, then knotted twice. The small space between the two tied threads on each carotid artery was examined to ensure that it lost colour after carotid ligation, indicating that blood flow through the carotid had indeed been prevented. The fascia was then sutured with absorbable sutures and the skin was closed using nylon thread. Bupivacaine was applied to the wound, and the rat was allowed to recover on a heating pad set at medium temperature for a minimum of 2 hours following surgery. One week later the sutures were removed under light isoflurane anaesthesia.

3.2.4. Open Field

The rats were exposed to a novel open field 48, 72 and 96 hours after carotid artery surgery. The open field consisted of a white plexiglass floor divided into 25 squares of equal size, surrounded by wooden walls painted white. Each rat was placed into the centre of the open field, then allowed to explore for 10 minutes. Behaviour was recorded using an overhead camera connected to the SMART tracking system (San Diego Instruments, San Diego, CA). Total distance travelled and number of lines crossed were recorded, along with the latency to enter the centre squares of the apparatus, the number

of entries into the centre and the distance travelled in the centre. Open field behaviour was again evaluated on three consecutive days 2 months after 2VO surgery.

3.2.5. Elevated Plus

Two weeks after carotid artery surgery, each rat was placed on an elevated plus maze for 10 minutes in a novel testing room. The maze was elevated 50cm above the ground, and consisted of four 45cm arms at 90° angles to each other. The two closed arms were made of grey plexiglass and were surrounded by 40cm high walls. The two open arms were constructed of white plexiglass, and were not walled. An overhead camera connected to a television was used so that the experimenter could watch the rat's behaviour without being visible to the rat. The number of closed and open arm entries as well as the number of vertical stretches, head dips, and stretch-attend postures were recorded. An arm entry was counted when all four of the animal's paws crossed the line dividing the arm from the central hub. Stretch-attend postures were counted when the animal stretched its head into the central hub or an open arm while standing in a closed arm.

3.2.6. Water Maze Testing

Beginning three weeks after carotid artery occlusion or sham surgery, the rats were tested in a working memory version of the Morris water maze. The pool was a white plastic cylinder fitted with a black plastic insert, measuring 162 cm in diameter, and filled to a depth of 61cm with room temperature water (22°C). The pool was located in a room with several extra-maze visual cues (black cut-outs and posters on the walls, a computer monitor, racks, sink, etc) to facilitate spatial navigation. On each day of testing

a platform was hidden in the pool 2cm below the water level. A different platform location was used on each of the five days of testing but was constant for each of the five daily trials. Each trial began with the rat being placed in a new start position around the perimeter of the maze, and the rat was then allowed 90 seconds to find the platform. If the rat failed to find the platform, it was gently guided to the platform by the experimenter. After each trial, the rat remained on the platform for 30 seconds before beginning the next trial. The latency to find the platform as well as the path length for each trial were recorded using an overhead video camera connected to the SMART tracking system (San Diego Instruments). Three days after completing working memory training, the rats were given a cued platform training session in which a large visual cue was hung from the ceiling directly above the platform. The rats were given 5 trials (90 seconds per trial) to swim to the platform. This was done to rule out the possibility that visual, motor, or motivational factors influenced performance during the working memory portion of training.

The working memory component of the maze was repeated 11 and 27 weeks after surgery to assess memory at increasing post-surgical intervals.

3.2.7. Pupillary Reflex

Since carotid artery occlusion results in degeneration of the retina and visual impairments in some rats (Stevens et al., 2002; Davidson et al., 2000), we tested pupillary reflexes at 5 and 28 weeks after 2VO or sham surgery. Both the direct and consensual pupillary responses to light were tested. The rats were thoroughly dark-adapted before testing began. An ophthalmoscope was held up to one eye, and the amount of time required for the pupil to fully constrict was recorded, to a maximum of 30 seconds. In

general the response either occurred quickly (within 10 seconds) or did not occur at all. The consensual response was then verified by quickly examining the other eye (which had not been exposed to the light) to determine whether the pupil had also constricted. The rats were fully dark-adapted again before testing the direct and consensual response of the other eye.

3.2.8. BrdU Administration

One week after the last training session on the water maze, the rats received 2 doses of 5-bromo-2-deoxyuridine (BrdU; 200mg/kg in 0.9% saline, intraperitoneal) spaced 24 hours apart. BrdU is not highly soluble, and large volumes of saline are required to achieve a dose of 200mg/kg. Therefore, in order to minimize discomfort to the rats, the total 200mg/kg dose was divided amongst two injections spaced one hour apart (each 100mg/kg; 37.5mg/ml). The rats were then left undisturbed (except for cage changing) for 28 days.

3.2.9. Tissue Collection

At the age of 13 months, the rats were given an overdose of sodium pentobarbital, and transcardially perfused with 100ml of heparinized saline. The brains were removed, taking care to avoid touching the brain with metal instruments, and bisected using a glass coverslip. The right hemisphere was quickly placed in 4% PFA in PB, and the left hemisphere was placed in Golgi fix (0.01% mercuric chloride, 0.01% potassium dichromate and 0.008% potassium chromate in distilled water; Glaser and Van der Loos 1981).

The right hemispheres were left in PFA overnight, then rinsed several times in PB

containing azide. They were then cut on a vibratome (World Precision Instruments, Sarasota, FL). Since different types of staining required different tissue thicknesses, the brains were cut into series of eight 50 μ m sections followed by two 100 μ m sections.

3.2.10. Verification of the Cholinergic Lesion

The first 50 μ m section from each series was stained for AChE. Floated sections containing the hippocampus were rinsed in 0.1M sodium acetate, then incubated overnight in a reaction solution of 0.68% sodium acetate, 0.1% cupric sulfate, 0.12% glycine and 0.1% acetylthiocholine iodide in distilled water, pH 5.0. The next day the sections were rinsed in sodium acetate, then developed in 1% sodium sulphide, pH 7.5 for 10 minutes. After rinsing in sodium acetate, the sections were washed in distilled water, mounted, air dried overnight, then dehydrated, cleared and coverslipped.

Sections containing the MS and diagonal band of Broca were immunohistochemically stained for p75^{NTR}, a nerve growth factor receptor that serves as a marker of forebrain cholinergic neurons. Briefly, sections were rinsed in 10mM PBS, then incubated overnight in a solution containing an antibody directed against p75^{NTR} (1:2000; Millipore, Temecula, CA), lambda carrageenan, bovine serum albumin and triton-X (Sigma, St. Louis, MO). On the following day the sections were incubated for 2 hours in biotinylated anti-mouse secondary antibody (1:100; GE Healthcare, Piscataway, NJ) followed by a 2-hour incubation in streptavidin-biotinylated horseradish-peroxidase complex (1:100; GE Healthcare). The sections were then reacted in DAB and hydrogen peroxide to visualize the antibody complex. The sections were mounted on gel-coated slides, air-dried, counterstained with pyronin Y, dehydrated, cleared and coverslipped. The number of p75+ cells was rated on a 4-point scale (1=complete loss of cells

compared to control, 2=moderate loss of cells compared to control, 3=slight loss of cells compared to control, and 4=no loss of cells compared to control). Rats with a rating of 3 or 4 were discarded from the study. As in experiment #1, cholinesterase-stained sections were used to confirm the lesion.

3.2.11. CA1 Pyramidal Cell Counts

The second 100 μ m-thick section from each series of sections (essentially yielding a 1 in 6 series of sections) was mounted onto gel-coated slides immediately after cutting, and allowed to air dry. The following day, the slides were progressively dehydrated by successive 2-minute washes in 70% ethanol, 95% ethanol and 100% ethanol, then placed in clearene for 3 minutes. The sections were then rehydrated in decreasing concentrations of ethanol. After a wash in distilled water, the sections were placed in 1% cresyl violet for 3 minutes, then rinsed twice in distilled water. Following a wash in 95% ethanol, the sections were placed in a mixture of 70% chloroform/30% ethanol, then washed once again in 95% ethanol followed by two rinses in distilled water. After sitting in differentiator for three minutes, the slides were dehydrated, cleared and coverslipped.

The number of CA1 pyramidal cells in cresyl-violet stained sections was counted stereologically using the optical fractionator function of StereoInvestigator software (MBF Biosciences, Williston, VT). Cells were counted in a three-dimensional 18 μ m x 18 μ m x 10 μ m box placed randomly within each square of a 75 x 75 μ m grid overlying the entire CA1 area of each tissue section.

3.2.12. GFAP Staining and Analysis

Astrocytic activation is a commonly used indicator of neural damage. To assess the astrocytic response to 2VO and cholinergic lesion, 7 sections from each brain containing the dorsal hippocampus were immunohistochemically stained to detect GFAP. Free-floating sections were rinsed three times in PBS with azide, blocked in 0.3% hydrogen peroxide, then rinsed a further three times in PBS with azide. The sections were incubated in primary mouse anti-GFAP antibody (1:600; Sigma, St. Louis, MO) at 4°C overnight, then thoroughly rinsed in PBS with azide before being incubated with anti-mouse secondary antibody (1:100; GE Healthcare) at room temperature. Following this 2-hour incubation, the sections were again rinsed in PBS, and incubated in streptavidin-biotinylated horseradish peroxidase complex (1:100; GE Healthcare) for 2 hours at room temperature. After rinsing in PBS, a DAB reaction was performed. The sections were then mounted on gelatin-coated slides, allowed to dry overnight, counterstained in pyronin Y, dehydrated, cleared and coverslipped. Sample photomicrographs showing GFAP staining can be found in Appendix 1 (Figure A1.7).

For each of the 7 sections examined from each rat, the entire CA1, CA3, DG and hilar areas were photographed. Images were obtained using an Olympus BX-51 microscope with a 20x objective coupled to StereoInvestigator software (MBF Biosciences). Using the thresholding function of ImageJ software (National Institutes of Health, Bethesda, MD) the percent area immunoreactive for GFAP was calculated for each image. These values were averaged across all images for each hippocampal sector to obtain an overall measure of astrocytic activation.

3.2.13. Ki-67 Staining and Analysis:

Seven 50 μ m sections spanning the hippocampus were chosen for detection of Ki-67, a marker of cell proliferation. The staining protocol was identical to that used for GFAP immunohistochemistry. The sections were incubated in primary anti-Ki-67 antibody (1:500; clone MIB-5; Dako, Mississauga, ON) at 4°C overnight, followed by 2-hour incubations in biotinylated anti-mouse secondary antibody (1:100; GE Healthcare) and streptavidin-biotinylated horseradish peroxidase complex (1:100; GE Healthcare) with rinsing between each incubation. A DAB reaction was performed to visualize the antibody complex, and the sections were counterstained in pyronin Y for 2 minutes before being dehydrated, cleared and coverslipped.

3.2.14. Doublecortin Staining and Analysis

In order to assess the number of newly born immature neurons in the dentate gyrus of the hippocampus, 50 μ m sections were immunohistochemically stained to detect doublecortin (DCX), a protein expressed in the adult brain by migrating neuroblasts (Brown et al., 2003b). Seven sections spanning the entire hippocampus were chosen from each brain. Free-floating sections were rinsed three times in PBS with azide, then blocked in 0.3% hydrogen peroxide, and rinsed a further three times in PBS with azide. After a 30 minute incubation in 3% normal horse serum (Vector Laboratories, Burlingame, CA), the sections were again rinsed, and incubated in primary goat anti-DCX antibody (1:200; Santa Cruz Biotechnology, Santa Cruz, CA) at room temperature overnight. The sections were then thoroughly rinsed in PBS with azide before being incubated in anti-goat secondary antibody (1:100; Vector Laboratories) at room temperature. Following this 2-hour incubation, the sections were again rinsed in PBS, and incubated in streptavidin-biotinylated horseradish peroxidase complex (1:100; GE Healthcare) for 2 hours at room

temperature. After rinsing in PBS, a 3,3-diaminobenzidine reaction was performed. The sections were then mounted on gelatin-coated slides, allowed to dry overnight, counterstained in pyronin Y (Sigma, St. Louis, MO), dehydrated, cleared and coverslipped.

DCX-positive cells in the dorsal and ventral dentate gyrus were counted manually on an Olympus BX-51 microscope with a 20x objective lens.

3.2.15. BrdU Staining and Analysis

The survival of newly born cells was assessed by immunohistochemical detection of BrdU 28 days after its incorporation into proliferating cells. Six free-floating hippocampal sections from each brain were stained to detect BrdU. The sections were rinsed in PBS with azide three times, then placed in 0.3% hydrogen peroxide to block endogenous peroxidases. Following three PBS rinses, the sections were placed in 2N HCl at 37°C for 60 minutes to denature the DNA. The sections were then neutralized in 0.1M boric acid buffer, pH 8.5 before being rinsed in PBS. The sections were then incubated in anti-BrdU antibody (1:500; Sigma, St. Louis, MO) at room temperature overnight. The following day, the sections were rinsed and incubated in anti-mouse secondary antibody (1:100; GE Healthcare) for 2 hours at room temperature, then rinsed again and incubated in streptavidin-biotinylated horseradish peroxidase complex (1:100; GE Healthcare) at room temperature for a further 2 hours. A DAB reaction was then performed, and the sections were mounted onto gelatin-coated slides and allowed to air dry overnight. The sections were then counterstained in pyronin Y before being dehydrated, cleared and coverslipped.

BrdU positive cells were counted manually in the dentate gyrus, hilus, CA1 and CA3 areas of the dorsal hippocampus using an Olympus BH-2 microscope with a 20x objective.

3.2.16. Golgi Analysis

The left hemisphere of each brain was left in Golgi solution for 14 days, then rinsed three times in distilled water, once for four hours, once for three hours, and the third time overnight. The brains were transferred to a 10% sucrose solution for 8 hours, then into a 20% sucrose solution overnight. The next day they were transferred to 30% sucrose for storage. After a minimum of 4 days in 30% sucrose, the brains were sliced on a vibratome (World Precision Instruments) at a thickness of 200 μ m, and mounted immediately on 2% gelatin-dipped slides. The sections were stored in a humidifying plastic box for up to five days, then stained. After a brief wash in distilled water, the sections were placed in ammonium hydroxide for 40 minutes, washed in distilled water, then incubated in diluted film fix (Kodak, Toronto, ON) for 40 minutes. The sections were then washed twice in distilled water, dehydrated in ethanol, cleared, and coverslipped with Permount (Fisher, Ottawa, ON).

The cell bodies and entire apical and basal dendritic fields of CA1 pyramidal cells from the dorsal hippocampus were traced using NeuroLucida software (MBF Biosciences) and an Olympus BX-51 microscope with a 100x oil objective. Cells within the middle third of the tissue section were chosen, and only cells with the entire dendritic structure contained within the three-dimensional space of a single section were traced. Additionally, only cells whose dendrites could clearly be distinguished from those of neighbouring cells were chosen. In total, 10 cells from each brain were traced.

NeuroLucida Explorer (MBF Biosciences) was used to obtain data on total dendritic length, dendritic branching and total number of spines and spine density.

3.3. Results

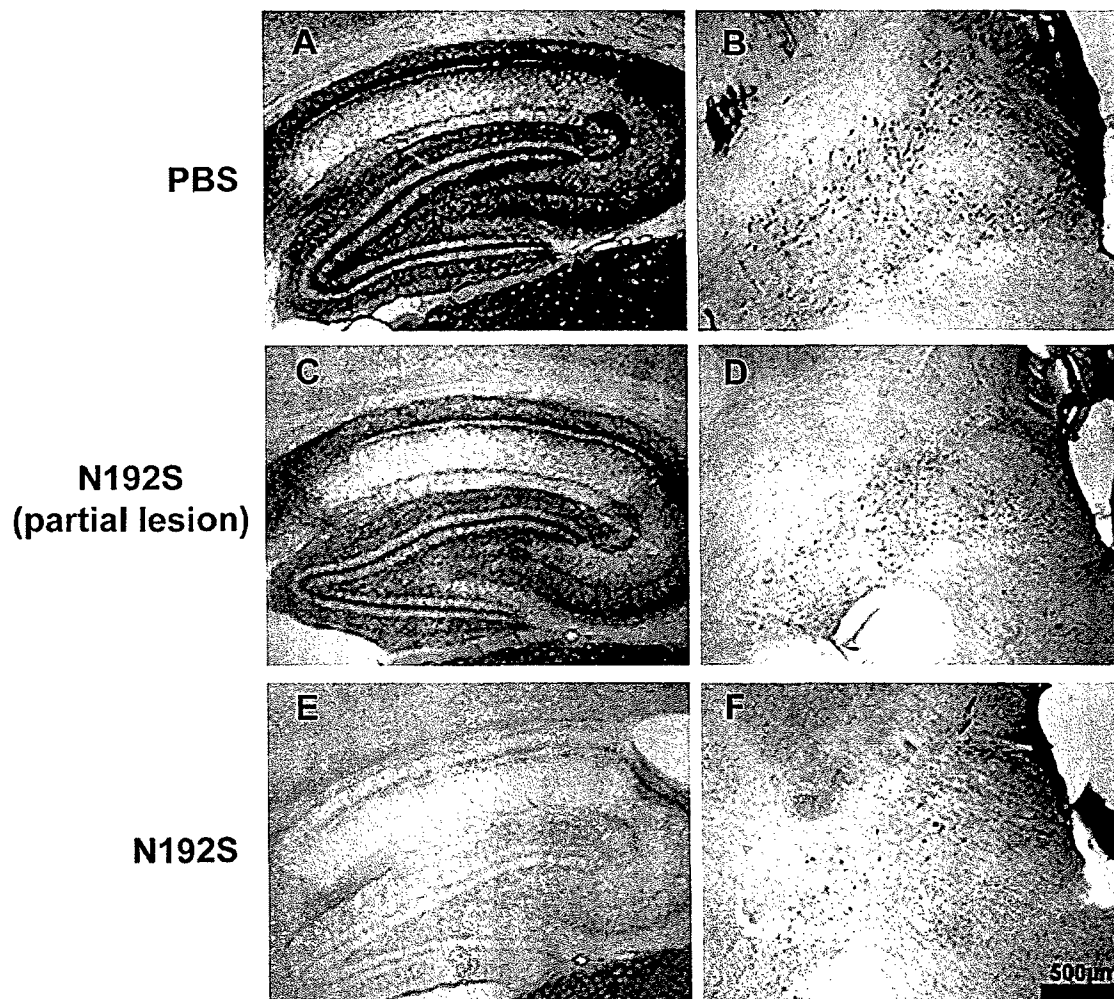
3.3.1. General

Two rats in the PBS-2VO group and one in the N192S-2VO group lost the pupillary reflex in both eyes and their behavioural data were therefore discarded, although the brains were used for histological assessment. A subset of the rats was tested only on the open field and the first two rounds of the water maze, and was sacrificed after the second round of water maze testing. The brains of these animals were not used for histological purposes, except to confirm the lesion. AChE and p75 staining were performed on tissue from all animals, revealing that six rats in the N192S-2VO group and five rats in the N192S-Sham group did not show a satisfactory lesion. The behavioural data from these animals were discarded, and their brains were not used for histological purposes. The final number of animals included in the first two runs (3 and 11 weeks post-surgery) of the water maze and the open field, the third run (27 weeks) of the water maze and elevated plus maze, and histological assessment, respectively, were as follows: PBS-injected rats subjected to sham occlusion (CONT; n=13, n=8 and n=8); PBS-injected rats subjected to carotid artery occlusion (2VO; n=10, n=6, and n=8); neonatal cholinergic lesioned rats subjected to sham occlusion (N192S; n=9, n=5 and n=5); N192S rats subjected to 2VO (DUAL; n=9, n=7 and n=7).

Figure 3.1 shows representative photomicrographs of hippocampal sections stained for cholinesterase and sections of the MS and diagonal band

Figure 3.1: Verification of the cholinergic lesion. Representative sections of the hippocampus stained for acetylcholinesterase (left) and sections of the diagonal band of Broca stained for p75 (right) from a PBS rat (A and B), a N192S rat showing an unsatisfactory lesion (C and D) and a N192S rat showing a satisfactory lesion (E and F).

Verification of the Cholinergic Lesion AChE and p75 Staining



immunohistochemically stained for p75 from a control animal (panels A and B), and a N192S animal showing a satisfactory lesion (panels E and F). Panels C and D show cholinesterase and p75 staining for a N192S animal showing an unacceptable lesion.

3.3.2. Open Field

The rats were exposed to a novel open field 48, 72 and 96 hours after carotid artery occlusion or sham surgery, and 2 months after surgery they were again exposed to the open field on three consecutive days. The data were analyzed using a repeated measures ANOVA with postsurgical interval (2 days or 2 months) and day (day 1,2 or 3) as within-subjects factors and lesion (N192S or PBS) and occlusion (2VO or sham) as between-subjects variables. Neither N192S nor 2VO affected the total distance travelled or the number of lines crossed, and there was no N192S by 2VO interaction effect on these measures (see Figures 3.2 and 3.3). However, there was a significant postsurgical interval by day by lesion interaction for both distance ($F_{2,74}=4.54$, $p=.014$) and line crosses ($F_{2,74}=4.29$, $p=.017$). On average, N192S animals travelled a significantly shorter distance in the inside squares ($F_{1,37}=6.36$, $p=.017$; see Figure 3.4), made fewer entries into the centre ($F_{1,37}=6.85$, $p=.013$; see Figure 3.5), and were slower to make an initial entry into the centre ($F_{1,37}=5.52$, $p=.024$; see Figure 3.6). Individual two-way ANOVAs on each of the six exposures to the open field indicated that the N192S effects on the number of entries into the centre and the distance travelled in the inside squares were not significant on the first day of testing at each postsurgical interval, but were evident with repeated exposure. In contrast, the lesion significantly increased the latency to enter the centre on the first and third days of testing, but not thereafter. 2VO had no effect on any

Figure 3.2: Distance travelled in the open field. The main effects of N192S and 2VO were both nonsignificant, as was the N192S by 2VO interaction effect. The postsurgical interval by day by lesion interaction effect was significant ($F_{2,74}=4.54$, $p=.014$).

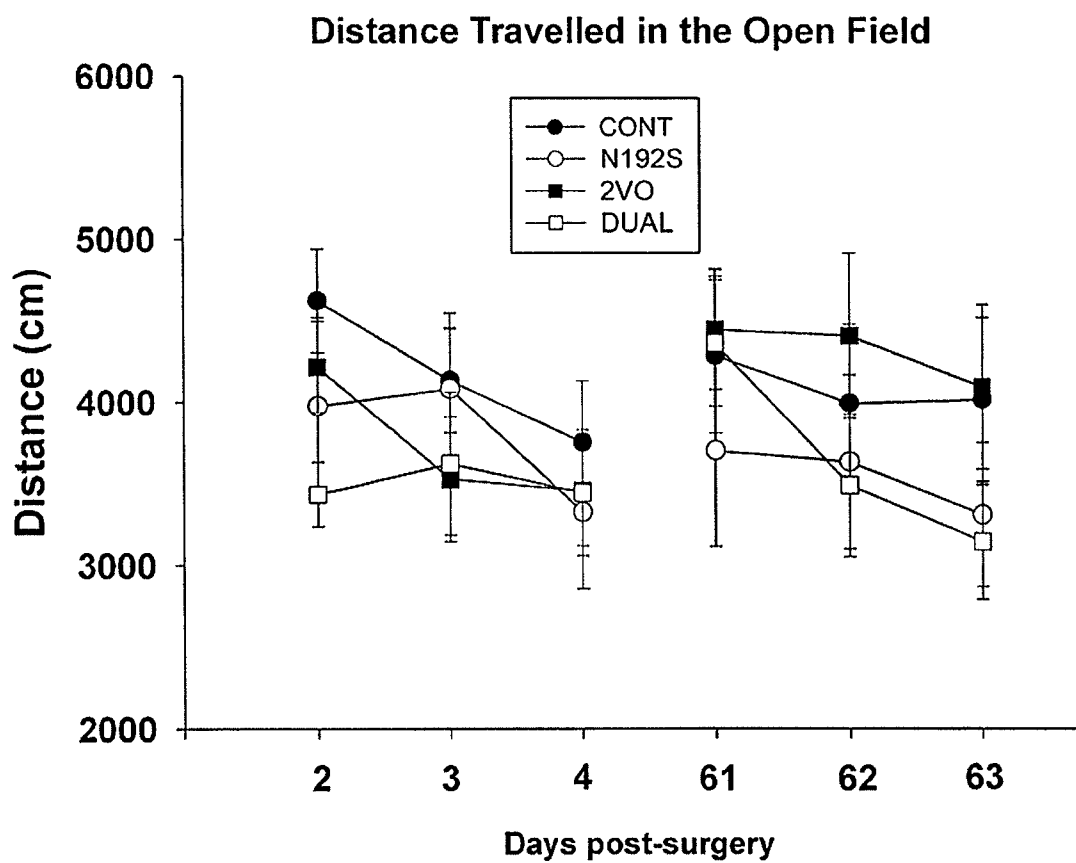


Figure 3.3: Number of lines crossed in the open field. The main effects of N192S and 2VO were both nonsignificant, as was the N192S by 2VO interaction effect. The postsurgical interval by day by lesion interaction effect was significant ($F_{2,74}=4.29$, $p=.017$).

Lines Crossed in the Open Field

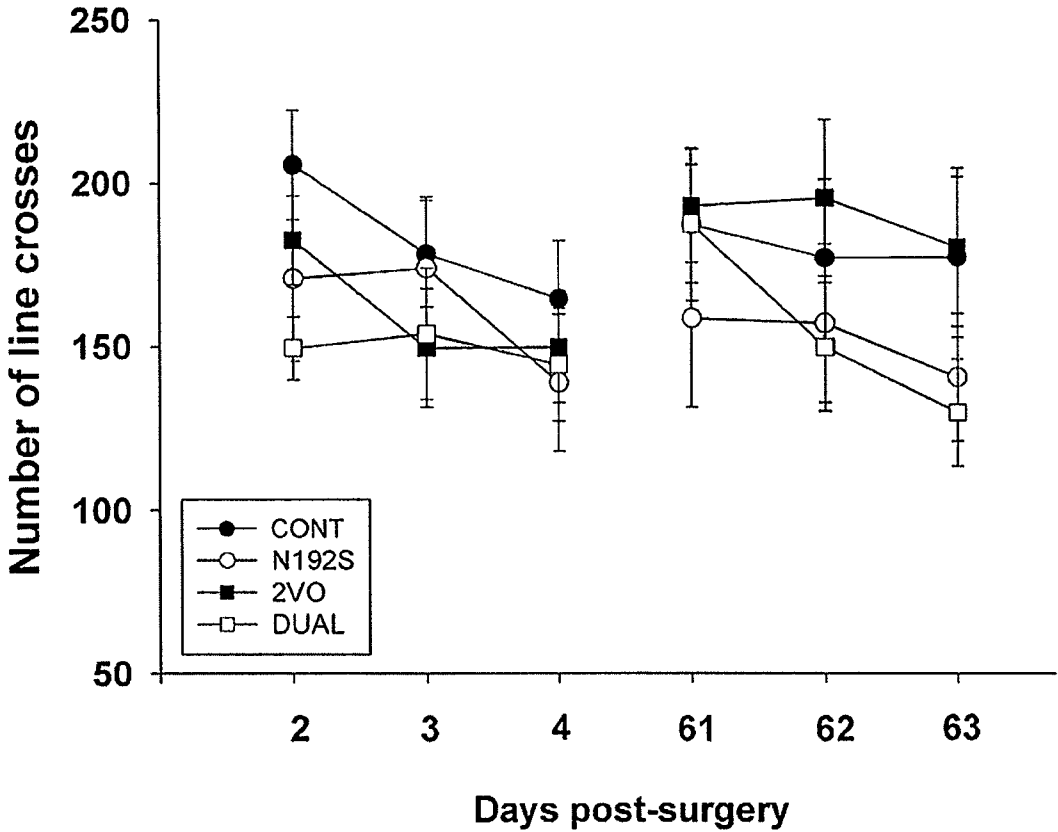


Figure 3.4: Distance travelled in the inner squares of the open field. N192S significantly reduced the distance travelled in the inner squares ($F_{1,37}=6.36$, $p=.017$). ‘*’ denotes a significant difference between combined PBS groups and combined N192S groups ($p<.05$).

Distance Travelled in the Inside Squares of the Open Field

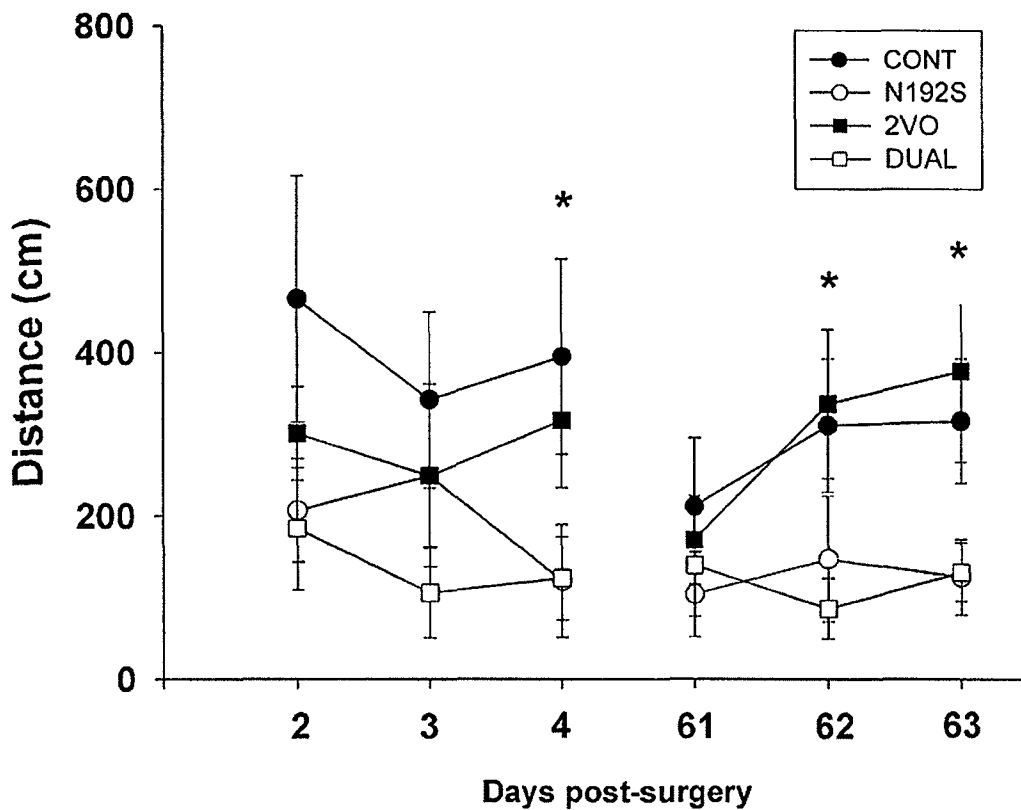


Figure 3.5: Number of entries into the central area of the open field. N192S significantly reduced the number of centre entries ($F_{1,37}=6.85$, $p=.013$). '*' denotes a significant difference between combined PBS groups and combined N192S groups ($p<.05$).

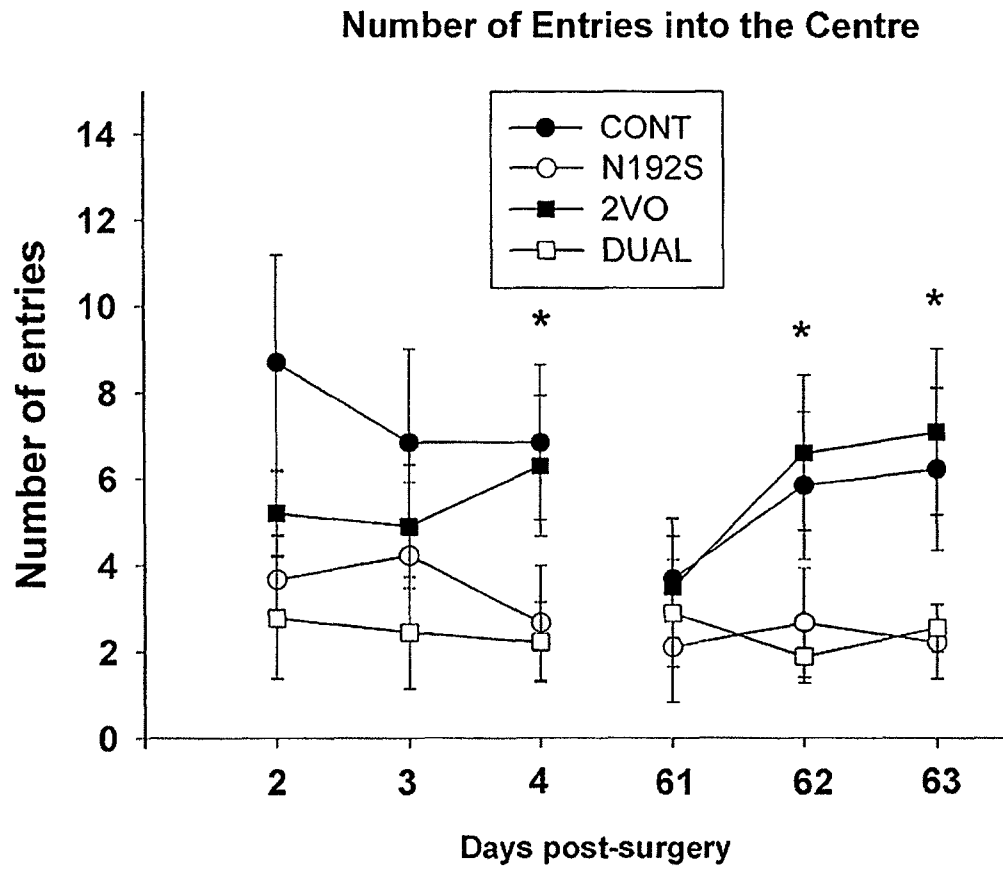
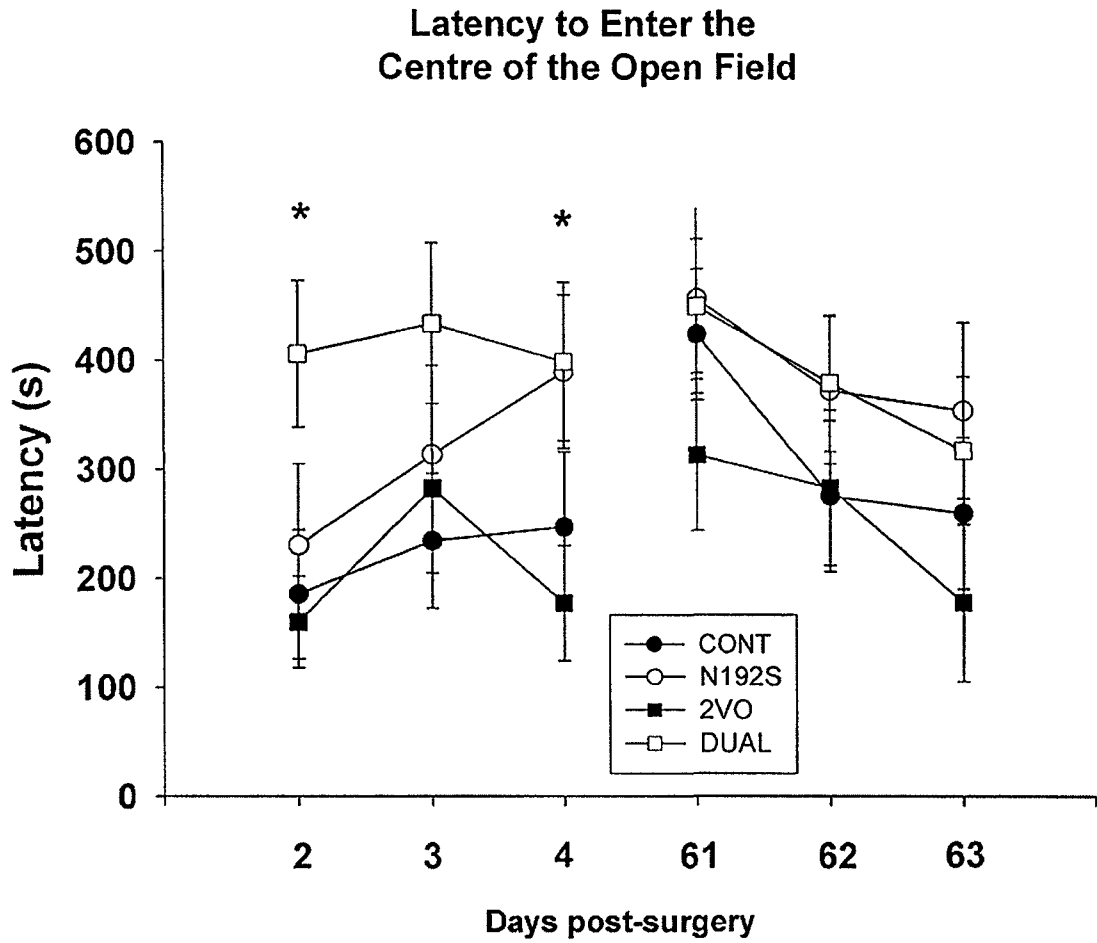


Figure 3.6: Latency to enter the central area of the open field during each exposure. N192S rats were slower to enter the central area ($F_{1,37}=5.52$, $p=.024$). ‘*’ denotes a significant difference between combined PBS groups and combined N192S groups ($p<.05$).



of these measures, and there were no overall 2VO by N192S interaction effects.

3.3.3. Elevated Plus

In order to explore the idea that the N192S animals displayed more anxiety-like behaviour, the rats were given a 10-minute exposure to an elevated plus maze in a novel testing room. The data were analyzed using two-way ANOVAs, with N192S and 2VO as the independent variables. Overall, there was a tendency for N192S rats to make fewer entries into the open arms which just missed significance ($F_{1,23} = .3.84, p=.062$). The N192S x 2VO interaction was significant ($F_{1,23} = 4.37, p<.05$). Further analysis of the data using a one-way ANOVA with post hoc Tukey test showed that the dual rats made significantly fewer open arm entries than rats subjected to 2VO alone ($p=.034$) while none of the other groups were significantly different from each other (see Figure 3.7). The number of closed arm entries did not differ between groups, nor did the number of vertical stretches or stretch-attend postures (all p 's $>.05$). However, N192S significantly reduced the number of head-dips ($F_{1,23} = 5.59, p<.03$; see Figure 3.8). These data further suggest that N192S, and in particular N192S in combination with 2VO caused rats to display more anxiety-like behaviour without affecting overall activity levels.

3.3.4. Water Maze

Latency and path length to find the platform were recorded for each trial. A repeated measures ANOVA was performed for each of the three runs on the water maze, with days and trials as within-subjects variables and lesion (PBS vs. N192S) and 2VO (sham vs. 2VO) as between-subjects variables.

3.3.4.1. Run 1 (3 weeks post-surgery)

Figure 3.7: Number of entries into the open (top panel) and closed (bottom panel) arms of the elevated plus maze. A significant N192S by 2VO interaction effect on open arm entries ($F_{1,23} = 4.37, p < .05$) was due to an increased number of open arm entries by 2VO rats compared to DUAL rats. The groups did not differ in terms of the number of closed arm entries.

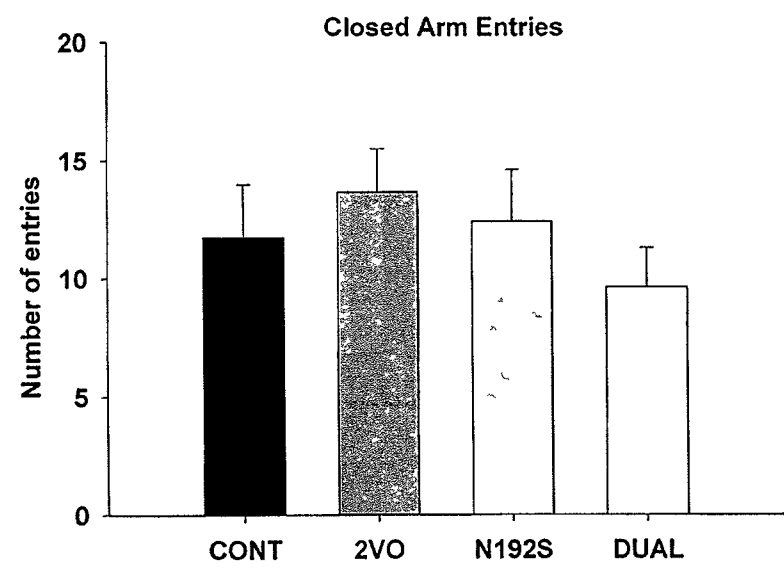
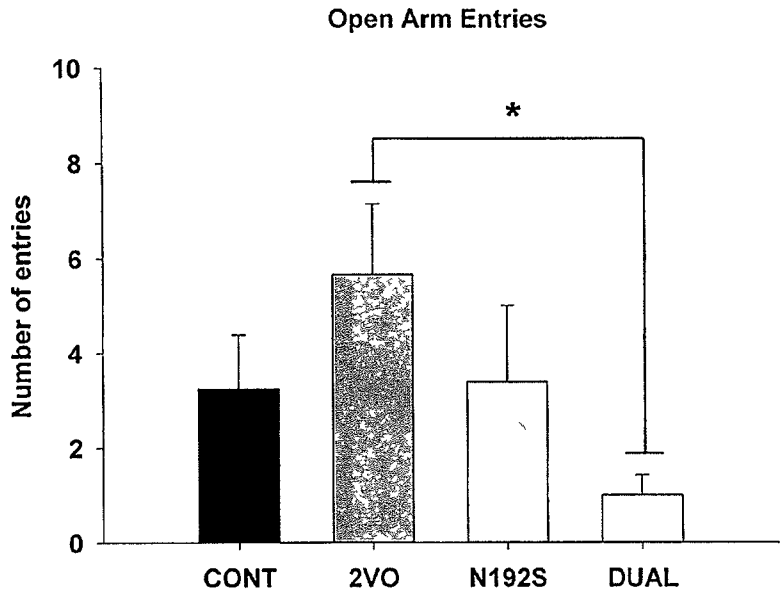
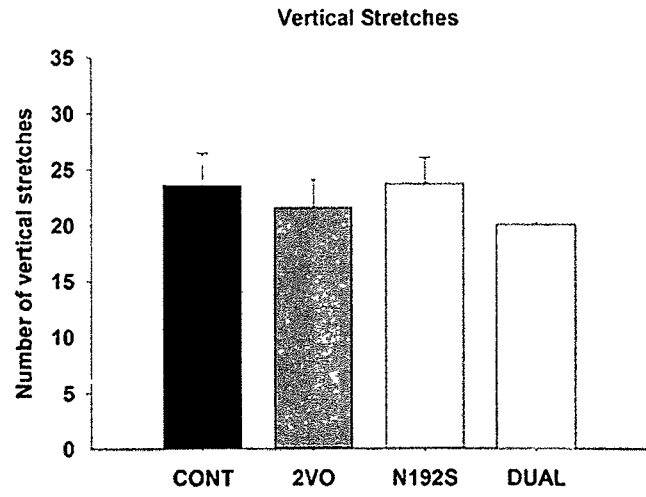
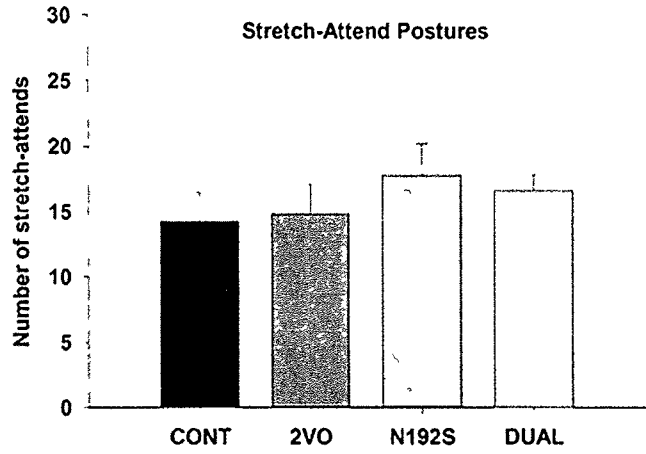
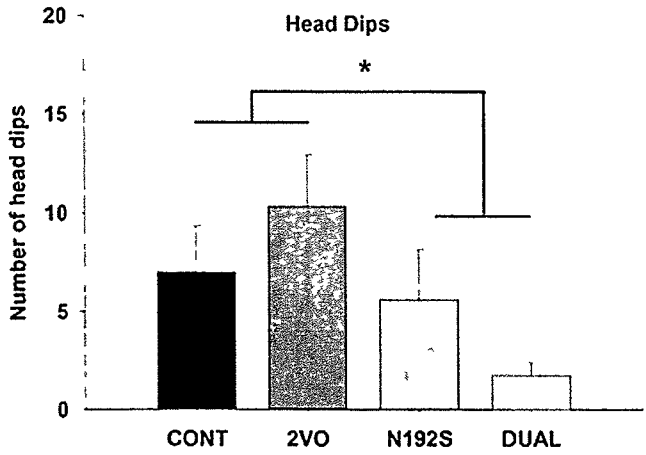


Figure 3.8: Number of head dips (top panel) stretch-attend postures (middle panel) and vertical stretches (bottom panel) on the elevated plus maze. N192S significantly reduced the number of head dips ($F_{1,23} = 5.59, p < .03$).



Overall there were no significant main effects of lesion or 2VO and no lesion by 2VO interaction effect on either path length or latency to find the platform. However, the analysis revealed a significant trial by lesion interaction effect on both path length ($F_{4,148}=4.26, p=.003$) and latency ($F_{4,148}=8.96, p<.001$), indicating that learning across the five trials within a day differed between the groups. On 19 out of 25 trials (76% of trials), the dual rats required the longest swim distances to find the hidden platform. A nonparametric binomial test for proportions indicated that this is a significantly greater proportion than would be expected by chance (25%; $p<.001$). Furthermore, individual one-way ANOVAs with post-hoc Tukey tests on each trial revealed that only the dual-treated group ever differed significantly from controls on any single trial in terms of swim distance (trial 1 on day 1, $p=.022$; trial 2 on day 5, $p=.011$) and latency (trial 1 on day 1, $p=.007$; trial 3 on day 2, $p=.046$ and trial 2 on day 5, $p=.007$). These data are depicted in Figures 3.9 (swim distance) and 3.10 (latency). Overall swim speed was not affected by the lesion ($F_{1,37}=.755, p=.39$) or by 2VO ($F_{1,37}=.761, p=.389$), and there was no lesion by 2VO interaction ($F_{1,37}=1.543, p=.222$). However, both the day by lesion ($F_{4,148}=4.078, p=.004$) and trial by lesion ($F_{4,148}=3.736, p=.006$) interactions were significant, indicating that N192S affected swim speeds only on certain days or trials. Individual two-way ANOVAs on each trial showed that N192S rats swam more slowly on trial 3 of day 2 ($F_{1,37}=5.442, p=.025$), trial 4 of day 2 ($F_{1,37}=4.318, p=.045$), trial 3 of day 3 ($F_{1,37}=5.94, p=.02$), and trial 5 of day 3 ($F_{1,37}=4.396, p=.043$), but swam more quickly on trial 2 of day 5 ($F_{1,37}=6.21, p=.017$). These data are shown in Figure 3.11.

3.3.4.2. Run 2 (11 weeks post- surgery)

Similar to the Run 1 data, there was a significant trial by lesion effect on both

Figure 3.9: Path length to find the hidden platform during the first run of the water maze (3 weeks post-surgery). There was a significant trial by N192S interaction effect ($F_{4,148}=4.26$, $p=.003$), indicating that learning across the 5 trials within a day differed between the groups. ‘*’ denotes trials on which DUAL rats differed significantly from CONT rats.

Water Maze Run 1: 3 Weeks Post-Surgery Path Length

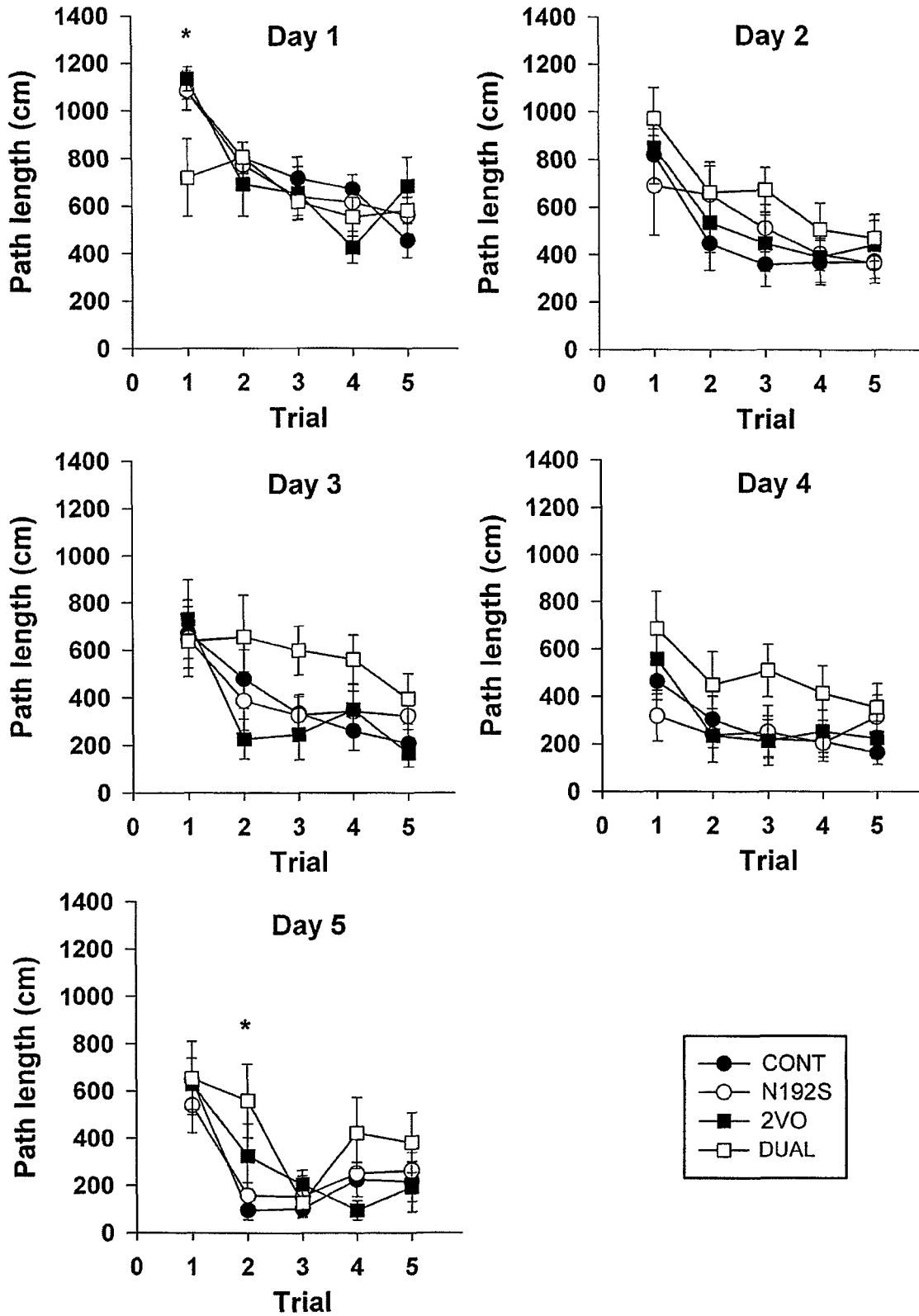


Figure 3.10: Latency to find the hidden platform during the first run of the water maze (3 weeks post-surgery). There was a significant trial by N192S interaction effect ($F_{4, 148} = 8.96, p < .001$), but no main effects of N192S or 2VO. ‘*’ denotes trials on which DUAL rats differed significantly from CONT rats.

**Water Maze Run 1: 3 Weeks Post-Surgery
Platform Latency**

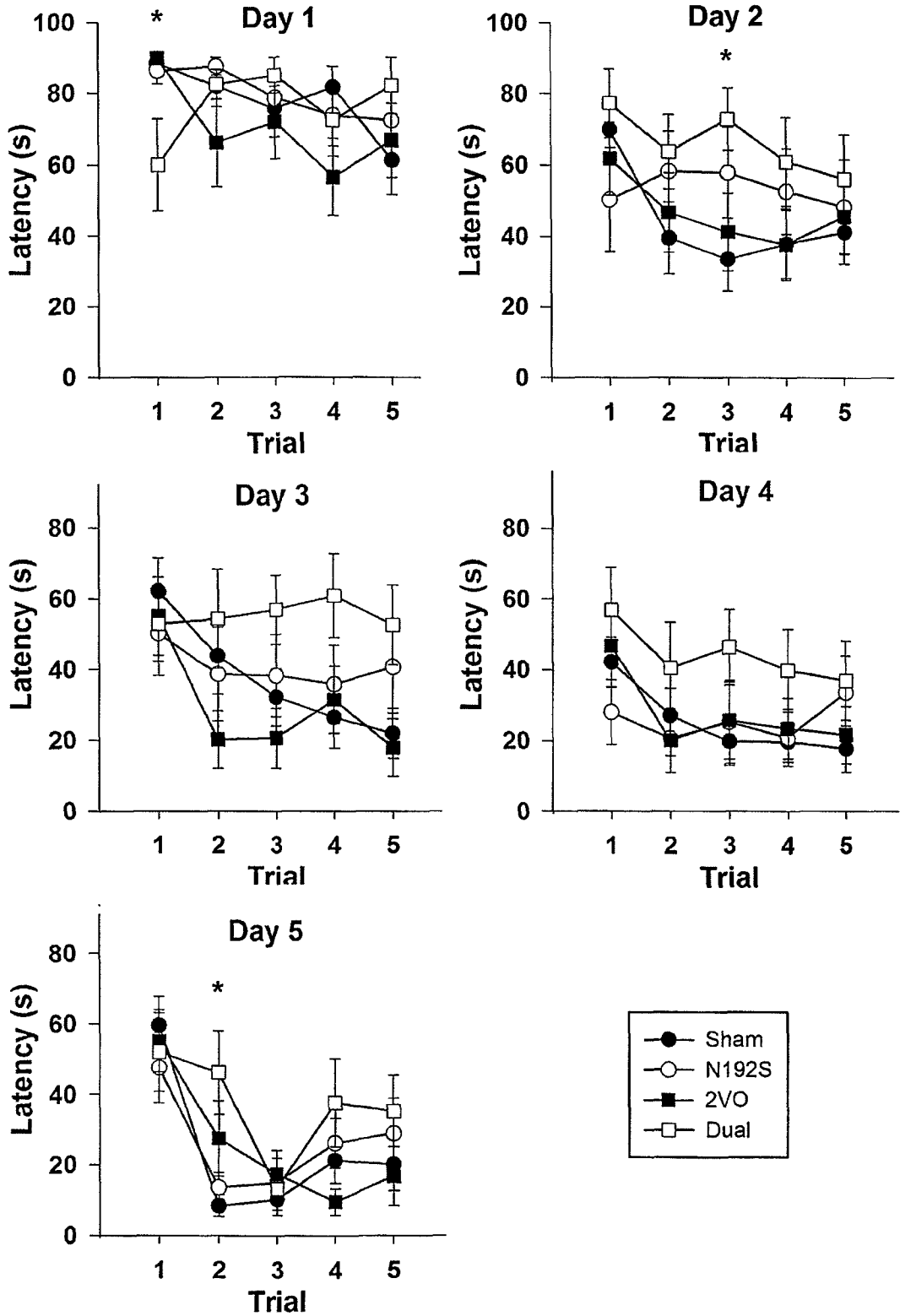
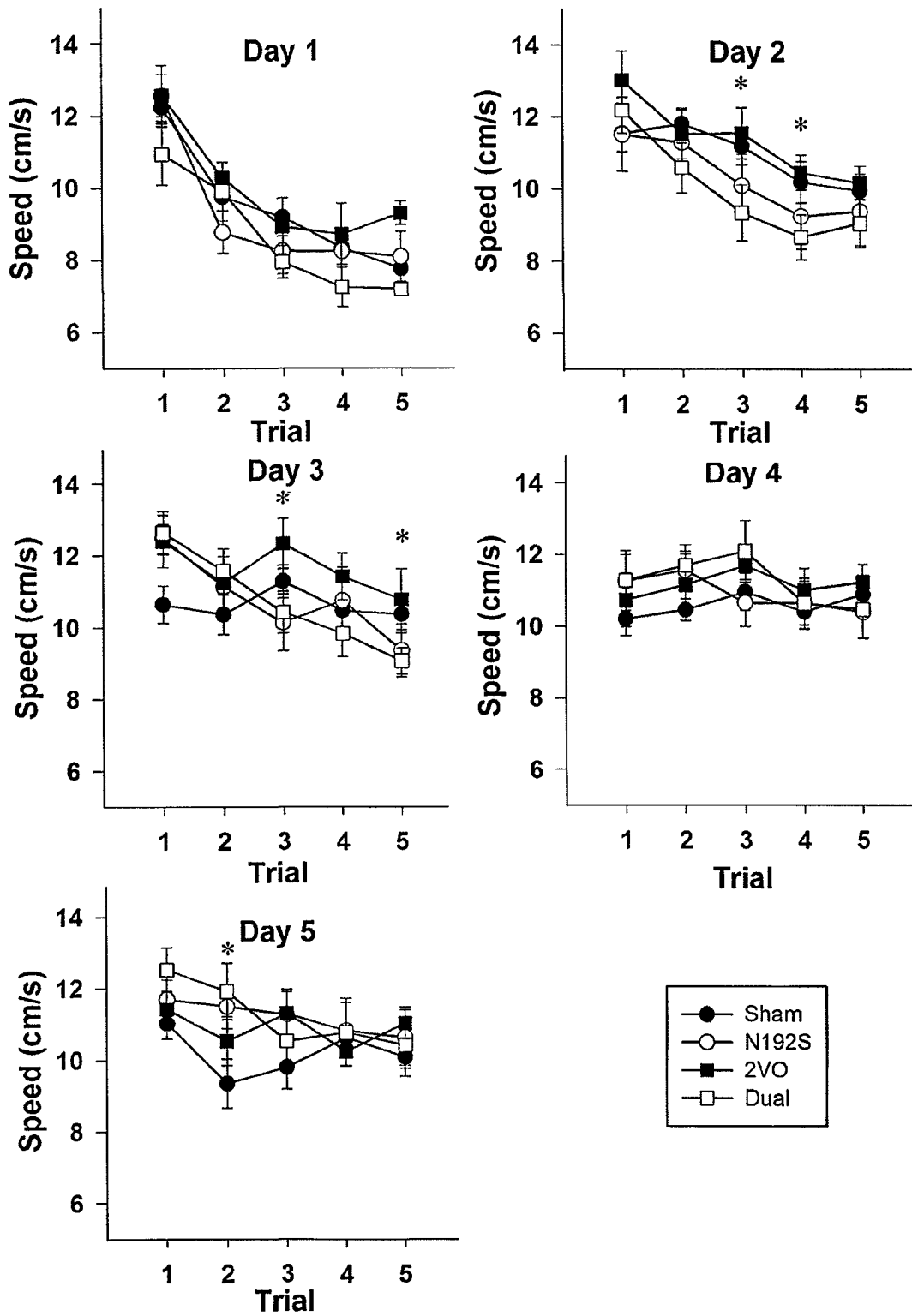


Figure 3.11: Swim speed during the first run of the water maze (3 weeks post-surgery). The main effects of N192S and 2VO, as well as the N192S by 2VO interaction were all nonsignificant, but the day by lesion ($F_{4,148}=4.078$, $p=.004$) and trial by lesion ($F_{4,148}=3.736$, $p=.006$) interaction effects were significant. ‘*’ denotes trials on which average swim speed for the combined N192S groups differed from the combined PBS groups.

Water Maze Run 1: 3 Weeks Post-Surgery Swim Speed



path length ($F_{4,148}=3.743$, $p=.006$) and latency to find the platform ($F_{4,148}=4.37$, $p=.002$), but no main effects of N192S or 2VO, and no N192S by 2VO interaction. Again, on 76% of trials the dual treated rats showed the poorest performance, which is a significantly greater proportion than would be expected by chance ($p<.001$). Dual-treated rats required significantly longer swim distances than controls on trial 5 of day 2 ($p=.042$), trial 3 of day 3 ($p=.047$) and trial 5 of day 5 ($p=.019$), and longer latencies on trial 2 of day 2 ($p=.026$), trial 5 of day 2 ($p=.013$), trial 3 of day 4 ($p=.03$) and trial 5 of day 5 ($p=.015$). The N192S ($F_{1,37}=.635$, $p=.431$), 2VO ($F_{1,37}=.077$, $p=.783$), and N192S by 2VO interaction effects ($F_{1,37}=.022$, $p=.884$) on swim speed were all nonsignificant, and there were no day or trial interaction effects (all p 's $>.05$). Figures 3.12, 3.13, and 3.14 show the Run 2 distance, latency, and swim speed data.

3.3.4.3. Run 3 (27 weeks post-surgery)

The overall N192S, 2VO, and N192S by 2VO interaction effects on both path length and latency were all nonsignificant (all p 's $>.05$). Only the day by trial by N192S by 2VO effect was significant, for both distance ($F_{16,352}=1.92$, $p=.018$) and latency ($F_{16,352}=1.90$, $p=.019$). N192S-sham rats differed significantly from PBS-sham rats on trial 1 of day 1 ($p=.048$ for distance, $p=.051$ for latency). There were no significant group differences on any other individual trial. While there were no overall effects of lesion ($F_{1,22}=.006$, $p=.93$) or 2VO ($F_{1,22}=.531$, $p=.474$) on swim speed, the N192S by 2VO interaction effect was significant ($F_{1,22}=4.599$, $p=.043$). Averaging the swim speed across all 25 trials indicated that N192S-sham animals swam the fastest, while N192S-2VO animals were the slowest swimmers. The water maze data for Run 3 are shown in Figures 3.15 (distance), 3.16 (latency) and 3.17 (speed).

Figure 3.12: Path length to find the hidden platform during the second run of the water maze (11 weeks post-surgery). There was a significant trial by N192S interaction effect ($F_{4,148}=3.91$, $p=.005$), indicating that learning across the 5 trials within a day differed between the groups. ‘*’ denotes trials on which DUAL rats differed significantly from CONT rats.

Water Maze Run 2: 11 Weeks Post-Surgery
Path Length

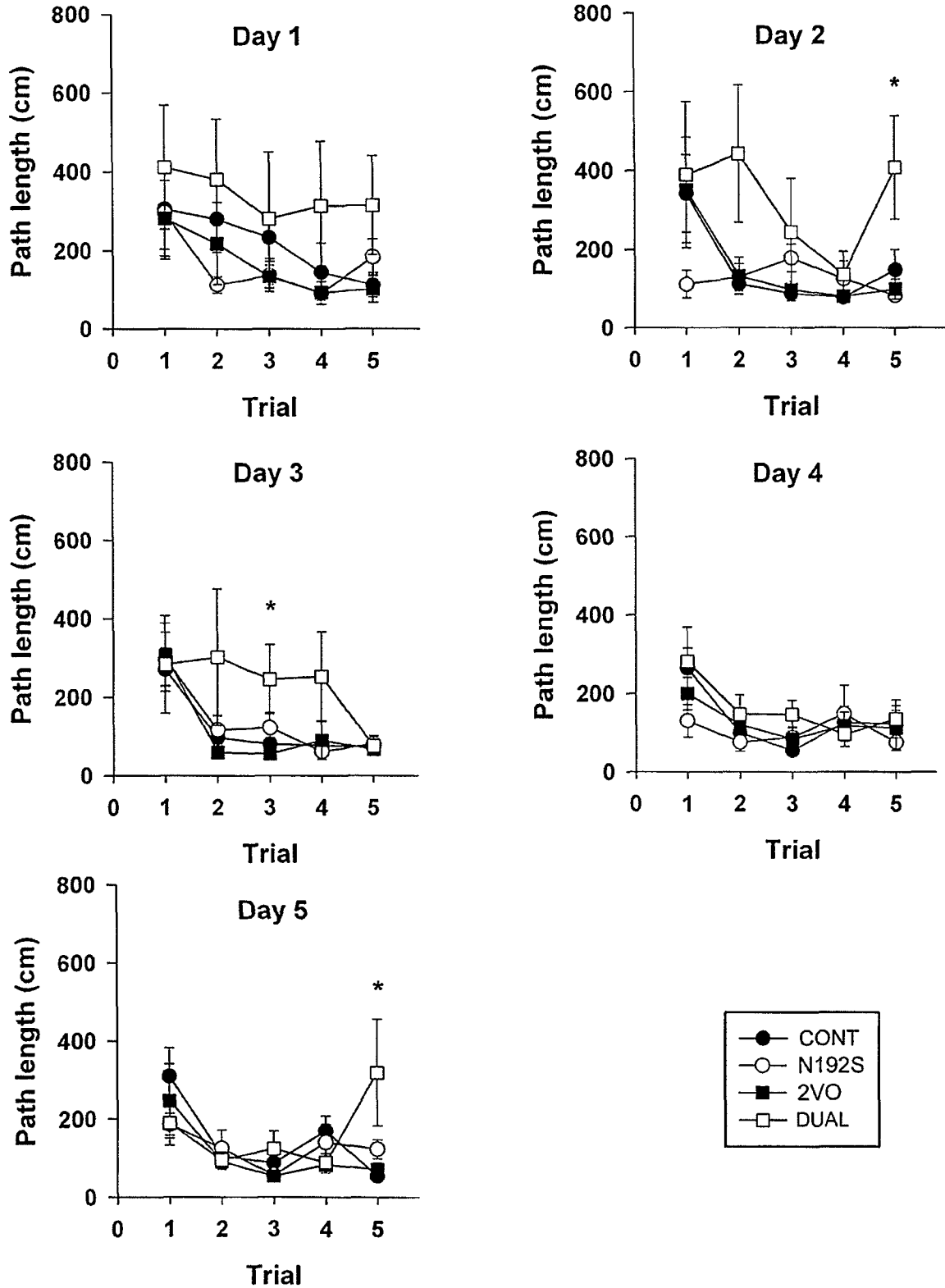


Figure 3.13: Latency to find the hidden platform during the second run of the water maze (11 weeks post-surgery). There was a significant trial by N192S interaction effect ($F_{4,148}=4.37$, $p=.002$), but no main effects of N192S or 2VO. ‘*’ denotes trials on which DUAL rats differed significantly from CONT rats.

**Water Maze Run 2: 11 Weeks Post-Surgery
Platform Latency**

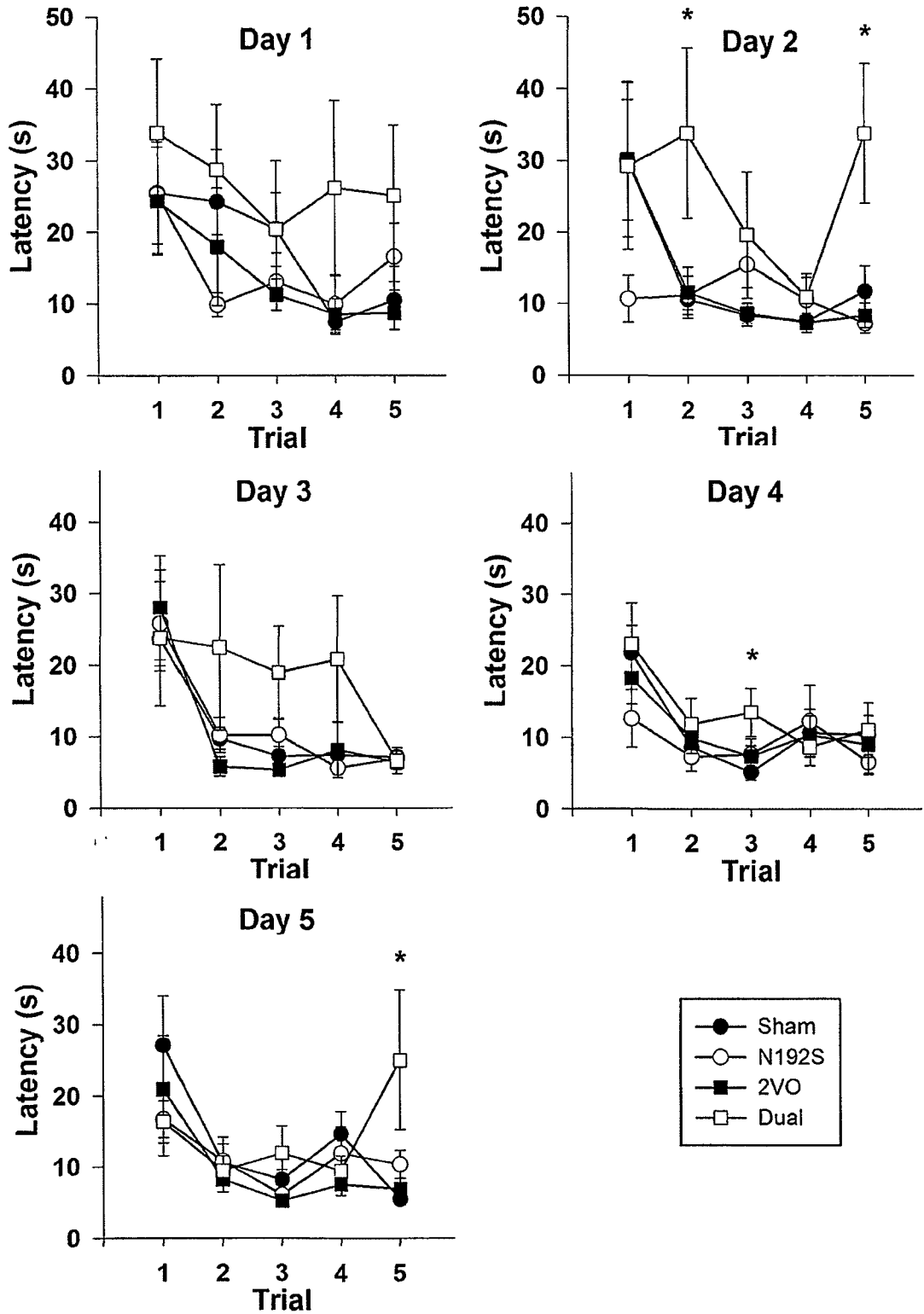


Figure 3.14: Swim speed during the second run of the water maze (11 weeks post-surgery). There were no main effects of N192S or 2VO on swim speed, and no significant interaction effects.

Water Maze Run 2: 11 Weeks Post-Surgery Swim Speed

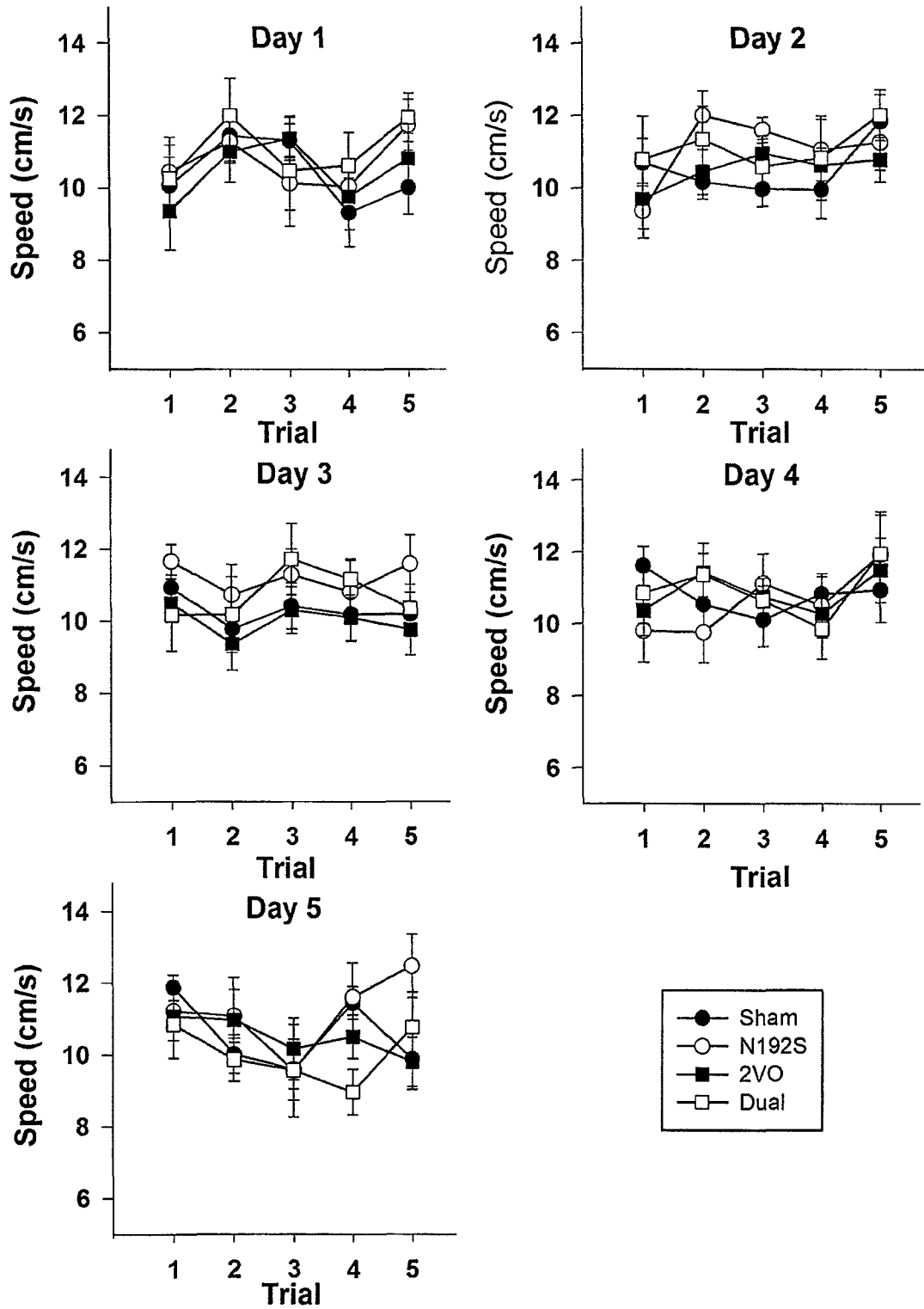


Figure 3.15: Path length to find the hidden platform during the third run of the water maze (27 weeks post-surgery). Only the day by trial by N192S by 2VO effect was significant ($F_{16, 352}=1.92, p=.018$). ‘*’ denotes trials on which N192S rats differed significantly from CONT rats.

**Water Maze Run 3: 27 Weeks Post-Surgery
Path Length**

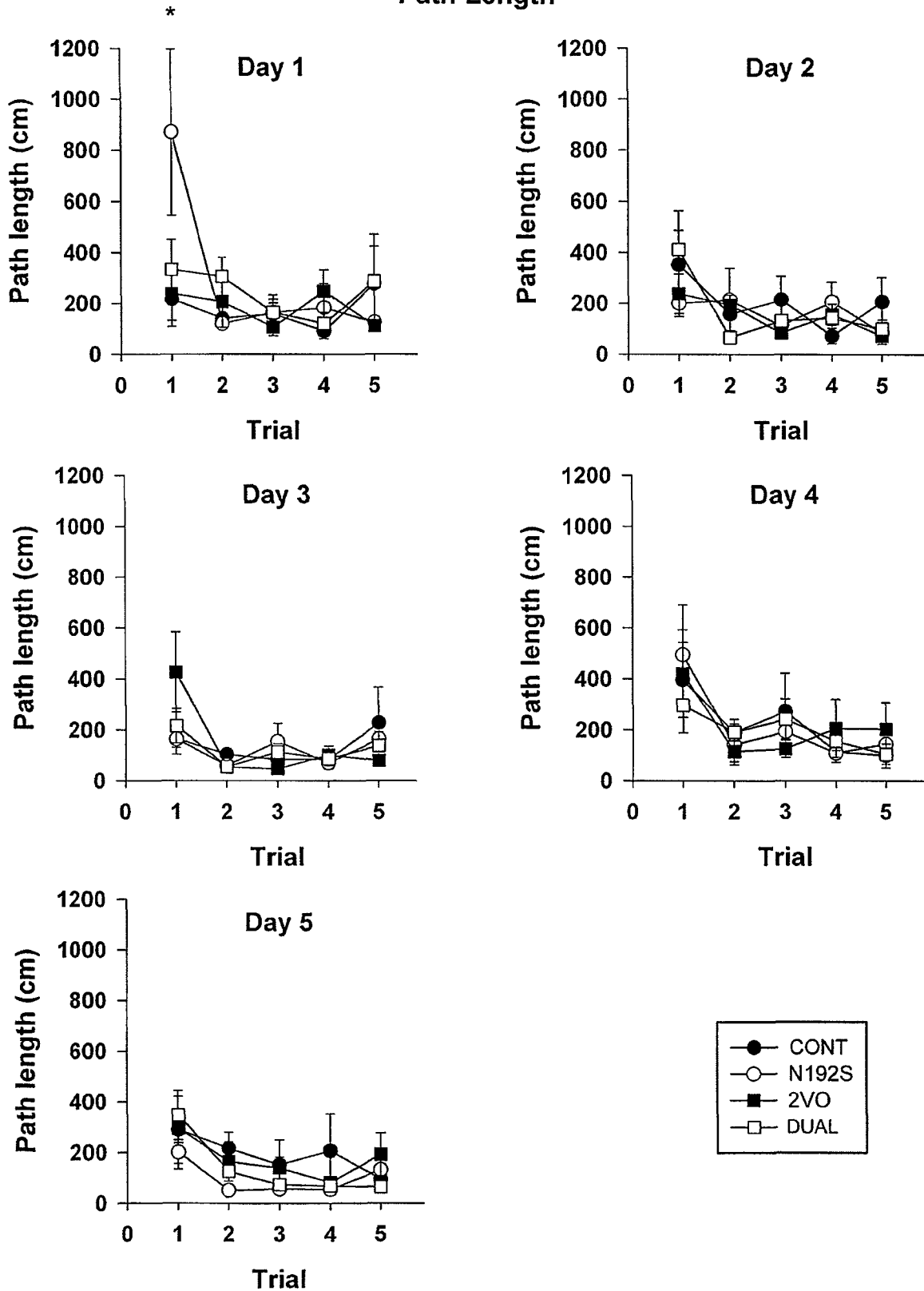


Figure 3.16: Latency to find the hidden platform during the third run of the water maze (27 weeks post-surgery). Only the day by trial by N192S by 2VO effect was significant ($F_{16,352}=1.90$, $p=.019$).

Water Maze Run 3: 27 Weeks Post-Surgery Platform Latency

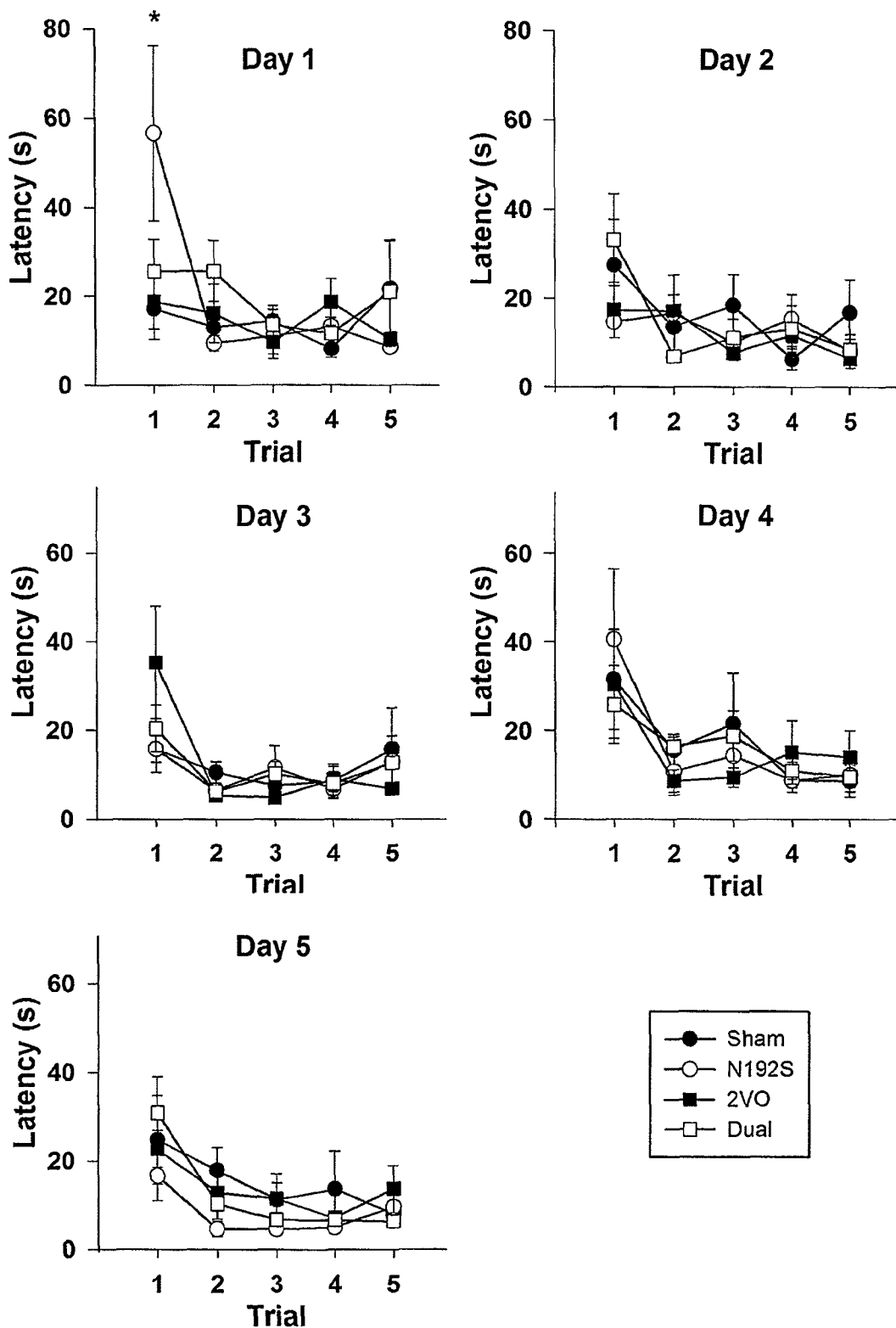


Figure 3.17: Swim speed during the third run of the water maze (27 weeks post-surgery). There was a significant N192S by 2VO interaction effect on swim speed ($F_{1,22}=4.599$, $p=.043$). ‘*’ denotes trials on which there was a significant N192S by 2VO interaction effect, and ‘#’ denotes trials on which there was a significant 2VO effect on swim speed.

Water Maze Run 3: 27 Weeks Post-Surgery
Swim Speed

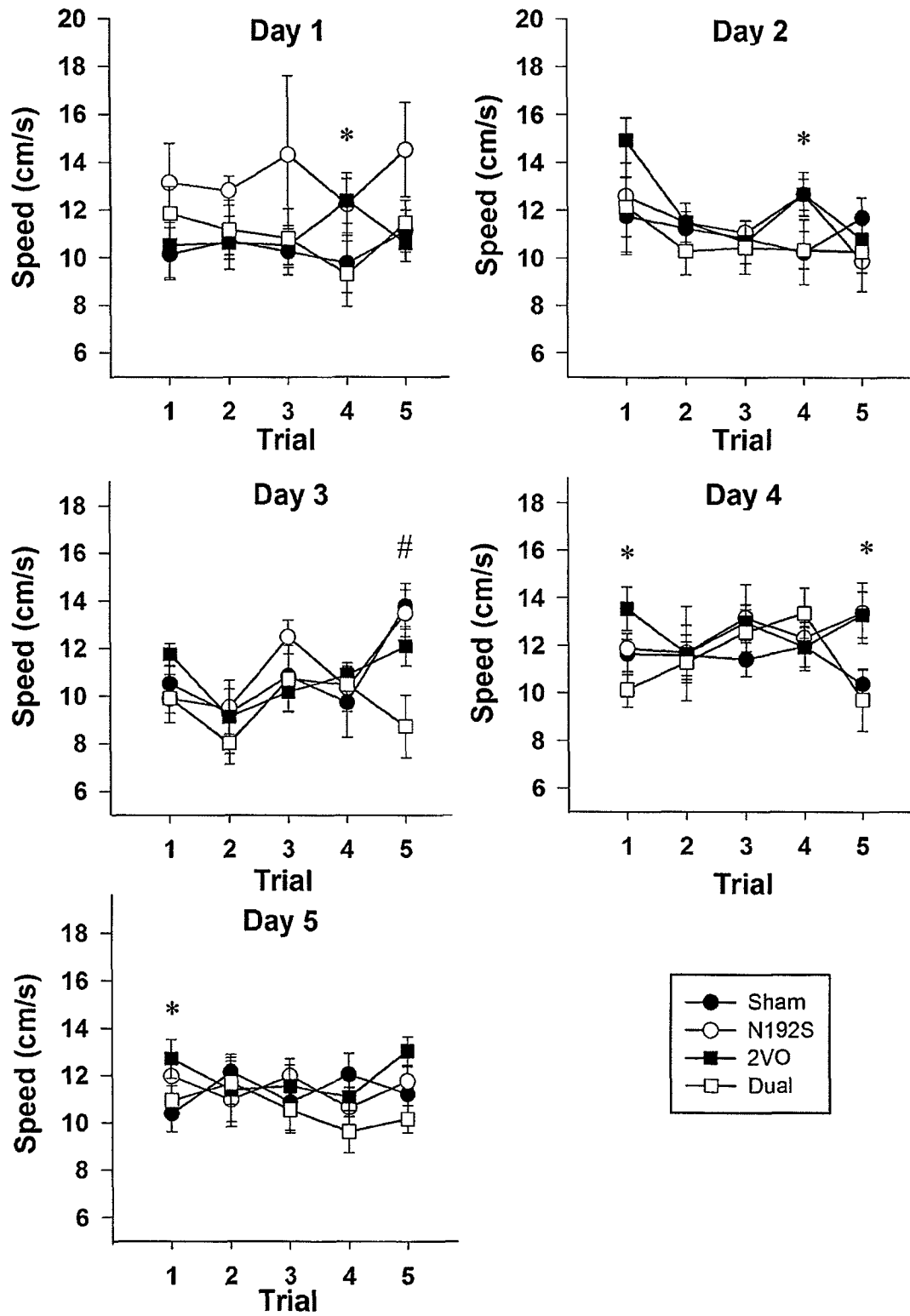
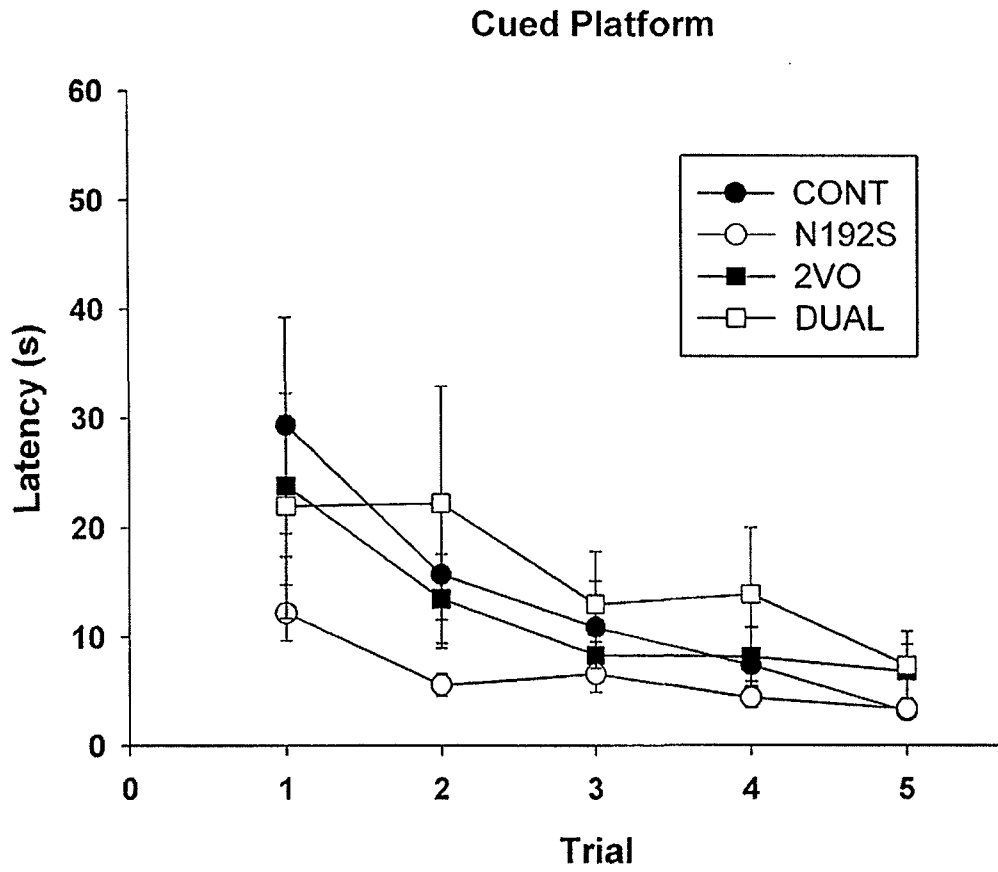


Figure 3.18: Latency to locate the cued platform. There were no group differences in the ability to find a cued platform.



3.3.4.4. Cued Platform

The results of the cued platform test are shown in Figure 3.18. There were no group differences on the latency to find the cued platform, indicating that any effects seen in the working memory version of the maze were unlikely to be due to motivational, visual or motor impairments.

3.3.5. CA1 Cell Number

Stereological counting of pyramidal cells in the CA1 region of the hippocampus revealed no loss of cells due to the cholinergic lesion ($F_{1,23} = .61$, NS) or 2VO ($F_{1,23} = .06$, NS). The N192S by 2VO interaction effect was also not significant ($F_{1,23} = .06$, NS). Figure 3.19 shows the average number of CA1 cells per group.

3.3.6. GFAP Immunoreactivity

Two-way ANOVA of the percent area of CA1, CA3, DG and hilus exhibiting GFAP immunoreactivity showed no effects of either N192S or 2VO in CA1, DG or hilus (all p 's $> .05$). However, N192S treatment increased GFAP staining in CA3 ($F_{1,24} = 4.819$, $p < .04$), while 2VO had no effect in this area. There were no N192S by 2VO interaction effects on GFAP staining in any hippocampal area (all p 's $> .05$). These data are presented in Figure 3.20.

3.3.7. Ki-67 Counts

The number of Ki-67-positive cells in the dorsal and ventral dentate gyrus were counted manually. Two-way analysis of variance indicated no significant effect of either

Figure 3.19: CA1 pyramidal cell number. CA1 cell number was equivalent amongst all groups.

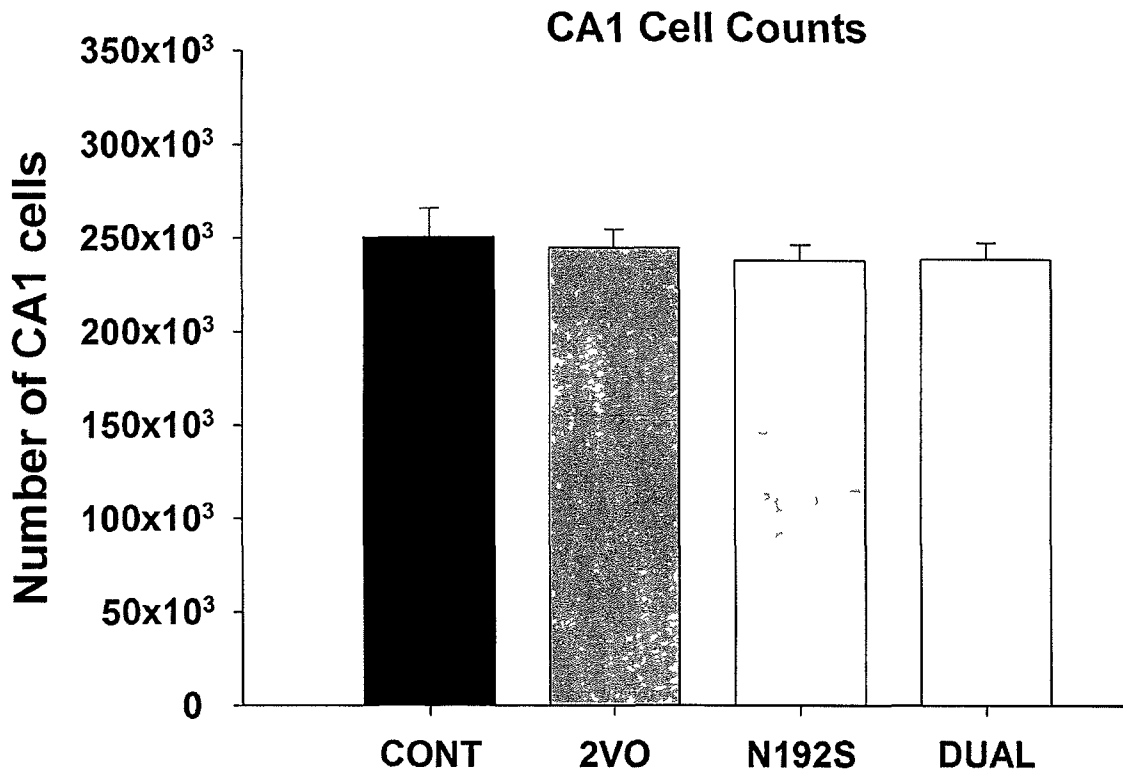
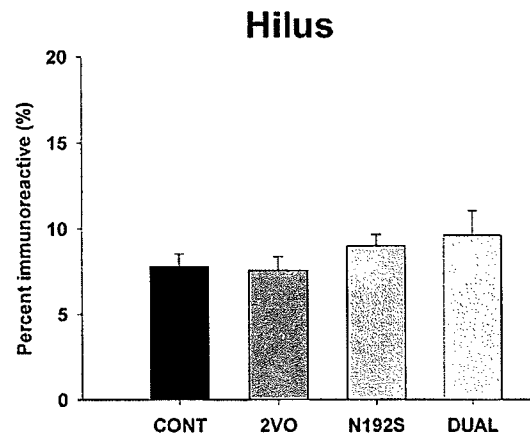
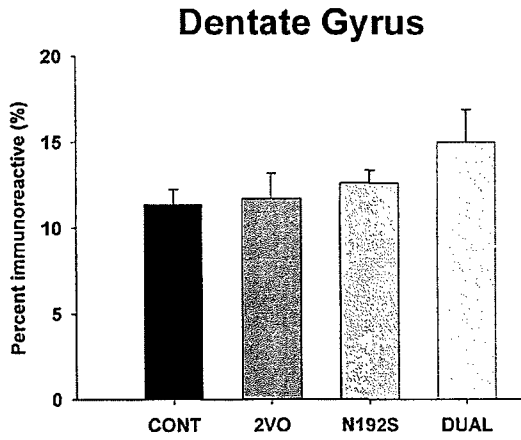
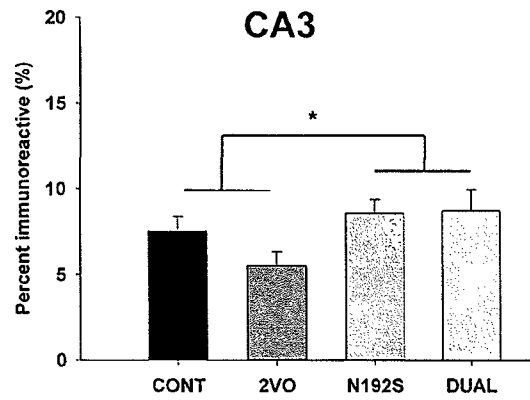
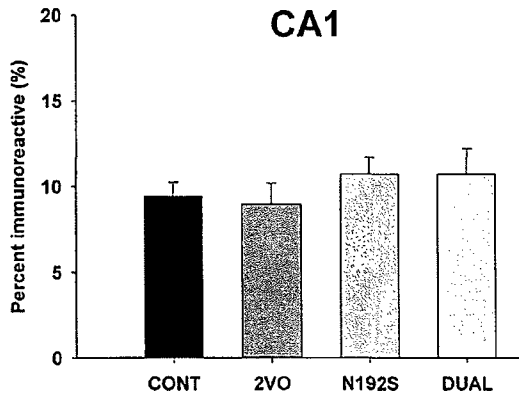


Figure 3.20: GFAP immunoreactivity in the hippocampus. N192S treatment increased GFAP expression in CA3 ($F_{1,24} = 4.819$, $p < .04$), but not in any other hippocampal sector (all p 's $> .05$).

GFAP Immunoreactivity in the Hippocampus



N192S or 2VO on Ki-67 labelled cells in either the dorsal or ventral sector, and no interaction effects (see Figure 3.21).

3.3.8. DCX Counts

As shown in Figure 3.22, manual cell counts of DCX-immunoreactive cells in the dentate gyrus revealed a significant effect of N192S in the dorsal dentate gyrus ($F_{1,24} = 6.14, p = .021$) but not the ventral dentate gyrus ($F_{1,24} = 2.016, p = .169$). Lesioned animals had 21% fewer DCX-positive cells in the dorsal DG compared to control rats. There was no effect of 2VO, and no N192S by 2VO interaction effect in either the dorsal or ventral dentate gyrus.

3.3.9. BrdU Counts

BrdU-positive cells in the dorsal dentate gyrus, hilus, CA1 and CA3 one month after BrdU injection were counted manually. Two-way ANOVAs demonstrated a lack of effect of either N192S or 2VO on the total number of surviving new cells in all four regions examined (see Figure 3.23). However, the effect of 2VO on BrdU cell number in CA3 approached significance ($F_{1,24} = 3.65, p = .068$), with 2VO animals tending to show higher numbers of BrdU-positive cells.

3.3.10. CA1 Pyramidal Cell Morphology

The cell body as well as the complete apical and basal dendritic trees of 10 dorsal CA1 pyramidal cells per brain were traced using NeuroLucida software. Representative cell tracings from each group are shown in Figure 3.24. 2VO significantly increased total apical branch length ($F_{1,18} = 5.24, p = .034$) by 16% and apical spines ($F_{1,18} = 6.45, p = .02$) by

Figure 3.21: Ki-67⁺ cell number in the dorsal (top panel) and ventral (bottom panel) dentate gyrus. All groups had similar numbers of Ki-67-labelled cells in both the dorsal and ventral DG.

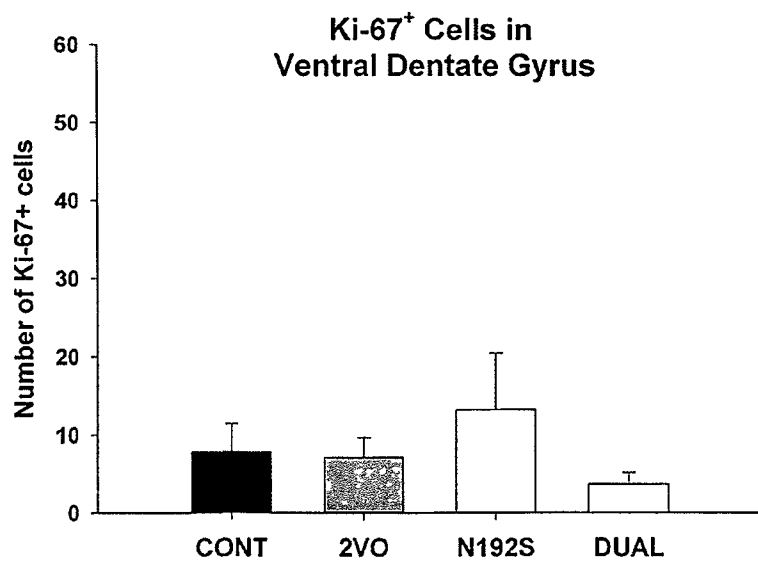
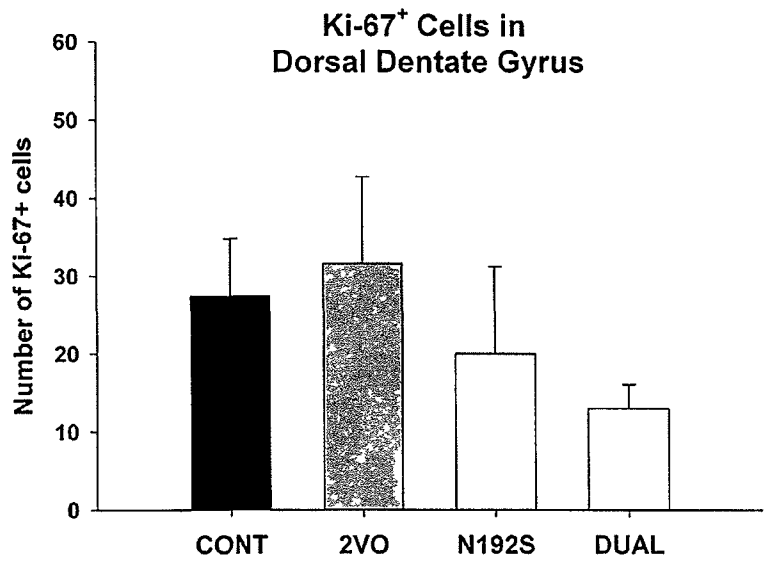


Figure 3.22: DCX⁺ cell number in the dorsal (top panel) and ventral (bottom panel) dentate gyrus. Animals in the combined N192S groups had 21% fewer DCX⁺ cells in the dorsal DG than rats in the combined PBS groups ($F_{1,24} = 6.14, p = .021$). There were no differences in the number of DCX⁺ cells in the ventral DG.

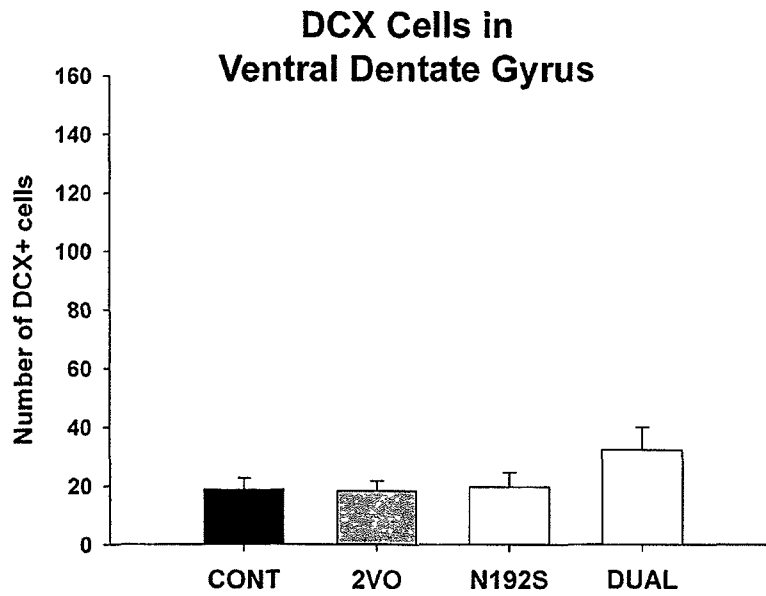
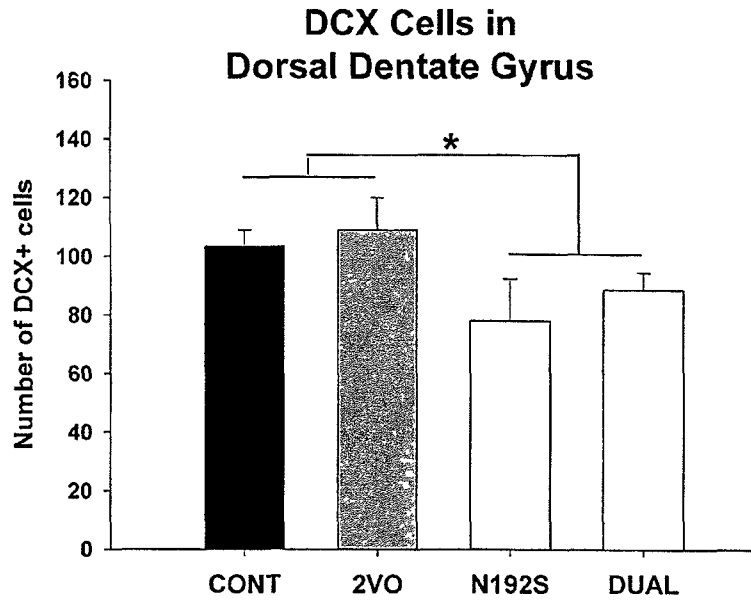
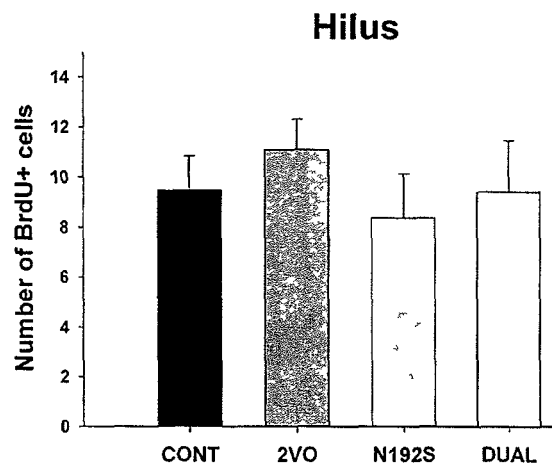
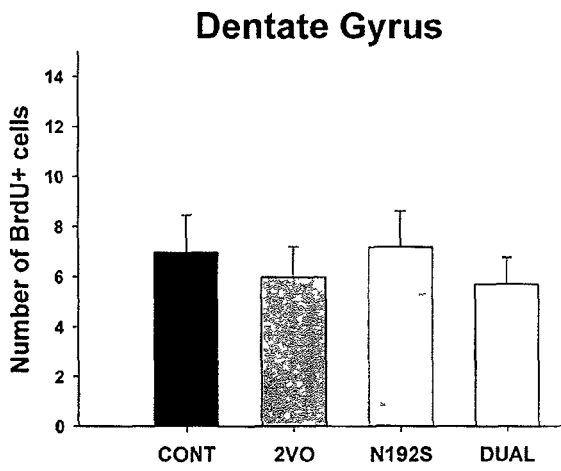
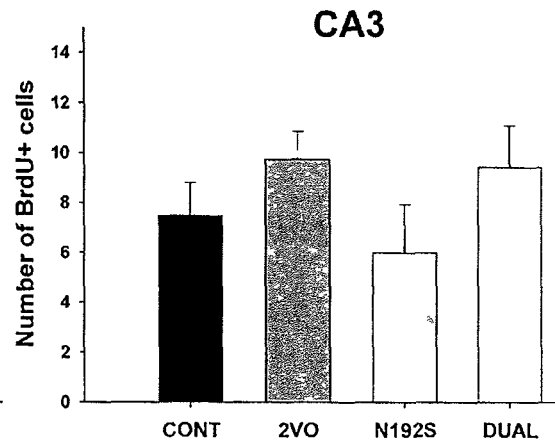
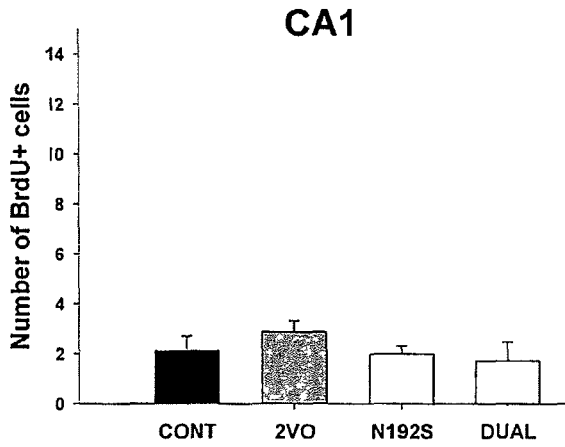


Figure 3.23: BrdU⁺ cell number in the hippocampus. Neither N192S nor 2VO affected the number of BrdU⁺ cells in any hippocampal sector (all p's >.05).



30% compared to control rats. The total number of basal segments was increased by 12% in 2VO rats compared to controls ($F_{1,18}=4.77$, $p=.042$). 2VO also increased the number of basal spines by 26% ($F_{1,18}=6.08$, $p=.024$). The effects of 2VO on cell body area, apical segments, apical and basal branching and spine density, and basal branch length were all non-significant (all p 's $>.05$). There were no effects of N192S, and no N192S by 2VO interaction effects on any overall measure of apical or basal dendritic complexity (all p 's $>.05$). Figure 3.25 shows the average total number of segments and branches as well as total branch length, and Figure 3.26 shows the number of spines and spine density for apical and basal dendrites.

Branch Order Analysis

Branch order analyses of the apical and basal trees were conducted to determine whether the distribution of branches, branch length, total spines or spine density were affected by N192S or 2VO. Repeated measures ANOVAs were used to detect any overall branch order by lesion or 2VO effects, and individual two-by-two ANOVAs were conducted to examine group differences at individual branch orders.

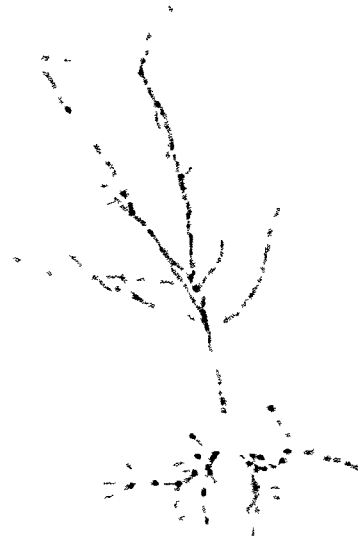
There was no overall branch order by N192S or 2VO effect on branch number for the apical dendrites. However, two-way ANOVAs of the data for each individual branch order revealed a significant effect of 2VO ($F_{1,18}=5.63$, $p=.032$), and a significant N192S by 2VO interaction effect ($F_{1,18}=6.23$, $p=.022$) on branch number at branch order 6. 2VO increased the number of 6th order branches mainly in N192S animals. Repeated measures ANOVA indicated a significant branch order by N192S by 2VO effect on basal branch number ($F_{8,144}=2.58$, $p=.011$). ANOVAs for each branch order revealed a significant 2VO

Figure 3.24: Representative CA1 cell tracings from a PBS-sham (top left), N192S-sham (top right), PBS-2VO (bottom left) and N192S-2VO rat (bottom right).

Representative Golgi Tracings of CA1 Pyramidal Cells



CONTROL



N192S



2VO



DUAL

Figure 3.25: Total number of segments (top), maximum branch order (middle), and total branch length for apical and basal dendrites of CA1 pyramidal cells. 2VO increased total apical branch length by 16% ($F_{1,18}=5.24$, $p=.034$) and the number of basal segments by 12% ($F_{1,18}=4.77$, $p=.042$). ‘*’ denotes a significant difference between the combined 2VO groups and the combined sham groups.

Golgi Analysis of CA1 Pyramidal Neurons Summary Measures of Dendritic Complexity

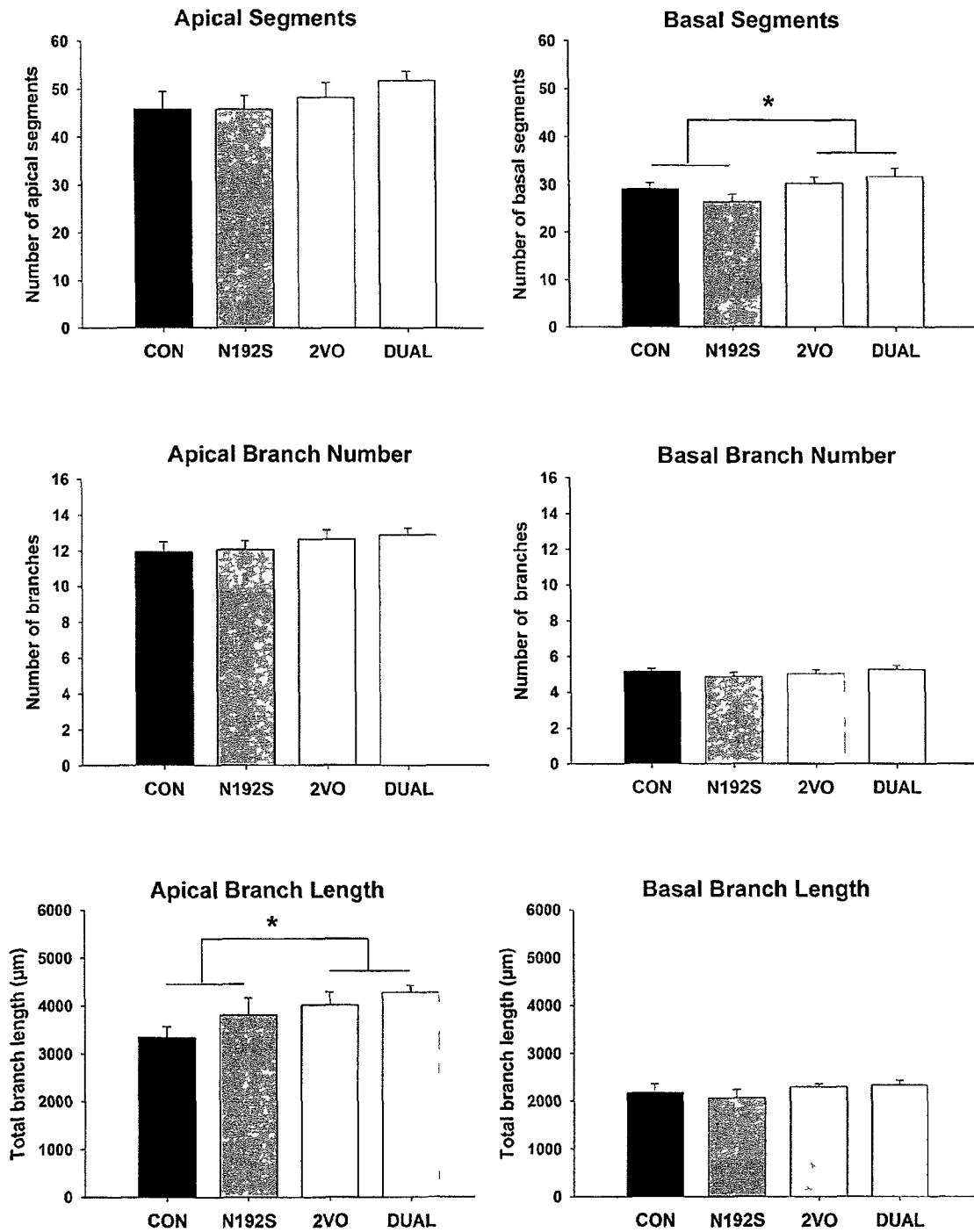
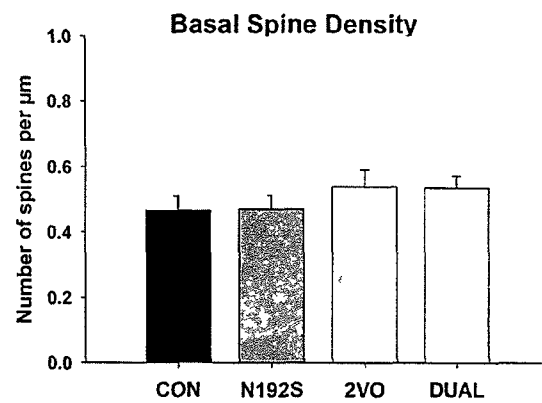
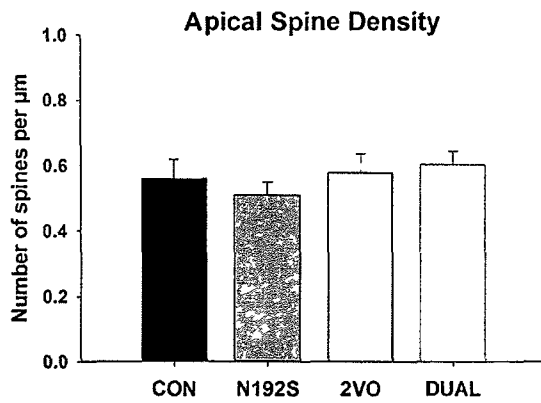
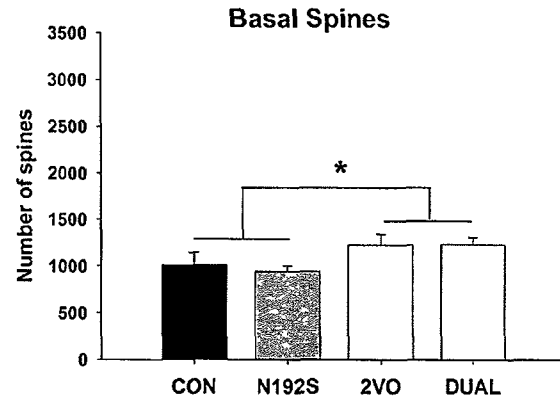
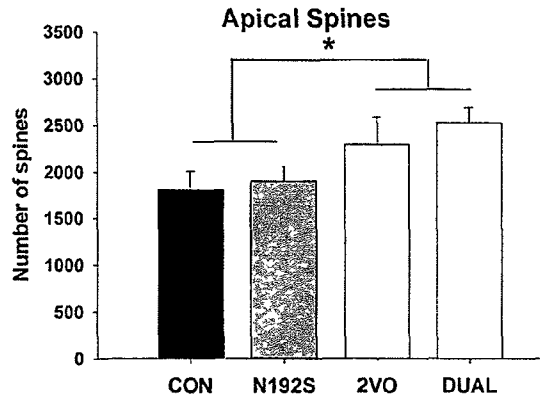


Figure 3.26: Total number of spines (top) and spine density (bottom) across the entire apical and basal dendritic trees of CA1 pyramidal cells. 2VO increased the total number of apical spines by 30% ($F_{1,18}=6.45$, $p=.02$) and the total number of basal spines by 26% ($F_{1,18}=6.08$, $p=.024$). ‘*’ denotes a significant difference between the combined 2VO groups and the combined sham groups.

Golgi Analysis of CA1 Pyramidal Neurons Summary of Spine Measures



effect on basal branch number at branch orders 1 and 2 ($F_{1,18}=5.26$, $p=.034$; $F_{1,18}=9.75$, $p=.006$), and a significant 2VO by N192S interaction effect at branch order 4 ($F_{1,18}=5.77$, $p=.027$). At branch orders 1 and 2, 2VO increased branch number in both PBS and N192S-treated animals, while at branch order 4, 2VO increased branch number only in the N192S animals. The branch number by branch order data are shown in Figure 3.27.

The overall branch order by N192S and branch order by 2VO effects on apical branch length were not significant. However, 2-way ANOVAs at each branch order indicated that 2VO increased apical branch length at branch orders 1 and 6 ($F_{1,18}=5.66$, $p=.029$; $F_{1,18}=4.96$, $p=.039$) while N192S increased branch length at orders 5 and 6 ($F_{1,18}=6.10$, $p=.024$; $F_{1,18}=4.67$, $p=.044$). The branch order by lesion, branch order by 2VO, and branch order by lesion by 2VO effects on basal branch length were nonsignificant. ANOVA revealed a significant 2VO by N192S interaction effect on branch length at branch order 2 ($F_{1,18}=5.65$, $p=.029$) with 2VO increasing basal dendritic length in PBS animals only. Figure 3.28 illustrates the branch length by branch order data for both the apical and basal trees.

There was an overall branch order by 2VO effect on apical spines ($F_{21, 378}=2.47$, $p<.001$), indicating that spine distribution across branch orders was affected by 2VO. ANOVAs at individual branch orders found that 2VO significantly increased spines at orders 1 ($F_{1,18}=14.09$, $p=.001$), 6 ($F_{1,18}=9.33$; $p=.007$), 7 ($F_{1,18}=8.12$, $p=.011$), and 11 ($F_{1,18}=9.40$, $p=.007$). N192S by itself did not affect apical spines at any branch order. However, at branch orders 6 and 7 there was a significant N192S by 2VO interaction (order 6: $F_{1,18}=4.4$, $p=.05$; order 7: $F_{1,18}=6.33$, $p=.022$). Inspection of the data indicates that the increase in apical spines induced by 2VO occurred mainly in the animals that

were also subjected to N192S. There was also a significant overall branch order by 2VO effect on basal spines ($F_{8,144}=3.00$, $p=.004$), indicating that basal spine distribution across branch orders was altered by 2VO. Two-by-two analysis indicated that 2VO significantly increased basal spines at branch order 4 ($F_{1,18}=7.42$, $p=.014$), and there was also a trend for 2VO to increase spines at branch orders 2 and 3 ($F_{1,18}=4.33$, $p=.052$; $F_{1,18}=3.48$, $p=.078$). The spines by branch order data are presented in Figure 3.29.

There were no branch order effects of 2VO or N192S, and no interaction effect on apical or basal spine density (see Figure 3.30). Individual ANOVAs at each branch order showed that 2VO increased basal spine density at branch order 4 ($F_{1,18}=5.24$, $p=.034$) while an increase at branch order 6 just missed significance ($F_{1,18}=3.64$, $p=.072$).

3.4. Discussion

3.4.1. Combined Effects of N192S and 2VO

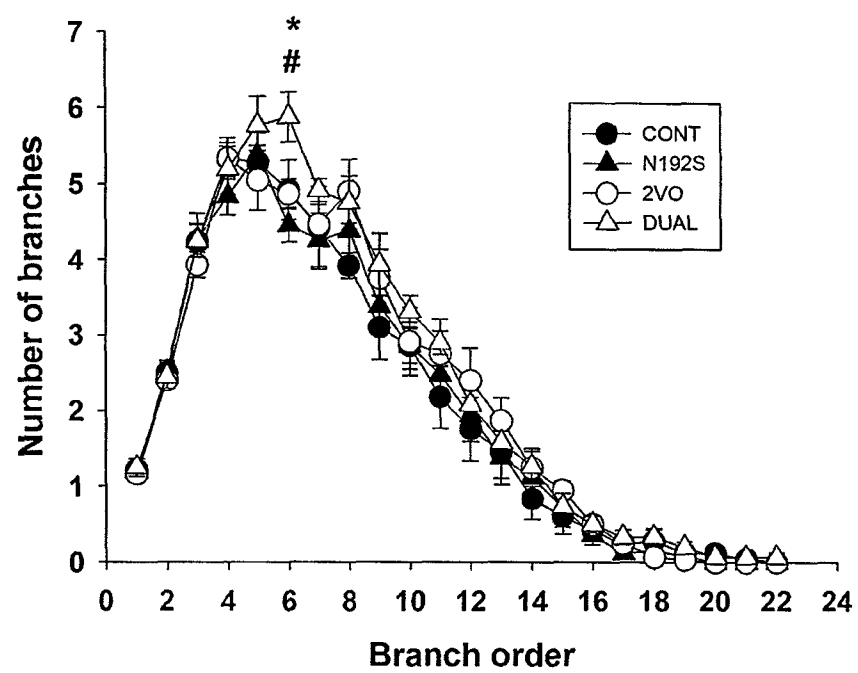
We predicted that a pre-existing cholinergic deficit would render the brain more vulnerable to the detrimental effects of 2VO, and we also expected that these dual-treated rats would exhibit more severe memory impairments and evidence of hippocampal damage than animals subjected to either treatment alone. In fact, dual rats did exhibit spatial working memory deficits as well as increased anxiety-like behaviour on the elevated plus maze, but did not show significant CA1 cell loss at 7 months post-surgery.

Our findings agree with a recent study which examined the combined effects of adult cholinergic lesion and subsequent mini-strokes. It was found that memory performance in the water maze was impaired in dual-treated animals, though hippocampal damage induced by the mini-strokes was not exacerbated by prior

Figure 3.27: Analysis of apical and basal branch number by branch order. Though the branch order by N192S, branch order by 2VO and branch order by N192S by 2VO effects were all nonsignificant for the apical dendrites, there was a significant branch order by N192S by 2VO effect on the basal dendrites ($F_{8,144}=2.58$, $p=.011$). ‘*’ denotes branch orders at which there was a significant N192S by 2VO interaction effect, ‘#’ denotes a significant 2VO effect, and ‘&’ denotes a significant N192S effect.

Branch Number by Branch Order Analysis

Apical Dendrites



Basal Dendrites

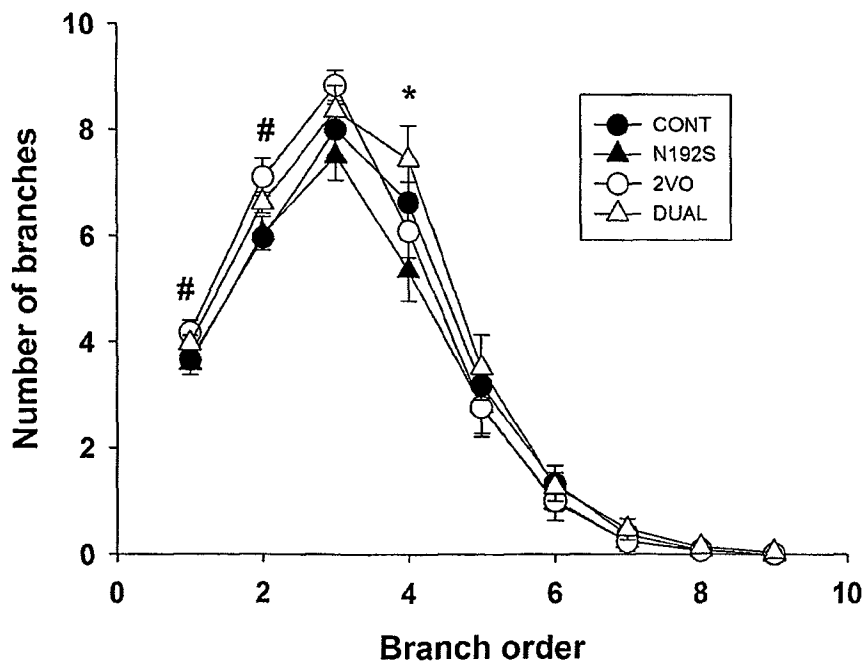
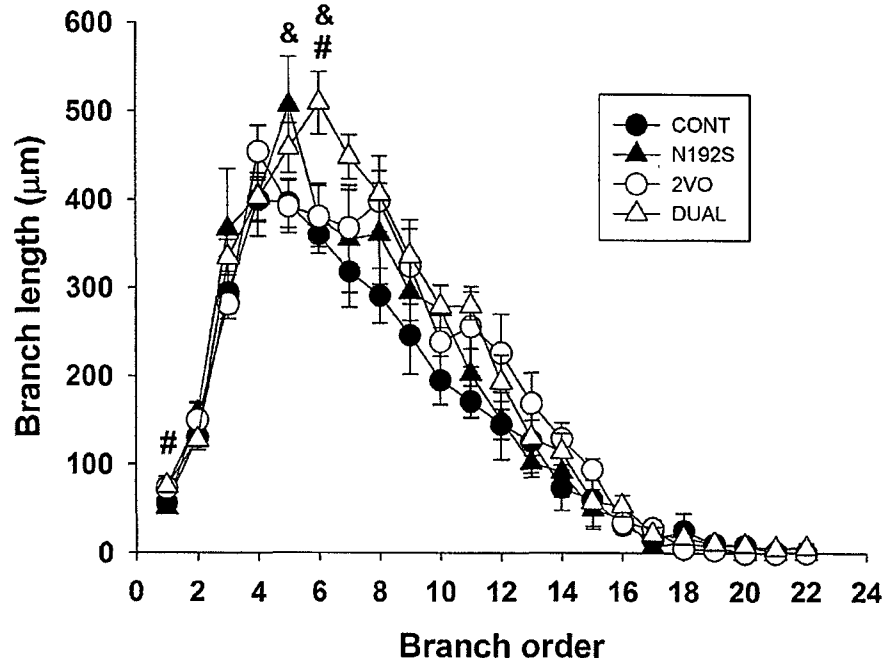


Figure 3.28: Analysis of apical and basal branch length by branch order. The overall branch order by N192S, branch order by 2VO and branch order by N192S by 2VO effects were all nonsignificant for both the apical and basal trees. However, two-by-two ANOVAs at each branch order indicated some N192S, 2VO, and N192S by 2VO effects at individual branch orders. ‘*’ denotes branch orders at which there was a significant N192S by 2VO interaction effect, ‘#’ denotes a significant 2VO effect, and ‘&’ denotes a significant N192S effect.

Branch Length by Branch Order Analysis

Apical Dendrites



Basal Dendrites

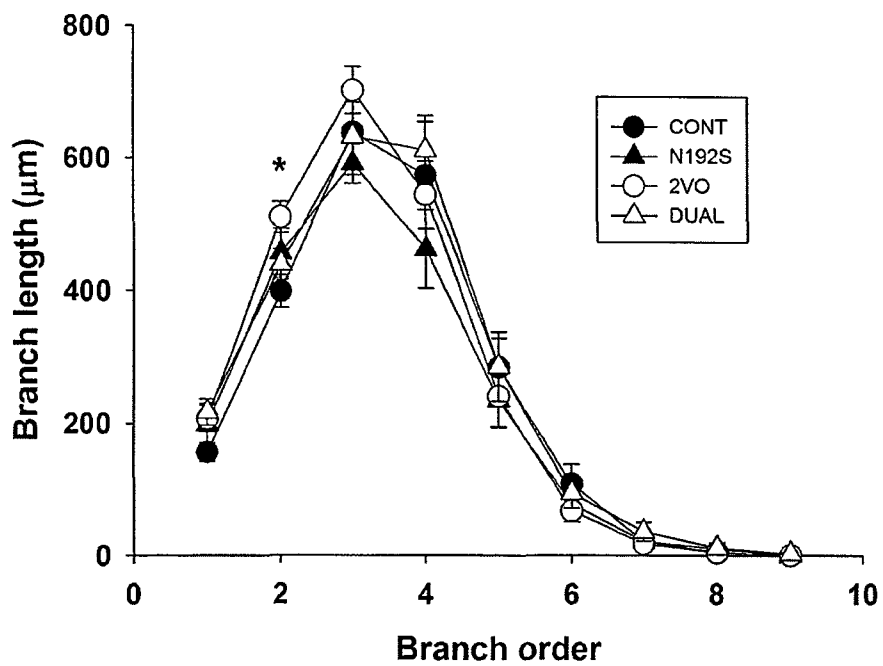
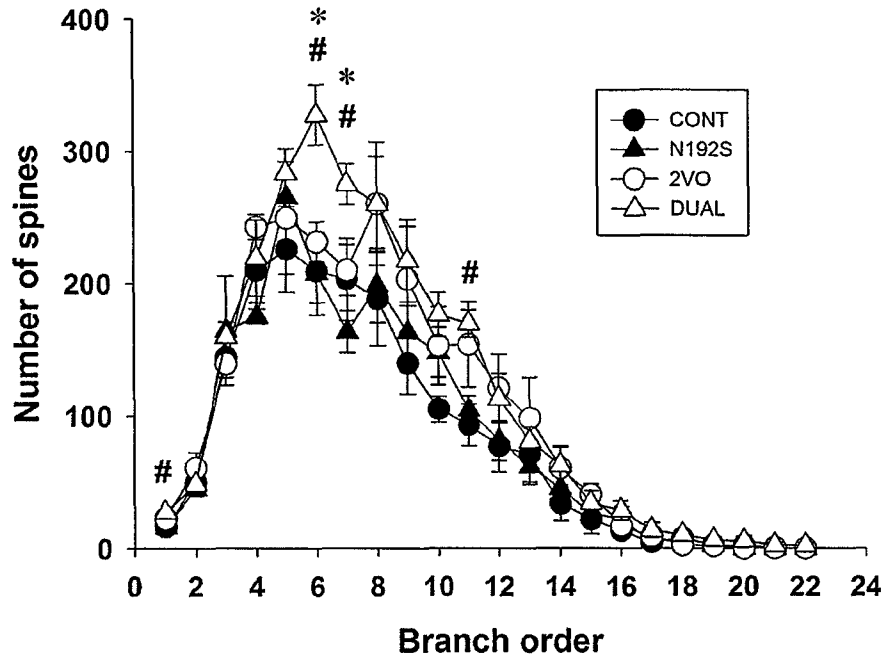


Figure 3.29: Analysis of apical and basal spines by branch order. 2VO significantly altered the distribution of both apical ($F_{21, 378}=2.47$, $p<.001$) and basal ($F_{8, 144}=3.00$, $p=.004$) spines. ‘*’ denotes branch orders at which there was a significant N192S by 2VO interaction effect, ‘#’ denotes a significant 2VO effect, and ‘&’ denotes a significant N192S effect.

Number of Spines by Branch Order Analysis

Apical Dendrites



Basal Dendrites

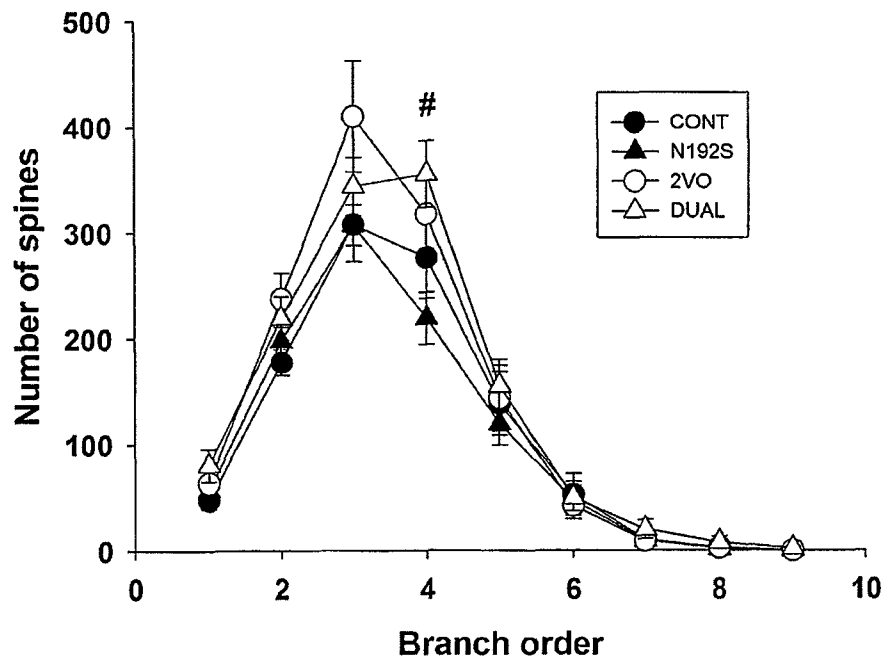
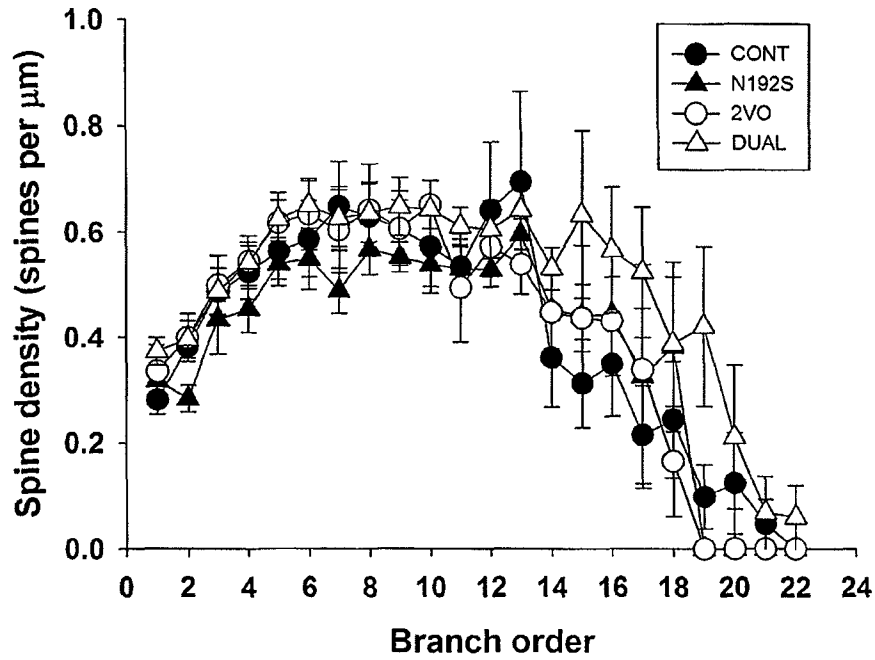


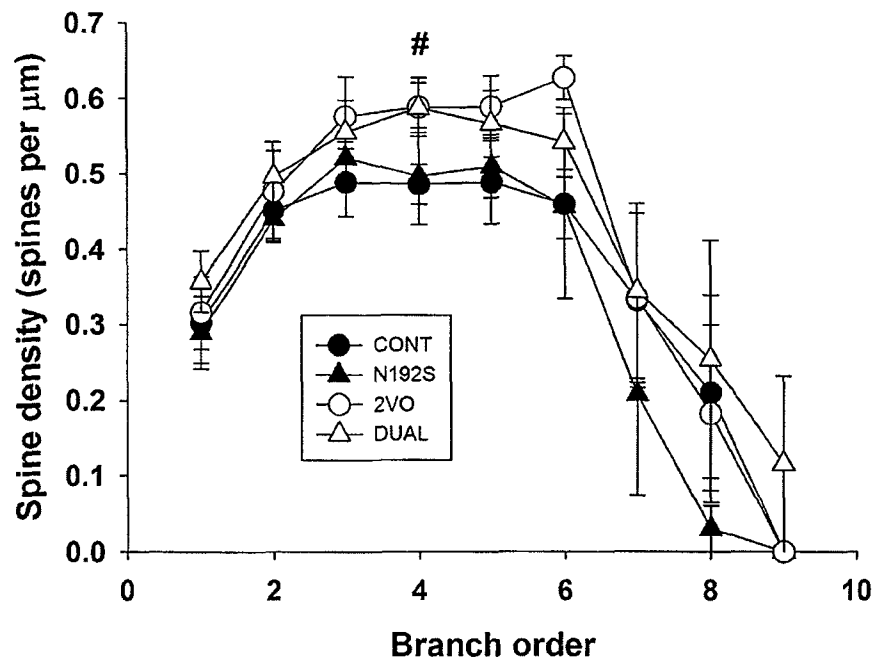
Figure 3.30: Analysis of apical and basal spine density by branch order. The overall branch order by N192S, branch order by 2VO and branch order by N192S by 2VO effects were all nonsignificant for both the apical and basal trees. 2VO increased basal spine density at branch order 4 ($F_{1,18}=5.24$, $p=.034$). ‘*’ denotes branch orders at which there was a significant N192S by 2VO interaction effect, ‘#’ denotes a significant 2VO effect, and ‘&’ denotes a significant N192S effect.

Analysis of Spine Density by Branch Order

Apical Dendrites



Basal Dendrites



cholinergic lesion (Craig et al., 2009). The dual rats in our experiment also showed no exacerbated hippocampal CA1 cell loss. Furthermore, there was no evidence of exacerbation of effects on the dendritic morphology of CA1 neurons that could explain their poor performance on the water maze. Surprisingly, the Golgi analyses showed the CA1 cells of dual treated rats largely resembled those of 2VO rats (both showed a marked dendritic hypertrophy), while their performance on the water maze was clearly different. However, branch order analysis did reveal interaction effects between N192S and 2VO in a few instances, whereby the stimulatory effects of 2VO on branch length and spines occurred only in lesioned animals. In these cases, N192S appeared to have had a permissive effect on 2VO-induced alterations in dendritic structure. Given the research indicating that cholinergic lesion impairs cortical plasticity (Conner et al., 2003; Ramanathan et al., 2009; Sachdev et al., 1998), this effect was unanticipated. One possible explanation for this finding is that whatever triggered the increased branching and spines in 2VO animals was more severe in dual rats. A second possibility is that nerve growth factor (NGF), which is increased in the hippocampi of adult cholinergic lesioned rats (Gu et al., 1998; Roßner et al., 1997) and which has been shown to induce dendritic remodelling in cortical pyramidal cells (Kolb et al., 1997), may have enabled some dendritic alterations in response to 2VO. In any case, it is clear that cholinergic denervation did not prevent the plastic response of CA1 dendrites to 2VO.

The lesion by 2VO interaction effect on the number of open arm entries suggests that the effects of 2VO on anxiety-like behaviour in the elevated plus maze were dependent on the status of the cholinergic system. Whereas non-lesioned rats subjected to 2VO made several entries into the open arms, N192S rats tended to avoid the open arms

after 2VO, on average making only one entry during the 10 minute testing period. Dual rats also exhibited behaviour indicative of anxiety in the open field, though this was no more pronounced than in rats subjected to N192S alone.

Neither CA1 cell loss nor changes in cytoarchitecture appear to explain the behavioural impairment seen in dual-treated rats. A neural correlate of the behavioural impairment remains to be uncovered. It is possible that 2VO-induced changes in dendritic morphology coupled with a loss of cholinergic activity at the time of testing is sufficient to explain the behavioural deficit. Of course, changes in cell number, activity, or morphology in other hippocampal sectors or other regions of the brain may also underlie the deficit.

3.4.2. Effects of 2VO

2VO has been shown to impair water maze performance at various postsurgical intervals, ranging from 7 days to 12 months (Cada et al., 2000; De Jong et al., 1999; Ohta et al., 1997; Pappas et al., 1996b), and these deficits occur regardless of the age at which the arteries are ligated. The failure to find an effect of 2VO on working memory performance here was unexpected.

The CA1 sector of the hippocampus is sensitive to cerebral hypoperfusion. Pappas et al. (1996b) demonstrated that CA1 cell loss after 2VO is slow to emerge, with no cell loss apparent 14 days post-surgery, but a ~10% reduction in cell number by 190 days after carotid ligation. Other reports have indicated a similar extent of cell loss at long post-surgical intervals (De Butte et al., 2002; Ritchie et al., 2004). Here, we found a non-significant 5% reduction in CA1 pyramidal cell number, although with larger group sizes, this may have reached statistical significance.

The failure to find a compelling effect of 2VO on spatial working memory and CA1 cell number is surprising, given the previous research showing both CA1 cell loss and memory impairment after 2VO. However, most prior studies have examined the consequences of 2VO in male rats only whereas we studied female rats. Females show reduced neural damage in response to focal ischemia (Alkayed et al., 1998; Takaba et al., 2004; Zhang et al., 1998), which appears to be a result of the neuroprotective actions of estrogen. It is possible that females may also be somewhat protected against the neuropathological effects of chronic cerebral hypoperfusion - to our knowledge the effects of 2VO in male and female rats have never been directly compared.

2VO had no effect on the generation of immature neurons, as indicated by counts of DCX-positive cells in the dentate gyrus. Notably, 2VO did not further decrease, or reverse the already reduced number of immature neurons in N192S rats. While Sivilia et al. (2008) found an increase in DCX-positive cells in the dentate gyri of 3-month-old rats 8 days after 2VO, the increase had disappeared by 75 days post-surgery. Furthermore, older animals (12 months at the time of 2VO surgery) did not exhibit enhanced neurogenesis in response to hypoperfusion. Our data are in agreement with this finding that there is no long-term neurogenesis-promoting effect of 2VO.

2VO induced dendritic hypertrophy in CA1 pyramidal cells. Increased apical branch length and spines, and increased basal segments and spines were observed in 2VO rats. These alterations were observed mainly in the low and middle branch orders, whereas higher branch orders were largely unaffected. CA1 pyramidal cells receive synaptic contacts arising from different cell populations on spatially distinct areas of the apical dendritic trees. While the distal apical branches receive perforant path input from

the entorhinal cortex, input to more proximal branches arises mainly from CA3 cells via Schaffer collaterals (Spruston 2008; Witter and Amaral 2004). The branch order-specific effects of 2VO found here may therefore reflect changes in the degree of connectivity of CA1 pyramidal cells with different input sources.

Increases in dendritic complexity and numbers of spines are assumed to reflect an increased number of synapses and therefore increased connectivity with other neurons (Kolb et al., 2001). The increased dendritic complexity seen in 2VO animals may reflect a compensatory response to damage in this area. Increased dendritic arborisation of pyramidal cells is associated with functional improvement after cortical damage (Kolb et al., 2001). However, it is unlikely that the increased arborisation seen here accounts for the spared spatial working memory in 2VO animals. Animals in both the 2VO and dual groups showed increased CA1 dendritic complexity, yet while the performance of 2VO animals on the spatial working memory task was unimpaired, dual animals showed clear working memory deficits. Thus, either the increased dendritic complexity is not related to spared performance on the water maze or it was not able to compensate for the deficit in dual-treated animals.

To our knowledge, this is the first examination of the effects of chronic cerebral hypoperfusion on dendritic morphology of CA1 cells. It would be particularly interesting to determine whether 2VO would have the same effects in male animals, as there is evidence for sex differences in structural plasticity in response to various types of manipulations, including environmental enrichment (Juraska et al., 1985), chronic stress (McLaughlin et al., 2009), and aging (Markham et al., 2005).

3.4.3. Effects of N192S

N192S alone did not elicit anxiety-like behaviour in the elevated plus maze. In contrast, rats subjected to N192S, either alone or in combination with 2VO, showed behavioural indications of anxiety in the open field, including reductions in the number of entries and distance travelled in the centre of the arena, and increases in the latency to enter the centre. Notably, at both post-surgical time points the groups performed equivalently during the first test day, and the differences between lesioned and non-lesioned rats became apparent only with repeated exposure to the open field. As seen particularly at the two month postsurgical interval, non-lesioned rats tended to show increased exploration of the centre of the open field with repeated exposures to the arena. In contrast, lesioned rats showed similar levels of exploration of the central area across the three days of testing. This might be indicative of a failure to habituate to anxiety-provoking situations in lesioned rats. Previous research has shown that cholinergic lesions of the MS or diagonal band of Broca in adult rats reduce the amount of time spent in the centre of an open field (Torres et al., 1994). Lamprea et al (2003) also found a reduction in the distance travelled in the centre of an open field after adult cholinergic lesion, though they showed similar reductions in distance travelled in the periphery. The authors concluded that the effect of the cholinergic lesion was to impair exploratory behaviour rather than increase anxiety-related behaviour. It is possible that a decrease in exploration may have contributed to the present results, as lesioned rats showed a nonsignificant trend towards decreased total distance travelled. However, the stronger effect of the lesion on number of entries into the centre, distance travelled in the centre, and latency to enter the centre suggests that the lesioned rats are indeed more anxious than controls. Interestingly, AD patients commonly suffer from anxiety (Seignourel et al.,

2008), and increased levels of anxiety have been reported in patients with mild cognitive impairment as well (Apostolova and Cummings 2008).

CA1 cell number was not affected by neonatal cholinergic lesion. This finding was not surprising, as previous work in this lab has found similar results (Pappas et al., 1996a). As a further measure of hippocampal damage, we examined GFAP expression in CA1, CA3, DG and hilus. The percent area immunoreactive for GFAP was increased only in the CA3 sector of rats subjected to N192S. The effects of cholinergic lesion on CA3 cell number or dendritic morphology have never been examined, but considering that CA3 was the only hippocampal sector to exhibit astrogliosis, such an investigation might be warranted.

As previously reported for male rats (Fréchette et al., 2009), here N192S also reduced the number of DCX-positive, newly born neurons in the dentate gyrus in female rats. Thus, not only does this effect occur in both sexes, it is still evident in middle-aged rats and it is restricted to the dorsal hippocampus.

Unexpectedly, N192S had virtually no effect on CA1 cytoarchitecture. This contrasts with previous research showing that N192S decreased apical branch number and spines, and reduced basal branch length of CA1 pyramidal cells in ~2 month old male rats (Fréchette et al., 2009). Similarly, neonatal cholinergic lesion has been shown to decrease dendritic complexity and/or spine density in visual cortex layer V pyramidal cells (Robertson et al., 1998), and in medial PFC layer V and granular retrosplenial cortex layer II/III pyramidal neurons (Sherren and Pappas 2005). All of the aforementioned studies examined cell morphology in relatively young (<6 months old) male animals. It is possible that the effect of the lesion changes dynamically over time

and/or the effects may be sex dependent. In support of this notion, Works et al. (2004) showed that the effect of adult cholinergic lesions on layer II-III frontal cortex cells was dependent on the age of the animal. While both young and aged rats showed apical dendritic atrophy, apical dendrites of middle-aged rats were unaffected by the lesion. It would be especially interesting to examine the cytoarchitecture of hippocampal cells in N192S and dual-treated rats at an older age, to determine whether lesion effects might emerge later, and whether they would interact with 2VO. Furthermore, an explicit comparison of the effects of sex on the outcome of cholinergic lesion is warranted.

3.5. Conclusions

Although combined neonatal cholinergic lesion and chronic cerebral hypoperfusion produced working memory impairments and increased anxiety, this model does not appear to mimic the neuropathological features of AD. The brains of AD patients are characterized by cell loss (West et al., 1994a; West et al., 2000) and dendritic regression (Hanks and Flood 1991) in the CA1 sector of the hippocampus while here, dual-treated animals exhibited no loss of cells and dendritic hypertrophy rather than regression. It would be interesting to examine the brains of these animals at longer post-surgical intervals to determine whether CA1 cell loss might become apparent, and whether the observed changes in dendritic morphology would be maintained with advancing age. As well, the effects of sex on the outcome of these treatments merit explicit examination.

4. Study #3: The Effects of Neonatal Cholinergic Lesion on Hippocampal Neurogenesis

4.1. Introduction

Environmental enrichment (EE) is an experimental paradigm in which rodents are housed in large cages containing toys, tunnels, ladders, swings, wheels and other objects. Rearing in such complex environments provides increased opportunities for motor, sensory, and cognitive stimulation, and promotes plasticity of the cortex and hippocampus (Nithianantharajah and Hannan 2006). Hebb was the first to report formally on the effects of enriched living conditions, in a study documenting the improved problem-solving capacity of rats raised at home and given the freedom to explore the house for several hours each day compared to rats raised under standard laboratory conditions (Hebb 1947). Since then, many studies have investigated the neural and behavioural effects of EE, and it is well established that it enhances learning and memory in normal animals (Kobayashi et al., 2002; Lee et al., 2003; Leggio et al., 2005; Marashi et al., 2003; Paylor et al., 1992; Schrijver et al., 2002; Tees 1999). In addition, EE has been shown to improve memory in animals that suffer from impairments associated with aging (Bennett et al., 2006; Frick and Fernandez 2003), Alzheimer's-like pathology (Jankowsky et al., 2005), traumatic brain injury (Hamm et al., 1996), and in transgenic mice modeling Down syndrome (Martínez-Cué et al., 2002).

Early research indicated that the behavioural changes stimulated by EE are accompanied by increases in cortical weight and thickness (Bennett et al., 1964; Rosenzweig et al., 1962; West and Greenough 1972), which were later shown to be a

result of an expansion of the dendritic material (Faherty et al., 2003; Gelfo et al., 2009; Green et al., 1983; Greenough et al., 1973; Greer et al., 1982; Juraska et al., 1985; Leggio et al., 2005; Mandolesi et al., 2008; Volkmar and Greenough 1972). While most studies have focused on EE-induced changes in the dendritic morphology of cortical neurons, (Faherty et al., 2003; Gelfo et al., 2009; Green et al., 1983; Greenough et al., 1973; Greer et al., 1982; Juraska et al., 1985; Leggio et al., 2005; Mandolesi et al., 2008; Volkmar and Greenough 1972), a handful of studies have shown the dendrites of hippocampal CA1 cells to be sensitive to EE (Bartesaghi et al., 2003; Faherty et al., 2003).

Enrichment also reportedly affects hippocampal neurogenesis. Increased neurogenesis in the hippocampi of rodents housed in EE was first described by Kempermann and colleagues (Kempermann et al., 1997). They demonstrated that the number of BrdU-labelled cells 4 weeks after BrdU administration was increased in the SGZ and GCL of the hippocampus after 10 weeks of EE in mice. Similar results have been reported after enrichment in the rat (Nilsson et al., 1999). EE may not affect all stages of neurogenesis equally. The increased number of newborn cells has been attributed to a survival-promoting influence of EE, while proliferation is unaffected (Brown et al., 2003a; Kempermann et al., 1997; Nilsson et al., 1999). Neuronal fate choice also seems to be unaltered by EE, as the proportion of newborn cells that become neurons is similar in rodents housed in standard and enriched conditions (Kempermann et al., 1997; Nilsson et al., 1999).

A recent study in our laboratory examined the combined effects of N192S on EE-induced changes in spatial working memory, CA1 dendritic morphology and neurogenesis, to determine whether cholinergic input contributes to EE-induced

plasticity. Rats subjected to N192S, like controls, showed improved performance on a working memory version of the water maze when housed under enriched conditions for 6 weeks (Fréchette et al., 2009). However, the lesioned rats exhibited reduced numbers of DCX-positive immature neurons in the DG, and there was a suggestion of impaired neurogenic responsiveness to enrichment in N192S rats. The stage-specific effects of cholinergic lesion on neurogenesis could not be determined in that study. The purpose of the present study was to examine the proliferation, differentiation and survival of new cells in rats subjected to N192S, as well as the ability of N192S rats to exhibit a neurogenic response to environmental enrichment.

4.2. Methods

4.2.1. Animals

All rats were housed throughout the experiment under a reversed light cycle with free access to standard rat chow and water. All care and handling of the animals followed established guidelines of the Canadian Council on Animal Care, and the experiment was approved by the Carleton University Animal Care Committee.

4.2.2. Breeding

Eight male and sixteen female Sprague-Dawley rats (Harlan, Indianapolis, IN) were used as breeders. After a one-week acclimation period, the rats were housed in groups of three (one male with two females). The females were inspected daily and were removed from the cage and single-housed when they began to show obvious indications of pregnancy. The females were monitored daily until the pups were born. The day of birth was designated as PND 0. On PND 3 or PND 4, the litters were culled to a

maximum of 10 pups. Though only males were used in this study, sufficient females were kept in order to maintain a minimum litter size of 8 whenever possible. The pups were subjected to stereotaxic surgery on PND 7 (see below) and weaned on PND 21-23. Some of the breeders were used to produce more than one litter. In these cases, the females were given a minimum of one week of rest after weaning before being paired with another male.

4.2.3. Cholinergic Lesion

On PND7, the pups underwent stereotaxic surgery to infuse either 192S (Advanced Targeting Systems, San Diego, CA), or vehicle (10mM pH 7.2 PBS) into the lateral ventricles. Pups were removed from the home cage 4 at a time and brought to the surgical suite, where they were placed on a heating pad. Each pup was anaesthetized using isoflurane/oxygen, then placed in a plaster mould mounted on a stereotaxic frame. The pups were maintained on 1.5-2% isoflurane for the duration of the surgery. One ear was punched for rat identification. A dorsal midline incision was made in the scalp and tissue overlying the skull was blunt deflected. Two holes were drilled in the skull at \pm 1.8mm lateral to Bregma. A needle attached to a 5 μ l syringe (Hamilton, Reno, NV) was lowered to a depth of 3.5mm ventral to the dura, aimed at the lateral ventricles. 1.5 μ l of 0.2 μ g/ μ l 192S was infused into each ventricle (300 ng per ventricle) over 2 minutes. The needle was left in place for a further 2 minutes to allow the solution to diffuse away from the injection site, then slowly retracted to prevent the toxin from being drawn back up into the needle. The incision was closed using tissue adhesive (Vetbond, 3M, London, ON), and the pup was placed with its littermates on a heating pad. When all pups had regained consciousness, they were placed back in the home cage. Approximately half of

the rats in each litter were assigned to each treatment group, such that group assignments were balanced as evenly as possible across litters.

4.2.4. Housing

Upon weaning at the age of 21-23 days, the rats were placed either into enriched housing conditions (EE), or were pair-housed under standard laboratory conditions (S). The enriched condition consisted of placing five or six rats from the same lesion condition in a large (72cm x 72cm x 52cm) two-level stainless steel cage with wire mesh sides and a plexiglass front panel. The cages contained different arrangements of toys, ladders, tunnels, hanging objects, and nesting material. Each day, one toy was replaced with a different toy. Each week, the rats were moved into a novel cage with a different complement and arrangement of objects. The standard condition involved housing pairs of rats from the same treatment group in plastic cages (44cm x 24cm x 20cm) with a small amount of paper nesting material. The enriched animals were housed in a separate room from the standard-housed rats and the conditions in the two rooms were kept as similar as possible (temperature, humidity, lighting level, etc). Housing assignments were distributed across the litters as evenly as possible.

4.2.5. Behavioural Monitoring

In order to explore the possibility that lesioned and control rats might respond differently to the enrichment experience, or display differences in behaviour during standard housing that might influence neurogenesis, the home-cage behaviour of the rats was monitored during the second, sixth and tenth weeks of the enrichment/standard housing period. Details are provided in Appendix 2.

4.2.6. BrdU Labelling

After six weeks in their respective housing conditions, all rats received BrdU to label proliferating cells. The BrdU was given in two intraperitoneal doses of 200mg/kg (dissolved in 0.9% saline), 24 hours apart. All injections were given between 9:00am and 12:00pm. A subset of the rats in each group was sacrificed 2 hours after the last injection (proliferation group). The remaining rats were returned to their respective housing conditions for another 28 days before being sacrificed (differentiation/survival group). Twenty-eight days was chosen as the 'survival' period, since it is known that the death of newly born cells occurs mostly within this period, and after this period the remaining cells are relatively permanent (Dayer et al., 2003).

4.2.7. Tissue Collection

Two hours or 28 days after the last BrdU injection, the rats were given an overdose of sodium pentobarbital, then transcardially perfused with 75ml of heparinized saline followed by 300ml of 4% PFA in PB. After removal, the brains were post-fixed in PFA overnight, then rinsed several times in PB containing azide over the next 24 hours. Over the next several days the brains were transferred into increasing concentrations of sucrose in PB (10%, 20% and 30%). Coronal sections were cut on a cryostat at a thickness of 40µm, and the sections were either stored in PB with azide (for immediate staining) or in cryoprotectant at -20°C for later processing.

4.2.8. Verification of the Cholinergic Lesion

AChE staining and p75^{NTR} immunohistochemistry were used to confirm the cholinergic lesion. For AChE, four sections spanning the hippocampus were stained.

Briefly, floated sections were rinsed in 0.1M sodium acetate, then incubated overnight in a reaction solution of 0.68% sodium acetate, 0.1% cupric sulfate, 0.12% glycine and 0.1% acetylthiocholine iodide in distilled water, pH 5.0. The next day the sections were rinsed in sodium acetate, then developed in 1% sodium sulphide, pH 7.5 for 10 minutes. After rinsing in sodium acetate, the sections were washed in distilled water, mounted, air dried overnight, then dehydrated, cleared and coverslipped. Images of the DG, CA1, CA3 and hilus regions were obtained using an Olympus BX-51 microscope (Markham, ON) at 20x magnification and captured using StereoInvestigator software (MBF Biosciences, Williston, VT). Using ImageJ software (National Institutes of Health, Bethesda, MD), the percent area of each region that showed positive staining for AChE was calculated.

Sections containing the vDB, hDB and MS were immunohistochemically stained to detect p75^{NTR}. Briefly, floated sections were rinsed in PBS and incubated overnight at room temperature in a dilution solution containing mouse anti-nerve growth factor receptor antibody (1:2000; Millipore, Temecula, CA), 0.3% lambda carrageenan, 0.3% bovine serum albumin and 0.3% triton x-100 in PBS. The sections were then incubated for 2 hours at room temperature in biotinylated sheep anti-mouse immunoglobulin (1:100; GE Healthcare, Oakville, ON), followed by a 2 hour incubation in streptavidin biotinylated horseradish peroxidase complex (1:100; GE Healthcare). In order to visualize the antibody complex, the sections were reacted in 0.02% DAB, 0.6% ammonium nickel sulphate and 0.01% hydrogen peroxide in 50mM Tris buffer, pH 7.4, then rinsed in PBS, mounted, and air-dried overnight. After counterstaining with 0.085% pyronin Y in acetate buffer, the sections were dehydrated, cleared and coverslipped. Cells in the MS/vDB and hDB that stained positive for p75 were counted manually using a

BX-51 microscope (Olympus) at 20x magnification. Any rat that suffered less than a 60% reduction in the number of p75⁺ cells or less than a 60% reduction in AChE staining compared to the average of the control group was excluded from further analyses. In all cases, the p75 and AChE data were in agreement.

4.2.9. Quantification of Cell Proliferation

Rats killed 2 hours after the last BrdU injection were used to assess the effects of the cholinergic lesion and enrichment on cell proliferation. Every 8th section throughout the entire hippocampus was immunohistochemically stained to detect the incorporation of BrdU into proliferating cells. Floated sections were rinsed three times in PBS with azide, then blocked for 30 minutes in 0.3% hydrogen peroxide in PBS. After a further three rinses in PBS, the sections were incubated in 2N HCl at 37°C for one hour, then placed in 0.1M boric acid buffer, pH 8.5 for 10 minutes. The sections were rinsed in PBS again before an overnight incubation at 4°C with mouse anti-BrdU antibody (1:500; Sigma-Aldrich clone BU-33, Oakville, ON). On the following day the sections were incubated first in sheep anti-mouse antibody (1:100; GE Healthcare) for 2 hours at room temperature, then in streptavidin biotinylated horseradish peroxidase complex (1:100; GE Healthcare). After a 2-hour incubation, the antibody complex was visualized using a DAB reaction as described above. The sections were counterstained in pyronin Y, then dehydrated, cleared and coverslipped. The total number of newly generated cells in the DG SGZ and GCL was estimated using stereological counting procedures. The SGZ was defined as an area 3 cell-diameters wide lying between the GCL and the hilus. The dorsal and ventral hippocampi were considered separately, as it has been noted that some treatments can preferentially affect dorsal or ventral hippocampal neurogenesis (Banar et

al., 2006). The optical fractionator feature of StereoInvestigator software, with the grid size set at $65\mu\text{m}$ by $65\mu\text{m}$, and the counting frame set at $50\mu\text{m} \times 50\mu\text{m} \times 10\mu\text{m}$ was used to quantify the number of BrdU-labelled cells. These counting parameters were such that approximately 1200 sampling sites were visited in the dorsal hippocampus, and approximately 500 sampling sites were visited in the ventral hippocampus. Figure A1.4 in Appendix 1 shows a representative photomicrograph of BrdU staining in the dentate gyrus 2 hours after the final BrdU injection.

The number of Ki-67 positive cells was used as an additional indication of the rate of cell proliferation. Sections adjacent to those used for BrdU staining from rats killed 2 hours after the last BrdU injection were immunohistochemically stained to detect Ki-67, a cell-cycle-related protein expressed during cell division. The staining protocol followed that described for BrdU, omitting the HCl and boric acid incubations. The primary mouse anti-Ki-67 antibody (Dako, Mississauga, ON) was used at a concentration of 1:500. The number of Ki-67 cells in the dorsal and ventral DG GCL and SGZ were quantified stereologically. The counting frame was set at $50\mu\text{m} \times 50\mu\text{m} \times 10\mu\text{m}$, and the grid size was $90\mu\text{m}$ by $90\mu\text{m}$, yielding approximately 750 sampling sites in the dorsal DG and 350 sampling sites in the ventral DG.

4.2.10. Quantification of Immature Neurons

Immature neurons were detected by immunohistochemical labelling of DCX, a marker for migrating neuroblasts. Every 8th section through the entire hippocampus of animals killed 2 hours after the final BrdU injection was stained. Briefly, sections were rinsed in PBS, blocked in 0.3% hydrogen peroxide, blocked in 3% normal horse serum, then incubated in primary goat anti-DCX antibody (1:250; Santa Cruz Biotechnology,

Santa Cruz, CA) overnight at room temperature. The sections were then incubated for 2 hours in biotinylated horse anti-goat antibody (1:100; Vector Laboratories, Burlingame, CA) followed by a 2-hour incubation in streptavidin-biotinylated horseradish peroxidase complex (1:100; GE Healthcare) and a DAB reaction. After counterstaining in pyronin Y, the sections were dehydrated, cleared and coverslipped. The DCX-positive cells were counted stereologically in the dorsal and ventral DG using StereoInvestigator (MBF Biosciences) with a counting frame of 40 μ m by 40 μ m by 10 μ m and a grid size of 60 μ m by 60 μ m. This produced an average of 1400 sampling sites in the dorsal DG and 600 sampling sites in the ventral DG.

4.2.11. Quantification of Cell Survival

The effects of cholinergic lesion and environmental enrichment on newborn cell survival were studied in rats killed 28 days after the last BrdU injection. Every 8th section throughout the entire hippocampus was immunohistochemically stained to detect cells that had incorporated BrdU. The staining protocol and counting parameters were as described above for the 2-hour post-injection group. Figure A1.4 in Appendix 1 shows a typical BrdU staining pattern in an animal sacrificed 28 days after the final BrdU injection.

The number of cells remaining 4 weeks after injection was expressed as a percentage of the number of proliferating cells that were present in rats in the corresponding experimental group killed at the 2-hour time point, to yield the proportion of newly generated cells that survived the first 4 weeks after their birth.

4.2.12. Determination of Cellular Fate Choice

The proportion of newborn cells that became neurons, astroglia, or neither was quantified by double immunofluorescent staining for BrdU/NeuN (a marker for mature neurons) and BrdU/S100 β (a marker for mature astrocytes) in 8 animals from each group. For BrdU/NeuN labelling, every 9th section through the dorsal hippocampus was stained. Sections were rinsed in PBS with azide, then blocked for 30 minutes in a solution of 0.3% bovine serum albumin, 0.3% lambda carrageenan, and 0.3% Triton X-100 in PBS with azide. The sections were then rinsed and placed in 45°C 2N HCl for 1 hour, followed by a 10 minute incubation in boric acid buffer, pH 8.5. After another rinse, the sections were incubated for 48 hours at 4°C in a mixture of mouse anti-NeuN (1:500; Millipore) and rat anti-BrdU (1:500; Novus Biologicals, Littleton, CO) in 0.3% Triton X-100 in PBS with azide. The sections were then rinsed and incubated for 1 hour in a mixture of goat anti-mouse Alexa 555 (1:500; Invitrogen, Burlington, ON) and goat anti-rat Alexa 488 (1:500; Invitrogen). The sections were rinsed three times in PBS, mounted onto gelatin-dipped slides, and coverslipped immediately with anti-fade mounting medium (Prolong Gold; Invitrogen).

For BrdU and S100B double-labelling, every 9th section through the dorsal hippocampus (adjacent to sections used for BrdU/NeuN) was stained. The staining protocol followed that used for BrdU/NeuN staining, with primary antibody concentrations of 1:1000 for rat anti-BrdU (Novus Biologicals), 1:2000 for mouse anti-S100B (BD Biosciences, Mississauga, ON), and 1:750 for both secondary antibodies (goat anti-rat Alexa 488 and goat anti-mouse Alexa 555; Invitrogen).

To determine the proportion of BrdU-labelled cells that also expressed NeuN or S100B, a minimum of 50 BrdU-labelled cells per brain were examined using a laser scanning confocal microscope (Nikon D-Eclipse C1, Nikon, Mississauga, ON) with a 100x objective. To avoid having to choose cells within sections to examine, and thereby possibly biasing the results, all of the BrdU⁺ cells in each section were examined. BrdU-labelled cells were found through the ocular lenses using widefield fluorescence, then scanned using EZ-C1 confocal software (Nikon). A series of images was taken at successive 0.5µm steps through the entire cell. The Z stacks were then examined to determine whether the BrdU-labelled cell co-expressed NeuN or S100B. The number of cells expressing NeuN or S100B was expressed as a percentage of the total number of BrdU-positive cells examined. Appendix 1 contains sample photomicrographs showing a BrdU⁺ cell that also expresses NeuN, a BrdU⁺ cell that does not express NeuN, a BrdU⁺ cells that expresses S100B, and a BrdU⁺ cell that does not express S100B (Figure A1.10).

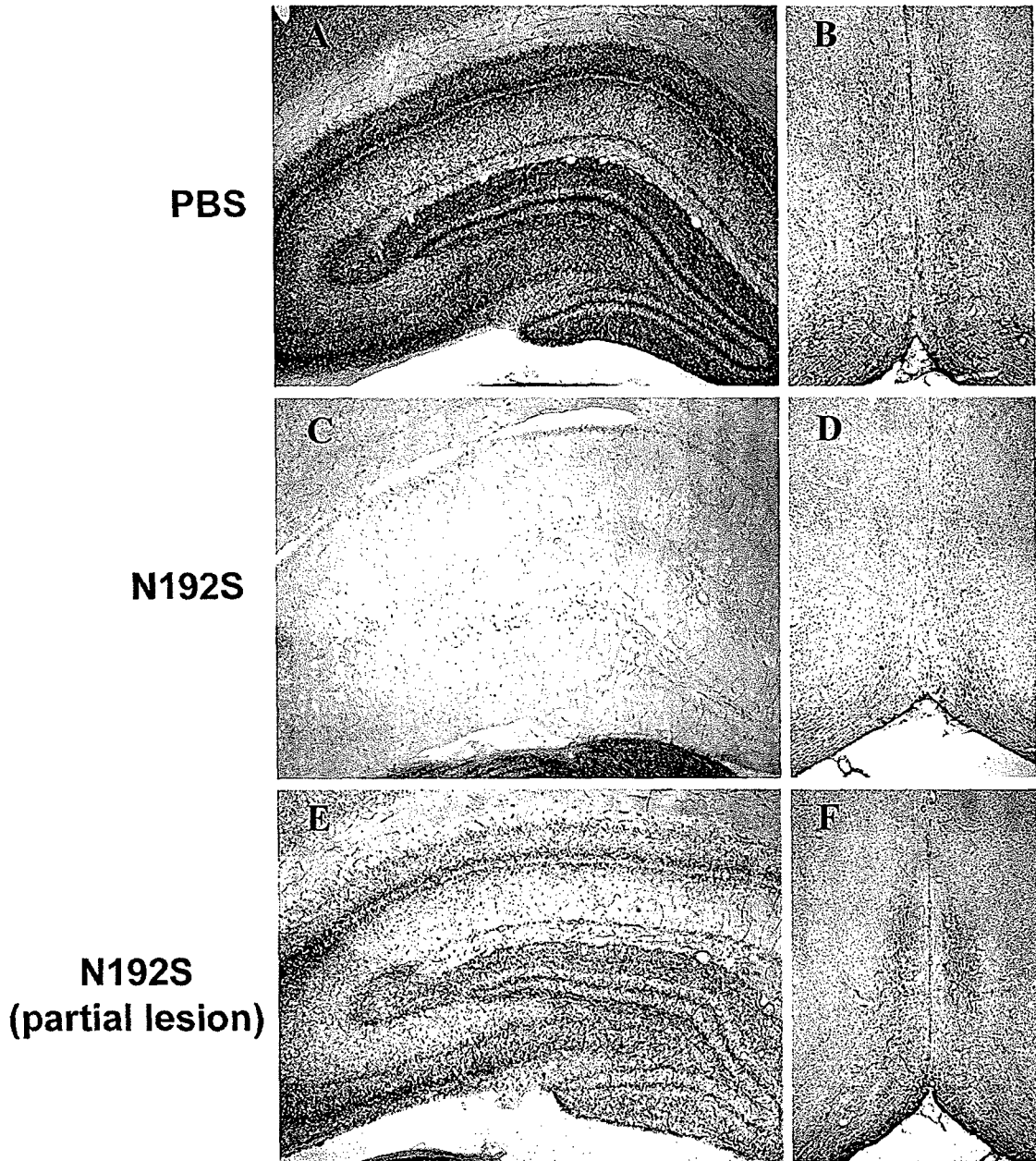
4.3. Results

4.3.1. General

One N192S pup was found dead 11 days post-surgery. All other rats recovered from neonatal surgery with no overt impairments. Administration of 192-IgG-saporin resulted in a severe loss of p75⁺ cells in the basal forebrain as well as a substantial reduction of AChE staining throughout the hippocampus. The percent area stained positive for AChE in lesioned rats was 5.4% of the control mean in CA1, 11.3% in CA3, 5.5% in DG and 6.5% in the hilus. The number of p75⁺ cells in the MS and vDB was reduced to 24% of control values, while the number of cells in the hDB was reduced to

Figure 4.1: Verification of the cholinergic lesion. Sample photomicrographs showing acetylcholinesterase staining in the hippocampus (A,C,E) and p75-positive cells in the medial septum and diagonal band of Broca (B,D,F) of a control rat (A,B), N192S rat (C,D) and a N192S rat with an incomplete lesion (E,F). All images were acquired using a 4X objective lens.

Verification of the Cholinergic Lesion AChE and p75 Staining



30.6% of controls. Rats in the lesioned groups that failed to show such losses of p75 and AChE staining were discarded from the study. The final numbers of animals included in each group were as follows: PBS-Standard (proliferation group: n=12, survival group: n=10); PBS-Enriched (proliferation group: n=15; survival group: n=18); N192S-Standard (proliferation group: n=8, survival group: n=8) and N192S-Enriched (proliferation group: n=8, survival group: n=11). Figure 4.1 shows representative photomicrographs of hippocampal sections stained for AChE and sections of the MS and vDB immunohistochemically stained for p75 from a control animal (panels A and B) and a N192S animal showing a satisfactory lesion (panels C and D). Panels E and F show AChE and p75 staining for a N192S animal showing an unacceptable lesion.

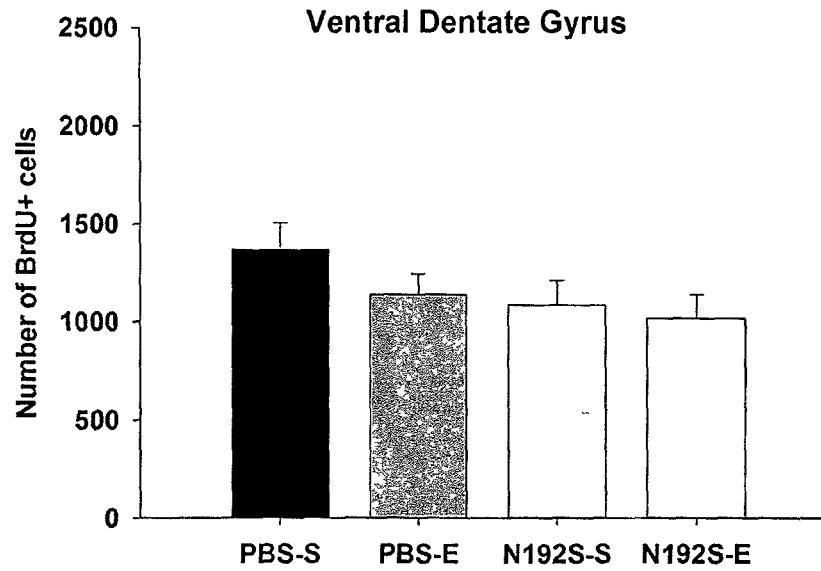
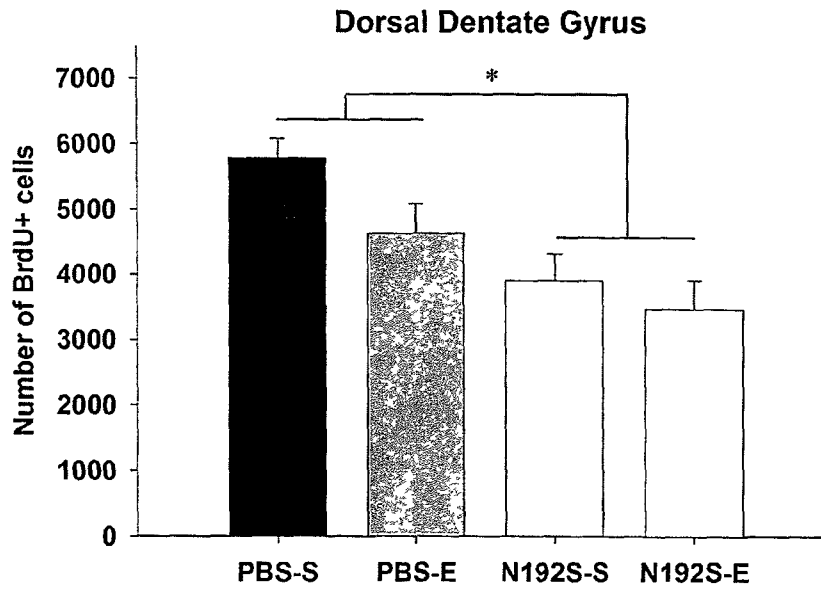
4.3.2. BrdU Counts- 2 Hour Survival

After 42 days in either standard or enriched housing, all rats received two BrdU injections spaced 24 hours apart. The number of BrdU⁺ cells in the dorsal and ventral DG GCL and SGZ 2 hours after the final BrdU injection were counted as an index of cell proliferation (see Figure 4.2). N192S decreased the number of BrdU⁺ cells in the dorsal DG ($F_{1,39}=32.38$, $p<.001$). Compared to the combined PBS groups, N192S rats had 34% fewer BrdU⁺ cells. N192S had no effect on the number of BrdU⁺ cells in the ventral DG ($F_{1,39}=2.59$, NS). The numbers of BrdU⁺ cells in both the dorsal and ventral DG were unaffected by the housing condition (dorsal: $F_{1,39}=1.54$, NS; ventral: $F_{1,39}=1.36$, NS). There were no N192S by housing interaction effects on dorsal or ventral BrdU⁺ cell number (dorsal: $F_{1,39}<1$; ventral: $F_{1,39}<1$).

4.3.3. Ki-67 Counts

Figure 4.2: BrdU⁺ cells in the dorsal (top panel) and ventral (bottom panel) DG 2 hours after the final BrdU injection. N192S rats had 34% fewer BrdU⁺ cells in the dorsal DG ($F_{1,39}=32.4$, $p<.001$). The number of BrdU cells in the ventral DG was unaffected by the lesion. The number of BrdU⁺ cells did not differ between enriched and standard-housed rats.

Number of BrdU+ Cells 2 Hours After the Final BrdU Injection



The number of Ki-67-positive cells in the DG was quantified as a secondary measure of cell proliferation in the animals described above. As illustrated in Figure 4.3, neither the N192S ($F_{1,40}>1$) nor EE ($F_{1,40}<1$) affected the number of Ki-67⁺ cells in the dorsal DG, and there was no N192S by housing interaction effect ($F_{1,40}<1$). Similarly, there were no significant N192S ($F_{1,40}<1$), housing ($F_{1,40}=1.73$, NS) or N192S by housing interaction ($F_{1,40}=2.86$, $p=.09$) effects on Ki-67-expressing cells in the ventral DG.

4.3.4. DCX Counts

The number of DCX-immunoreactive immature neurons in the dorsal DG was reduced by N192S ($F_{1,38}=7.28$, $p=.01$). Lesioned animals had 14% fewer dorsal DCX-positive cells than controls. This effect was not observed in the ventral DG ($F_{1,38}<1$). EE did not affect the number of DCX⁺ cells in either the dorsal ($F_{1,38}=1.46$, NS) or ventral ($F_{1,38}<1$) DG. The N192S by housing interaction effect was not significant in either the dorsal ($F_{1,38}<1$) or ventral DG ($F_{1,38}<1$). These data are shown in Figure 4.4.

4.3.5. Correlations

In the dorsal DG, Ki67 counts were not significantly correlated with either the BrdU counts ($r=.10$, $p=.53$) or the DCX counts ($r=-.10$, $p=.52$). However, the BrdU and DCX counts were significantly positively correlated ($r=.52$, $p<.001$). Ventral BrdU counts were positively correlated with Ki67 counts ($r=.35$, $p=.019$) but not DCX counts ($r=.01$, $p=.93$). DCX and Ki67 counts in the ventral DG were not significantly correlated ($r=.24$, $p=.11$).

4.3.6. BrdU Counts-28 Day Survival

Figure 4.3: Ki-67⁺ cells in the dorsal (top panel) and ventral (bottom panel) DG 2 hours after the final BrdU injection. Neither N192S nor the housing condition affected the number of Ki-67⁺ cells, in either the dorsal or ventral DG.

Number of Ki-67+ Cells

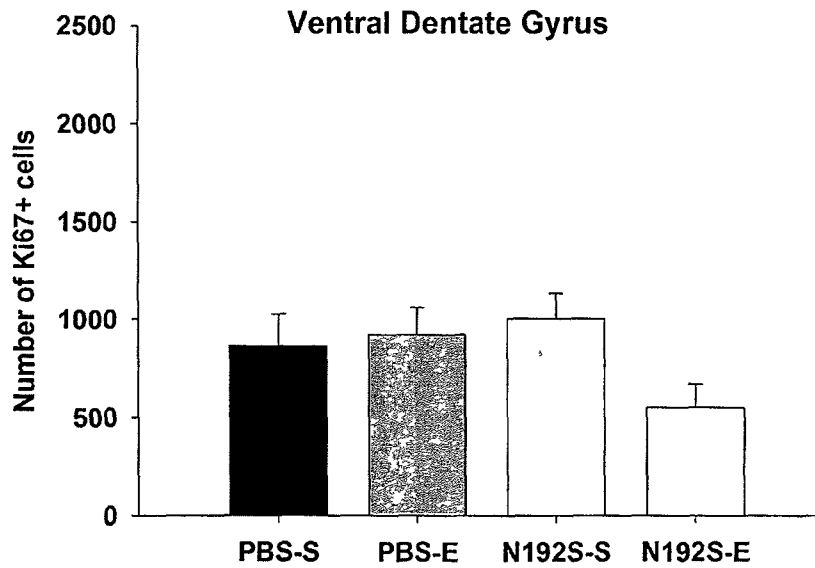
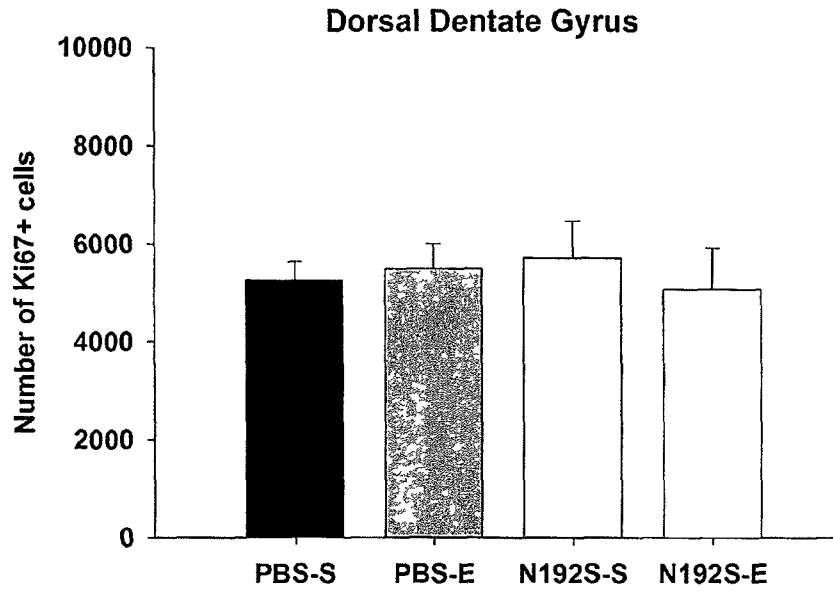
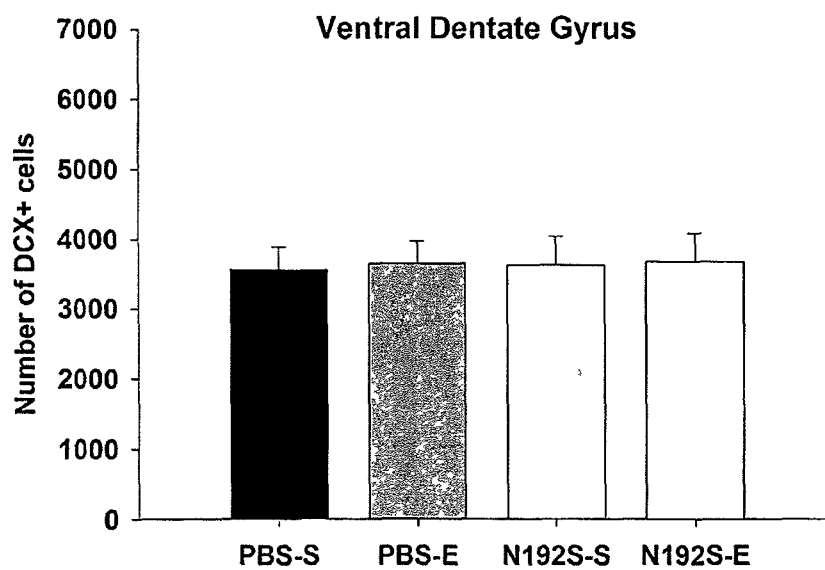
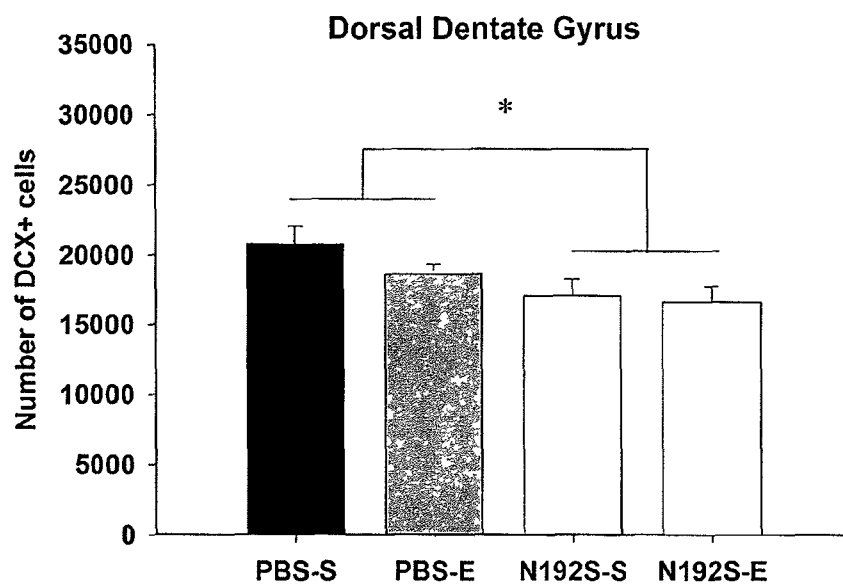


Figure 4.4: DCX⁺ cells in the dorsal (top panel) and ventral (bottom panel) DG 2 hours after the final BrdU injection. N192S rats had 14% fewer DCX⁺ cells in the dorsal DG than did control rats ($F_{1,38}=7.3$, $p=.01$) but did not show any differences in the ventral DG. The housing condition did not have a significant effect on the number of DCX⁺ cells in either the dorsal or ventral DG.

Number of DCX+ Cells



The numbers of BrdU⁺ cells remaining 28 days after the final BrdU injection indicate the total number of new cells produced. As shown in Figure 4.5, this measure was unaffected in the dorsal DG by either N192S ($F_{1,42}=1.29$, NS) or the housing condition ($F_{1,42}<1$). Also, there was no N192S by housing interaction effect on BrdU⁺ cells in the dorsal DG ($F_{1,42}<1$). Similarly, there were no N192S ($F_{1,42}=1.85$, NS), housing ($F_{1,42}<1$) or N192S by housing interaction effects ($F_{1,42}=1.376$, NS) on the number in the ventral DG.

The percentage of surviving cells was calculated by dividing the number of BrdU⁺ cells remaining 28 days after the last injection by the average cell count in each animal's respective treatment group 2 hours after the last injection (Figure 4.6). N192S increased the percentage of BrdU⁺ cells in the dorsal DG that survived the period from 2 h to 28 days ($F_{1,42}=5.60$, $p=.02$). Survival rates were 34% in N192S rats compared to 23% in PBS rats. EE had no effect on cell survival in the dorsal DG ($F_{1,42}<1$) nor was there a N192S by housing interaction ($F_{1,42}<1$). In the ventral DG, there were no main effects of N192S ($F_{1,42}<1$) or housing ($F_{1,42}<1$). However, there was a significant N192S by housing interaction effect ($F_{1,42}=4.67$, $p=.04$). Figure 4.6 indicates that PBS-treated rats showed an increased percent of surviving cells in the ventral DG when housed under EE ($t_{25}=-2.53$, $p=.02$), while no such effect was observed for the lesioned rats who in fact showed slightly reduced levels of survival after EE ($t_{17}<1$).

4.3.7. Differentiation

The percentage of BrdU-positive cells expressing the mature neuronal marker NeuN or the mature astrocytic marker S100B were analyzed using two-way ANOVAs. As shown in Figure 4.7, neither N192S ($F_{1,28}=1.97$, NS) nor enrichment ($F_{1,28}<1$) altered

Figure 4.5: BrdU⁺ cells in the dorsal (top panel) and ventral (bottom panel) DG 28 days after the final BrdU injection. Neither the lesion nor the housing condition altered the number of BrdU-positive cells.

Number of BrdU+ Cells 28 Days After the Final BrdU Injection

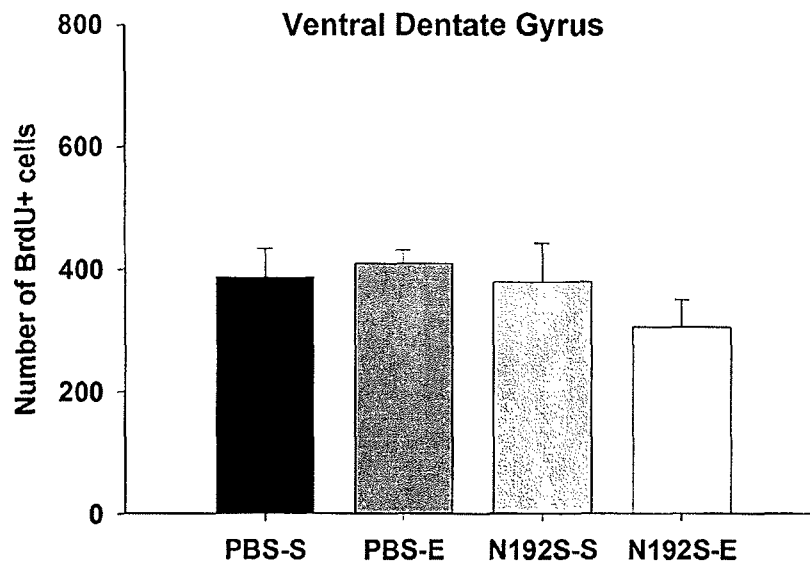
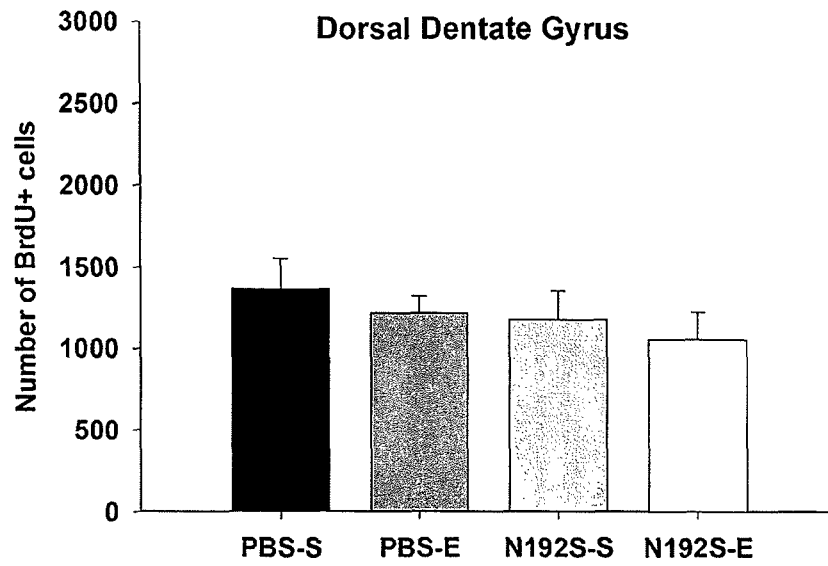
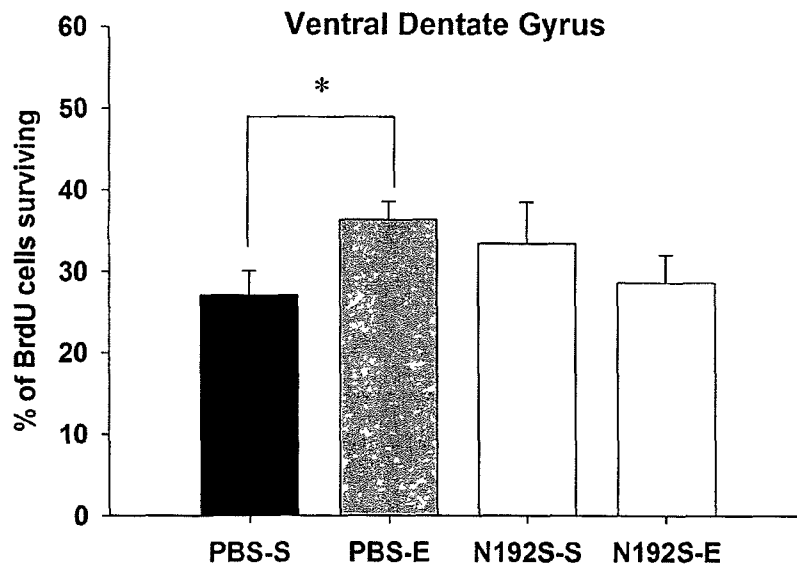
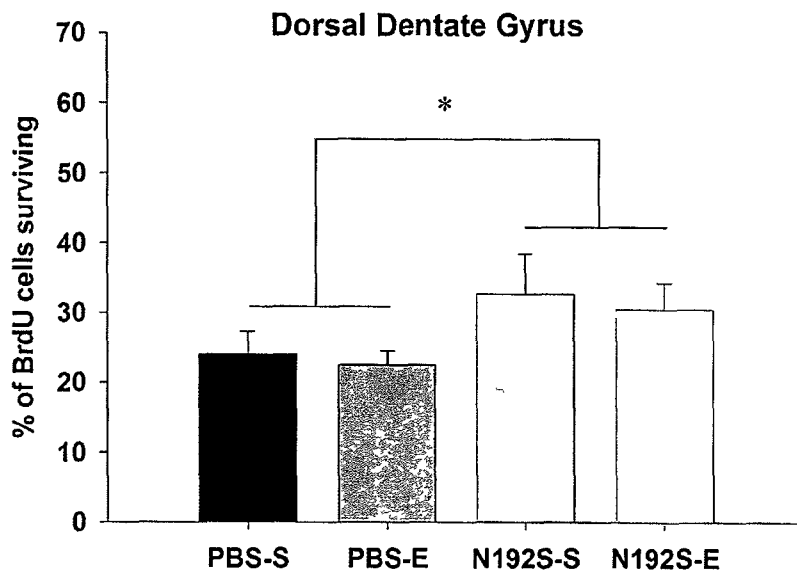


Figure 4.6: Percentage of surviving BrdU⁺ cells in the dorsal (top panel) and ventral (bottom panel) DG 28 days after the final BrdU injection. N192S increased the percentage of surviving cells in the dorsal DG ($F_{1,42}=5.6$, $p=.02$), but this effect was not seen in the ventral DG. While the housing condition did not affect the percentage of surviving cells in the dorsal DG, PBS-treated rats showed an increased percent of surviving cells in the ventral DG when housed under EE ($t_{25}=-2.53$, $p=.02$). This effect was not observed in N192S rats.

Survival of BrdU+ Cells



the proportion of newborn cells expressing NeuN, and there was no N192S by housing interaction ($F_{1,28} < 1$). The percentage of BrdU-positive cells that also expressed S100B was unaffected by N192S ($F_{1,28} = 2.50$, NS) and housing conditions ($F_{1,28} < 1$), and the N192S by housing interaction effect was nonsignificant ($F_{1,28} < 1$). Across all groups, the average percentage of BrdU⁺ cells that expressed NeuN was 80.3%, and the average percentage of BrdU-labelled cells that expressed S100B was 1.4%. 17% of BrdU immunoreactive cells expressed neither NeuN nor S100B, and this was unaffected by the N192S ($F_{1,28} = 1.41$, NS) or housing condition ($F_{1,28} < 1$) and there was no N192S by housing interaction effect ($F_{1,28} < 1$).

The total number of new neurons, defined as the total number of BrdU-positive cells 28 days after BrdU injection, multiplied by the proportion of new cells that expressed NeuN at that time point, was unaffected by both N192S ($F_{1,28} < 1$) and housing ($F_{1,28} = 1.79$, NS). The N192S by housing interaction effect was also nonsignificant ($F_{1,28} < 1$). On average, 926 new neurons were produced in the dorsal DG. These data are shown in Figure 4.8.

As illustrated in Figure 4.9, neither N192S ($F_{1,28} = 1.18$, NS), housing ($F_{1,28} < 1$), nor the N192S by housing interaction ($F_{1,28} < 1$) affected the total number of new astrocytes (total number of BrdU-positive cells 28 days after BrdU injection multiplied by the proportion of new cells that expressed S100B). On average, 24 new astrocytes were generated in the dorsal DG.

4.4. Discussion

4.4.1. Effects of N192S on Neurogenesis

Figure 4.7: Percentage of BrdU⁺ cells expressing NeuN, S100B, or neither. The phenotypic fate of BrdU⁺ cells was unaffected by N192S or the housing condition.

Neuronal and Glial Differentiation of BrdU+ Cells

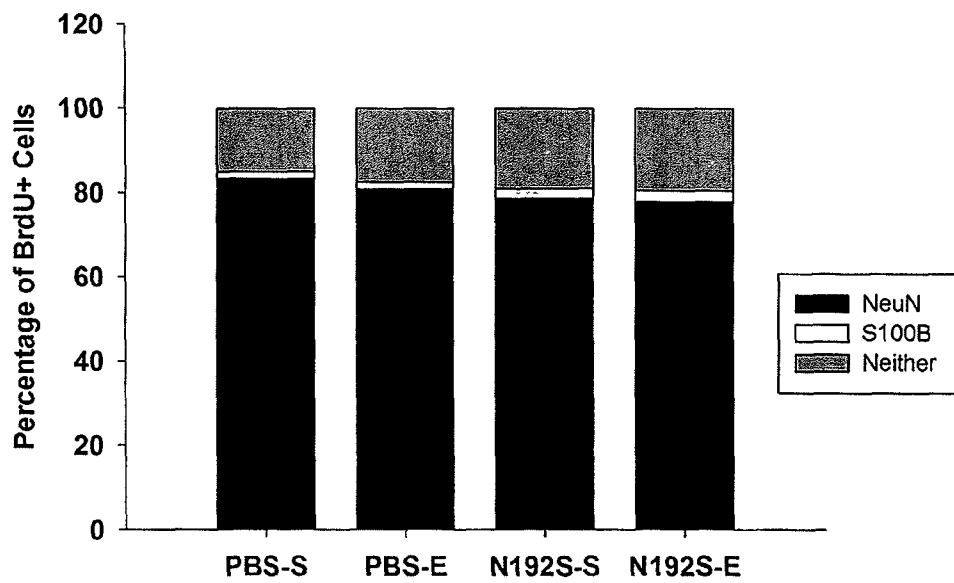


Figure 4.8: Total neurogenesis. Neither N192S nor enrichment altered the total number of new neurons generated.

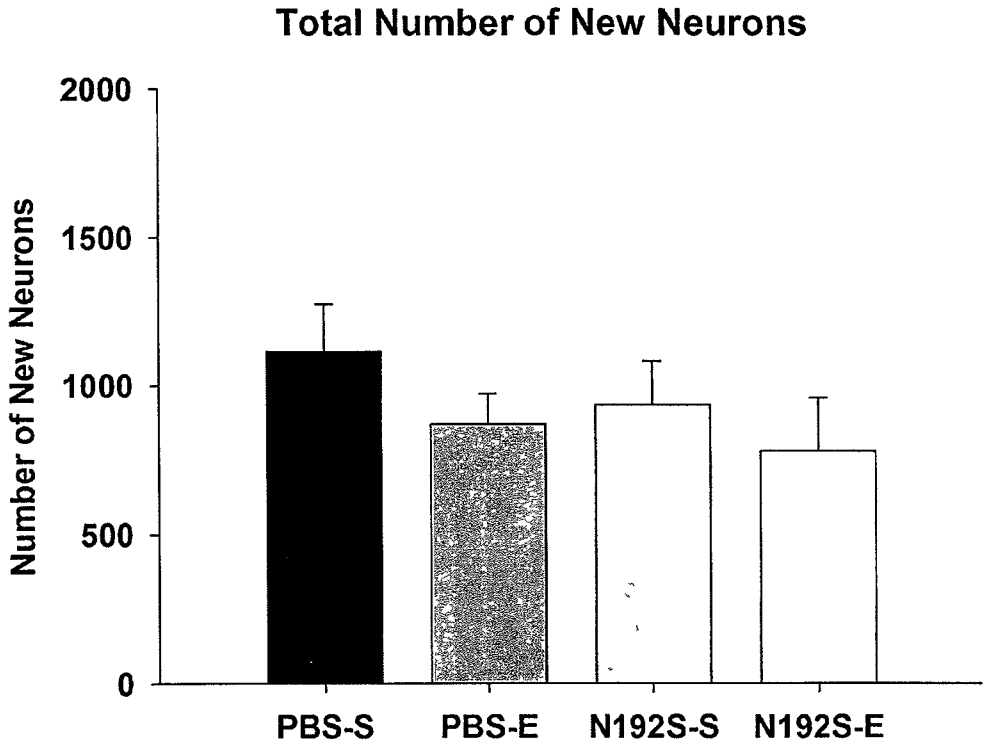
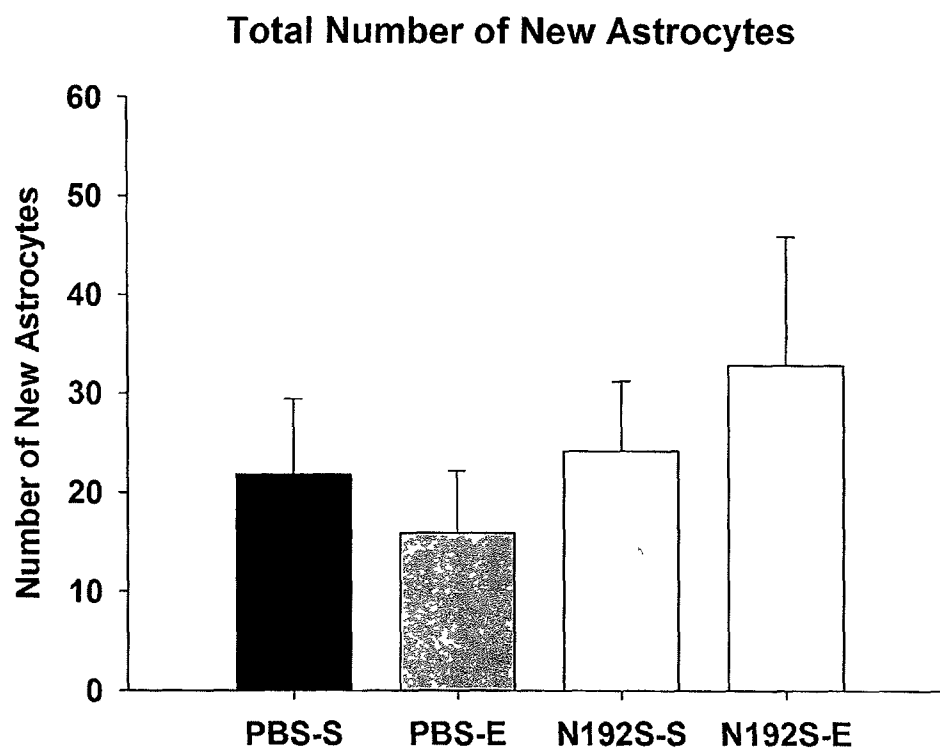


Figure 4.9: Total astrogliogenesis. Neither N192S nor enrichment altered the total number of new astrocytes generated.



N192S reduced the number of BrdU-labelled cells detected in the dorsal DG 2 hours after the last BrdU injection, suggesting a negative effect on cell proliferation. To confirm this, we performed stereological counts of cells expressing Ki-67, an endogenous mitotic marker which is expressed throughout all stages of the cell cycle except the resting phase (Gerdes et al., 1984). Counts of Ki-67⁺ cells and BrdU-labelled cells were previously shown to be altered in parallel after some treatments that up- or downregulated proliferation (Kee et al., 2002), and it was expected here that Ki-67 counts would mirror the BrdU data. Unexpectedly, N192S had no effect on Ki-67 expressing cell number, indicating that proliferation was unaffected. Furthermore, the BrdU and Ki-67 counts in the dorsal DG were not correlated. The lack of agreement between the BrdU and Ki-67 data might indicate that brain levels of BrdU were not equivalent between N192S and control rats, possibly due to unequal passage through the blood-brain barrier or unequal rates of removal of BrdU from the body. However, the observed effect of the lesion on BrdU counts is not likely simply an artefact of unequal BrdU availability, as BrdU counts were significantly correlated with the number of cells expressing DCX, an endogenous marker of immature neurons. The disagreement between the BrdU and Ki-67 data suggests that they measured different aspects of neurogenesis. While Ki-67 strictly labels cells that are in the process of dividing at the time of sacrifice, BrdU remains detectable after the newborn cell becomes postmitotic. In the current study, cells born during the first pulse of BrdU should have exited the cell cycle by the time the animals were sacrificed, and therefore the BrdU counts not only reflect cell proliferation, but would also be influenced by an effect of N192S on the short term survival of the post-mitotic cells. Given the lack of group differences in Ki-67 labelling, it therefore seems

likely that N192S reduced short term survival of the newly born cells, rather than their proliferation.

Four weeks after the last BrdU injection, the number of surviving BrdU-labelled cells was equivalent for the N192S and PBS groups. The most plausible explanation of these results is that N192S hastened but did not amplify the death of newly born cells, such that a reduction of cells was evident 2 hours after the last BrdU injection but not 4 weeks later. This implies that PBS-treated rats, compared to N192S rats, would lose a larger number of cells between 2 hours and 4 weeks after the last BrdU injection. This is supported by the finding that the ratio of cells remaining 4 weeks after the last BrdU injection to the number of cells present 2 hours after the last BrdU pulse was decreased in the dorsal DG of PBS rats compared to the N192S rats. We suggest that N192S accelerates the early post-mitotic demise of newborn DG cells but over an extended time, does not affect their survival rate. In other words, normally a proportion of newborn cells survive, while the rest are destined for apoptotic death (unless they receive additional survival-promoting signals). N192S does not change this proportion, but rather causes the cells that were destined for apoptosis to die sooner.

N192S did not alter the proportion of new cells that became neurons or astrocytes. The majority (80%) of new cells expressed NeuN 28 days after their birth, indicating that they had acquired a neuronal phenotype. Less than 2% of new cells differentiated into S100B-expressing astrocytes. It appears that N192S does not affect cell fate decisions during neurogenesis in adulthood.

In the present study we have expanded on our previous work showing reduced DCX⁺ immature neurons in the DG after N192S (Fréchette et al., 2009), and

demonstrated that N192S appears to reduce the short term survival of new cells without impacting on their proliferation, long-term survival or differentiation. Mohapel et al. (2005) also suggested that adult cholinergic lesion reduced either proliferation or short-term survival of new cells, but they did not distinguish between the two possibilities. Other studies using adult cholinergic lesion (Itou et al., 2010) or pharmacological manipulations (Kaneko et al., 2006; Kotani et al., 2006) agree that the cholinergic system appears to regulate survival rather than proliferation or differentiation of new cells. However, Van Kampen and Eckman (2010) reported that cholinergic lesioned rats showed reductions in the numbers of proliferating cell nuclear antigen (PCNA) –positive cells, suggesting an effect of the lesion on proliferation. However, PCNA is expressed long after the new cell exits the cell cycle (Mandyam et al., 2007), and therefore it is not clear whether the results of Van Kampen and Eckman (2010) reflect an effect of the lesion on proliferation or the short term survival of the new cells.

Both muscarinic (M1 and M4) and nicotinic ($\alpha 7$ and $\beta 2$ subunit-containing) cholinergic receptors are expressed on immature cells in the SGZ of the DG (Kaneko et al., 2006; Mohapel et al., 2005). Furthermore, AChE staining (see Figure 1) and ChAT-positive fibres (Kaneko et al., 2006) are found at high densities in the inner GCL and SGZ, and ChAT⁺ fibres have been found to be in contact with cells expressing PSA-NCAM, a marker for new cells (Kaneko et al., 2006). These findings suggest that cholinergic input is positioned to affect the survival of newborn cells. In support of this, a number of studies have demonstrated neuroprotective and/or anti-apoptotic effects of cholinergic signalling in vitro (Akaike et al., 2010; Akaike et al., 1994; Garrido et al., 2001; Rosa et al., 2006; Yu et al., 2009). Cholinergic signalling through either nicotinic

or muscarinic ACh receptors upregulates Bcl-2 (an anti-apoptotic molecule), and nicotinic receptor activation leads to the phosphorylation and inactivation of the pro-apoptotic proteins Bad and Bax (Resende and Adhikari 2009). Furthermore, cholinergic lesion increases dying cells in the DG, assessed either morphologically (pyknotic cells; Van Kampen and Eckman 2010) or by the TUNEL assay for apoptotic cells (Cooper-Kuhn et al., 2004). Thus, the lack of direct cholinergic stimulation of newborn cells might impair their survival through a failure to inhibit apoptosis.

N192S might also impact newborn cell survival indirectly. For example, cholinergic lesion might influence neurogenesis through changes in brain derived neurotrophic factor (BDNF) signalling. Knockdown of BDNF specifically in the DG using RNA interference was found to decrease neurogenesis (Taliaz et al., 2010), and BDNF knockout mice show reductions in the survival of newborn cells (Sairanen et al., 2005). Conversely, BDNF infusion into the hippocampus upregulates neurogenesis (Scharfman et al., 2005). BDNF expression is modulated by the BFCS. Specific ablation of BFCS neurons in adult rats using 192S has been shown to decrease BDNF mRNA in the hippocampus (Berchtold et al., 2002; Ferencz et al., 1997; Kokaia et al., 1996), though other studies report no change (Gu et al., 1998; Yu et al., 1995) or increases (Paban et al., 2009) in hippocampal BDNF mRNA or protein expression. We recently found that neonatal cholinergic lesion decreased the hippocampal protein content of pro-BDNF, the precursor to BDNF (Ward, Rennie and Pappas, unpublished observations). Though none of these studies has examined the relationship between BDNF expression and neurogenesis after cholinergic lesion, it is reasonable to hypothesize that lesion-

induced decreases in BDNF might account for the reduction in short term survival of new cells seen here.

It has been reported that in the adult rodent, neurosphere-producing (i.e. proliferating) cells in the SVZ, which supplies new neurons to the olfactory bulb, express the p75 receptor (Young et al., 2007). It is not known whether precursor cells in the DG SGZ express p75, and in particular whether they express p75 at the time of toxin exposure on PND7. If this is the case, these cells would be expected to suffer direct immunotoxic effects from 192S, thereby reducing the population of precursor cells. While this possibility can't be ruled out entirely, it seems an unlikely explanation for the reduction in BrdU-labelled cells seen here. If the toxin killed the SGZ progenitor cells, one would expect to see reductions in cell proliferation, rather than changes in the short term survival of new cells.

The number of immature DCX⁺ neurons was reduced by N192S. While intuitively this reduction might seem to be of little functional consequence given the finding that net neurogenesis was unchanged, the decreased number of DCX⁺ neurons after cholinergic lesion may have functional relevance in its own right. Immature neurons have unique properties that have been hypothesized to allow them to make a special contribution to hippocampal function (Doetsch and Hen 2005). Newborn neurons are more easily excited, have lowered thresholds for LTP induction (Schmidt-Hieber et al., 2004; Wang et al., 2000) and are integrated into hippocampal circuits where they are thought to participate in supporting spatial memory (Kee et al., 2007). Recently it was shown in vivo that specific, transient ablation of immature neurons results in impaired long-term memory retention in mice (Deng et al., 2009), suggesting that these cells play a

role in hippocampal memory function. It would be interesting to test N192S rats on a task such as the long-term memory task used by Deng et al. which is known to be sensitive to reductions in immature neurons. Notably, though N192S rats exhibit normal cognitive ability on most tasks when tested as adults, long-term but not short-term retention of a socially-transmitted food preference was impaired in N192S rats (Ricceri et al., 2004). Whether this is related to impaired neurogenesis is unknown, but the possibility is intriguing.

While in this case, we found no difference in the total number of new neurons generated, it is possible to imagine circumstances in which a reduction of short-term survival could impair net neurogenesis. Kempermann (2008) theorizes that the role of cell proliferation in the adult hippocampus is to provide a pool of new cells that can be recruited and integrated into networks under conditions where computational needs arise, such as while learning a novel task. Accordingly, cognitive tasks have been shown to increase the survival of new cells in the DG if learning takes place when the cells are at a specific developmental stage (Epp et al., 2007). N192S rats, having reduced levels of immature cells, would have a correspondingly reduced potential for incorporation of new cells into circuits. In circumstances where an appropriate survival-promoting signal is present (e.g. cognitive demand), N192S rats might show reductions in net neurogenesis. Given the hypothesized role of neurogenesis in learning and memory (Deng et al., 2010; Kitabatake et al., 2007; Leuner et al., 2006) this might also be expected to impair performance on cognitive tasks. It would be of great interest to determine whether behaviourally tested N192S rats would exhibit decreased net neurogenesis compared to tested controls, as predicted by the above hypothesis.

The reduction in both DCX⁺ cells and BrdU⁺ cells in lesioned animals was seen only in the dorsal DG while ventral neurogenesis was unaffected by the lesion. This may be due to the fact that the lesion is less complete in the ventral hippocampus compared to the dorsal sector. Leanza et al. (1996) reported that the density of cholinesterase-positive fibres remaining in the ventral hippocampus after neonatal cholinergic lesion was greater than in the dorsal hippocampus. Visual inspection of cholinesterase-stained sections of the ventral hippocampi of animals used in the present study indicated a similar dorsal-ventral gradient in lesion severity. Alternatively, neurogenesis may be regulated differently in the dorsal and ventral sectors. Some evidence exists to support the idea that dorsal and ventral hippocampal neurogenesis can be regulated independently of each other. For example, the ventral hippocampus is more sensitive to the neurogenesis-enhancing effects of the antidepressant agomelatine (Banasr et al., 2006), as well as the negative effects of chronic mild stress (Jayatissa et al., 2006) and corticosterone treatment on neurogenesis (Brummelte and Galea 2010).

The dorsal/ventral gradient in neurogenic sensitivity to cholinergic deafferentation might be functionally important. The dorsal and ventral hippocampi are thought to contribute preferentially to memory and emotion/anxiety processing, respectively (Bannerman et al., 2004; Bertoglio et al., 2006; Degroot and Treit 2004; Esclassan et al., 2009; McEown and Treit 2009). Accordingly, dorsal and ventral neurogenesis have been hypothesized to be functionally distinct, with changes in ventral neurogenesis being related to affect, anxiety and the behavioural response to antidepressants, and changes in dorsal neurogenesis being associated with learning and memory processes (Jinno 2010; Sahay and Hen 2007). N192S-induced changes in short term survival or the number of

immature neurons in the dorsal DG would therefore be expected to influence learning and memory processes, but not anxiety/affect.

4.4.2. Combined Effects of N192S and Enrichment

While several laboratories have shown that EE upregulates DG neurogenesis (Brown et al., 2003a; Kempermann et al., 1997; Kempermann et al., 1998; Nilsson et al., 1999; Rossi et al., 2006), we did not observe that effect here. Surprisingly, EE had no impact on cell proliferation, newborn cell survival, differentiation, or total overall levels of neurogenesis in the dorsal DG in either the control or lesioned rats. In addition, while enrichment increased the long-term survival of BrdU⁺ cells in the ventral DG of PBS rats, this was insufficient to result in an overall increase in net neurogenesis. We previously found that rats housed under the same enrichment conditions as we used in the current study showed a tendency towards increased numbers of DCX⁺ cells in the DG, but that this effect just failed to reach statistical significance. We suggested that result was due to the use of DCX as a marker for neurogenesis, which likely underestimates the effects of enrichment (see discussion in Fréchette et al., 2009). However, based on the present results, it appears that our enrichment protocol simply does not produce robust changes in neurogenesis. The reason for the lack of enrichment effects is unclear. Enrichment parameters (duration of enrichment, specifics of the environment, and number of cagemates), subjects (species, sex, and age at onset of enrichment) and methods of quantifying levels of neurogenesis (timing and number of BrdU injections, interval between BrdU injections and sacrifice) vary widely between studies, and may explain the discrepant results found here. Unfortunately, the lack of enrichment effects prevented a

principal aim of this project, namely to ascertain the effect of N192S on EE-induced neurogenesis.

The lack of effect of EE on neurogenesis is puzzling as we have previously reported that this EE regimen had a robust enhancing effect on spatial learning and as well, it eliminated the reduction of CA1 dendritic spines that was observed in N192S rats housed in standard conditions (Fréchette et al., 2009). It seems that not all EE procedures promote neurogenesis despite their effect on behaviour and neuronal cytoarchitecture. This adds to the existing evidence (Meshi et al., 2006) that enrichment-induced improvements in at least some types of learning and memory are independent of the effects of enrichment on neurogenesis. While this study provided some indication that the cholinergic system may also be involved in the neurogenic response to EE at least for the ventral DG, further research is warranted using an EE protocol that has robust effects on neurogenesis in the dorsal DG. Very few studies have specifically examined the effects of enrichment on the ventral hippocampus in terms of neurogenesis, or other outcomes such as changes in protein expression, cell morphology, neurotrophin levels, neurotransmitter dynamics or synaptic plasticity. The current findings suggest that the ventral DG may be sensitive to enrichment, and detailed examinations of the enrichment-induced changes in the ventral hippocampus are warranted.

4.5. Conclusions

N192S impaired the short-term survival of newborn cells in both standard housed and EE rats. Furthermore, N192S rats did not show the enhanced survival of new cells that was seen in the ventral DG of PBS rats after enrichment, suggesting that the cholinergic system may be important for the neurogenic response to enrichment. It would

be interesting to examine neurogenesis in N192S rats after training on a learning task which is known to promote the survival of new cells, to determine whether neurogenic responsiveness is generally impaired in N192S rats. It would also be informative to test standard and enriched-housed N192S rats on tasks that are sensitive to reductions in neurogenesis, especially one for which enhanced performance after enrichment requires an upregulation of neurogenesis (Buel-Jungerman et al., 2005).

5. General Discussion and Conclusions

Three experiments were carried out here. The first two were based on the hypothesis that neonatal lesioning of the BFCS in the rat would lead to more severe cognitive and neural impairments during aging, or when accompanied by aging-related physiological changes, in this instance chronic cerebral hypoperfusion. It was further hypothesized that the cognitive and neural impairments would mimic those observed in Alzheimer's disease. The latter did not occur. However, there were several indications of an interaction between the lesion and both aging and chronic hypoperfusion.

The first experiment showed that N192S and aging interact to produce deficits in spatial working memory, while neither aging nor N192S alone resulted in memory impairment. Despite the cognitive decline observed in aged N192S rats, the neural effects of N192S in aged rats did not mimic the changes associated with AD. Substantial CA1 pyramidal cell loss occurs in the AD brain (in the range of 50-70%; (Bobinski et al., 1998; Kril et al., 2002; Rössler et al., 2002; West et al., 1994b)), along with severe regression of both the apical and basal dendritic trees (Hanks and Flood 1991). In addition, AD brains show increased astrocytic reactivity in the hippocampus and temporal cortex (Muramori et al., 1998; Sheng et al., 1994; Van Eldik and Griffin 1994; Vijayan et al., 1991). In contrast, compared to age-matched controls, 21-month-old N192S rats did not show CA1 cell loss in the dorsal or ventral hippocampus, nor did they exhibit astrogliosis in any hippocampal subfield. Finally, rather than exhibiting widespread dendritic atrophy, the CA1 cells of aged N192S rats showed subtle alterations in the distribution of dendritic material along the length of the dendritic tree. Thus the combination of aging and cholinergic lesion is not sufficient to reproduce the

neuropathological features of AD. However, the altered dendritic morphology of CA1 cells in aged N192S rats could potentially affect hippocampal function. Furthermore, as pointed out by Flood (1993), the ability of dendrites to continue to exhibit plasticity with age might be just as, or more, important than the absolute size or complexity of the dendritic arbour at any given time. Thus, it would be informative to determine whether age-related changes in dendritic plasticity are modified by N192S lesion.

The second experiment indicated that while N192S lesion combined with chronic cerebral hypoperfusion produced working memory impairments and increased anxiety, this model also does not mimic the neuropathological features of AD. These animals exhibited no loss of CA1 cells and showed dendritic hypertrophy rather than regression in these neurons. However, it would be interesting to examine the brains of these animals at longer post-surgical intervals to determine whether CA1 cell loss might become apparent, and whether the observed changes in dendritic morphology would be maintained with advancing age. As well, the effects of sex on the outcome of these treatments merit explicit examination.

The third experiment examined whether N192S affected the proliferation, differentiation and survival of newborn hippocampal neurons. It meant to determine if N192S rats show an altered neurogenic response to environmental enrichment. Surprisingly, enrichment was not found to affect neurogenesis in the dorsal dentate gyrus in either control or N192S rats and as a result, the aforementioned aim could not be assessed. However, it was discovered that N192S impaired the short-term survival of newborn cells in both standard housed and EE rats. Furthermore, N192S rats did not show the enhanced survival of new cells that was seen in the ventral DG of PBS rats after

enrichment, suggesting that the cholinergic system may be important for the neurogenic response to enrichment.

These three experiments revealed significant new information concerning the effects of neonatal lesioning of the BFCS.

Rats subjected to N192S were more susceptible to the effects of both aging and 2VO on spatial working memory. It does not seem likely that aging and 2VO each have a subthreshold effect on working memory, which when added to the effects of N192S results in observable impairment. Neither aged control rats, nor rats subjected to 2VO or N192S alone, showed a tendency towards impaired working memory. Rather, N192S seems to synergise with both aging and 2VO. N192S might prevent or impair a compensatory response to aging or 2VO that normally allows for intact working memory in these animals. Cellular dysfunction caused by aging or 2VO (whether related to the observed dendritic remodelling of CA1 cells or not) may be compounded by a lack of acetylcholine at the time of behavioural testing. In other words, damaged cells may be more sensitive to reduced levels of ACh. Alternatively, the lack of ACh during and after 2VO, or over the course of aging, may have exacerbated the cellular damage or dysfunction associated with these factors, resulting in impaired memory. Furthermore, both aging and 2VO are associated with impaired cholinergic function (Bartus et al., 1982; Terry and Buccafusco 2003), and it has been suggested that memory may be impaired only when cholinergic dysfunction surpasses a certain threshold (Wrenn et al., 1999). It is possible that by combining N192S with 2VO- or aging-induced changes in the cholinergic system, this threshold was exceeded, resulting in memory impairment. Future studies should aim to determine the neural basis of impaired working memory in

aged N192S and N192S-2VO rats. One area of the brain that might be of particular interest in this regard is the prefrontal cortex (PFC), which is known to mediate working memory. Pyramidal cells in this area show reduced dendritic complexity in adult rats after N192S (Sherren and Pappas 2005), and an examination of PFC pyramidal cells in aged N192S and N192S-2VO rats might provide insight into the neural correlates of cognitive impairments in these animals. Additionally, it is important to determine which factors in the aging brain interact with N192S. The current research suggests that cerebral hypoperfusion may be one such factor, but there are likely to be several others.

N192S by itself or in combination with 2VO (experiment two) induced anxiety-like behaviour in the open field that was evident with repeated exposure to the apparatus. This suggests that habituation to anxiety-provoking situations is impaired in N192S rats. Conversely, it might be argued that instead of increased anxiety, the behaviour of N192S rats in the open field reflected a failure to remember the apparatus. However, this is unlikely for two reasons. First, N192S rats did show a typical habituation profile (reduced locomotor activity with repeated exposure) in terms of the total distance traveled, indicating intact memory for the open field. Secondly, the consistent finding that N192S rats are not impaired in terms of spatial reference memory further supports the notion that these results are due to increased anxiety rather than impaired memory. Further research on the effects of cholinergic lesion on anxiety-like behaviour is warranted.

Whereas previous work in our laboratory has shown reduced apical branching and spines, as well as a decrease in the length of the basal dendrites of CA1 cells from young male rats after N192S (Fréchette et al., 2009), the present studies found either no change in middle-aged females (study 2) or subtle alterations in aged males that were

qualitatively different from those seen in the CA1 cells of the young rat (experiment 1). Collectively these results indicate that the effects of the lesion on dendritic morphology change dynamically over time, as is also the case for adult cholinergic lesions (Works et al., 2004). Future research might examine whether the effects of cholinergic lesion on dendritic morphology are dependent on the age at which the lesion occurs. For example, if animals were subjected to cholinergic lesion at an advanced age, would we observe the same dendritic alterations as in aged rats subjected to N192S?

Whether changes in CA1 dendritic structure in the aged N192S rat account for, or at least contribute to, the working memory impairment seen in these rats is unknown. However, despite the dendritic reductions seen in young animals after N192S, working memory is unimpaired in these rats (Fréchette et al., 2009), suggesting that changes in dendritic structure of CA1 cells are not necessarily correlated with behavioural outcomes. It would be of interest to examine the dendritic morphology of other cell types in the aged N192S rat, particularly in areas of the brain known to mediate working memory, such as the prefrontal cortex.

We have previously observed reductions in the number of DCX-positive cells in the DG after N192S (Fréchette et al., 2009), and this result was replicated here in young male and middle-aged female rats, but not middle-aged or aged male rats. Thus, the effects of cholinergic lesion on neurogenesis may be both age- and sex-dependent. The results of the third experiment suggest that the reduction in immature DCX+ cells in N192S rats is due to impaired short-term survival of new cells, rather than to reductions in proliferation. The functional implications of the alterations in neurogenesis seen in N192S rats are currently unknown. Adult neurogenesis is believed to be involved in

certain forms of learning and memory (Raber et al., 2004; Saxe et al., 2006; Shors et al., 2001; Shors et al., 2002; Snyder et al., 2005; Winocur et al., 2006), and in particular, immature neurons may play a unique role in cognitive functions (Deng et al., 2009). While learning and memory abilities are relatively intact in N192S rats, it is possible that the reduction in immature neurons might result in impaired memory in certain tasks, particularly those that are sensitive to disruptions in neurogenesis. Furthermore, the hypothesis that the reduction in short-term survival of new cells would translate into a reduction in the overall rate of neurogenesis in N192S rats when a survival-promoting signal is applied warrants further investigation. Indeed, it was hoped that the enrichment study would answer this question, but the surprising lack of effect of enrichment on newborn cell survival prevented us from making any conclusions in this regard. Recent research suggests that the effects of enrichment on cell survival are strongest after short periods of EE (Llorens-Martin et al., 2010), so an examination of short-duration enrichment-induced neurogenesis in N192S rats might help resolve this issue.

N192S did not result in CA1 cell loss in either aged male (experiment one) or middle-aged female (experiment two) rats, suggesting that cholinergic input is not required for the survival of mature CA1 cells. Conversely, N192S impaired the short-term survival of newborn cells in the dentate gyrus. Cholinergic signalling therefore appears to be vital for some survival-promoting process in the young DG cell that is either not necessary to maintain the survival of mature CA1 cells, or which is independent of cholinergic signalling in these cells.

References

- Akaike, A., Takada-Takatori, Y., Kume, T., Izumi, Y., 2010. Mechanisms of neuroprotective effects of nicotine and acetylcholinesterase inhibitors: Role of alpha4 and alpha7 receptors in neuroprotection. *J Mol Neurosci.* 40, 211-216.
- Akaike, A., Tamura, Y., Yokota, T., Shimohama, S., Kimura, J., 1994. Nicotine-induced protection of cultured cortical neurons against N-methyl-D-aspartate receptor-mediated glutamate cytotoxicity. *Brain Res.* 644, 181-187.
- Alkayed, N.J., Harukuni, I., Kimes, A.S., London, E.D., Traystman, R.J., Hurn, P.D., Grady, P.A., 1998. Gender-linked brain injury in experimental stroke • editorial comment. *Stroke.* 29, 159-166.
- Altman, J., 1969. Autoradiographic and histological studies of postnatal neurogenesis. IV. cell proliferation and migration in the anterior forebrain, with special reference to persisting neurogenesis in the olfactory bulb. *J Comp Neurol.* 137, 433-457.
- Altman, J., Das, G.D., 1965. Autoradiographic and histological evidence of postnatal hippocampal neurogenesis in rats. *J Comp Neurol.* 124, 319-335.
- Apostolova, L.G., Cummings, J.L., 2008. Neuropsychiatric manifestations in mild cognitive impairment: A systematic review of the literature. *Dement Geriatr Cogn Disord.* 25, 115-126.
- Armstrong, D.M., Bruce, G., Hersh, L.B., Gage, F.H., 1987. Development of cholinergic neurons in the septal/diagonal band complex of the rat. *Brain Res.* 433, 249-256.
- Arters, J., Hohmann, C.F., Mills, J., Olaghery, O., Berger-Sweeney, J., 1998. Sexually dimorphic responses to neonatal basal forebrain lesions in mice: I. behavior and neurochemistry.. *J Neurobiol.* 37, 582-594.
- Auld, D.S., Kornecook, T.J., Bastianetto, S., Quirion, R., 2002. Alzheimer's disease and the basal forebrain cholinergic system: Relations to β -amyloid peptides, cognition, and treatment strategies. *Prog Neurobiol.* 68, 209-245.
- Aznavour, N., Mechawar, N., Descarries, L., 2002. Comparative analysis of cholinergic innervation in the dorsal hippocampus of adult mouse and rat: A quantitative immunocytochemical study. *Hippocampus.* 12, 206-217.
- Aztiria, E., Capodici, G., Arancio, L., Leanza, G., 2007. Extensive training in a maze task reduces neurogenesis in the adult rat dentate gyrus probably as a result of stress. *Neurosci Lett.* 416, 133-137.

- Banasr, M., Soumier, A., Hery, M., Mocaër, E., Daszuta, A., 2006. Agomelatine, a new antidepressant, induces regional changes in hippocampal neurogenesis. *Biol Psychiatry*. 59, 1087-1096.
- Bannerman, D.M., Rawlins, J.N.P., McHugh, S.B., Deacon, R.M.J., Yee, B.K., Bast, T., Zhang, W.-., Pothuizen, H.H.J., Feldon, J., 2004. Regional dissociations within the hippocampus—memory and anxiety. *Neuroscience & Biobehavioral Reviews*. 28, 273-283.
- Bannister, N.J., Larkman, A.U., 1995. Dendritic morphology of CA1 pyramidal neurones from the rat hippocampus: I. branching patterns. *J Comp Neurol*. 360, 150-160.
- Bannon, A.W., Curzon, P., Gunther, K.L., Decker, M.W., 1996. Effects of intraseptal injection of 192-IgG-saporin in mature and aged long-evans rats. *Brain Res*. 718, 25-36.
- Bartesaghi, R., Severi, S., Guidi, S., 2003. Effects of early environment on pyramidal neuron morphology in field CA1 of the guinea-pig. *Neuroscience*. 116, 715-732.
- Bartus, R., Dean, R., 3rd, Beer, B., Lippa, A., 1982. The cholinergic hypothesis of geriatric memory dysfunction. *Science*. 217, 408-414.
- Baskin, D.S., Browning, J.L., Pirozzolo, F.J., Korporaal, S., Baskin, J.A., Appel, S.H., 1999. Brain choline acetyltransferase and mental function in Alzheimer disease. *Arch Neurol*. 56, 1121-1123.
- Baxter, M.G., Bucci, D.J., Sobel, T.J., Williams, M.J., Gorman, L.K., Gallagher, M., 1996. Intact spatial learning following lesions of basal forebrain cholinergic neurons. *Neuroreport*. 7, 1417-1420.
- Belleville, S., Rouleau, N., Van der Linden, M., Collette, F., 2003. Effect of manipulation and irrelevant noise on working memory capacity of patients with Alzheimer's dementia. *Neuropsychology*. 17, 69-81.
- Belleville, S., Peretz, I., Malenfant, D., 1996. Examination of the working memory components in normal aging and in dementia of the Alzheimer type. *Neuropsychologia*. 34, 195-207.
- Bennett, S.A., Tenniswood, M., Chen, J.H., Davidson, C.M., Keyes, M.T., Fortin, T., Pappas, B.A., 1998. Chronic cerebral hypoperfusion elicits neuronal apoptosis and behavioral impairment. *Neuroreport*. 9, 161-166.
- Bennett, E.L., Krech, D., Rosenzweig, M.R., 1964. Reliability and regional specificity of cerebral effects of environmental complexity and training. *J Comp Physiol Psychol*. 57, 440-441.

- Bennett, J.C., McRae, P.A., Levy, L.J., Frick, K.M., 2006. Long-term continuous, but not daily, environmental enrichment reduces spatial memory decline in aged male mice. *Neurobiol Learn Mem.* 85, 139-152.
- Berchtold, N.C., Kesslak, J.P., Cotman, C.W., 2002. Hippocampal brain-derived neurotrophic factor gene regulation by exercise and the medial septum. *J Neurosci Res.* 68, 511-521.
- Berger-Sweeney, J., 1998. The effects of neonatal basal forebrain lesions on cognition: Towards understanding the developmental role of the cholinergic basal forebrain. *Int J Dev Neurosci.* 16, 603-612.
- Bertoglio, L.J., Joca, S.R.L., Guimarães, F.S., 2006. Further evidence that anxiety and memory are regionally dissociated within the hippocampus. *Behav Brain Res.* 175, 183-188.
- Bierer, L.M., Haroutunian, V., Gabriel, S., Knott, P.J., Carlin, L.S., Purohit, D.P., Perl, D.P., Schmeidler, J., Kanof, P., 1995. Neurochemical correlates of dementia severity in Alzheimer's disease: Relative importance of the cholinergic deficits. *J Neurochem.* 64, 749-760.
- Bizon, J.L., Gallagher, M., 2003. Production of new cells in the rat dentate gyrus over the lifespan: Relation to cognitive decline. *Eur J Neurosci.* 18, 215-219.
- Bobinski, M., de Leon, M.J., Tarnawski, M., Wegiel, J., Bobinski, M., Reisberg, B., Miller, D.C., Wisniewski, H.M., 1998. Neuronal and volume loss in CA1 of the hippocampal formation uniquely predicts duration and severity of Alzheimer disease. *Brain Res.* 805, 267-269.
- Bohnen, N.I., Kaufer, D.I., Hendrickson, R., Ivanco, L.S., Lopresti, B., Davis, J.G., Constantine, G., Mathis, C.A., Moore, R.Y., DeKosky, S.T., 2005. Cognitive correlates of alterations in acetylcholinesterase in Alzheimer's disease. *Neurosci Lett.* 380, 127-132.
- Bowen, D.M., Smith, C.B., White, P., Davison, A.N., 1976. Neurotransmitter-related enzymes and indices of hypoxia in senile dementia and other abiotrophies. *Brain.* 99, 459-496.
- Brabander, d., Kramers, Uylings, 1998. Layer-specific dendritic regression of pyramidal cells with ageing in the human prefrontal cortex. *Eur J Neurosci.* 10, 1261-1269.
- Brown, J., Cooper-Kuhn, C.M., Kempermann, G., Van Praag, H., Winkler, J., Gage, F.H., Kuhn, H.G., 2003a. Enriched environment and physical activity stimulate hippocampal but not olfactory bulb neurogenesis. *Eur J Neurosci.* 17, 2042-2046.

- Brown, J.P., Couillard-Després, S., Cooper-Kuhn, C.M., Winkler, J., Aigner, L., Kuhn, H.G., 2003b. Transient expression of doublecortin during adult neurogenesis. *J Comp Neurol.* 467, 1-10.
- Bruel-Jungerman, E., Laroche, S., Rampon, C., 2005. New neurons in the dentate gyrus are involved in the expression of enhanced long-term memory following environmental enrichment. *Eur J Neurosci.* 21, 513-521.
- Brummelte, S., Galea, L.A.M., 2010. Chronic high corticosterone reduces neurogenesis in the dentate gyrus of adult male and female rats. *Neuroscience.* 168, 680-690.
- Burk, J.A., Herzog, C.D., Porter, M.C., Sarter, M., 2002. Interactions between aging and cortical cholinergic deafferentation on attention. *Neurobiol Aging.* 23, 467-477.
- Caceres, A., Steward, O., 1983. Dendritic reorganization in the denervated dentate gyrus of the rat following entorhinal cortical lesions: A golgi and electron microscopic analysis. *J Comp Neurol.* 214, 387-403.
- Cada, A., de la Torre, J.C., Gonzalez-Lima, F., 2000. Chronic cerebrovascular ischemia in aged rats: Effects on brain metabolic capacity and behavior. *Neurobiol Aging.* 21, 225-233.
- Cameron, H.A., McKay, R.D., 2001. Adult neurogenesis produces a large pool of new granule cells in the dentate gyrus. *J Comp Neurol.* 435, 406-417.
- Cameron, H.A., McKay, R.D., 1999. Restoring production of hippocampal neurons in old age. *Nat Neurosci.* 2, 894-897.
- Carlesimo, G.A., Mauri, M., Graceffa, A.M., Fadda, L., Loasses, A., Lorusso, S., Caltagirone, C., 1998. Memory performances in young, elderly, and very old healthy individuals versus patients with Alzheimer's disease: Evidence for discontinuity between normal and pathological aging. *J Clin Exp Neuropsychol.* 20, 14-29.
- Caserta, M.T., Bannon, Y., Fernandez, F., Giunta, B., Schoenberg, M.R., Tan, J., 2009. Normal brain aging clinical, immunological, neuropsychological, and neuroimaging features. *Int Rev Neurobiol.* 84, 1-19.
- Chappell, J., McMahan, R., Chiba, A., Gallagher, M., 1998. A re-examination of the role of basal forebrain cholinergic neurons in spatial working memory. *Neuropharmacology.* 37, 481-487.
- Christie, B.R., Cameron, H.A., 2006. Neurogenesis in the adult hippocampus. *Hippocampus.* 16, 199-207.
- Clarke, D.J., 1985. Cholinergic innervation of the rat dentate gyrus: An immunocytochemical and electron microscopical study. *Brain Res.* 360, 349-354.

- Cohen-Cory, S., Dreyfus, C.F., Black, I.B., 1989. Expression of high- and low-affinity nerve growth factor receptors by purkinje cells in the developing rat cerebellum. *Exp Neurol.* 105, 104-109.
- Conner, J.M., Culberson, A., Packowski, C., Chiba, A.A., Tuszynski, M.H., 2003. Lesions of the basal forebrain cholinergic system impair task acquisition and abolish cortical plasticity associated with motor skill learning. *Neuron.* 38, 819-829.
- Connor, D.J., Thal, L.J., Mandel, R.J., Langlais, P.J., Masliah, E., 1992. Independent effects of age and nucleus basalis magnocellularis lesion: Maze learning, cortical neurochemistry, and morphometry. *Behav Neurosci.* 106, 776-788.
- Cooper-Kuhn, C.M., Winkler, J., Kuhn, H.G., 2004. Decreased neurogenesis after cholinergic forebrain lesion in the adult rat. *J Neurosci Res.* 77, 155-165.
- Court, J., Martin-Ruiz, C., Piggott, M., Spurdin, D., Griffiths, M., Perry, E., 2001. Nicotinic receptor abnormalities in Alzheimer's disease. *Biol Psychiatry.* 49, 175-184.
- Craig, L.A., Hong, N.S., Kopp, J., McDonald, R.J., 2009. Selective lesion of medial septal cholinergic neurons followed by a mini-stroke impairs spatial learning in rats. *Exp Brain Res.* 193, 29-42.
- Crain, B., Cotman, C., Taylor, D., Lynch, G., 1973. A quantitative electron microscopic study of synaptogenesis in the dentate gyrus of the rat. *Brain Res.* 63, 195-204.
- Cummings, B.J., Su, J.H., Geddes, J.W., Van Nostrand, W.E., Wagner, S.L., Cunningham, D.D., Cotman, C.W., 1992. Aggregation of the amyloid precursor protein within degenerating neurons and dystrophic neurites in Alzheimer's disease. *Neuroscience.* 48, 763-777.
- Davidson, C.M., Pappas, B.A., Stevens, W.D., Fortin, T., Bennett, S.A.L., 2000. Chronic cerebral hypoperfusion: Loss of pupillary reflex, visual impairment and retinal neurodegeneration. *Brain Res.* 859, 96-103.
- Davies, P., Maloney, A.J.F., 1976. Selective loss of central cholinergic neurons in Alzheimer's disease. *The Lancet.* 308, 1403-1403.
- Dayer, A.G., Ford, A.A., Cleaver, K.M., Yassaee, M., Cameron, H.A., 2003. Short-term and long-term survival of new neurons in the rat dentate gyrus. *J Comp Neurol.* 460, 563-572.
- De Butte, M., Fortin, T., Pappas, B.A., 2002. Pinealectomy: Behavioral and neuropathological consequences in a chronic cerebral hypoperfusion model. *Neurobiol Aging.* 23, 309-317.

- de Fockert, J.W., 2005. Keeping priorities: The role of working memory and selective attention in cognitive aging. *Sci Aging Knowledge Environ.* 2005, pe34.
- De Jong, G.I., Farkas, E., Stienstra, C.M., Plass, J.R.M., Keijser, J.N., de la Torre, J.C., Luiten, P.G.M., 1999. Cerebral hypoperfusion yields capillary damage in the hippocampal CA1 area that correlates with spatial memory impairment. *Neuroscience.* 91, 203-210.
- De Jong, G.I., De Vos, R.A., Steur, E.N., Luiten, P.G., 1997. Cerebrovascular hypoperfusion: A risk factor for Alzheimer's disease? animal model and postmortem human studies. *Ann N Y Acad Sci.* 826, 56-74.
- de la Torre, J.C., 2002. Vascular basis of Alzheimer's pathogenesis. *Ann N Y Acad Sci.* 977, 196-215.
- de la Torre, J.C., 2009. Cerebrovascular and cardiovascular pathology in Alzheimer's disease. *Int Rev Neurobiol.* 84, 35-48.
- de la Torre, J.C., 2006. How do heart disease and stroke become risk factors for Alzheimer's disease? *Neurol Res.* 28, 637-644.
- de la Torre, J.C., Nelson, N., Sutherland, R.J., Pappas, B.A., 1998. Reversal of ischemic-induced chronic memory dysfunction in aging rats with a free radical scavenger-glycolytic intermediate combination. *Brain Res.* 779, 285-288.
- de la Torre, J.C., 2004. Is Alzheimer's disease a neurodegenerative or a vascular disorder? data, dogma, and dialectics. *The Lancet Neurology.* 3, 184-190.
- Degroot, A., Treit, D., 2004. Anxiety is functionally segregated within the septo-hippocampal system. *Brain Res.* 1001, 60-71.
- Deng, W., Aimone, J.B., Gage, F.H., 2010. New neurons and new memories: How does adult hippocampal neurogenesis affect learning and memory? *Nat Rev Neurosci.* 11, 339-350.
- Deng, W., Saxe, M.D., Gallina, I.S., Gage, F.H., 2009. Adult-born hippocampal dentate granule cells undergoing maturation modulate learning and memory in the brain. *J Neurosci.* 29, 13532-13542.
- Dickstein, D.L., Walsh, J., Brautigam, H., Stockton, S.D., Jr, Gandy, S., Hof, P.R., 2010. Role of vascular risk factors and vascular dysfunction in Alzheimer's disease. *Mt Sinai J Med.* 77, 82-102.
- Dickstein, D.L., Kabaso, D., Rocher, A.B., Luebke, J.I., Wearne, S.L., Hof, P.R., 2007. Changes in the structural complexity of the aged brain. *Aging Cell.* 6, 275-284.

- Dobbs, A.R., Rule, B.G., 1989. Adult age differences in working memory. *Psychol Aging*. 4, 500-503.
- Doetsch, F., 2003. The glial identity of neural stem cells. *Nat Neurosci*. 6, 1127-1134.
- Doetsch, F., Hen, R., 2005. Young and excitable: The function of new neurons in the adult mammalian brain. *Curr Opin Neurobiol*. 15, 121-128.
- Dornan, W.A., McCampbell, A.R., Tinkler, G.P., Hickman, L.J., Bannon, A.W., Decker, M.W., Gunther, K.L., 1996. Comparison of site-specific injections into the basal forebrain on water maze and radial arm maze performance in the male rat after immunolesioning with 192 IgG saporin. *Behav Brain Res*. 82, 93-101.
- Drag, L.L., Bieliauskas, L.A., 2010. Contemporary review 2009: Cognitive aging. *J Geriatr Psychiatry Neurol*. 23, 75-93.
- Drapeau, E., Montaron, M.F., Aguerre, S., Abrous, D.N., 2007. Learning-induced survival of new neurons depends on the cognitive status of aged rats. *J Neurosci*. 27, 6037-6044.
- Drapeau, E., Mayo, W., Aurousseau, C., Le Moal, M., Piazza, P.V., Abrous, D.N., 2003. Spatial memory performances of aged rats in the water maze predict levels of hippocampal neurogenesis. *Proc Natl Acad Sci U S A*. 100, 14385-14390.
- Dudchenko, P.A., 2004. An overview of the tasks used to test working memory in rodents. *Neuroscience & Biobehavioral Reviews*. 28, 699-709.
- Durkin, T.P., 1994. Spatial working memory over long retention intervals: Dependence on sustained cholinergic activation in the septohippocampal or nucleus basalis magnocellularis-cortical pathways? *Neuroscience*. 62, 681-693.
- Durkin, T.P., Toumane, A., 1992. Septo-hippocampal and nBM-cortical cholinergic neurones exhibit differential time-courses of activation as a function of both type and duration of spatial memory testing in mice. *Behav Brain Res*. 50, 43-52.
- Duzel, S., Munte, T.F., Lindenberger, U., Bunzeck, N., Schutze, H., Heinze, H.J., Duzel, E., 2010. Basal forebrain integrity and cognitive memory profile in healthy aging. *Brain Res*. 1308, 124-136.
- Eckenstein, F.P., Baughman, R.W., Quinn, J., 1988. An anatomical study of cholinergic innervation in rat cerebral cortex. *Neuroscience*. 25, 457-474.
- Epp, J.R., Spritzer, M.D., Galea, L.A.M., 2007. Hippocampus-dependent learning promotes survival of new neurons in the dentate gyrus at a specific time during cell maturation. *Neuroscience*. 149, 273-285.

- Esclassan, F., Coutureau, E., Scala, G.D., Marchand, A.R., 2009. Differential contribution of dorsal and ventral hippocampus to trace and delay fear conditioning. *Hippocampus*. 19, 33-44.
- Fadda, F., Melis, F., Stancampiano, R., 1996. Increased hippocampal acetylcholine release during a working memory task. *Eur J Pharmacol*. 307, R1-R2.
- Fadel, J., Sarter, M., Bruno, J.P., 1999. Age-related attenuation of stimulated cortical acetylcholine release in basal forebrain-lesioned rats. *Neuroscience*. 90, 793-802.
- Faherty, C.J., Kerley, D., Smeyne, R.J., 2003. A golgi-cox morphological analysis of neuronal changes induced by environmental enrichment. *Dev Brain Res*. 141, 55-61.
- Farkas, E., Luiten, P.G.M., Bari, F., 2007. Permanent, bilateral common carotid artery occlusion in the rat: A model for chronic cerebral hypoperfusion-related neurodegenerative diseases. *Brain Res Rev*. 54, 162-180.
- Ferencz, I., Kokaia, M., Keep, M., Elmér, E., Metsis, M., Kokaia, Z., Lindvall, O., 1997. Effects of cholinergic denervation on seizure development and neurotrophin messenger RNA regulation in rapid hippocampal kindling. *Neuroscience*. 80, 389-399.
- Filippov, V., Kronenberg, G., Pivneva, T., Reuter, K., Steiner, B., Wang, L., Yamaguchi, M., Kettenmann, H., Kempermann, G., 2003. Subpopulation of nestin-expressing progenitor cells in the adult murine hippocampus shows electrophysiological and morphological characteristics of astrocytes. *Molecular and Cellular Neuroscience*. 23, 373-382.
- Fitz, N.F., Gibbs, R.B., Johnson, D.A., 2006. Aversive stimulus attenuates impairment of acquisition in a delayed match to position T-maze task caused by a selective lesion of septo-hippocampal cholinergic projections. *Brain Res Bull*. 69, 660-665.
- Fletcher, B.R., Baxter, M.G., Guzowski, J.F., Shapiro, M.L., Rapp, P.R., 2007. Selective cholinergic depletion of the hippocampus spares both behaviorally induced arc transcription and spatial learning and memory. *Hippocampus*. 17, 227-234.
- Flood, D.G., 1993. Critical issues in the analysis of dendritic extent in aging humans, primates, and rodents. *Neurobiol Aging*. 14, 649-654.
- Fontana, X., Nacher, J., Soriano, E., del Rio, J.A., 2006. Cell proliferation in the adult hippocampal formation of rodents and its modulation by entorhinal and fimbria-fornix afferents. *Cereb Cortex*. 16, 301-312.
- Foos, P.W., Wright, L., 1992. Adult age differences in the storage of information in working memory. *Exp Aging Res*. 18, 51-57.

- Fréchette, M., Rennie, K., Pappas, B.A., 2009. Developmental forebrain cholinergic lesion and environmental enrichment: Behaviour, CA1 cytoarchitecture and neurogenesis. *Brain Res.* 1252, 172-182.
- Frick, K.M., Baxter, M.G., Markowska, A.L., Olton, D.S., Price, D.L., 1995. Age-related spatial reference and working memory deficits assessed in the water maze. *Neurobiol Aging.* 16, 149-160.
- Frick, K.M., Fernandez, S.M., 2003. Enrichment enhances spatial memory and increases synaptophysin levels in aged female mice. *Neurobiol Aging.* 24, 615-626.
- Frotscher, M., Léránth, C., 1986. The cholinergic innervation of the rat fascia dentata: Identification of target structures on granule cells by combining choline acetyltransferase immunocytochemistry and golgi impregnation. *J Comp Neurol.* 243, 58-70.
- Frotscher, M., Léránth, C., 1985. Cholinergic innervation of the rat hippocampus as revealed by choline acetyltransferase immunocytochemistry: A combined light and electron microscopic study. *J Comp Neurol.* 239, 237-246.
- Gallagher, M., Colombo, P.J., 1995. Ageing: The cholinergic hypothesis of cognitive decline. *Curr Opin Neurobiol.* 5, 161-168.
- Garcia, A.D., Doan, N.B., Imura, T., Bush, T.G., Sofroniew, M.V., 2004. GFAP-expressing progenitors are the principal source of constitutive neurogenesis in adult mouse forebrain. *Nat Neurosci.* 7, 1233-1241.
- Garrido, R., Mattson, M.P., Hennig, B., Toborek, M., 2001. Nicotine protects against arachidonic-acid-induced caspase activation, cytochrome c release and apoptosis of cultured spinal cord neurons. *J Neurochem.* 76, 1395-1403.
- Gelfo, F., De Bartolo, P., Giovine, A., Petrosini, L., Leggio, M.G., 2009. Layer and regional effects of environmental enrichment on the pyramidal neuron morphology of the rat. *Neurobiol Learn Mem.* 91, 353-365.
- Gerdes, J., Lemke, H., Baisch, H., Wacker, H., Schwab, U., Stein, H., 1984. Cell cycle analysis of a cell proliferation-associated human nuclear antigen defined by the monoclonal antibody ki-67. *J Immunol.* 133, 1710-1715.
- Germano, C., Kinsella, G.J., 2005. Working memory and learning in early Alzheimer's disease. *Neuropsychol Rev.* 15, 1-10.
- Glaser, E.M., Van der Loos, H., 1981. Analysis of thick brain sections by obverse—reverse computer microscopy: Application of a new, high clarity Golgi—Nissl stain. *J Neurosci Methods.* 4, 117-125.

Gleeson, J.G., Lin, P.T., Flanagan, L.A., Walsh, C.A., 1999. Doublecortin is a microtubule-associated protein and is expressed widely by migrating neurons. *Neuron*. 23, 257-271.

Gould, E., 2007. How widespread is adult neurogenesis in mammals? *Nat Rev Neurosci*. 8, 481-488.

Gould, E., Tanapat, P., Hastings, N.B., Shors, T.J., 1999. Neurogenesis in adulthood: A possible role in learning. *Trends Cogn Sci (Regul Ed)*. 3, 186-192.

Gould, E., Woolf, N.J., Butcher, L.L., 1991. Postnatal development of cholinergic neurons in the rat: I. forebrain. *Brain Res Bull*. 27, 767-789.

Grady, C.L., Craik, F.I., 2000. Changes in memory processing with age. *Curr Opin Neurobiol*. 10, 224-231.

Green, E.J., Greenough, W.T., Schlumpf, B.E., 1983. Effects of complex or isolated environments on cortical dendrites of middle-aged rats. *Brain Res*. 264, 233-240.

Greenough, W.T., Volkmar, F.R., Juraska, J.M., 1973. Effects of rearing complexity on dendritic branching in frontolateral and temporal cortex of the rat. *Exp Neurol*. 41, 371-378.

Greer, E.R., Diamond, M.C., Murphy Jr., G.M., 1982. Increased branching of basal dendrites on pyramidal neurons in the occipital cortex of homozygous brattleboro rats in standard and enriched environmental conditions: A golgi study. *Exp Neurol*. 76, 254-262.

Gu, Z., Yu, J., Perez-Polo, J.R., 1998. Responses in the aged rat brain after total immunolesion. *J Neurosci Res*. 54, 7-16.

Hamm, R.J., Temple, M.D., O'Dell, D.M., Pike, B.R., Lyeth, B.G., 1996. Exposure to environmental complexity promotes recovery of cognitive function after traumatic brain injury. *J Neurotrauma*. 13, 41-47.

Hanks, S.D., Flood, D.G., 1991. Region-specific stability of dendritic extent in normal human aging and regression in Alzheimer's disease. I. CA1 of hippocampus. *Brain Res*. 540, 63-82.

Hastings, N.B., Gould, E., 1999. Rapid extension of axons into the CA3 region by adult-generated granule cells. *J Comp Neurol*. 413, 146-154.

Hebb, D.O., 1947. The effects of early experience on problem-solving at maturity. *Amer Psychol*. 2, 306-307.

- Heckers, S., Ohtake, T., Wiley, R., Lappi, D., Geula, C., Mesulam, M., 1994. Complete and selective cholinergic denervation of rat neocortex and hippocampus but not amygdala by an immunotoxin against the p75 NGF receptor. *J Neurosci.* 14, 1271-1289.
- Heine, V.M., Maslam, S., Joëls, M., Lucassen, P.J., 2004. Prominent decline of newborn cell proliferation, differentiation, and apoptosis in the aging dentate gyrus, in absence of an age-related hypothalamus–pituitary–adrenal axis activation. *Neurobiol Aging.* 25, 361-375.
- Henke, H., Lang, W., 1983. Cholinergic enzymes in neocortex, hippocampus and basal forebrain of non-neurological and senile dementia of Alzheimer-type patients. *Brain Res.* 267, 281-291.
- Hohmann, C.F., Berger-Sweeney, J., 1998. Sexually dimorphic responses to neonatal basal forebrain lesions in mice: II. cortical morphology. *J Neurobiol.* 37, 595-606.
- Holtmaat, A., Svoboda, K., 2009. Experience-dependent structural synaptic plasticity in the mammalian brain. *Nat Rev Neurosci.* 10, 647-658.
- Ikegami, S., 1994. Behavioral impairment in radial-arm maze learning and acetylcholine content of the hippocampus and cerebral cortex in aged mice. *Behav Brain Res.* 65, 103-111.
- Itou, Y., Nochi, R., Kuribayashi, H., Saito, Y., Hisatsune, T., 2010. Cholinergic activation of hippocampal neural stem cells in aged dentate gyrus. *Hippocampus.* 9999, NA.
- Jankowsky, J.L., Melnikova, T., Fadale, D.J., Xu, G.M., Slunt, H.H., Gonzales, V., Younkin, L.H., Younkin, S.G., Borchelt, D.R., Savonenko, A.V., 2005. Environmental enrichment mitigates cognitive deficits in a mouse model of Alzheimer's disease. *J Neurosci.* 25, 5217-5224.
- Jayatissa, M.N., Bisgaard, C., Tingström, A., Papp, M., Wiborg, O., 2006. Hippocampal cytochrome correlates to escitalopram-mediated recovery in a chronic mild stress rat model of depression. *Neuropsychopharmacology.* 31, 2395-2404.
- Jessberger, S., Kempermann, G., 2003. Adult-born hippocampal neurons mature into activity-dependent responsiveness. *Eur J Neurosci.* 18, 2707-2712.
- Jinno, S., 2010. Topographic differences in adult neurogenesis in the mouse hippocampus: A stereology-based study using endogenous markers. *Hippocampus.* 9999, NA.
- Johnson, K.A., Jones, K., Holman, B.L., Becker, J.A., Spiers, P.A., Satlin, A., Albert, M.S., 1998. Preclinical prediction of Alzheimer's disease using SPECT. *Neurology.* 50, 1563-1571.

- Johnson, K.A., Albert, M.S., 2000. Perfusion abnormalities in prodromal AD. *Neurobiol Aging*. 21, 289-292.
- Juraska, J.M., Fitch, J.M., Henderson, C., Rivers, N., 1985. Sex differences in the dendritic branching of dentate granule cells following differential experience. *Brain Res*. 333, 73-80.
- Kalaria, R.N., 1996. Cerebral vessels in ageing and Alzheimer's disease. *Pharmacol Ther*. 72, 193-214.
- Kalaria, R.N., 2000. The role of cerebral ischemia in Alzheimer's disease. *Neurobiol Aging*. 21, 321-330.
- Kaneko, N., Okano, H., Sawamoto, K., 2006. Role of the cholinergic system in regulating survival of newborn neurons in the adult mouse dentate gyrus and olfactory bulb. *Genes to Cells*. 11, 1145-1159.
- Kaplan, M.S., Bell, D.H., 1983. Neuronal proliferation in the 9-month-old rodent-radioautographic study of granule cells in the hippocampus. *Exp Brain Res*. 52, 1-5.
- Kaplan, M.S., Hinds, J.W., 1977. Neurogenesis in the adult rat: Electron microscopic analysis of light radioautographs. *Science*. 197, 1092-1094.
- Kee, N., Teixeira, C.M., Wang, A.H., Frankland, P.W., 2007. Preferential incorporation of adult-generated granule cells into spatial memory networks in the dentate gyrus. *Nat Neurosci*. 10, 355-362.
- Kee, N., Sivalingam, S., Boonstra, R., Wojtowicz, J.M., 2002. The utility of ki-67 and BrdU as proliferative markers of adult neurogenesis. *J Neurosci Methods*. 115, 97-105.
- Kempermann, G., Kuhn, H.G., Gage, F.H., 1997. More hippocampal neurons in adult mice living in an enriched environment. *Nature*. 386, 493-495.
- Kempermann, G., 2008. The neurogenic reserve hypothesis: What is adult hippocampal neurogenesis good for? *Trends Neurosci*. 31, 163-169.
- Kempermann, G., Jessberger, S., Steiner, B., Kronenberg, G., 2004. Milestones of neuronal development in the adult hippocampus. *Trends Neurosci*. 27, 447-452.
- Kempermann, G., Gast, D., Kronenberg, G., Yamaguchi, M., Gage, F.H., 2003. Early determination and long-term persistence of adult-generated new neurons in the hippocampus of mice. *Development*. 130, 391-399.
- Kempermann, G., 2002. Why new neurons? possible functions for adult hippocampal neurogenesis. *J Neurosci*. 22, 635-638.

- Kempermann, G., Kuhn, H.G., Gage, F.H., 1998. Experience-induced neurogenesis in the senescent dentate gyrus. *J Neurosci.* 18, 3206-3212.
- Kensinger, E.A., Shearer, D.K., Locascio, J.J., Growdon, J.H., Corkin, S., 2003. Working memory in mild Alzheimer's disease and early parkinson's disease. *Neuropsychology.* 17, 230-239.
- Kitabatake, Y., Sailor, K.A., Ming, G., Song, H., 2007. Adult neurogenesis and hippocampal memory function: New cells, more plasticity, new memories? *Neurosurg Clin N Am.* 18, 105-113.
- Klempin, F., Kempermann, G., 2007. Adult hippocampal neurogenesis and aging. *Eur Arch Psychiatry Clin Neurosci.* 257, 271-280.
- Kobayashi, S., Ohashi, Y., Ando, S., 2002. Effects of enriched environments with different durations and starting times on learning capacity during aging in rats assessed by a refined procedure of the hebb-williams maze task. *J Neurosci Res.* 70, 340-346.
- Koh, S., Higgins, G.A., 1991. Differential regulation of the low-affinity nerve growth factor receptor during postnatal development of the rat brain. *J Comp Neurol.* 313, 494-508.
- Koh, S., Loy, R., 1989. Localization and development of nerve growth factor-sensitive rat basal forebrain neurons and their afferent projections to hippocampus and neocortex. *J Neurosci.* 9, 2999-318.
- Kokaia, M., Ferencz, I., Leanza, G., Elmér, E., Metsis, M., Kokaia, Z., Wiley, R.G., Lindvall, O., 1996. Immunolesioning of basal forebrain cholinergic neurons facilitates hippocampal kindling and perturbs neurotrophin messenger RNA regulation. *Neuroscience.* 70, 313-327.
- Kolb, B., Brown, R., Witt-Lajeunesse, A., Gibb, R., 2001. Neural compensations after lesion of the cerebral cortex. *Neural Plast.* 8, 1-16.
- Kolb, B., Gorny, G., Côté, S., Ribeiro-da-Silva, A., Cuello, A.C., 1997. Nerve growth factor stimulates growth of cortical pyramidal neurons in young adult rats. *Brain Res.* 751, 289-294.
- Kotani, S., Yamauchi, T., Teramoto, T., Ogura, H., 2006. Pharmacological evidence of cholinergic involvement in adult hippocampal neurogenesis in rats. *Neuroscience.* 142, 505-514.
- Kril, J.J., Patel, S., Harding, A.J., Halliday, G.M., 2002. Neuron loss from the hippocampus of Alzheimer's disease exceeds extracellular neurofibrillary tangle formation. *Acta Neuropathol.* 103, 370-376.

- Kronenberg, G., Reuter, K., Steiner, B., Brandt, M.D., Jessberger, S., Yamaguchi, M., Kempermann, G., 2003. Subpopulations of proliferating cells of the adult hippocampus respond differently to physiologic neurogenic stimuli. *J Comp Neurol.* 467, 455-463.
- Kuhn, H., Dickinson-Anson, H., Gage, F., 1996. Neurogenesis in the dentate gyrus of the adult rat: Age-related decrease of neuronal progenitor proliferation. *J Neurosci.* 16, 2027-2033.
- Lamprea, M.R., Cardenas, F.P., Silveira, R., Walsh, T.J., Morato, S., 2003. Effects of septal cholinergic lesion on rat exploratory behavior in an open-field. *Braz J Med Biol Res.* 36, 233-238.
- Lauder, J.M., Schambra, U.B., 1999. Morphogenetic roles of acetylcholine. *Environ Health Perspect.* 107, 65-69.
- Leanza, G., Nilsson, O.G., Nikkhah, G., Wiley, R.G., Bjorklund, A., 1996. Effects of neonatal lesions of the basal forebrain cholinergic system by 192 immunoglobulin G-saporin: Biochemical, behavioural and morphological characterization. *Neuroscience.* 74, 119-141.
- Leanza, G., 1998. Chronic elevation of amyloid precursor protein expression in the neocortex and hippocampus of rats with selective cholinergic lesions. *Neurosci Lett.* 257, 53-56.
- Lee, E.H.Y., Hsu, W.L., Ma, Y.L., Lee, P.J., Chao, C.C., 2003. Enrichment enhances the expression of *sgk*, a glucocorticoid-induced gene, and facilitates spatial learning through glutamate AMPA receptor mediation. *Eur J Neurosci.* 18, 2842-2852.
- Leggio, M.G., Mandolesi, L., Federico, F., Spirito, F., Ricci, B., Gelfo, F., Petrosini, L., 2005. Environmental enrichment promotes improved spatial abilities and enhanced dendritic growth in the rat. *Behav Brain Res.* 163, 78-90.
- Leranth, C., Hajszan, T., 2007. Extrinsic afferent systems to the dentate gyrus. In *Progress in Brain Research. The Dentate Gyrus: A Comprehensive Guide to Structure, Function, and Clinical Implications*, Vol. Volume 163, Helen E. Scharfman, ed. Elsevier, pp. 63-84, 799.
- Leuner, B., Gould, E., 2010. Structural plasticity and hippocampal function. *Annu Rev Psychol.* 61, 111-40, C1-3.
- Leuner, B., Gould, E., Shors, T.J., 2006. Is there a link between adult neurogenesis and learning? *Hippocampus.* 16, 216-224.
- Lin, L., LeBlanc, C.J., Deacon, T.W., Isacson, O., 1998. Chronic cognitive deficits and amyloid precursor protein elevation after selective immunotoxin lesions of the basal forebrain cholinergic system. *Neuroreport.* 9, 547-552.

- Lindsay, J., Laurin, D., Verreault, R., Hebert, R., Helliwell, B., Hill, G.B., McDowell, I., 2002. Risk factors for Alzheimer's disease: A prospective analysis from the canadian study of health and aging. *Am J Epidemiol.* 156, 445-453.
- Lister, J.P., Barnes, C.A., 2009. Neurobiological changes in the hippocampus during normative aging. *Arch Neurol.* 66, 829-833.
- Liu, H., Zhang, J., Zheng, P., Zhang, Y., 2005. Altered expression of MAP-2, GAP-43, and synaptophysin in the hippocampus of rats with chronic cerebral hypoperfusion correlates with cognitive impairment. *Mol Brain Res.* 139, 169-177.
- Llorens-Martin, M., Tejada, G.S., Trejo, J.L., 2010. Differential regulation of the variations induced by environmental richness in adult neurogenesis as a function of time: A dual birthdating analysis. *PLoS One.* 5, e12188.
- Lolova, I., 1989. Dendritic changes in the hippocampus of aged rats. *Acta Morphol Hung.* 37, 3-10.
- London, E.D., Ball, M.J., Waller, S.B., 1989. Nicotinic binding sites in cerebral cortex and hippocampus in Alzheimer's dementia. *Neurochem Res.* 14, 745-750.
- Ma, W., Maric, D., Li, B.S., Hu, Q., Andreadis, J.D., Grant, G.M., Liu, Q.Y., Shaffer, K.M., Chang, Y.H., Zhang, L., Pancrazio, J.J., Pant, H.C., Stenger, D.A., Barker, J.L., 2000. Acetylcholine stimulates cortical precursor cell proliferation in vitro via muscarinic receptor activation and MAP kinase phosphorylation. *Eur J Neurosci.* 12, 1227-1240.
- Mainen, Z.F., Sejnowski, T.J., 1996. Influence of dendritic structure on firing pattern in model neocortical neurons. *Nature.* 382, 363-366.
- Mandolesi, L., De Bartolo, P., Foti, F., Gelfo, F., Federico, F., Leggio, M.G., Petrosini, L., 2008. Environmental enrichment provides a cognitive reserve to be spent in the case of brain lesion. *J Alzheimers Dis.* 15, 11-28.
- Mandyam, C.D., Harburg, G.C., Eisch, A.J., 2007. Determination of key aspects of precursor cell proliferation, cell cycle length and kinetics in the adult mouse subgranular zone. *Neuroscience.* 146, 108-122.
- Marashi, V., Barnekow, A., Ossendorf, E., Sachser, N., 2003. Effects of different forms of environmental enrichment on behavioral, endocrinological, and immunological parameters in male mice. *Horm Behav.* 43, 281-292.
- Markakis, E.A., Gage, F.H., 1999. Adult-generated neurons in the dentate gyrus send axonal projections to field CA₃ and are surrounded by synaptic vesicles. *J Comp Neurol.* 406, 449-460.

- Markham, J.A., McKian, K.P., Stroup, T.S., Juraska, J.M., 2005. Sexually dimorphic aging of dendritic morphology in CA1 of hippocampus. *Hippocampus*. 15, 97-103.
- Martínez-Cué, C., Baamonde, C., Lumbreras, M., Paz, J., Davisson, M.T., Schmidt, C., Dierssen, M., Flórez, J., 2002. Differential effects of environmental enrichment on behavior and learning of male and female Ts65Dn mice, a model for down syndrome. *Behav Brain Res*. 134, 185-200.
- Mash, D.C., Flynn, D.D., Potter, L.T., 1985. Loss of M2 muscarine receptors in the cerebral cortex in Alzheimer's disease and experimental cholinergic denervation.. *Science*. 228, 1115-1117.
- Mathisen, J.S., Blackstad, T.W., 1964. Cholinesterase in the hippocampal region. distribution and relation to architectonics and afferent systems. *. Acta Anat*. 56, 216-253.
- McEown, K., Treit, D., 2009. The role of the dorsal and ventral hippocampus in fear and memory of a shock-probe experience. *Brain Res*. 1251, 185-194.
- McLaughlin, K.J., Baran, S.E., Conrad, C.D., 2009. Chronic stress- and sex-specific neuromorphological and functional changes in limbic structures. *Mol Neurobiol*. 40, 166-182.
- McMahan, R.W., Sobel, T.J., Baxter, M.G., 1997. Selective immunolesions of hippocampal cholinergic input fail to impair spatial working memory. *Hippocampus*. 7, 130-136.
- Means, L.W., Kennard, K.J., 1991. Working memory and the aged rat: Deficient two-choice win-stay water-escape acquisition and retention. *Physiol Behav*. 49, 301-307.
- Meshi, D., Drew, M.R., Saxe, M., Ansorge, M.S., David, D., Santarelli, L., Malapani, C., Moore, H., Hen, R., 2006. Hippocampal neurogenesis is not required for behavioral effects of environmental enrichment. *Nat Neurosci*. 9, 729-731.
- Mesulam, M.M., Mufson, E.J., Wainer, B.H., Levey, A.I., 1983. Central cholinergic pathways in the rat: An overview based on an alternative nomenclature (Ch1-Ch6). *Neuroscience*. 10, 1185-1201.
- Mesulam, M., 2004. The cholinergic lesion of Alzheimer's disease: Pivotal factor or side show? *Learning & Memory*. 11, 43-49.
- Ming, G.L., Song, H., 2005. Adult neurogenesis in the mammalian central nervous system. *Annu Rev Neurosci*. 28, 233-250.

- Minger, S.L., Esiri, M.M., McDonald, B., Keene, J., Carter, J., Hope, T., Francis, P.T., 2000. Cholinergic deficits contribute to behavioral disturbance in patients with dementia. *Neurology*. 55, 1460-1467.
- Mohapel, P., Leanza, G., Kokaia, M., Lindvall, O., 2005. Forebrain acetylcholine regulates adult hippocampal neurogenesis and learning. *Neurobiol Aging*. 26, 939-946.
- Morris, R., 1984. Developments of a water-maze procedure for studying spatial learning in the rat. *J Neurosci Methods*. 11, 47-60.
- Mufson, E.J., Ma, S.Y., Dills, J., Cochran, E.J., Leurgans, S., Wu, J., Bennett, D.A., Jaffar, S., Gilmore, M.L., Levey, A.I., Kordower, J.H., 2002. Loss of basal forebrain P75^{NTR} immunoreactivity in subjects with mild cognitive impairment and Alzheimer's disease. *J Comp Neurol*. 443, 136-153.
- Muramori, F., Kobayashi, K., Nakamura, I., 1998. A quantitative study of neurofibrillary tangles, senile plaques and astrocytes in the hippocampal subdivisions and entorhinal cortex in Alzheimer's disease, normal controls and non-Alzheimer neuropsychiatric diseases. *Psychiatry Clin Neurosci*. 52, 593-599.
- Nakamura, S., Akiguchi, I., Kameyama, M., Mizuno, N., 1985. Age-related changes of pyramidal cell basal dendrites in layers III and V of human motor cortex: A quantitative golgi study. *Acta Neuropathol*. 65, 281-284.
- Ni, J., Ohta, H., Matsumoto, K., Watanabe, H., 1994. Progressive cognitive impairment following chronic cerebral hypoperfusion induced by permanent occlusion of bilateral carotid arteries in rats. *Brain Res*. 653, 231-236.
- Ni, J.W., Matsumoto, K., Li, H.B., Murakami, Y., Watanabe, H., 1995. Neuronal damage and decrease of central acetylcholine level following permanent occlusion of bilateral common carotid arteries in rat. *Brain Res*. 673, 290-296.
- Nieuwenhuys, R., 1994. The neocortex. an overview of its evolutionary development, structural organization and synaptology. *Anat Embryol (Berl)*. 190, 307-337.
- Nilsson, L., Nordberg, A., Hardy, J., Wester, P., Winblad, B., 1986. Physostigmine restores 3H-acetylcholine efflux from Alzheimer brain slices to normal level.. *J Neural Transm*. 67, 275-285.
- Nilsson, M., Perfilieva, E., Johansson, U., Orwar, O., Eriksson, P.S., 1999. Enriched environment increases neurogenesis in the adult rat dentate gyrus and improves spatial memory. *J Neurobiol*. 39, 569-578.
- Nishimura, A., Hohmann, C.F., Johnston, M.V., Blue, M.E., 2002. Neonatal electrolytic lesions of the basal forebrain stunt plasticity in mouse barrel field cortex. *Int J Dev Neurosci*. 20, 481-489.

- Nithianantharajah, J., Hannan, A.J., 2006. Enriched environments, experience-dependent plasticity and disorders of the nervous system. *Nat Rev Neurosci.* 7, 697-709.
- Ohta, H., Nishikawa, H., Kimura, H., Anayama, H., Miyamoto, M., 1997. Chronic cerebral hypoperfusion by permanent internal carotid ligation produces learning impairment without brain damage in rats. *Neuroscience.* 79, 1039-1050.
- Okamura, N., Arai, H., Maruyama, M., Higuchi, M., Matsui, T., Tanji, H., Seki, T., Hirai, H., Chiba, H., Itoh, M., Sasaki, H., 2002. Combined analysis of CSF tau levels and [(123)I]iodoamphetamine SPECT in mild cognitive impairment: Implications for a novel predictor of Alzheimer's disease. *Am J Psychiatry.* 159, 474-476.
- Olariu, A., Cleaver, K.M., Cameron, H.A., 2007a. Decreased neurogenesis in aged rats results from loss of granule cell precursors without lengthening of the cell cycle. *J Comp Neurol.* 501, 659-667.
- Olariu, A., Cleaver, K.M., Cameron, H.A., 2007b. Decreased neurogenesis in aged rats results from loss of granule cell precursors without lengthening of the cell cycle. *J Comp Neurol.* 501, 659-667.
- Paban, V., Jaffard, M., Chambon, C., Malafosse, M., Alescio-Lautier, B., 2005. Time course of behavioral changes following basal forebrain cholinergic damage in rats: Environmental enrichment as a therapeutic intervention. *Neuroscience.* 132, 13-32.
- Paban, V., Chambon, C., Manrique, C., Touzet, C., Alescio-Lautier, B., 2009. Neurotrophic signaling molecules associated with cholinergic damage in young and aged rats: Environmental enrichment as potential therapeutic agent. *Neurobiol Aging.* Epub, .
- Pappas, B.A., Bayley, P.J., Bui, B.K., Hansen, L.A., Thal, L.J., 2000. Choline acetyltransferase activity and cognitive domain scores of Alzheimer's patients. *Neurobiol Aging.* 21, 11-17.
- Pappas, B.A., Payne, K.B., Fortin, T., Sherren, N., 2005. Neonatal lesion of forebrain cholinergic neurons: Further characterization of behavioral effects and permanency. *Neuroscience.* 133, 485-492.
- Pappas, B.A., Davidson, C.M., Fortin, T., Nallathamby, S., Park, G.A.S., Mohr, E., Wiley, R.G., 1996a. 192 IgG-saporin lesion of basal forebrain cholinergic neurons in neonatal rats. *Dev Brain Res.* 96, 52-61.
- Pappas, B.A., de la Torre, J.C., Davidson, C.M., Keyes, M.T., Fortin, T., 1996b. Chronic reduction of cerebral blood flow in the adult rat: Late-emerging CA1 cell loss and memory dysfunction. *Brain Res.* 708, 50-58.

- Pappas, B.A., Sherren, N., 2003. Neonatal 192 IgG-saporin lesion of forebrain cholinergic neurons: Focus on the life span? *Neuroscience & Biobehavioral Reviews*. 27, 365-376.
- Pappas, B.A., Nguyen, T., Brownlee, B., Tanasoiu, D., Fortin, T., Sherren, N., 2000. Ectopic noradrenergic hyperinnervation does not functionally compensate for neonatal forebrain acetylcholine lesion. *Brain Res*. 867, 90-99.
- Paxinos, G., Watson, C., 1998. *The Rat Brain in Stereotaxic Coordinates*. Academic Press, New York.
- Paylor, R., Morrison, S.K., Rudy, J.W., Waltrip, L.T., Wehner, J.M., 1992. Brief exposure to an enriched environment improves performance on the morris water task and increases hippocampal cytosolic protein kinase C activity in young rats. *Behav Brain Res*. 52, 49-59.
- Preclinical Alzheimer's Disease Workgroup. 2010. Criteria for preclinical Alzheimer's disease. Presented at the Alzheimer's Association International Conference on Alzheimer's Disease. June 2010.
- Pyapali, G.K., Turner, D.A., 1996. Increased dendritic extent in hippocampal CA1 neurons from aged F344 rats. *Neurobiol Aging*. 17, 601-611.
- Raber, J., Rola, R., LeFevour, A., Morhardt, D., Curley, J., Mizumatsu, S., VandenBerg, S.R., Fike, J.R., 2004. Radiation-induced cognitive impairments are associated with changes in indicators of hippocampal neurogenesis. *Radiat Res*. 162, 39-47.
- Ramanathan, D., Tuszyński, M.H., Conner, J.M., 2009. The basal forebrain cholinergic system is required specifically for behaviorally mediated cortical map plasticity. *J Neurosci*. 29, 5992-6000.
- Ramirez-Amaya, V., Marrone, D.F., Gage, F.H., Worley, P.F., Barnes, C.A., 2006. Integration of new neurons into functional neural networks. *J Neurosci*. 26, 12237-12241.
- Rao, M.S., Hattiangady, B., Shetty, A.K., 2006a. The window and mechanisms of major age-related decline in the production of new neurons within the dentate gyrus of the hippocampus. *Aging Cell*. 5, 545-558.
- Rao, M.S., Hattiangady, B., Shetty, A.K., 2006b. The window and mechanisms of major age-related decline in the production of new neurons within the dentate gyrus of the hippocampus. *Aging Cell*. 5, 545-558.
- Rao, M.S., Hattiangady, B., Abdel-Rahman, A., Stanley, D.P., Shetty, A.K., 2005. Newly born cells in the ageing dentate gyrus display normal migration, survival and neuronal fate choice but endure retarded early maturation. *Eur J Neurosci*. 21, 464-476.

- Renner, M.J., Rosenzweig, M.R., 1986. Social interactions among rats housed in grouped and enriched conditions. *Dev Psychobiol.* 19, 303-313.
- Rennie, K., Butte, M.D., Pappas, B.A., 2009. Melatonin promotes neurogenesis in dentate gyrus in the pinealectomized rat. *J Pineal Res.* 47, 313-317.
- Resende, R., Adhikari, A., 2009. Cholinergic receptor pathways involved in apoptosis, cell proliferation and neuronal differentiation. *Cell Commun Signal.* 7, 20.
- Ricceri, L., Usiello, A., Valanzano, A., Calamandrei, G., Frick, K., Berger-Sweeney, J., 1999. Neonatal 192 IgG-saporin lesions of basal forebrain cholinergic neurons selectively impair response to spatial novelty in adult rats. *Behav Neurosci.* 113, 1204-1215.
- Ricceri, L., 2003. Behavioral patterns under cholinergic control during development: Lessons learned from the selective immunotoxin 192 IgG saporin. *Neurosci Biobehav Rev.* 27, 377-384.
- Ricceri, L., Calamandrei, G., Berger-Sweeney, J., 1997. Different effects of postnatal day 1 versus 7 192 immunoglobulin G-saporin lesions on learning, exploratory behaviors, and neurochemistry in juvenile rats. *Behav Neurosci.* 111, 1292-1302.
- Ricceri, L., Minghetti, L., Moles, A., Popoli, P., Confaloni, A., De Simone, R., Piscopo, P., Scattoni, M.L., di Luca, M., Calamandrei, G., 2004. Cognitive and neurological deficits induced by early and prolonged basal forebrain cholinergic hypofunction in rats. *Exp Neurol.* 189, 162-172.
- Ricceri, L., Hohmann, C., Berger-Sweeney, J., 2002. Early neonatal 192 IgG saporin induces learning impairments and disrupts cortical morphogenesis in rats. *Brain Res.* 954, 160-172.
- Riley, K.P., Snowdon, D.A., Desrosiers, M.F., Markesbery, W.R., 2005. Early life linguistic ability, late life cognitive function, and neuropathology: Findings from the nun study. *Neurobiol Aging.* 26, 341-347.
- Ritchie, L.J., De Butte, M., Pappas, B.A., 2004. Chronic mild stress exacerbates the effects of permanent bilateral common carotid artery occlusion on CA1 neurons. *Brain Res.* 1014, 228-235.
- Robertson, R., Gallardo, K., Claytor, K., Ha, D., Ku, K., Yu, B., Lauterborn, J., Wiley, R., Yu, J., Gall, C., Leslie, F., 1998. Neonatal treatment with 192 IgG-saporin produces long-term forebrain cholinergic deficits and reduces dendritic branching and spine density of neocortical pyramidal neurons. *Cereb Cortex.* 8, 142-155.
- Rosa, A.O., Egea, J., Gandía, L., López, M.G., García, A.G., 2006. Neuroprotection by nicotine in hippocampal slices subjected to oxygen-glucose deprivation: Involvement of the alpha7 nAChR subtype. *J Mol Neurosci.* 30, 61-62.

- Rosenzweig, M.R., Krech, D., Bennett, E.L., Zolman, J.F., 1962. Variation in environmental complexity and brain measures. *J Comp Physiol Psychol.* 55, 1092-1095.
- Rossi, C., Angelucci, A., Costantin, L., Braschi, C., Mazzantini, M., Babbini, F., Fabbri, M.E., Tessarollo, L., Maffei, L., Berardi, N., Caleo, M., 2006. Brain-derived neurotrophic factor (BDNF) is required for the enhancement of hippocampal neurogenesis following environmental enrichment. *Eur J Neurosci.* 24, 1850-1856.
- Rössler, M., Zarski, R., Bohl, J., Ohm, T.G., 2002. Stage-dependent and sector-specific neuronal loss in hippocampus during Alzheimer's disease. *Acta Neuropathol.* 103, 363-369.
- Roßner, S., Wörtwein, G., Gu, Z., Yu, J., Schliebs, R., Bigl, V., 1997. Cholinergic control of nerve growth factor in adult rats: Evidence from cortical cholinergic deafferentation and chronic drug treatment. *J Neurochem.* 69, 947-953.
- Rylett, R.J., Ball, M.J., Colhoun, E.H., 1983. Evidence for high affinity choline transport in synaptosomes prepared from hippocampus and neocortex of patients with Alzheimer's disease. *Brain Res.* 289, 169-175.
- Sabolek, H.R., Bunce, J.G., Giuliana, D., Chrobak, J.J., 2004. Within-subject memory decline in middle-aged rats: Effects of intraseptal tacrine. *Neurobiol Aging.* 25, 1221-1229.
- Sachdev, R.N.S., Lu, S., Wiley, R.G., Ebner, F.F., 1998. Role of the basal forebrain cholinergic projection in somatosensory cortical plasticity. *J Neurophysiol.* 79, 3216-3228.
- Sahay, A., Hen, R., 2007. Adult hippocampal neurogenesis in depression. *Nat Neurosci.* 10, 1110-1115.
- Sairanen, M., Lucas, G., Ernfors, P., Castren, M., Castren, E., 2005. Brain-derived neurotrophic factor and antidepressant drugs have different but coordinated effects on neuronal turnover, proliferation, and survival in the adult dentate gyrus. *J Neurosci.* 25, 1089-1094.
- Salthouse, T.A., Babcock, R.L., Shaw, R.J., 1991. Effects of adult age on structural and operational capacities in working memory. *Psychol Aging.* 6, 118-127.
- Sarter, M., Bruno, J.P., 1998. Age-related changes in rodent cortical acetylcholine and cognition: Main effects of age versus age as an intervening variable. *Brain Res Brain Res Rev.* 27, 143-156.
- Sarter, M., Bruno, J.P., 2004. Developmental origins of the age-related decline in cortical cholinergic function and associated cognitive abilities. *Neurobiol Aging.* 25, 1127-1139.

- Sarti, C., Pantoni, L., Bartolini, L., Inzitari, D., 2002. Persistent impairment of gait performances and working memory after bilateral common carotid artery occlusion in the adult wistar rat. *Behav Brain Res.* 136, 13-20.
- Sato, A., Sato, Y., Uchida, S., 2002. Regulation of cerebral cortical blood flow by the basal forebrain cholinergic fibers and aging. *Auton Neurosci.* 96, 13-19.
- Saunders, N.L., Summers, M.J., 2010. Attention and working memory deficits in mild cognitive impairment. *J Clin Exp Neuropsychol.* 32, 350-357.
- Saxe, M.D., Battaglia, F., Wang, J., Malleret, G., David, D.J., Monckton, J.E., Garcia, A.D.R., Sofroniew, M.V., Kandel, E.R., Santarelli, L., Hen, R., Drew, M.R., 2006. Ablation of hippocampal neurogenesis impairs contextual fear conditioning and synaptic plasticity in the dentate gyrus. *Proc Nat Acad Sci U S A.* 103, 17501-17506.
- Scattoni, M.L., Adriani, W., Calamandrei, G., Laviola, G., Ricceri, L., 2006. Long-term effects of neonatal basal forebrain cholinergic lesions on radial maze learning and impulsivity in rats. *Behav Pharmacol.* 17, 517-524.
- Scattoni, M.L., Calamandrei, G., Ricceri, L., 2003. Neonatal cholinergic lesions and development of exploration upon administration of the GABA_A receptor agonist muscimol in preweaning rats. *Pharmacol Biochem Behav.* 76, 213-221.
- Schade, J.P., Baxter, C.F., 1960. Changes during growth in the volume and surface area of cortical neurons in the rabbit. *Exp Neurol.* 2, 158-178.
- Scharfman, H., Goodman, J., Macleod, A., Phani, S., Antonelli, C., Croll, S., 2005. Increased neurogenesis and the ectopic granule cells after intrahippocampal BDNF infusion in adult rats. *Exp Neurol.* 192, 348-356.
- Scheibel, M.E., Lindsay, R.D., Tomiyasu, U., Scheibel, A.B., 1975. Progressive dendritic changes in aging human cortex. *Exp Neurol.* 47, 392-403.
- Schmidt-Hieber, C., Jonas, P., Bischofberger, J., 2004. Enhanced synaptic plasticity in newly generated granule cells of the adult hippocampus. *Nature.* 429, 184-187.
- Schrijver, N.C.A., Bahr, N.I., Weiss, I.C., Würbel, H., 2002. Dissociable effects of isolation rearing and environmental enrichment on exploration, spatial learning and HPA activity in adult rats. *Pharmacology Biochemistry and Behavior.* 73, 209-224.
- Seignourel, P.J., Kunik, M.E., Snow, L., Wilson, N., Stanley, M., 2008. Anxiety in dementia: A critical review. *Clin Psychol Rev.* 28, 1071-1082.
- Semba, K., Fibiger, H.C., 1988. Time of origin of cholinergic neurons in the rat basal forebrain. *J Comp Neurol.* 269, 87-95.

Seri, B., García-Verdugo, J.M., Collado-Morente, L., McEwen, B.S., Alvarez-Buylla, A., 2004. Cell types, lineage, and architecture of the germinal zone in the adult dentate gyrus. *J Comp Neurol.* 478, 359-378.

Seri, B., Garcia-Verdugo, J.M., McEwen, B.S., Alvarez-Buylla, A., 2001. Astrocytes give rise to new neurons in the adult mammalian hippocampus. *J Neurosci.* 21, 7153-7160.

Shen, J., Barnes, C.A., Wenk, G.L., McNaughton, B.L., 1996. Differential effects of selective immunotoxic lesions of medial septal cholinergic cells on spatial working and reference memory. *Behav Neurosci.* 110, 1181-1186.

Sheng, J.G., Mrak, R.E., Griffin, W.S., 1994. S100 beta protein expression in Alzheimer disease: Potential role in the pathogenesis of neuritic plaques. *J Neurosci Res.* 39, 398-404.

Sherren, N., 2003. Neurochemistry, cortical morphology and behaviour after single and combined neonatal acetylcholine and dopamine lesions in rats.

Sherren, N., Pappas, B.A., 2005. Selective acetylcholine and dopamine lesions in neonatal rats produce distinct patterns of cortical dendritic atrophy in adulthood. *Neuroscience.* 136, 445-456.

Sherren, N., Pappas, B.A., Fortin, T., 1999. Neural and behavioral effects of intracranial 192 IgG-saporin in neonatal rats: Sexually dimorphic effects? *Dev Brain Res.* 114, 49-62.

Shors, T.J., Miesegaes, G., Beylin, A., Zhao, M., Rydel, T., Gould, E., 2001. Neurogenesis in the adult is involved in the formation of trace memories. *Nature.* 10, 372-376.

Shors, T.J., 2004. Memory traces of trace memories: Neurogenesis, synaptogenesis and awareness. *Trends Neurosci.* 27, 250-256.

Shors, T.J., Townsend, D.A., Zhao, M., Kozorovitskiy, Y., Gould, E., 2002. Neurogenesis may relate to some but not all types of hippocampal-dependent learning. *Hippocampus.* 12, 578-584.

Shukitt-Hale, B., Mouzakis, G., Joseph, J.A., 1998. Psychomotor and spatial memory performance in aging male fischer 344 rats. *Exp Gerontol.* 33, 615-624.

Sivanandam, T.M., Thakur, M.K., 2010. Amyloid precursor protein (APP) mRNA level is higher in the old mouse cerebral cortex and is regulated by sex steroids. *J Mol Neurosci.*

- Sivilia, S., Giuliani, A., Del Vecchio, G., Giardino, L., Calzà, L., 2008. Age-dependent impairment of hippocampal neurogenesis in chronic cerebral hypoperfusion. *Neuropathol Appl Neurobiol.* 34, 52-61.
- Snowdon, D.A., Kemper, S.J., Mortimer, J.A., Greiner, L.H., Wekstein, D.R., Markesbery, W.R., 1996. Linguistic ability in early life and cognitive function and Alzheimer's disease in late life. findings from the nun study. *JAMA.* 275, 528-532.
- Snyder, J.S., Hong, N.S., McDonald, R.J., Wojtowicz, J.M., 2005. A role for adult neurogenesis in spatial long-term memory. *Neuroscience.* 130, 843-852.
- Song, H.J., Stevens, C.F., Gage, F.H., 2002. Neural stem cells from adult hippocampus develop essential properties of functional CNS neurons. *Nat Neurosci.* 5, 438-445.
- Spruston, N., 2008. Pyramidal neurons: Dendritic structure and synaptic integration. *Nat Rev Neurosci.* 9, 206-221.
- Stampfer, M.J., 2006. Cardiovascular disease and Alzheimer's disease: Common links. *J Intern Med.* 260, 211-223.
- Stanfield, B.B., Trice, J.E., 1988. Evidence that granule cells generated in the dentate gyrus of adult rats extend axonal projections. *Exp Brain Res.* 72, 399-406.
- Steele, R.J., Morris, R.G., 1999. Delay-dependent impairment of a matching-to-place task with chronic and intrahippocampal infusion of the NMDA-antagonist D-AP5. *Hippocampus.* 9, 118-136.
- Stevens, W.D., Fortin, T., Pappas, B.A., 2002. Retinal and optic nerve degeneration after chronic carotid ligation: Time course and role of light exposure. *Stroke.* 33, 1107-1112.
- Stoehr, J.D., Mobley, S.L., Roice, D., Brooks, R., Baker, L.M., Wiley, R.G., Wenk, G.L., 1997. The effects of selective cholinergic basal forebrain lesions and aging upon expectancy in the rat. *Neurobiol Learn Mem.* 67, 214-227.
- Stopford, C.L., Snowden, J.S., Thompson, J.C., Neary, D., 2007. Distinct memory profiles in Alzheimer's disease. *Cortex.* 43, 846-857.
- Takaba, H., Fukuda, K., Yao, H., 2004. Substrain differences, gender, and age of spontaneously hypertensive rats critically determine infarct size produced by distal middle cerebral artery occlusion. *Cell Mol Neurobiol.* 24, 589-598.
- Taliaz, D., Stall, N., Dar, D.E., Zangen, A., 2010. Knockdown of brain-derived neurotrophic factor in specific brain sites precipitates behaviors associated with depression and reduces neurogenesis. *Mol Psychiatry.* 15, 80-92.

- Tanaka, K., Ogawa, N., Asanuma, M., Kondo, Y., Nomura, M., 1996. Relationship between cholinergic dysfunction and discrimination learning disabilities in wistar rats following chronic cerebral hypoperfusion. *Brain Res.* 729, 55-65.
- Tees, R.C., 1999. The influences of rearing environment and neonatal choline dietary supplementation on spatial learning and memory in adult rats. *Behav Brain Res.* 105, 173-188.
- Terry, A.V., Buccafusco, J.J., 2003. The cholinergic hypothesis of age and Alzheimer's disease-related cognitive deficits: Recent challenges and their implications for novel drug development. *J Pharmacol Exp Ther.* 306, 821-827.
- Torres, E.M., Perry, T.A., Blockland, A., Wilkinson, L.S., Wiley, R.G., Lappi, D.A., Dunnet, S.B., 1994. Behavioural, histochemical and biochemical consequences of selective immunolesions in discrete regions of the basal forebrain cholinergic system. *Neuroscience.* 63, 95-122.
- Tsuchiya, M., Sako, K., Yura, S., Yonemasu, Y., 1992. Cerebral blood flow and histopathological changes following permanent bilateral carotid artery ligation in wistar rats. *Exp Brain Res.* 89, 87-92.
- Van der Borght, K., Mulder, J., Keijser, J.N., Eggen, B.J.L., Luiten, P.G.M., Van der Zee, E.A., 2005. Input from the medial septum regulates adult hippocampal neurogenesis. *Brain Res Bull.* 67, 117-125.
- Van Eldik, L.J., Griffin, W.S., 1994. S100 beta expression in Alzheimer's disease: Relation to neuropathology in brain regions. *Biochim Biophys Acta.* 1223, 398-403.
- Van Kampen, J.M., Eckman, C.B., 2010. Agonist-induced restoration of hippocampal neurogenesis and cognitive improvement in a model of cholinergic denervation. *Neuropharmacology.* 58, 921-929.
- van Praag, H., Schinder, A.F., Christie, B.R., Toni, N., Palmer, T.D., Gage, F.H., 2002. Functional neurogenesis in the adult hippocampus. *Nature.* 415, 1030-1034.
- van Praag, H., Kempermann, G., Gage, F.H., 1999. Running increases cell proliferation and neurogenesis in the adult mouse dentate gyrus. *Nat Neurosci.* 2, 266-270.
- Vaucher, E., Hamel, E., 1995. Cholinergic basal forebrain neurons project to cortical microvessels in the rat: Electron microscopic study with anterogradely transported phaseolus vulgaris leucoagglutinin and choline acetyltransferase immunocytochemistry. *J Neurosci.* 15, 7427-7441.
- Vecchi, T., Saveriano, V., Paciaroni, L., 1998. Storage and processing working memory functions in Alzheimer-type dementia. *Behav Neurol.* 11, 227-231.

- Veng, L.M., Mesches, M.H., Browning, M.D., 2003. Age-related working memory impairment is correlated with increases in the L-type calcium channel protein alpha1D (Cav1.3) in area CA1 of the hippocampus and both are ameliorated by chronic nimodipine treatment. *Brain Res Mol Brain Res.* 110, 193-202.
- Vijayan, V.K., Geddes, J.W., Anderson, K.J., Chang-Chui, H., Ellis, W.G., Cotman, C.W., 1991. Astrocyte hypertrophy in the Alzheimer's disease hippocampal formation. *Exp Neurol.* 112, 72-78.
- Volkmar, F.R., Greenough, W.T., 1972. Rearing complexity affects branching of dendrites in the visual cortex of the rat. *Science.* 176, 1445-1447.
- Vuckovich, J.A., Semel, M.E., Baxter, M.G., 2004. Extensive lesions of cholinergic basal forebrain neurons do not impair spatial working memory. *Learn Memory.* 11, 87-94.
- Waite, J.J., Wardlow, M.L., Chen, A.C., Lappi, D.A., Wiley, R.G., Thal, L.J., 1994. Time course of cholinergic and monoaminergic changes in rat brain after immunolesioning with 192 IgG-saporin. *Neurosci Lett.* 169, 154-158.
- Walsh, T.J., Herzog, C.D., Gandhi, C., Stackman, R.W., Wiley, R.G., 1996. Injection of IgG 192-saporin into the medial septum produces cholinergic hypofunction and dose-dependent working memory deficits. *Brain Res.* 726, 69-79.
- Walter, J., Keiner, S., Witte, O.W., Redecker, C., 2010. Differential stroke-induced proliferative response of distinct precursor cell subpopulations in the young and aged dentate gyrus. *Neuroscience.* 169, 1279-1286.
- Wang, S., Scott, B.W., Wojtowicz, J.M., 2000. Heterogenous properties of dentate granule neurons in the adult rat. *J Neurobiol.* 42, 248-257.
- Wang, T.-., Chen, J.-., Wang, Y.-., Tseng, G.-., 2009. The cytoarchitecture and soma-dendritic arbors of the pyramidal neurons of aged rat sensorimotor cortex: An intracellular dye injection study. *Neuroscience.* 158, 776-785.
- Waters, G., Caplan, D., 2002. Working memory and online syntactic processing in Alzheimer's disease: Studies with auditory moving window presentation. *J Gerontol B Psychol Sci Soc Sci.* 57, P298-311.
- Wellman, C.L., Pellemounter, M.A., 1999. Differential effects of nucleus basalis lesions in young adult and aging rats. *Neurobiol Aging.* 20, 381-393.
- West, M.J., Kawas, C.H., Martin, L.J., Troncoso, J.C., 2000. The CA1 region of the human hippocampus is a hot spot in Alzheimer's disease. *Ann N Y Acad Sci.* 908, 255-259.

- West, M.J., Coleman, P.D., Flood, D.G., Troncoso, J.C., 1994a. Differences in the pattern of hippocampal neuronal loss in normal ageing and Alzheimer's disease. *The Lancet*. 344, 769-772.
- West, M.J., Coleman, P.D., Flood, D.G., Troncoso, J.C., 1994b. Differences in the pattern of hippocampal neuronal loss in normal ageing and Alzheimer's disease. *The Lancet*. 344, 769-772.
- West, R.W., Greenough, W.T., 1972. Effect of environmental complexity on cortical synapses of rats: Preliminary results. *Behav Biol*. 7, 279-284.
- White, K.G., Ruske, A.C., 2002. Memory deficits in Alzheimer's disease: The encoding hypothesis and cholinergic function. *Psychon Bull Rev*. 9, 426-437.
- Wiley, R.G., Oeltmann, T.N., Lappi, D.A., 1991. Immunolesioning: Selective destruction of neurons using immunotoxin to rat NGF receptor. *Brain Res*. 562, 149-153.
- Williams, S.R., Stuart, G.J., 2003. Role of dendritic synapse location in the control of action potential output. *Trends Neurosci*. 26, 147-154.
- Wingfield, A., Stine, E.A., Lahar, C.J., Aberdeen, J.S., 1988. Does the capacity of working memory change with age? *Exp Aging Res*. 14, 103-107.
- Winocur, G., Wojtowicz, J.M., Sekeres, M., Snyder, J.S., Wang, S., 2006. Inhibition of neurogenesis interferes with hippocampus-dependent memory function. *Hippocampus*. 16, 296-304.
- Witter, M.P., Amaral, D.G., 2004. Hippocampal formation. In *The Rat Nervous System*. G. Paxinos, ed. Elsevier, San Diego, CA, pp. 635-704.
- Works, S.J., Wilson, R.E., Wellman, C.L., 2004. Age-dependent effect of cholinergic lesion on dendritic morphology in rat frontal cortex. *Neurobiol Aging*. 25, 963-974.
- Wrenn, C.C., Wiley, R.G., 1998. The behavioral functions of the cholinergic basal forebrain: Lessons from 192 IgG-saporin. *Int J Dev Neurosci*. 16, 595-602.
- Wrenn, C.C., Lappi, D.A., Wiley, R.G., 1999. Threshold relationship between lesion extent of the cholinergic basal forebrain in the rat and working memory impairment in the radial maze. *Brain Res*. 847, 284-298.
- Yan, Q., Johnson, E., Jr, 1988. An immunohistochemical study of the nerve growth factor receptor in developing rats. *J Neurosci*. 8, 3481-3498.
- Yankner, B.A., Lu, T., Loerch, P., 2008. The aging brain. *Annu Rev Pathol*. 3, 41-66.

- Young, K.M., Merson, T.D., Sotthibundhu, A., Coulson, E.J.B., P.F., 2007. p75 neurotrophin receptor expression defines a population of BDNF-responsive neurogenic precursor cells. *J Neurosci.* 27, 5146-5155.
- Yu, J., Huang, N.F., Wilson, K.D., Velotta, J.B., Huang, M., Li, Z., Lee, A., Robbins, R.C., Cooke, J.P., Wu, J.C., 2009. nAChRs mediate human embryonic stem cell-derived endothelial cells: Proliferation, apoptosis, and angiogenesis. *PloS One.* 4, e7040. doi:10.1371/journal.pone.0007040.
- Yu, J., Pizzo, D.P., Hutton, L.A., Perez-Polo, J.R., 1995. Role of the cholinergic system in the regulation of neurotrophin synthesis. *Brain Res.* 705, 247-254.
- Zec, R.F., 1995. The neuropsychology of aging. *Exp Gerontol.* 30, 431-442.
- Zhang, Y., Shi, J., Rajakumar, G., Day, A.L., Simpkins, J.W., 1998. Effects of gender and estradiol treatment on focal brain ischemia. *Brain Res.* 784, 321-324.
- Zhu, X.O., Waite, P.M., 1998. Cholinergic depletion reduces plasticity of barrel field cortex. *Cereb Cortex.* 8, 63-72.

Appendix 1: Anatomy and Sample Photomicrographs

Figure A1.1: Diagram showing dorsal and ventral hippocampus (adapted from Paxinos and Watson, 1998)

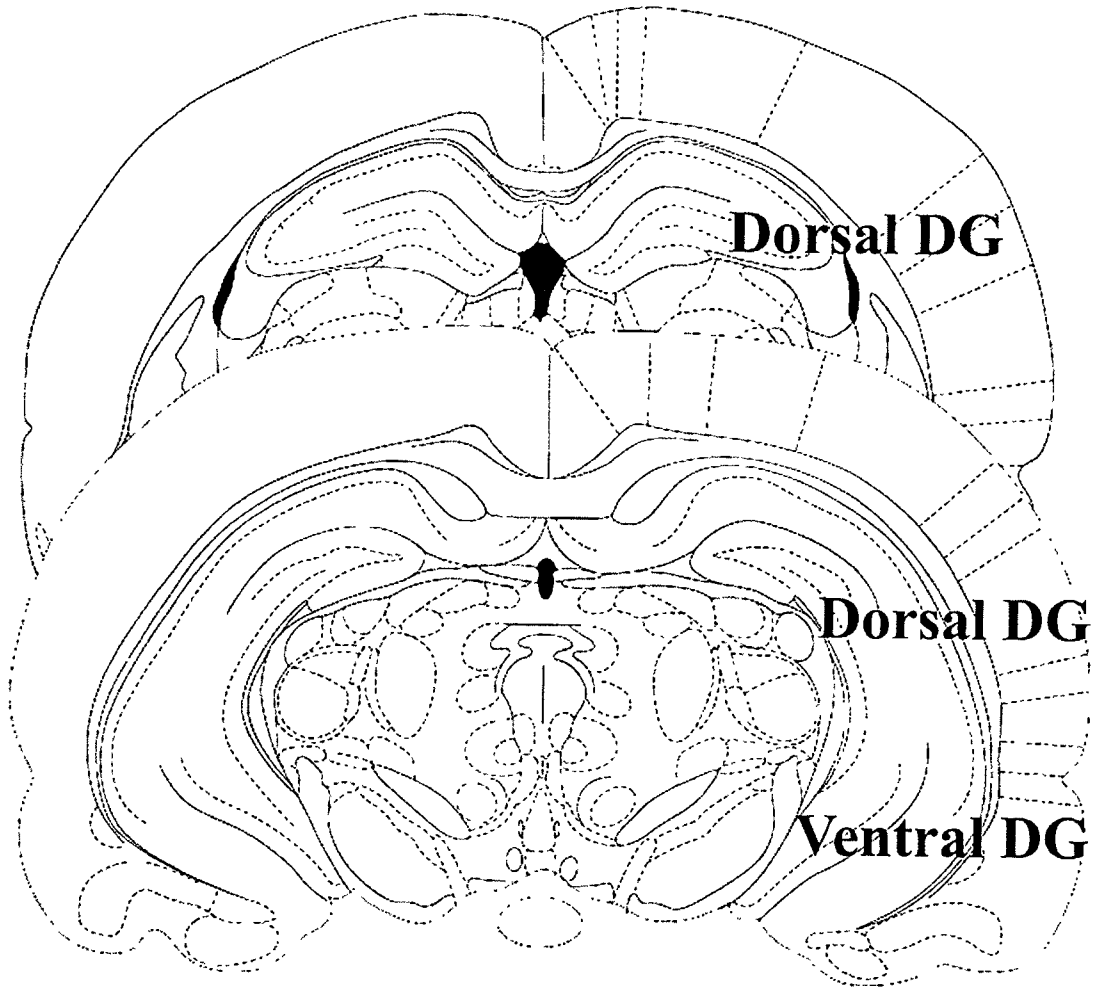
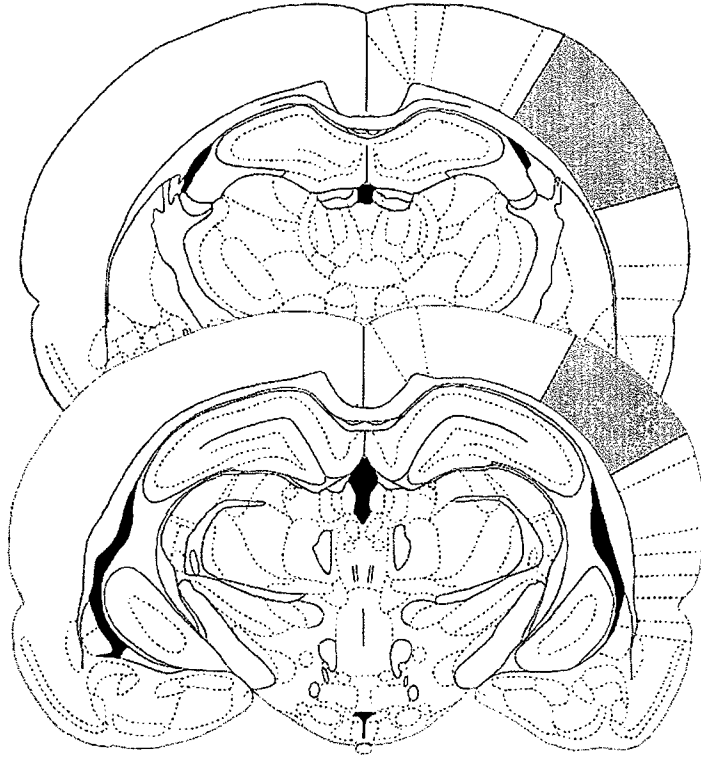


Figure A1.2: Diagrams showing the areas of parietal (top plates) and entorhinal cortices (bottom plates) selected for APP analysis. The plates show the most anterior and posterior sections that were used for each cortical area. Adapted from Paxinos and Watson, 1998.

Parietal Cortex
(Primary Somatosensory/Barrel Field Cortex)



Entorhinal Cortex

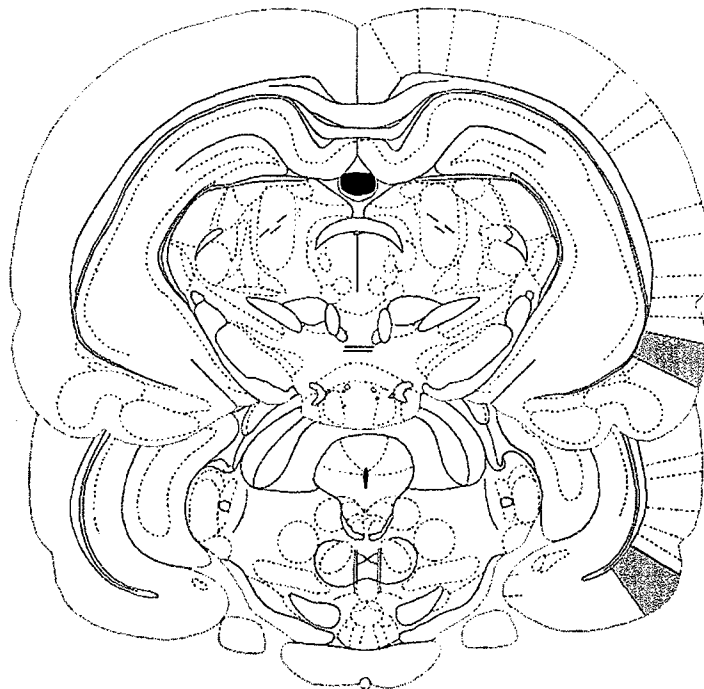


Figure A1.3: Sample cresyl violet staining. Top panel: image of the dorsal hippocampus acquired using a 4x objective lens. Bottom panel: image of the CA1 sector acquired using a 40x objective lens.



Figure A1.4: Sample BrdU staining. The top image shows BrdU⁺ cells 2 hours after the final BrdU injection. At this time point, BrdU⁺ cells were frequently found in clusters of irregularly shaped cells. The bottom image shows BrdU⁺ cells 28 days after the final BrdU injection. At this time point, individual BrdU⁺ cells were frequently found within the granule cell layer, and had a rounder morphology. Both images were acquired using a 4x objective lens.



Figure A1.5: Sample Ki-67 staining. Top panel: image of the dorsal hippocampus acquired using a 4x objective lens. Bottom panel: image of the dentate gyrus acquired using a 40x objective lens.

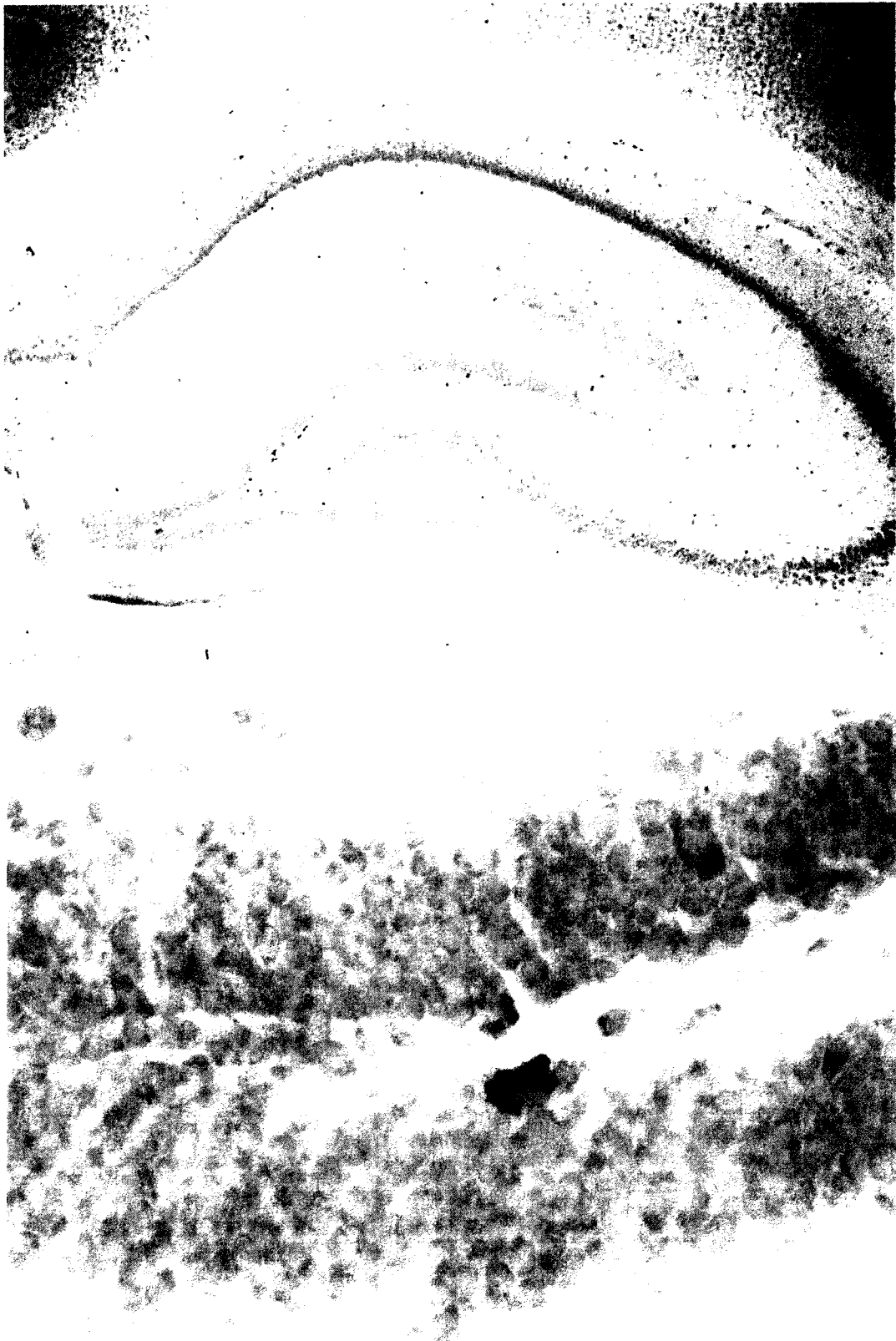


Figure A1.6: Sample DCX staining. Top panel: image of the dorsal hippocampus acquired using a 4x objective lens. Bottom panel: image of the dentate gyrus acquired using a 40x objective lens.

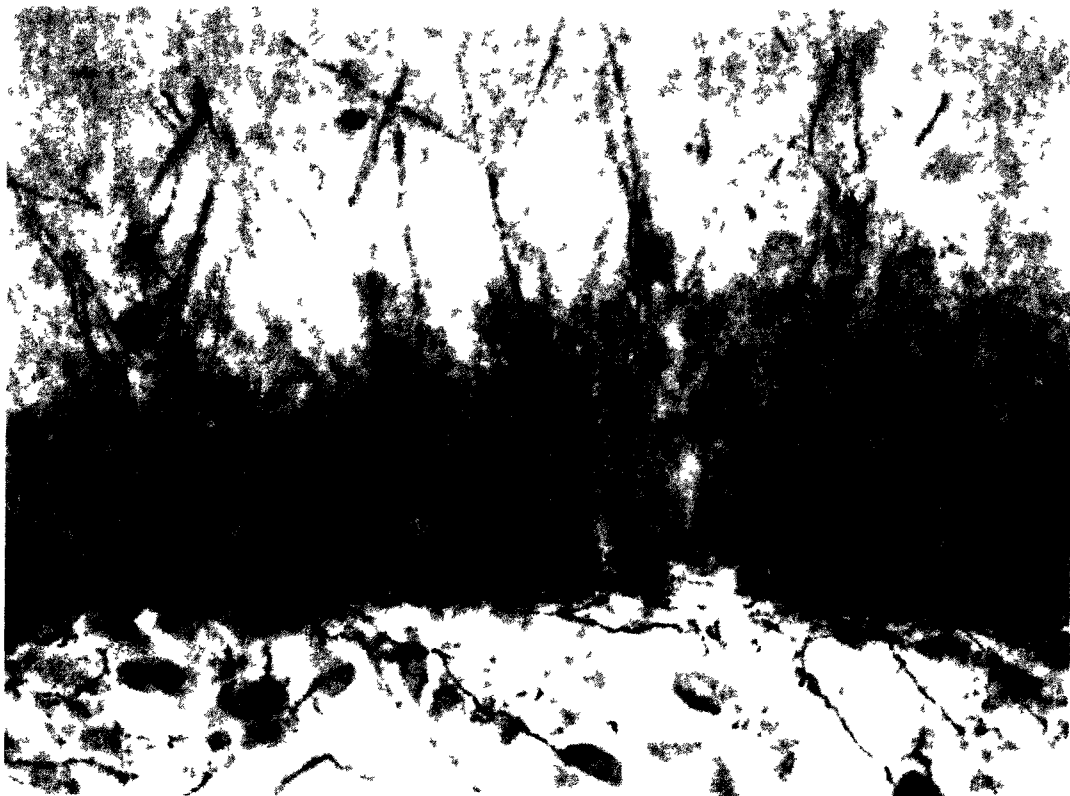


Figure A1.7: Sample GFAP staining (DAB method). Top panel: image of the dorsal hippocampus acquired using a 4x objective lens. Bottom panel: image of the CA1 sector acquired using a 40x objective lens.

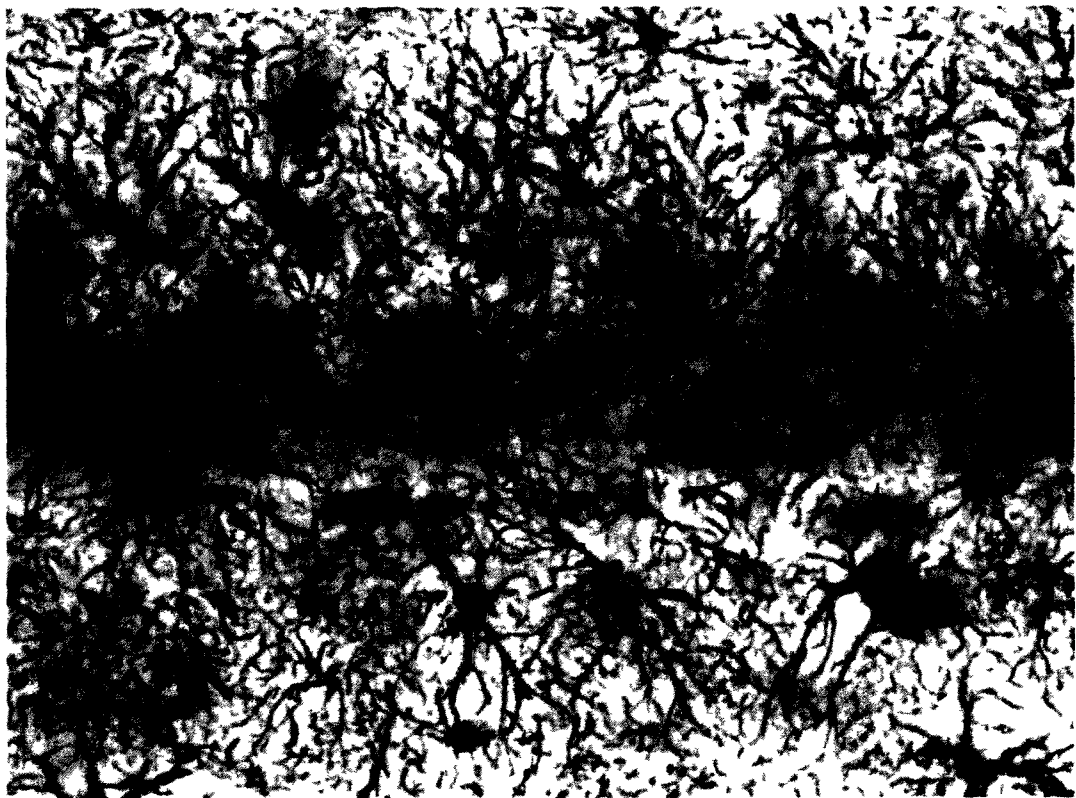


Figure A1.8: Sample GFAP staining (fluorescent method). Top panel: image of the dorsal hippocampus acquired using a 4x objective lens. Bottom panel: image of the CA1 sector acquired using a 40x objective lens.



Figure A1.9: Sample APP staining in the hippocampus. Top panel: image of the dorsal hippocampus acquired using a 4x objective lens. Bottom panel: image of the CA1 sector acquired using a 40x objective lens.

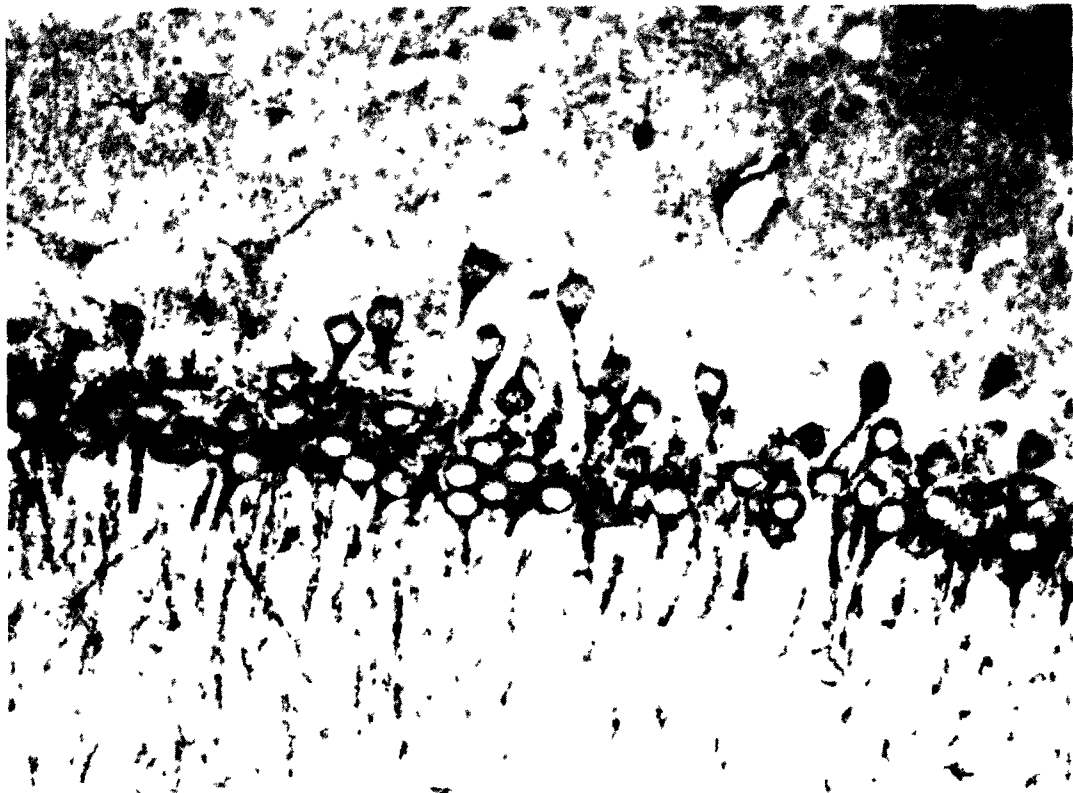


Figure A1.10: Sample photomicrographs showing BrdU-labelled cells expressing NeuN or S100B, or that do not double-label with either NeuN or S100B in the granule cell layer. A,B,C: A BrdU⁺ cell (green) expressing NeuN (red). D,E,F: A BrdU⁺ cell (green) that does not express NeuN (red). G,H,I: A BrdU⁺ cell (green) expressing S100B (red). J,K,L: A BrdU⁺ cell that does not express S100B (red).

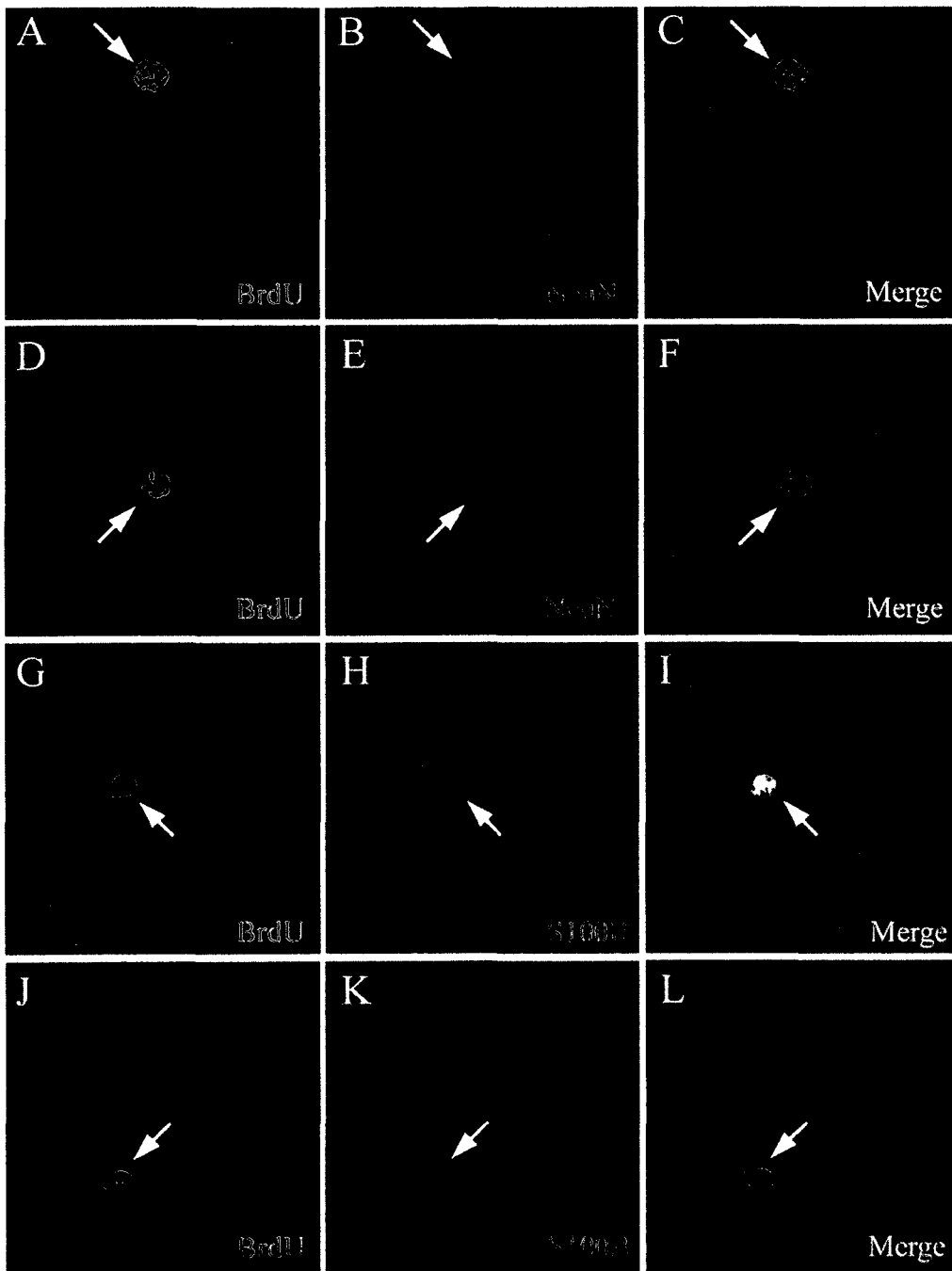


Figure A.11: Sample Golgi staining. Top panel: image of the dorsal hippocampus acquired using a 4x objective lens. Bottom left panel: image of a CA1 cell used for analysis. The dendrites of this cell are entirely contained within the 200 μ m thickness of the tissue section, and are not occluded by the dendrites of neighbouring cells or by blood vessels. This image was acquired using a 20x objective lens. Bottom right panel: image of dendritic spines obtained using a 100x objective lens.



8. Appendix 2. Supplementary Material for Study 3

8.1 Behavioural Monitoring

In order to explore the possibility that lesioned and control rats might respond differently to the enrichment experience, or display differences in behaviour during standard housing that might influence neurogenesis, the home-cage behaviour of the rats was monitored during the second, sixth and tenth weeks of the enrichment/standard housing period. A low-light video camera (Sanyo, model VCB-3524, Woodbridge, ON) was used to record activity for one hour at the beginning of the dark cycle on one day at each time point. The first hour of the dark cycle corresponded with a time when human activity and noise in the vivarium were minimal.

The rats' behaviour during enrichment was scored according to the categories used by Renner and Rosenzweig (Renner and Rosenzweig 1986). The behaviours were divided into social activities, object interactions, and solitary activities. Social activities included wrestling, chasing, sniffing/nose-to-nose contact, anogenital sniffing/mounting, passive contact, social grooming, or paw contact with a cagemate. Object interactions included sniffing/nose contact, paw contact, climbing/entering an object, biting an object, colliding with an object, and object motions. Solitary activities included locomotion, cage climbing, digging, sniffing at the cage, rearing, scratching, grooming, eating, drinking, yawning/stretching, and immobility (described in Renner and Rosenzweig, 1986). The rats in the standard housing condition were scored for social behaviours and solitary activities, but not for object activities, since their cages did not contain any added objects. Behaviours were scored during the first five seconds of each thirty second interval during the one-hour recording session. For each of the behaviours listed above, it was

determined whether the behaviour occurred or did not occur during the five-second interval. For each behaviour, the number of intervals during which that behaviour occurred was then tallied. Since the number of rats per cage was different between standard and enriched housing groups, as was the availability of toys and the amount of space, the data for the enriched rats and the standard-housed rats were not compared to each other, and differences between lesioned and control rats were assessed in each housing condition separately. The data were analyzed using independent samples t-tests (PBS vs. N192S). Data for each time point were considered separately. The data were analyzed as aggregates for each cage, as it was impossible to identify individual rats on the video recordings. The data are illustrated in Figures A2.1-A2.7.

8.2. Results

8.2.1. Standard Housing

No group differences were observed on any social or solitary behaviour during the second week of standard housing (all p 's $>.05$). During the sixth week of standard housing, control animals engaged in more individual grooming behaviours ($t_{15}=-3.66$, $p<.01$) and drank more often ($t_{15}=-2.34$, $p=.03$) than did N192S rats. All other behaviours were observed equally frequently in both treatment groups at this time point (all p 's $>.05$). N192S rats were significantly less likely to make paw contact with a cagemate ($t_9=-3.41$, $p<.01$) and were observed in locomotion less often ($t_9=-2.47$, $p=.04$) than control rats during the tenth week of standard housing, while all other behaviours were unaltered by cholinergic lesion (all p 's $>.05$).

8.2.2. Enriched Housing

Social, object-directed, and solitary behaviours were not affected by cholinergic lesion during the second week of enrichment (all p 's $>.05$). However, lesioned rats showed increased locomotor behaviour during the sixth week of enriched housing ($t_6=5.576$, $p<.01$), and increased social grooming ($t_{10}=2.433$, $p=.04$) and decreased chasing behaviour ($t_{10}=-2.907$, $p=.02$) compared to controls during the tenth week of enrichment. No other behaviours were significantly altered by cholinergic lesion at either the six or ten week time points (all p 's $>.05$).

8.3. Discussion

We anticipated the possibility that lesion-induced changes in home-cage behaviour and activity levels might account for the difference in neurogenesis between control and N192S rats, and therefore we periodically recorded the rats' behaviour in the home cage. However as outlined above, only a few minor changes in behaviour were noted - it is unlikely that these could account for the difference in neurogenesis. Both standard-housed and enriched N192S rats showed reduced numbers of BrdU⁺ and DCX⁺ cells, but none of the behavioural changes were observed in both housing groups. Furthermore, some of the behaviours were seen so rarely (for example, chasing at the 10 week time point), that it seems implausible that differences in these behaviours could have any impact on neurogenesis. Finally, some of the changes would be expected, if anything, to increase neurogenesis (such as increased locomotion; van Praag et al., 1999), but the opposite effect was observed. As such, behavioural changes cannot explain the effect of the cholinergic lesion on neurogenesis.

Figure A2.1: Solitary behaviours observed after 2, 6 and 10 weeks of enriched housing (Set A: locomotor and exploratory behaviours). No group differences on any behaviour were observed during the second or tenth week. N192S rats showed increased locomotor behaviour during the sixth week of enriched housing ($t_6=5.576$, $p=.001$).

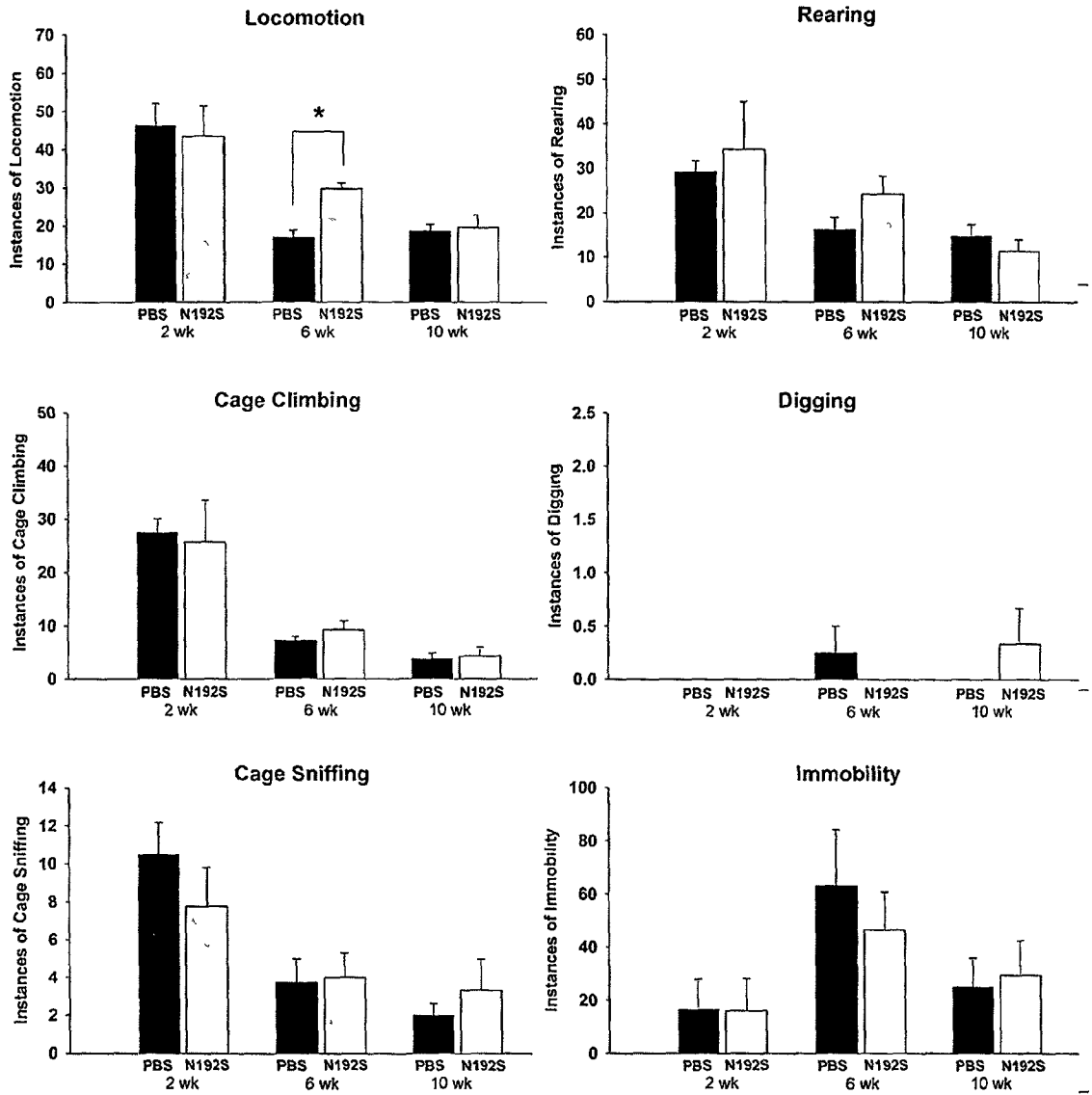


Figure A2.2: Solitary behaviours observed after 2, 6 and 10 weeks of enriched housing (Set B: Ingestive and self-maintenance behaviours). No group differences were observed at any time point.

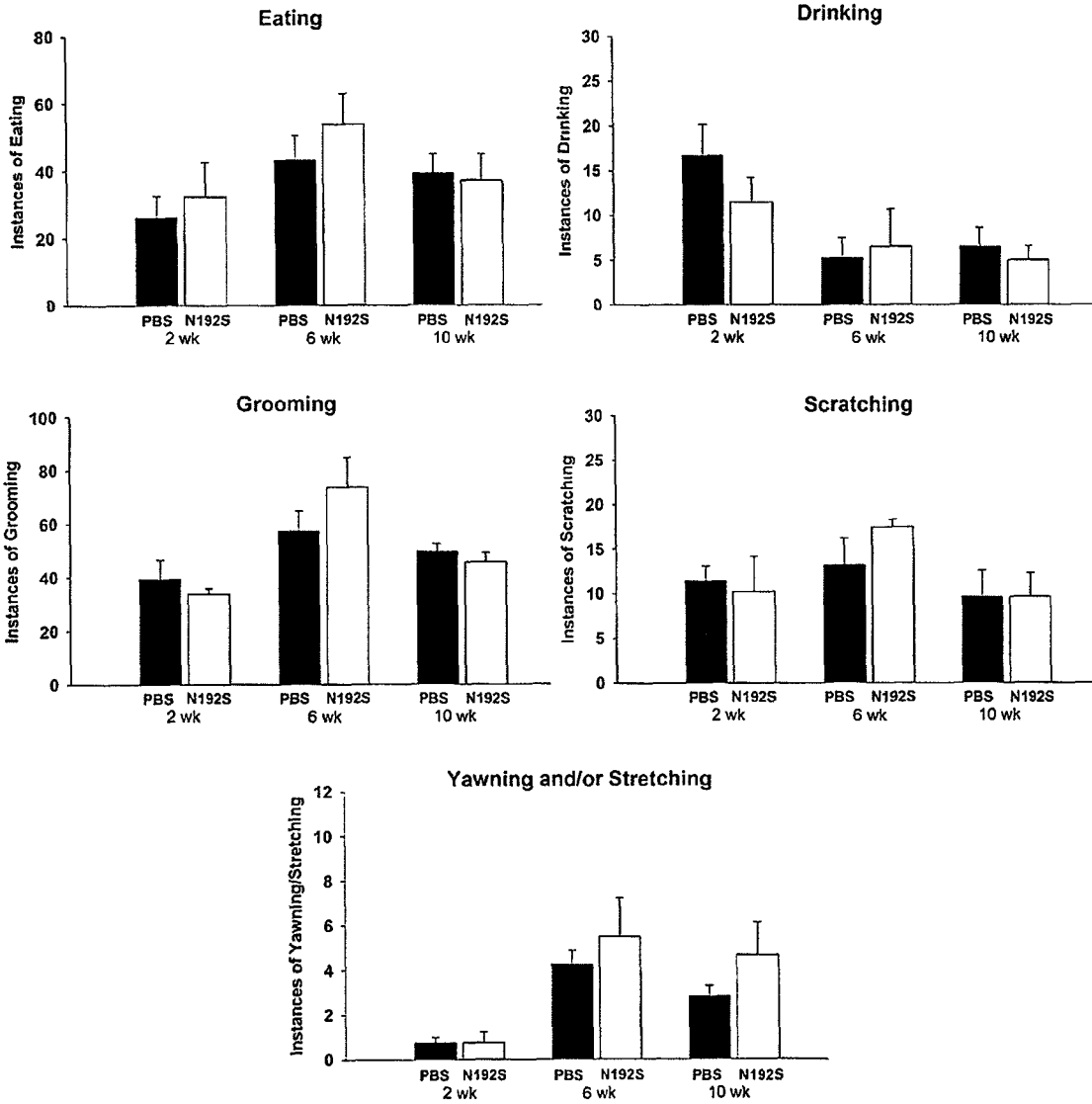


Figure A2.3: Social behaviours observed after 2, 6 and 10 weeks of enriched housing. No group differences were observed during the second or sixth week. N192S rats displayed increased social grooming ($t_{10}=2.433$, $p=.035$) and decreased chasing behaviour ($t_{10}=-2.907$, $p=.016$) compared to controls during the tenth week of enrichment.

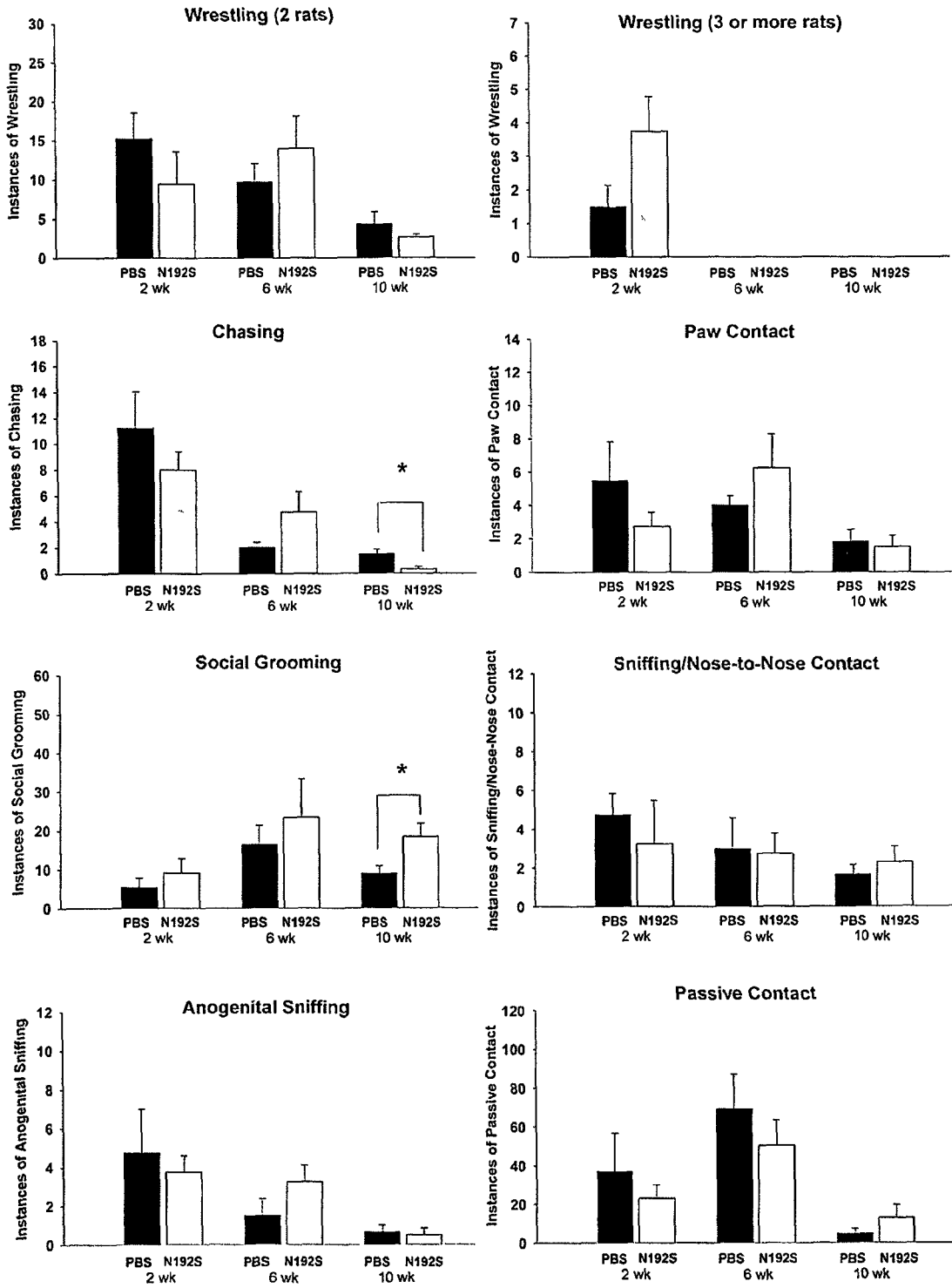


Figure A2.4: Object-directed behaviours observed after 2, 6 and 10 weeks of enriched housing. No group differences were observed at any time point.

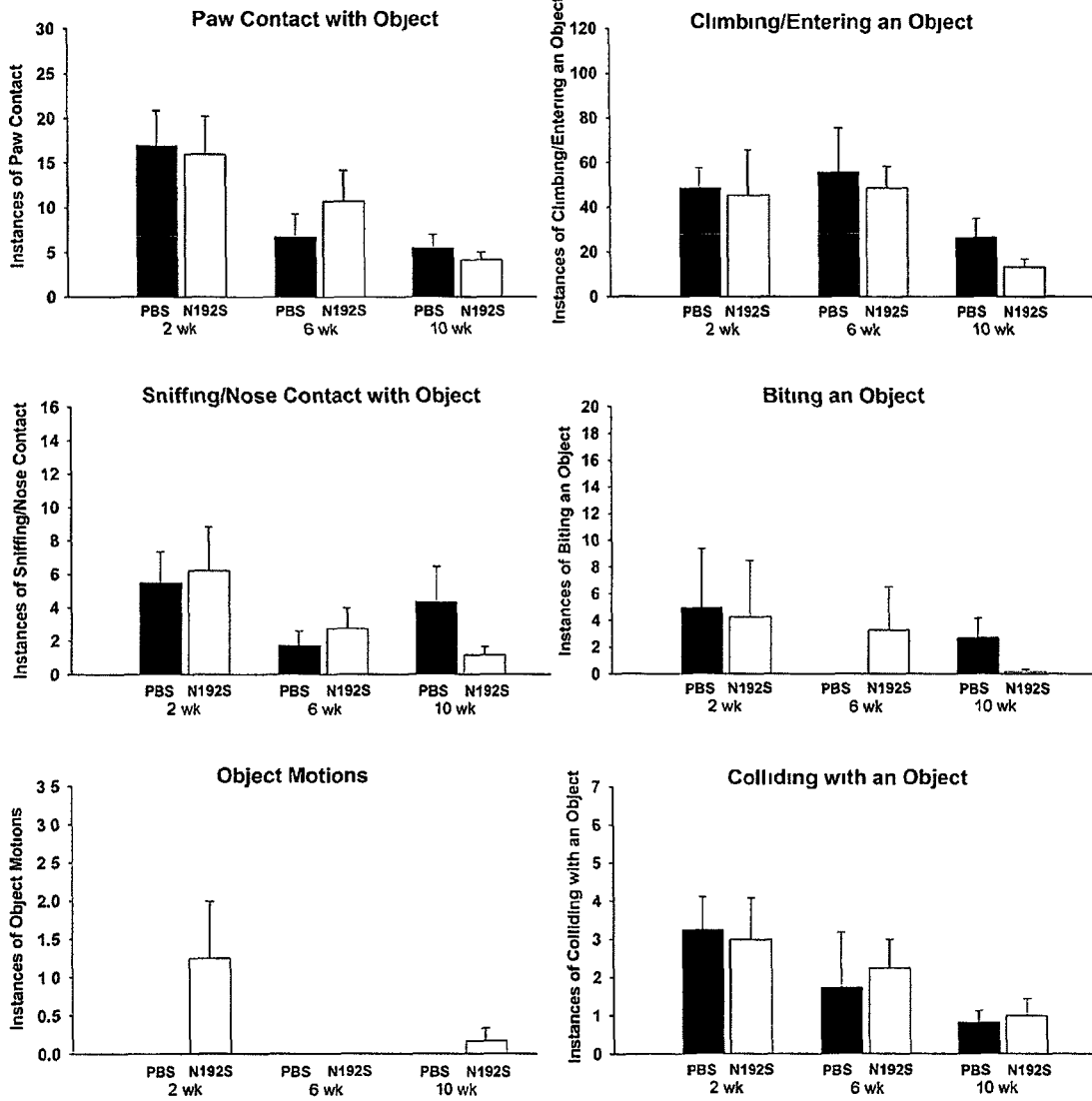


Figure A2.5: Solitary behaviours observed after 2, 6 and 10 weeks of standard housing (Set A: locomotor and exploratory behaviours). No group differences on any behaviour were observed during the second or sixth week. N192S rats were observed in locomotion less often ($t_9=-2.47$, $p=.036$) than control rats during the tenth week.

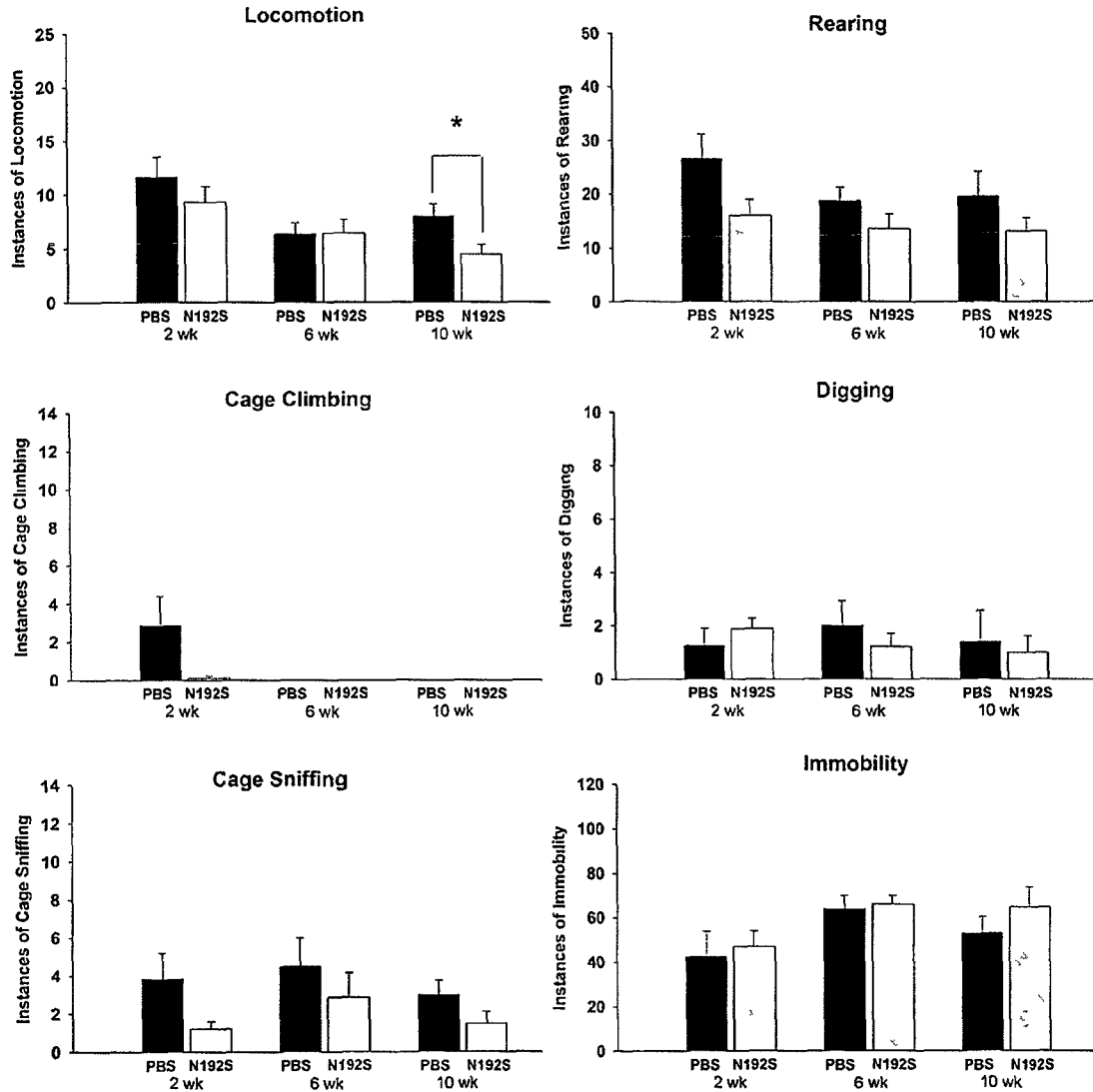


Figure A2.6: Solitary behaviours observed after 2,6 and 10 weeks of standard housing (Set B: Ingestive and self-maintenance behaviours). No group differences on any behaviour were observed during the second or tenth week. During the sixth week, control animals engaged in more individual grooming episodes ($t_{15}=-3.66$, $p=.002$) and drank more often ($t_{15}=-2.34$, $p=.033$) than did N192S rats.

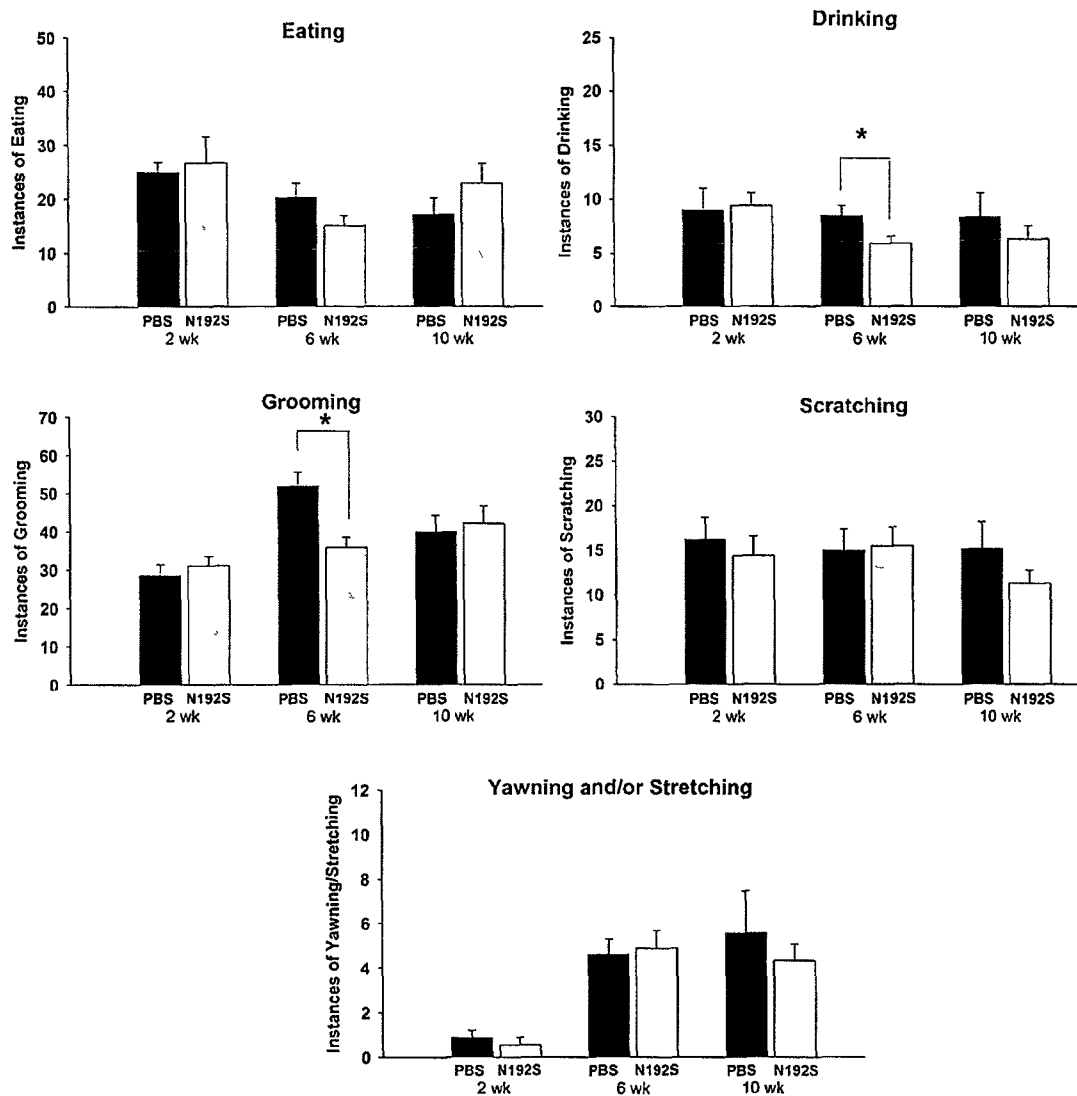
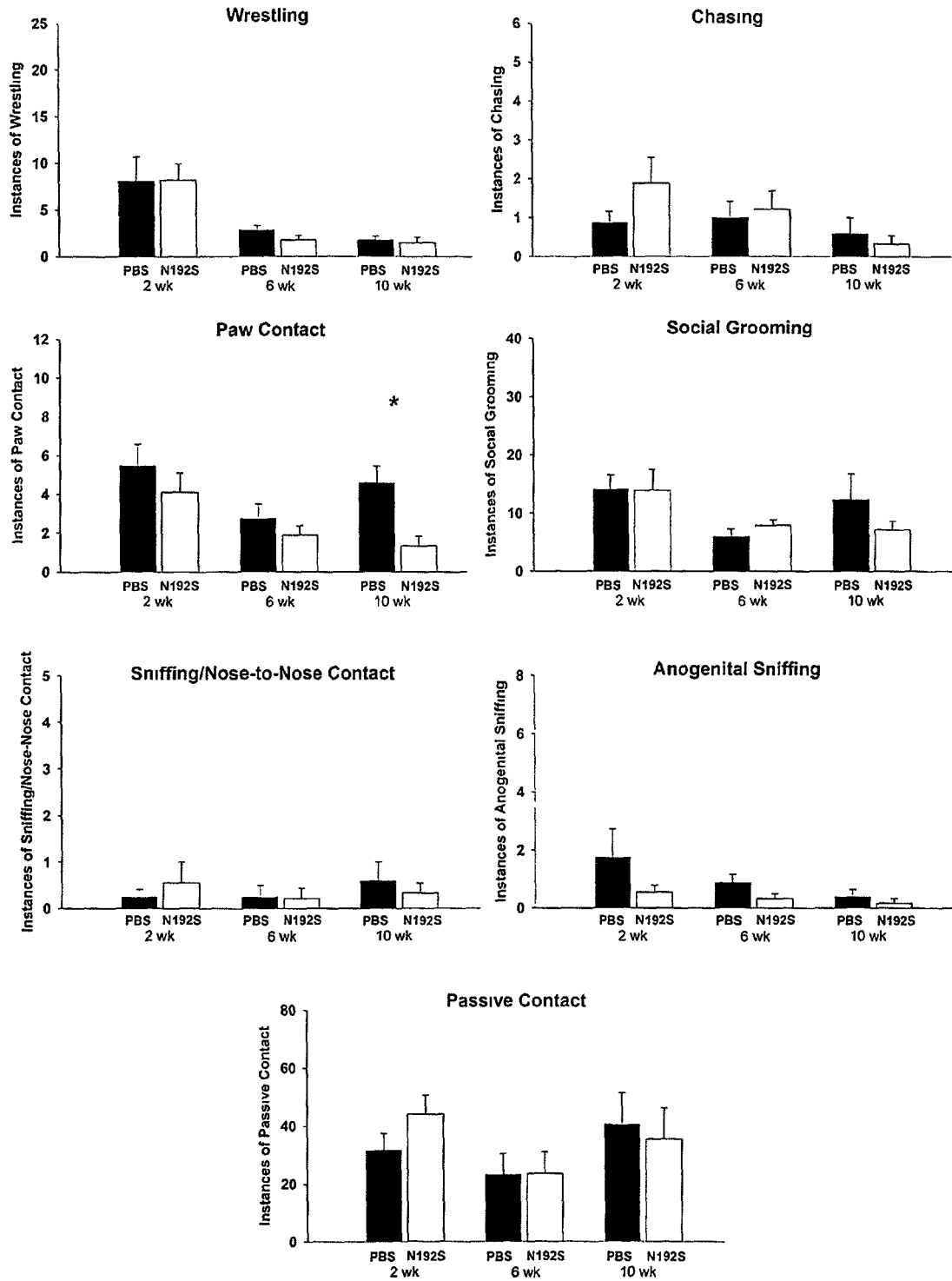


Figure A2.7: Social behaviours observed after 2, 6 and 10 weeks of standard housing. No group differences on any behaviour were observed during the second or sixth week. During the tenth week N192S rats were less likely to make paw contact with a cagemate ($t_9 = -3.41$, $p = .008$).



9. Appendix 3: ANOVA Summary Tables

N192S-Aging Study

Water Maze: Swim Speed

Source	df	MS	F	p
days	4	483.676	6.266	0.000
days * N192S	4	11.492	0.149	0.963
days * age	4	753.143	9.757	0.000
days * N192S * age	4	173.744	2.251	0.068
Error(days)	108	77.191		
trials	4	187.451	3.740	0.007
trials * N192S	4	38.044	0.759	0.554
trials * age	4	50.078	0.999	0.411
trials * N192S * age	4	89.477	1.785	0.137
Error(trials)	108	50.121		
days * trials	16	155.815	2.987	0.000
days * trials * N192S	16	115.333	2.211	0.005
days * trials * age	16	67.712	1.298	0.194
days * trials * N192S * age	16	111.370	2.135	0.007
Error(days*trials)	432	52.158		
N192S	1	2224.767	7.628	0.010
age	1	2505.562	8.591	0.007
N192S * age	1	1842.195	6.316	0.018
Error	27	291.650		

N192S-Aging Study
Water Maze: Distance

Source	df	MS	F	p
Day	4	33360000.000	58.954	0.000
Day * N192S	4	535198.381	0.946	0.441
Day * age	4	1010428.497	1.786	0.137
Day * N192S * age	4	2183759.673	3.859	0.006
Error(Day)	108	565854.842		
Trial	4	14710000.000	24.948	0.000
Trial * N192S	4	393866.296	0.668	0.615
Trial * age	4	526358.428	0.893	0.471
Trial * N192S * age	4	897934.593	1.523	0.200
Error(Trial)	108	589458.252		
Day * Trial	16	605900.175	1.202	0.263
Day * Trial * N192S	16	316562.926	0.628	0.862
Day * Trial * age	16	706817.261	1.402	0.136
Day * Trial * N192S * age	16	647710.755	1.285	0.203
Error(Day*Trial)	432	504154.375		
N192S	1	1560633.538	0.916	0.347
age	1	6166363.545	3.621	0.068
N192S * age	1	545123.206	0.320	0.576
Error	27	1702905.549		

N192S-Aging Study
Cued Platform: Distance

Source	df	MS	F	p
Trials	4	516761.135	1.800	0.144
Trials * N192S	4	24663.381	0.086	0.986
Error(Trials)	48	287168.115		
N192S	1	1801367.376	2.798	0.120
Error	12	643714.918		

N192S-Aging Study
Ki-67: Dorsal DG

Source	df	MS	F	p
N192S	1	1.695	0.009	0.927
age	1	3744.554	19.093	0.000
N192S * age	1	49.517	0.252	0.619
Error	28	196.119		
Total	32			

N192S-Aging Study
Ki-67: Ventral DG

Source	df	MS	F	p
N192S	1	0.116	0.004	0.951
age	1	209.575	6.972	0.013
N192S * age	1	57.212	1.903	0.179
Error	28	30.062		
Total	32			

N192S-Aging Study

DCX: Dorsal DG

Source	df	MS	F	p
N192S	1	1098.919	0.426	0.519
age	1	85827.568	33.298	0.000
N192S * age	1	394.379	0.153	0.699
Error	28	2577.563		
Total	32			

N192S-Aging Study

DCX: Ventral DG

Source	df	MS	F	p
N192S	1	379.893	0.954	0.337
age	1	15365.767	38.580	0.000
N192S * age	1	564.218	1.417	0.244
Error	28	398.282		
Total	32			

N192S-Aging Study

Hippocampal GFAP Expression

Sector	t	df	p
CA1	0.065	15	0.949
CA3	0.618	15	0.546
DG	-0.760	15	0.459
Hilus	-0.177	15	0.862

N192S-Aging Study
CA1 Cell Counts in 21-Month-Old Rats

Measure	t	df	p
Dorsal CA1	1.154	15	0.266
Ventral CA1	0.665	15	0.516
Total CA1	0.992	15	0.337

N192S-Aging Study
Golgi Analysis: Summary Measures

Measure	t	df	p
Cell area	0.278	8	0.788
Apical trees	0.000	8	1.000
Apical branches	-0.228	8	0.825
Apical segments	-0.046	8	0.965
Apical length	0.120	8	0.908
Apical spines	0.202	8	0.845
Apical spine density	0.226	8	0.827
Basal trees	0.000	8	1.000
Basal branches	-0.606	8	0.562
Basal segments	0.589	8	0.572
Basal length	0.131	8	0.899
Basal spines	0.699	8	0.504
Basal spine density	0.973	8	0.359

N192S-Aging Study

Golgi Analysis: Apical Branch Number by Branch Order

Source	df	MS	F	p
BranchOrder	29	29.763	27.288	.000
BranchOrder * N192S	29	1.491	1.367	.108
Error(BranchOrder)	232	1.091		
N192S	1	.504	.075	.791
Error	53.494	8	6.687	

N192S-Aging Study

Golgi Analysis: Apical Branch Length by Branch Order

Source	df	MS	F	p
BranchOrder	29	131386.966	14.724	.000
BranchOrder * N192S	29	15202.821	1.704	.017
Error(BranchOrder)	232	8923.193		
N192S	1	5881.410	.114	.745
Error	8	51808.502		

N192S-Aging Study

Golgi Analysis: Apical Spines by Branch Order

Source	df	MS	F	p
BranchOrder	29	111000.314	32.711	.000
BranchOrder * N192S	29	4984.908	1.469	.064
Error(BranchOrder)	232	3393.402		
N192S	1	1040.969	.025	.879
Error	8	42429.958		

N192S-Aging Study

Golgi Analysis: Apical Spine Density by Branch Order

Source	df	MS	F	p
BranchOrder	19	.183	17.159	.000
BranchOrder * N192S	19	.021	2.000	.011
Error(BranchOrder)	152	.011		
N192S	1	.000	.000	.999
Error	8	.478		

N192S-Aging Study

Golgi Analysis: Basal Branch Number by Branch Order

Source	df	MS	F	p
BranchOrder	8	156.595	144.629	.000
BranchOrder * N192S	8	2.347	2.168	.042
Error(BranchOrder)	64	1.083		
N192S	1	2.703	.578	.469
Error	8	4.675		

N192S-Aging Study

Golgi Analysis: Basal Branch Length by Branch Order

Source	df	MS	F	p
BranchOrder	8	635922.031	51.520	.000
BranchOrder * N192S	8	37710.952	3.055	.006
Error(BranchOrder)	64	12343.090		
N192S	1	2031.217	.034	.859
Error	8	60536.883		

N192S-Aging Study

Golgi Analysis: Basal Spines by Branch Order

Source	df	MS	F	p
BranchOrder	8	417496.979	88.960	.000
BranchOrder * N192S	8	19086.854	4.067	.001
Error(BranchOrder)	64	4693.079		
N192S	1	906.006	.042	.843
Error	8	21550.793		

N192S-Aging Study

Golgi Analysis: Basal Spine Density by Branch Order

Source	df	MS	F	p
BranchOrder	6	.384	8.710	.000
BranchOrder * N192S	6	.039	.892	.509
Error(BranchOrder)	48	.044		
N192S	1	.006	.040	.847
Error	8	.152		

2VO-N192S Study

Open Field : Total Distance Traveled

Source	df	MS	F	p
Postsurgical Interval	1	701066.092	0.401	0.531
Postsurgical Interval * N192S	1	1324502.623	0.757	0.390
Postsurgical Interval * 2VO	1	4260977.100	2.436	0.127
Postsurgical Interval * N192S * 2VO	1	218191.396	0.125	0.726
Error(Postsurgical Interval)	37	1748982.692		
Exposure	2	6351070.257	15.798	0.000
Exposure * N192S	2	312370.632	0.777	0.463
Exposure * 2VO	2	154677.933	0.385	0.682
Exposure * N192S * 2VO	2	207035.522	0.515	0.600
Error(Exposure)	74	402019.603		
Postsurgical Interval * Exposure	2	70024.335	0.185	0.832
Postsurgical Interval * Exposure * N192S	2	1720771.122	4.542	0.014
Postsurgical Interval * Exposure * 2VO	2	952085.629	2.513	0.088
Postsurgical Interval * Exposure * N192S * 2VO	2	727173.621	1.919	0.154
Error(Postsurgical Interval*Exposure)	74	378868.707		
N192S	1	12290000.000	1.494	0.229
2VO	1	598459.857	0.073	0.789
N192S*2VO	1	6484.981	0.001	0.978
Error	37	8225532.413		

N192S-2VO Study
 Open Field: Number of Line
 Crosses

Source	df	MS	F	p
Postsurgical Interval	1	2288.032	0.559	0.459
Postsurgical Interval * N192S	1	3268.089	0.799	0.377
Postsurgical Interval * 2VO	1	8222.972	2.010	0.165
Postsurgical Interval * N192S * 2VO	1	913.619	0.223	0.639
Error(Postsurgical Interval)	37	4090.467		
Exposure	2	13661.216	15.549	0.000
Exposure * N192S	2	917.927	1.045	0.357
Exposure * 2VO	2	264.244	0.301	0.741
Exposure * N192S * 2VO	2	555.862	0.633	0.534
Error(Exposure)	74	878.577		
Postsurgical Interval * Exposure	2	49.802	0.057	0.945
Postsurgical Interval * Exposure * N192S	2	3774.407	4.293	0.017
Postsurgical Interval * Exposure * 2VO	2	2034.123	2.314	0.106
Postsurgical Interval * Exposure * N192S * 2VO	2	1297.399	1.476	0.235
Error(Postsurgical Interval*Exposure)	74	879.106		
N192S	1	34225.724	1.834	0.184
2VO	1	1767.064	0.095	0.760
N192S * 2VO	1	89.111	0.005	0.945
Error	37	18664.119		

N192S-2VO Study
 Open Field: Distance Traveled in the
 Inner Squares

Source	df	MS	F	p
Postsurgical Interval	1	151515.468	1.411	0.243
Postsurgical Interval * N192S	1	3375.620	0.031	0.860
Postsurgical Interval * 2VO	1	115707.642	1.077	0.306
Postsurgical Interval * N192S * 2VO	1	23764.271	0.221	0.641
Error(Postsurgical Interval)	37	107416.425		
Exposure	2	4804.081	0.198	0.821
Exposure * N192S	2	49406.287	2.040	0.137
Exposure * 2VO	2	22972.542	0.948	0.392
Exposure * N192S * 2VO	2	40105.195	1.656	0.198
Error(Exposure)	74	24220.380		
Postsurgical Interval * Exposure	2	103631.336	4.580	0.013
Postsurgical Interval * Exposure * N192S	2	54127.758	2.392	0.098
Postsurgical Interval * Exposure * 2VO	2	1187.204	0.052	0.949
Postsurgical Interval * Exposure * N192S * 2VO	2	3301.033	0.146	0.864
Error(Postsurgical Interval*Exposure)	74	22625.228		
N192S	1	1792252.662	6.306	0.017
2VO	1	93007.752	0.327	0.571
N192S * 2VO	1	4908.524	0.017	0.896
Error	37	284196.056		

N192S-2VO Study
 Open Field: Number of
 Centre Entries

Source	df	MS	F	p
Postsurgical Interval	1	37.542	1.115	0.298
Postsurgical Interval * N192S	1	1.928	0.057	0.812
Postsurgical Interval * 2VO	1	49.245	1.462	0.234
Postsurgical Interval * N192S * 2VO	1	6.584	0.195	0.661
Error(Postsurgical Interval)	37	33.684		
Exposure	2	4.577	0.557	0.575
Exposure * N192S	2	16.127	1.963	0.148
Exposure * 2VO	2	6.628	0.807	0.450
Exposure * N192S * 2VO	2	8.622	1.049	0.355
Error(Exposure)	74	8.216		
Postsurgical Interval * Exposure	2	24.026	3.044	0.054
Postsurgical Interval * Exposure * N192S	2	21.340	2.704	0.074
Postsurgical Interval * Exposure * 2VO	2	2.415	0.306	0.737
Postsurgical Interval * Exposure * N192S * 2VO	2	0.444	0.056	0.945
Error(Postsurgical Interval*Exposure)	74	7.892		
N192S	1	648.877	6.855	0.013
2VO	1	22.445	0.237	0.629
N192S * 2VO	1	1.317	0.014	0.907
Error	37	94.657		

N192S-2VO Study
Open Field: Latency
to Enter Centre

Source	df	MS	F	p
Postsurgical Interval	1	152354.841	3.703	0.062
Postsurgical Interval * N192S	1	34880.423	0.848	0.363
Postsurgical Interval * 2VO	1	96132.742	2.336	0.135
Postsurgical Interval * N192S * 2VO	1	17423.261	0.423	0.519
Error(Postsurgical Interval)	37	41145.637		
Exposure	2	33029.629	1.377	0.259
Exposure * N192S	2	10511.017	0.438	0.647
Exposure * 2VO	2	41518.398	1.731	0.184
Exposure * N192S * 2VO	2	18826.772	0.785	0.460
Error(Exposure)	74	23991.571		
Postsurgical Interval * Exposure	2	206041.888	10.900	0.000
Postsurgical Interval * Exposure * N192S	2	3367.942	0.178	0.837
Postsurgical Interval * Exposure * 2VO	2	13739.497	0.727	0.487
Postsurgical Interval * Exposure * N192S * 2VO	2	1281.612	0.068	0.935
Error(Postsurgical Interval*Exposure)	74	18902.825		
N192S	1	915009.989	5.527	0.024
2VO	1	503.591	0.003	0.956
N192S * 2VO	1	104512.599	0.631	0.432
Error	37	165541.731		

N192S-2VO Study

Elevated Plus: Closed Arm Entries

Source	df	MS	F	p
N192S	1	18.654	0.677	0.419
2VO	1	1.195	0.043	0.837
N192S * 2VO	1	35.695	1.295	0.267
Error	23	27.561		
Total	27			

N192S-2VO Study

Elevated Plus: Open Arm Entries

Source	df	MS	F	p
N192S	1	33.082	3.842	0.062
2VO	1	0.000	0.000	0.994
N192S * 2VO	1	37.622	4.370	0.048
Error	23	8.610		
Total	27			

N192S-2VO Study

Elevated Plus: Number of Vertical Stretches

Source	df	MS	F	p
N192S	1	3.029	0.065	0.801
2VO	1	51.461	1.099	0.305
N192S * 2VO	1	4.779	0.102	0.752
Error	23	46.821		
Total	27			

N192S-2VO Study

Elevated Plus: Number of Stretch-Attend Postures

Source	df	MS	F	p
N192S	1	46.270	1.708	0.204
2VO	1	0.568	0.021	0.886
N192S * 2VO	1	5.014	0.185	0.671
Error	23	27.087		
Total	27			

N192S-2VO Study

Elevated Plus: Number of Head

Dips

Source	df	MS	F	p
N192S	1	161.622	5.598	0.027
2VO	1	0.433	0.015	0.904
N192S * 2VO	1	83.676	2.898	0.102
Error	23	28.871		
Total	27			

N192S-2VO Study
Water Maze, 1st Run: Latency

Source	df	MS	F	p
days	4	76718.561	63.850	0.000
days * N192S	4	1128.258	0.939	0.443
days * 2VO	4	1817.390	1.513	0.201
days * N192S * 2VO	4	647.566	0.539	0.707
Error(days)	148	1201.541		
trials	4	12670.279	25.682	0.000
trials * N192S	4	4423.368	8.966	0.000
trials * 2VO	4	121.421	0.246	0.912
trials * N192S * 2VO	4	328.909	0.667	0.616
Error(trials)	148	493.347		
days * trials	16	1058.790	1.823	0.025
days * trials * N192S	16	367.777	0.633	0.858
days * trials * 2VO	16	730.011	1.257	0.220
days * trials * N192S * 2VO	16	525.985	0.906	0.563
Error(days*trials)	592	580.736		
N192S	1	23832.552	3.889	0.056
2VO	1	4700.526	0.767	0.387
N192S * 2VO	1	10026.859	1.636	0.209
Error	37	6127.486		

N192S-2VO Study
 Water Maze, 1st Run: Distance

Source	df	MS	F	p
days	4	5573601.953	46.430	0.000
days * N192S	4	182538.229	1.521	0.199
days * 2VO	4	237941.703	1.982	0.100
days * N192S * 2VO	4	139250.548	1.160	0.331
Error(days)	148	120042.342		
trials	4	4665622.699	71.474	0.000
trials * N192S	4	278269.729	4.263	0.003
trials * 2VO	4	9958.029	0.153	0.962
trials * N192S * 2VO	4	89980.094	1.378	0.244
Error(trials)	148	65277.652		
days * trials	16	112786.663	1.569	0.072
days * trials * N192S	16	37244.562	0.518	0.938
days * trials * 2VO	16	96193.430	1.339	0.168
days * trials * N192S * 2VO	16	85861.934	1.195	0.267
Error(days*trials)	592	71864.248		
N192S	1	1147701.327	1.670	0.204
2VO	1	1004515.693	1.462	0.234
N192S * 2VO	1	757943.201	1.103	0.300
Error	37	687136.583		

N192S-2VO Study

Water Maze, 1st Run: Speed

Source	df	MS	F	p
Days	4	98.462	16.642	0.000
Days * N192S	4	24.128	4.078	0.004
Days * 2VO	4	2.822	0.477	0.753
Days * N192S * 2VO	4	1.391	0.235	0.918
Error(Days)	148	5.916		
Trials	4	124.421	29.741	0.000
Trials * N192S	4	15.630	3.736	0.006
Trials * 2VO	4	2.444	0.584	0.674
Trials * N192S * 2VO	4	0.912	0.218	0.928
Error(Trials)	148	4.183		
Days * Trials	16	17.386	7.970	0.000
Days * Trials * N192S	16	2.206	1.011	0.442
Days * Trials * 2VO	16	2.299	1.054	0.397
Days * Trials * N192S * 2VO	16	2.057	0.943	0.519
Error(Days*Trials)	592	2.181		
N192S	1	17.652	0.755	0.390
2VO	1	17.785	0.761	0.389
N192S * 2VO	1	36.048	1.543	0.222
Error	37	23.364		

N192S-2VO Study

Water Maze, 2nd Run: Latency

Source	df	MS	F	p
days	4	1737.036	6.022	.000
days * N192S	4	235.746	.817	.516
days * 2VO	4	346.750	1.202	.312
days * N192S * 2VO	4	314.647	1.091	.363
Error(days)	148	288.464		
trials	4	5570.109	34.589	.000
trials * N192S	4	703.981	4.372	.002
trials * 2VO	4	95.891	.595	.666
trials * N192S * 2VO	4	104.482	.649	.629
Error(trials)	148	161.038		
days * trials	16	201.655	1.324	.176
days * trials * N192S	16	288.982	1.898	.018
days * trials * 2VO	16	189.380	1.244	.229
days * trials * N192S * 2VO	16	189.719	1.246	.228
Error(days*trials)	592	152.260		
N192S	1	2471.389	1.212	.278
2VO	1	2696.624	1.323	.258
N192S * 2VO	1	5964.468	2.925	.096
Error	37	2038.940		

N192S-2VO Study

Water Maze, 2nd Run: Distance

Source	df	MS	F	p
days	4	299509.380	5.100	0.001
days * N192S	4	50892.383	0.867	0.486
days * 2VO	4	69624.642	1.186	0.320
days * N192S * 2VO	4	70938.451	1.208	0.310
Error(days)	148	58725.122		
trials	4	758845.865	30.220	0.000
trials * N192S	4	98282.674	3.914	0.005
trials * 2VO	4	24684.332	0.983	0.419
trials * N192S * 2VO	4	13711.404	0.546	0.702
Error(trials)	148	25110.783		
days * trials	16	32287.657	1.316	0.181
days * trials * N192S	16	40575.770	1.653	0.051
days * trials * 2VO	16	27709.579	1.129	0.324
days * trials * N192S * 2VO	16	34700.741	1.414	0.129
Error(days*trials)	592	24540.113		
N192S	1	484273.119	1.125	0.296
2VO	1	548803.098	1.275	0.266
N192S * 2VO	1	1102593.472	2.561	0.118
Error	37	430459.947		

N192S-2VO Study

Water Maze, 3rd Run: Speed

Source	df	MS	F	p
days	4	2.968	0.474	0.755
days * N192S	4	6.540	1.043	0.387
days * 2VO	4	6.598	1.053	0.382
days * N192S * 2VO	4	4.334	0.691	0.599
Error(days)	148	6.268		
trials	4	12.564	2.671	0.034
trials * N192S	4	9.072	1.929	0.109
trials * 2VO	4	2.942	0.625	0.645
trials * N192S * 2VO	4	4.576	0.973	0.424
Error(trials)	148	4.704		
days * trials	16	10.181	2.954	0.000
days * trials * N192S	16	4.258	1.235	0.235
days * trials * 2VO	16	3.180	0.923	0.543
days * trials * N192S * 2VO	16	3.539	1.027	0.426
Error(days*trials)	592	3.447		
N192S	1	34.166	0.635	0.431
2VO	1	4.123	0.077	0.783
N192S * 2VO	1	1.165	0.022	0.884
Error	37	53.809		

N192S-2VO Study
 Water Maze, 3rd Run: Latency

Source	df	MS	F	p
days	4	807.211	3.397	.012
days * N192S	4	331.240	1.394	.243
days * 2VO	4	41.608	.175	.951
days * N192S * 2VO	4	71.928	.303	.875
Error(days)	88	237.645		
trials	4	5526.390	24.864	.000
trials * N192S	4	165.460	.744	.564
trials * 2VO	4	71.260	.321	.863
trials * N192S * 2VO	4	217.917	.980	.422
Error(trials)	88	222.261		
days * trials	16	123.867	.609	.877
days * trials * N192S	16	202.979	.998	.459
days * trials * 2VO	16	261.116	1.283	.205
days * trials * N192S * 2VO	16	388.522	1.909	.019
Error(days*trials)	352	203.478		
N192S	1	1.866	.002	.964
2VO	1	3.810	.004	.948
N192S * 2VO	1	258.690	.291	.595
Error	22	889.191		

N192S-2VO Study
 Water Maze, 3rd Run: Distance

Source	df	MS	F	p
days	4	197821.982	4.211	.004
days * N192S	4	97857.067	2.083	.090
days * 2VO	4	6854.578	.146	.964
days * N192S * 2VO	4	19195.643	.409	.802
Error(days)	88	46975.089		
trials	4	909950.411	21.084	.000
trials * N192S	4	29142.684	.675	.611
trials * 2VO	4	13532.131	.314	.868
trials * N192S * 2VO	4	52496.482	1.216	.310
Error(trials)	88	43158.479		
days * trials	16	26192.338	.656	.837
days * trials * N192S	16	45652.418	1.143	.314
days * trials * 2VO	16	56063.247	1.404	.137
days * trials * N192S * 2VO	16	76836.634	1.924	.018
Error(days*trials)	352	39943.767		
N192S	1	449.505	.003	.960
2VO	1	10513.476	.062	.806
N192S * 2VO	1	1331.672	.008	.930
Error	22	170861.793		

N192S-2VO Study

Water Maze, 3rd Run: Speed

Source	df	MS	F	p
Days	4	31.693	4.597	0.002
Days * N192S	4	24.505	3.554	0.010
Days * 2VO	4	8.072	1.171	0.329
Days * N192S * 2VO	4	3.230	0.468	0.759
Error(Days)	88	6.895		
Trials	4	10.773	1.655	0.168
Trials * N192S	4	7.743	1.189	0.321
Trials * 2VO	4	11.376	1.747	0.147
Trials * N192S * 2VO	4	5.901	0.906	0.464
Error(Trials)	88	6.511		
Days * Trials	16	12.586	2.075	0.009
Days * Trials * N192S	16	4.574	0.754	0.737
Days * Trials * 2VO	16	3.657	0.603	0.882
Days * Trials * N192S * 2VO	16	7.438	1.226	0.245
Error(Days*Trials)	352	6.067		
N192S	1	0.228	0.006	0.937
2VO	1	19.060	0.531	0.474
N192S * 2VO	1	164.916	4.599	0.043
Error	22	35.861		

N192S-2VO Study

Water Maze Cued Platform: Latency

Source	df	MS	F	p
trials	4	1080.017	7.760	.000
trials * N192S	4	128.651	.924	.453
trials * 2VO	4	31.341	.225	.924
trials * N192S * 2VO	4	82.875	.595	.667
Error(trials)	92	139.184		
N192S	1	87.941	.133	.718
2VO	1	531.098	.806	.379
N192S * 2VO	1	881.476	1.338	.259
Error	23	659.010		

N192S-2VO Study

CA1 Cell Count

Source	df	MS	F	p
N192S	1	542500000	0.611	0.443
2VO	1	47810000	0.054	0.819
N192S * 2VO	1	61340000	0.069	0.795
Error	23	888600000		
Total	27			

N192S-2VO Study

GFAP Immunoreactivity in CA1

Source	df	MS	F	p
N192S	1	15.559	1.587	0.220
2VO	1	0.368	0.037	0.848
N192S * 2VO	1	0.398	0.041	0.842
Error	24	9.806		
Total	28			

N192S-2VO Study

GFAP Immunoreactivity in CA3

Source	df	MS	F	p
N192S	1	30.348	4.819	0.038
2VO	1	5.844	0.928	0.345
N192S * 2VO	1	7.697	1.222	0.280
Error	24	6.298		
Total	28			

N192S-2VO Study

GFAP Immunoreactivity in the Dentate Gyrus

Source	df	MS	F	p
N192S	1	34.665	2.572	0.122
2VO	1	12.419	0.921	0.347
N192S * 2VO	1	6.889	0.511	0.482
Error	24	13.480		
Total	28			

N192S-2VO Study

GFAP Immunoreactivity in the Hilus

Source	df	MS	F	p
N192S	1	17.373	2.674	0.115
2VO	1	0.239	0.037	0.850
N192S * 2VO	1	1.194	0.184	0.672
Error	24	6.498		
Total	28			

N192S-2VO Study

Number of Ki-67+ Cells in the Dorsal Dentate Gyrus

Source	df	MS	F	p
N192S	1	1151.231	2.162	0.154
2VO	1	13.942	0.026	0.873
N192S * 2VO	1	208.761	0.392	0.537
Error	24	532.495		
Total	28			

N192S-2VO Study

Number of Ki-67+ Cells in the Ventral Dentate Gyrus

Source	df	MS	F	p
N192S	1	6.181	0.068	0.797
2VO	1	176.720	1.933	0.177
N192S * 2VO	1	128.720	1.408	0.247
Error	24	91.416		
Total	28			

N192S-2VO Study

Number of DCX+ Cells in the Dorsal Dentate Gyrus

Source	df	MS	F	p
N192S	1	3540.948	6.137	0.021
2VO	1	447.170	0.775	0.387
N192S* 2VO	1	42.713	0.074	0.788
Error	24	576.960		
Total	28			

N192S-2VO Study

Number of DCX+ Cells in the Ventral Dentate Gyrus

Source	df	MS	F	p
N192S	1	365.907	2.016	0.169
2VO	1	248.124	1.367	0.254
N192S * 2VO	1	290.727	1.602	0.218
Error	24	181.521		
Total	28			

N192S-2VO Study

Number of BrdU+ Cells in CA1

Source	df	MS	F	p
N192S	1	2.788	1.213	0.282
2VO	1	0.364	0.158	0.694
N192S * 2VO	1	1.809	0.787	0.384
Error	24	2.299		
Total	28			

N192S-2VO Study

Number of BrdU+ Cells in CA3

Source	df	MS	F	p
N192S	1	5.596	0.376	0.546
2VO	1	54.391	3.654	0.068
N192S * 2VO	1	2.343	0.157	0.695
Error	24	14.884		
Total	28			

N192S-2VO Study

Number of BrdU+ Cells in the Dentate Gyrus

Source	df	MS	F	p
N192S	1	0.012	0.001	0.975
2VO	1	10.422	0.856	0.364
N192S * 2VO	1	0.398	0.033	0.858
Error	24	12.176		
Total	28			

N192S-2VO Study

Number of BrdU+ Cells in the Hilus

Source	df	MS	F	p
N192S	1	13.190	0.754	0.394
2VO	1	11.877	0.679	0.418
N192S * 2VO	1	0.600	0.034	0.855
Error	24	17.491		
Total	28			

N192S-2VO Study

Golgi Analysis: Apical Branch Number

Source	df	MS	F	p
N192S	1	.152	.123	.730
2VO	1	3.096	2.507	.131
N192S * 2VO	1	.024	.020	.890
Error	18	1.235		
Total	22			

N192S-2VO Study

Golgi Analysis: Apical Branch Length

Source	df	MS	F	p
N192S	1	719614.766	2.147	.160
2VO	1	1758863.752	5.249	.034
N192S * 2VO	1	60778.569	.181	.675
Error	18	335115.983		
Total	22			

N192S-2VO Study

Golgi Analysis: Apical Segments

Source	df	MS	F	p
N192S	1	16.800	.382	.544
2VO	1	97.829	2.222	.153
N192S * 2VO	1	17.575	.399	.535
Error	18	44.029		
Total	22			

N192S-2VO Study

Golgi Analysis: Apical Spines

Source	df	MS	F	p
N192S	1	135318.273	0.531	0.476
2VO	1	1646302.074	6.458	0.020
N192S * 2VO	1	28218.793	0.111	0.743
Error	18	254931.627		
Total	22			

N192S-2VO Study

Golgi Analysis: Apical Spine Density

Source	df	MS	F	p
N192S	1	.001	.064	.804
2VO	1	.017	1.248	.279
N192S * 2VO	1	.007	.544	.470
Error	18	.013		
Total	22			

N192S-2VO Study

Golgi Analysis: Basal Branch Number

Source	df	MS	F	p
N192S	1	.009	.041	.841
2VO	1	.064	.279	.604
N192S * 2VO	1	.364	1.587	.224
Error	18	.229		
Total	22			

N192S-2VO Study

Golgi Analysis: Basal Branch Length

Source	df	MS	F	p
N192S	1	8492.151	.093	.764
2VO	1	182452.727	2.005	.174
N192S * 2VO	1	29340.667	.322	.577
Error	18	91002.553		
Total	22			

N192S-2VO Study

Golgi Analysis: Basal Segments

Source	df	MS	F	p
N192S	1	2.199	.182	.675
2VO	1	57.791	4.779	.042
N192S * 2VO	1	23.712	1.961	.178
Error	18	12.093		
Total	22			

N192S-2VO Study

Golgi Analysis: Basal Spines

Source	df	MS	F	p
N192S	1	4911.273	.087	.771
2VO	1	342866.438	6.087	.024
N192S * 2VO	1	7256.204	.129	.724
Error	18	56328.996		
Total	22			

N192S-2VO Study

Golgi Analysis: Basal Spine Density

Source	df	MS	F	p
N192S	1	.000	.001	.980
2VO	1	.026	2.460	.134
N192S * 2VO	1	.000	.006	.938
Error	18	.011		
Total	22			

N192S-2VO Study

Golgi Analysis: Apical Branch Number by Branch Order

Source	df	MS	F	p
branchorder	21	81.179	313.695	0.000
branchorder * N192S	21	0.139	0.538	0.954
branchorder * 2VO	21	0.331	1.279	0.185
branchorder * N192S * 2VO	21	0.265	1.025	0.431
Error(branchorder)	378	0.259		
N192S	1	.580	.285	.600
2VO	1	4.932	2.423	.137
N192S * 2VO	1	.536	.263	.614
Error	18	2.035		

N192S-2VO Study

Golgi Analysis: Apical Branch Length by Branch Order

Source	df	MS	F	p
BranchOrder	21	564368.746	29.862	.000
BranchOrder * N192S	21	17426.186	.922	.562
BranchOrder * 2VO	21	24894.573	1.317	.159
BranchOrder * N192S * 2VO	21	14490.474	.767	.761
Error(BranchOrder)	378	18899.350		
N192S	1	4782.247	.130	.723
2VO	1	151257.110	4.107	.058
N192S * 2VO	1	25193.526	.684	.419
Error	18	36832.301		

N192S-2VO Study

Golgi Analysis: Apical Spines by Branch Order

Source	df	MS	F	p
BranchOrder	21	184256.343	130.281	.000
BranchOrder * N192S	21	1514.953	1.071	.377
BranchOrder * 2VO	21	3505.300	2.478	.000
BranchOrder * N192S * 2VO	21	1347.506	.953	.522
Error(BranchOrder)	378	1414.299		
N192S	1	6831.243	.605	.447
2VO	1	72538.713	6.422	.021
N192S * 2VO	1	1603.083	.142	.711
Error	18	11296.111		

N192S-2VO Study

Golgi Analysis: Apical Spine Density by Branch Order

Source	df	MS	F	p
BranchOrder	21	.871	32.581	.000
BranchOrder * N192S	21	.032	1.203	.245
BranchOrder * 2VO	21	.017	.639	.890
BranchOrder * N192S * 2VO	21	.019	.721	.812
Error(BranchOrder)	378	.027		
N192S	1	.130	.814	.379
2VO	1	.392	2.461	.134
N192S * 2VO	1	.359	2.257	.150
Error	18	.159		

N192S-2VO Study

Golgi Analysis: Basal Branch Number by Branch Order

Source	df	MS	F	p
BranchOrder	8	212.715	453.056	.000
BranchOrder * N192S	8	.206	.438	.897
BranchOrder * 2VO	8	.802	1.708	.101
BranchOrder * N192S * 2VO	8	1.214	2.586	.011
Error(BranchOrder)	144	.470		
N192S	1	.173	.112	.742
2VO	1	6.033	3.889	.064
N192S * 2VO	1	2.635	1.699	.209
Error	18	1.551		

N192S-2VO Study

Golgi Analysis: Basal Branch Length by Branch Order

Source	df	MS	F	p
BranchOrder	8	1321199.282	237.952	0.000
BranchOrder * N192S	8	3079.247	0.555	0.813
BranchOrder * 2VO	8	3975.745	0.716	0.677
BranchOrder * N192S * 2VO	8	10125.770	1.824	0.077
Error(BranchOrder)	144	5552.380		
N192S	1	1501.415	.144	.709
2VO	1	22634.416	2.167	.158
N192S * 2VO	1	4239.906	.406	.532
Error	18	10446.583		

N192S-2VO Study

Golgi Analysis: Basal Spines by Branch Order

Source	df	MS	F	p
BranchOrder	8	369707.106	188.999	.000
BranchOrder * N192S	8	922.070	.471	.875
BranchOrder * 2VO	8	5880.179	3.006	.004
BranchOrder * N192S * 2VO	8	2693.012	1.377	.211
Error(BranchOrder)	144	1956.137		
N192S	1	338.000	.055	.817
2VO	1	36178.807	5.909	.026
N192S * 2VO	1	548.453	.090	.768
Error	18	6122.755		

N192S-2VO Study

Golgi Analysis: Basal Spine Density by Branch Order

Source	df	MS	F	p
BranchOrder	8	.762	32.243	.000
BranchOrder * N192S	8	.008	.326	.955
BranchOrder * 2VO	8	.004	.188	.992
BranchOrder * N192S * 2VO	8	.016	.668	.719
Error(BranchOrder)	144	.024		
N192S	1	.003	.039	.847
2VO	1	.271	3.630	.073
N192S * 2VO	1	.023	.314	.582
Error	18	.075		

N192S-Enrichment Study
Behavioural Monitoring, Week 2, Standard Housing

Behaviour	t	df	p
Wrestling	0.032	15	0.975
Chasing	1.351	15	0.197
Sniff/nose-nose contact	0.614	15	0.548
Anogenital sniff	-1.253	15	0.229
Passive contact	1.402	15	0.181
Social grooming	-0.053	15	0.959
Paw contact with a cagemate	-0.939	15	0.362
Locomotion	-0.958	15	0.353
Cage climbing	-1.905	15	0.076
Digging	0.868	15	0.399
Cage sniffing	-1.977	15	0.067
Rearing	-2.023	15	0.061
Scratching	-0.559	15	0.585
Grooming	0.684	15	0.505
Eating	0.327	15	0.748
Drinking	0.194	15	0.849
Yawning/stretching	-0.655	15	0.522
Immobility	0.339	15	0.739

N192S-Enrichment Study
 Behavioural Monitoring, Week 6, Standard Housing

Behaviour	t	df	p
Wrestling	-1.640	15	0.122
Chasing	0.350	15	0.731
Sniff/nose-nose contact	-0.083	15	0.935
Anogenital sniff	-1.647	15	0.120
Passive contact	0.028	15	0.978
Social grooming	1.225	15	0.240
Paw contact with a cagemate	-0.987	15	0.339
Locomotion	0.042	15	0.967
Cage climbing	*	*	*
Digging	-0.766	15	0.456
Cage sniffing	-0.824	15	0.423
Rearing	-1.404	15	0.181
Scratching	0.178	15	0.861
Grooming	-3.660	15	0.002
Eating	-1.700	15	0.110
Drinking	-2.343	15	0.033
Yawning/stretching	0.247	15	0.809
Immobility	0.282	15	0.782

* test could not be conducted because both groups scored 0 on this measure.

N192S-Enrichment Study
Behavioural Monitoring, Week 10, Standard Housing

Behaviour	t	df	p
Wrestling	-0.424	9	0.682
Chasing	-0.621	9	0.550
Sniff/nose-nose contact	-0.621	9	0.550
Anogenital sniff	-0.811	9	0.438
Passive contact	-0.332	9	0.747
Social grooming	-1.230	9	0.250
Paw contact with a cagemate	-3.409	9	0.008
Locomotion	-2.465	9	0.036
Cage climbing	*	*	*
Digging	-0.317	9	0.759
Cage sniffing	-1.533	9	0.160
Rearing	-1.306	9	0.224
Scratching	-1.211	9	0.257
Grooming	0.339	9	0.742
Eating	1.172	9	0.271
Drinking	-0.858	9	0.413
Yawning/stretching	-0.675	9	0.517
Immobility	0.986	9	0.350

* test could not be conducted because both groups scored 0 on this measure.

N192S-Enrichment Study
Behavioural Monitoring, Week 2, Enrichment

Behaviour	t	df	p
Wrestling (2 rats)	-1.087	6	0.319
Wrestling (3 or more rats)	1.850	6	0.114
Chasing	-1.033	6	0.341
Sniff/nose-nose contact	-0.598	6	0.572
Anogenital sniff	-0.416	6	0.692
Passive contact	-0.683	6	0.520
Social grooming	0.861	6	0.422
Paw contact with a cagemate	-1.109	6	0.310
Sniff/nose contact with an object	0.235	6	0.822
Paw contact with an object	-0.174	6	0.868
Climb/enter object	-0.147	6	0.888
Bite object	-0.123	6	0.906
Collide with object	-0.182	6	0.862
Object motions	1.667	6	0.147
Locomotion	-0.279	6	0.789
Cage climbing	-0.214	6	0.837
Digging	*	*	*
Cage sniffing	-1.041	6	0.338
Rearing	0.454	6	0.666
Scratching	-0.291	6	0.781
Grooming	-0.736	6	0.490
Eating	0.518	6	0.623
Drinking	-1.184	6	0.281
Yawning/stretching	0.000	6	1.000
Immobility	-0.030	6	0.977

* test could not be conducted because both groups scored 0 on this measure.

N192S-Enrichment Study
Behavioural Monitoring, Week 6, Enrichment

Behaviour	t	df	p
Wrestling	0.901	6	0.402
Chasing	1.718	6	0.137
Sniff/nose-nose contact	-0.132	6	0.899
Anogenital sniff	1.439	6	0.200
Passive contact	-0.851	6	0.427
Social grooming	0.637	6	0.548
Paw contact with a cagemate	1.073	6	0.324
Sniff/nose contact with an object	0.661	6	0.533
Paw contact with an object	0.923	6	0.392
Climb/enter object	-0.334	6	0.749
Bite object	1.000	6	0.356
Collide with object	0.309	6	0.768
Object motions	*	*	*
Locomotion	5.576	6	0.001
Cage climbing	1.102	6	0.313
Digging	-1.000	6	0.356
Cage sniffing	0.139	6	0.894
Rearing	1.652	6	0.150
Scratching	1.368	6	0.220
Grooming	1.224	6	0.267
Eating	0.911	6	0.397
Drinking	0.264	6	0.801
Yawning/stretching	0.687	6	0.518
Immobility	-0.662	6	0.533

* test could not be conducted because both groups scored 0 on this measure.

N192S-Enrichment Study
Behavioural Monitoring, Week 10, Enrichment

Behaviour	t	df	p
Wrestling	-1.043	10	0.322
Chasing	-2.907	10	0.016
Sniff/nose-nose contact	0.707	10	0.496
Anogenital sniff	-0.349	10	0.734
Passive contact	1.153	10	0.276
Social grooming	2.433	10	0.035
Paw contact with a cagemate	-0.343	10	0.739
Sniff/nose contact with an object	-1.445	10	0.179
Paw contact with an object	-0.768	10	0.460
Climb/enter object	-1.430	10	0.183
Bite object	-1.658	10	0.128
Collide with object	0.307	10	0.765
Object motions	1.000	10	0.341
Locomotion	0.218	10	0.832
Cage climbing	0.259	10	0.801
Digging	1.000	10	0.341
Cage sniffing	0.764	10	0.462
Rearing	-0.944	10	0.367
Scratching	0.000	10	1.000
Grooming	-0.908	10	0.385
Eating	-0.241	10	0.814
Drinking	-0.570	10	0.581
Yawning/stretching	1.182	10	0.265
Immobility	0.256	10	0.803

N192S-Enrichment Study

BrdU (2 hours after final injection): Dorsal DG

Source	df	MS	F	p
N192S	1	36990000	32.386	0.000
housing	1	1763459	1.544	0.221
N192S * housing	1	4851	0.004	0.948
Error	39	1142263		
Total	43			

N192S-Enrichment Study

BrdU (2 hours after final injection): Ventral DG

Source	df	MS	F	p
N192S	1	425604	2.599	0.115
housing	1	223596	1.365	0.250
N192S * housing	1	65738	0.401	0.530
Error	39	163769		
Total	43			

N192S-Enrichment Study

Ki-67: Dorsal DG

Source	df	MS	F	p
N192S	1	111.210	0.000	0.996
housing	1	424694.721	0.111	0.741
N192S * housing	1	1970220.612	0.513	0.478
Error	40	3840445.954		
Total	44			

N192S-Enrichment Study

Ki-67: Ventral DG

Source	df	MS	F	p
N192S	1	140399.773	0.600	0.443
housing	1	405957.113	1.734	0.195
N192S * housing	1	670924.108	2.866	0.098
Error	40	234136.678		
Total	44			

N192S-Enrichment Study
DCX: Dorsal DG

Source	df	MS	F	p
N192S	1	82930000	7.283	0.010
housing	1	16720000	1.468	0.233
N192S * housing	1	7647069	0.672	0.418
Error	38	11390000		
Total	42			

N192S-Enrichment Study
DCX: Ventral DG

Source	df	MS	F	p
N192S	1	24263.717	0.018	0.894
housing	1	46772.724	0.035	0.854
N192S * housing	1	5646.469	0.004	0.949
Error	38	1354047.448		
Total	42			

N192S-Enrichment Study
BrdU (4 weeks after final injection): Dorsal DG

Source	df	MS	F	p
N192S	1	336303.671	1.297	0.261
housing	1	199763.139	0.770	0.385
N192S * housing	1	2298.996	0.009	0.925
Error	42	259291.511		
Total	46			

N192S-Enrichment Study

BrdU (4 weeks after final injection): Ventral DG

Source	df	MS	F	p
N192S	1	33255.051	1.850	0.181
housing	1	6956.933	0.387	0.537
N192S * housing	1	24738.347	1.376	0.247
Error	42	17974.412		
Total	46			

N192S-Enrichment Study

BrdU (percent survival): Dorsal DG

Source	df	MS	F	p
N192S	1	730.129	5.609	0.023
housing	1	37.198	0.286	0.596
N192S * housing	1	1.446	0.011	0.917
Error	42	130.173		
Total	46			

N192S-Enrichment Study

BrdU (percent survival): Ventral DG

Source	df	MS	F	p
N192S	1	5.157	0.046	0.832
housing	1	50.857	0.449	0.507
N192S * housing	1	529.756	4.674	0.036
Error	42	113.333		
Total	46			

N192S-Enrichment Study

Percent of BrdU+ Cells Expressing NeuN

Source	df	MS	F	p
N192S	1	115.283	1.975	0.171
housing	1	18.466	0.316	0.578
N192S * housing	1	6.599	0.113	0.739
Error	28	58.375		
Total	32			

N192S-Enrichment Study

Percent of BrdU+ Cells Expressing S100B

Source	df	MS	F	p
N192S	1	5.206	2.508	0.124
housing	1	0.020	0.010	0.922
N192S * housing	1	0.186	0.090	0.767
Error	28	2.076		
Total	32			

N192S-Enrichment Study

Percent of BrdU+ Cells Expressing Neither NeuN or S100B

Source	df	MS	F	p
N192S	1	71.491	1.413	0.244
housing	1	17.270	0.341	0.564
N192S * housing	1	9.002	0.178	0.676
Error	28	50.582		
Total	32			

N192S-Enrichment Study

Total Neurogenesis

Source	df	MS	F	p
N192S	1	144115.922	0.808	0.376
housing	1	320378.765	1.797	0.191
N192S * housing	1	15646.302	0.088	0.769
Error	28	178264.943		
Total	32			

N192S-Enrichment Study

Total Gliogenesis

Source	df	MS	F	p
N192S	1	742.790	1.183	0.286
housing	1	15.532	0.025	0.876
N192S * housing	1	420.709	0.670	0.420
Error	28	627.972		
Total	32			